Integrable Boundary Flows and the g-function

Ruth Margaret Wilbourne

A thesis presented for the degree of
Doctor of Philosophy

Centre for Particle Theory
Department of Mathematical Sciences
Durham University

May 2012

Integrable Boundary Flows and the g-function

Ruth Margaret Wilbourne

Submitted for the degree of Doctor of Philosophy

May 2012

Abstract

This thesis explores renormalisation group flows in integrable quantum field theories with boundaries, as described by the g-function. The main focus is on the g-function in the staircase model, the renormalisation group flow of which passes close to the unitary minimal models. This g-function is used to identify flows between boundary conditions both within and between the minimal models. In certain limits the $\mathcal{M}A_m^{(+)}$ theories which interpolate between pairs of minimal models emerge from the staircase model, and exact expressions for the g-function in these models are extracted from the staircase g-function. Perturbative tests on the $\mathcal{M}A_4^{(+)}$ g-function are discussed, as is initial work on the g-function for the $\mathcal{M}A_4^{(-)}$ theory, which describes flows that emerge when the bulk coupling is taken to have the opposite sign to that in $\mathcal{M}A_4^{(+)}$. Expressions are also found for excited state versions of the $\mathcal{M}A_m^{(+)}$ g-function, and these allow the unique identification of certain boundary flows.

Declaration

The work in this thesis is based on research carried out in the Department of Mathematical Sciences at Durham University. No part of this thesis has been submitted elsewhere for any other degree or qualification. Chapters 1-4.1 consist of a review of the necessary background material, for which no originality is claimed. Chapters 4.2 and 5 are based on original work done in collaboration with Patrick Dorey and Roberto Tateo, which was published in [1]. Chapter 6 consists of unpublished original work which grew from discussions with Patrick Dorey and also, in the case of section 6.3.2, Balázs Pozsgay.

Acknowledgements

I am very grateful to my supervisor Patrick Dorey for his generosity with his time and expertise. I would also like to thank Balázs Pozsgay for helpful and interesting discussions, and my friends and family for keeping me in touch with the real world during the preparation of this thesis. Finally I would like to thank the Science and Technology Facilities Council whose financial support enabled this research.

Contents

List of Figures

Chapter 1

The Renormalisation Group and Conformal Field Theory

1.1 Statistical Mechanics

Materials that exhibit sudden changes in their properties have long been the subject of scientific study. Such changes, known as phase transitions, encompass a wide variety of physical phenomena, from the changes in the state of water as it moves from solid ice to liquid to gas, to materials whose magnetic properties are suddenly lost or gained. Everyday observations show that such transitions are induced by changes in external variables such as temperature, but it was not until the development of statistical mechanics that the process of these phase transitions could be described in detail through the microscopic properties of the materials in question.

Statistical mechanics allows the analysis of systems involving an infinite number of degrees of freedom (see, for example, [2–5]), and the focus here will be on systems defined on a lattice. Thermodynamic quantities such as entropy, internal energy, free energy and magnetisation can be extracted purely from the knowledge of the Boltzmann weights $e^{-\beta H}$ which encode each configuration of the system. These weights are determined by the Hamiltonian H which gives the energy for each configuration, and by $\beta = k_B/T$, where T is the temperature and k_B is the Boltzmann constant. The Boltzmann weights are summed over to form the partition function

Z

$$Z = \mathrm{Tr}\, e^{-\beta H}, \tag{1.1.1}$$

where the trace is taken over all the possible configurations of the system. The probability of a system being in a particular configuration $\{\sigma\}$ with energy $H_{\{\sigma\}}$ is then given by

$$p_\sigma = \frac{1}{Z} e^{-\beta H_{\{\sigma\}}} \tag{1.1.2}$$

and the thermodynamic variables can also be calculated as functions of Z and its derivatives. For example, the free energy F is defined as

$$F = -\frac{1}{\beta} \ln Z. \tag{1.1.3}$$

The focus here will be on models describing magnetic systems. The simplest and most famous of these is the Ising model, which describes the behaviour of ferromagnetic materials, and in particular their property of spontaneous magnetisation. This property means that below a certain temperature they retain their magnetisation even when the external magnetic field is removed, and it is through the Ising model that statistical mechanics can be used to describe this sudden change in behaviour that occurs as the temperature is varied. The Ising model can be defined in any number of dimensions, but it is the model defined on a two-dimensional square lattice that is of relevance to this thesis. The sites of the lattice are occupied by spins pointing either 'up' or 'down', and the more the spins are aligned with one another the greater the magnetisation of the system. In order to better illustrate certain concepts that will be important throughout this thesis, the details of this model will be introduced in the context of a more complex model, the Blume-Capel or tricritical Ising model (see, for example [6]). The difference between its set-up and that of the Ising model is that vacant sites are allowed in the lattice. The situation at each lattice site is described by the variable σ_i, which can take one of three values: 0 for the vacant sites and ± 1 for spin up and spin down, respectively. The Hamiltonian

for the model in a particular configuration $\{\sigma_i\}$ is

$$H(\{\sigma_i\}) = -J \sum_{<i,j>} \sigma_i \sigma_j + \mu \sum_i \sigma_i^2 - h \sum_i \sigma_i \tag{1.1.4}$$

where $<,>$ denotes the sum over nearest-neighbour pairs in the lattice. $J > 0$ is the coupling constant for the interaction between neighbouring spins, μ is viewed as a chemical potential for the vacancies, h is the external magnetic field, and $\sum_i \sigma_i$ is equal to the magnetisation of the system in this configuration. The partition function is

$$Z = \sum_{\{\sigma_i \in \{0,\pm 1\}\}} e^{-\beta H(\{\sigma_i\})} \tag{1.1.5}$$

where the first sum is over all possible configurations of the σ_i's. The expectation value of the magnetisation, M, is given by

$$M = \sum_{\{\sigma_i \in \{0,\pm 1\}\}} p_\sigma \sum_i \sigma_i = \frac{1}{\beta Z} \frac{\partial Z}{\partial h} = -\frac{\partial F}{\partial h}. \tag{1.1.6}$$

In the $\mu \to -\infty$ limit, the contribution to the partition function from configurations where one or more lattice sites is vacant becomes insignificant with respect to configurations with all sites occupied, and the model reduces to the Ising model which has partition function

$$Z = \sum_{\{\sigma_i \in \{\pm 1\}\}} e^{\beta\left(J \sum_{<i,j>} \sigma_i \sigma_j + h \sum_i \sigma_i\right)}. \tag{1.1.7}$$

For $J > 0$, at temperatures less than a certain critical temperature T_C known as the Curie temperature, the Ising model is dominated either by the configuration with all spins up (for $h > 0$), or with all spins down (for $h < 0$). These ordered phases persist for $h \to 0^+$ and $h \to 0^-$, respectively. The system is therefore magnetised even when there is no external magnetic field, meaning that the model describes a uniaxial ferromagnet.

A statistical system is characterised by its correlation length, ξ. This measures the distance over which the degrees of freedom (e.g. spin) of particles occupying the various lattice sites are correlated to one another, and so defines the scale at

which microscopic properties have a significant impact on the system. The two point correlation function $G(r)$ between spins separated by a distance r is

$$G(r) = \langle \sigma(r)\sigma(0) \rangle = \frac{1}{Z} \sum_{\{\sigma_i\}} \sigma(r)\sigma(0) e^{-\beta H(\{\sigma_i\})} \tag{1.1.8}$$

and the correlation length is defined via its decay:

$$G(r) \propto \frac{e^{-r/\xi}}{r^{(d-1)/2}} \qquad \text{for } r \gg \xi \tag{1.1.9}$$

where d is the number of dimensions. The correlation length is dependent on the external parameters such as temperature, pressure and the external magnetic field, and as such enters into the description of critical points of the system. A critical point in the space of the external parameters occurs when one or more of the thermodynamic variables exhibits a sudden change as the external parameters are smoothly varied. Such behaviour usually indicates a phase transition in the system. If a thermodynamic variable defined in terms of a first derivative of the partition function has a discontinuity for some values of the external parameters then this indicates a first-order phase transition. If, instead, a first-derivative-type thermodynamic variable is continuous but its own derivative is divergent then such a critical point indicates a second-order or continuous phase transition. The continuous behaviour is due to the correlation length becoming infinite at the critical point, so that at this point the system must exist in one unique phase. As the critical point is approached from either side, the correlation length tends smoothly to infinity, and the difference between the thermodynamic quantities in question tends smoothly to zero.

The tricritical Ising model (1.1.4) exhibits both types of phase transition. In its $\mu \to -\infty$ Ising model limit, at every point on the line $h = 0$, $T < T_C$ there is a discontinuity in the magnetisation $M(h)$ signalling a first-order phase transition with finite correlation length between the ordered phases with all spins up and all spins down. As $T \to T_C$, the discontinuity tends to zero so that $M(h)$ becomes continuous at $T = T_C$, and the two phases become indistinguishable. However, the magnetic susceptibility $\chi \sim \frac{\partial M}{\partial h}$ diverges at this point, as does the correlation length,

meaning that $(h, T) = (0, T_C)$ is a critical point associated to a second-order phase transition. For $T > T_C$ there is a single, disordered phase. The phase diagram for the Ising model is depicted in figure 1.1, and the behaviour of the magnetisation $M(h)$ at $h = 0$ is shown in figure 1.2.

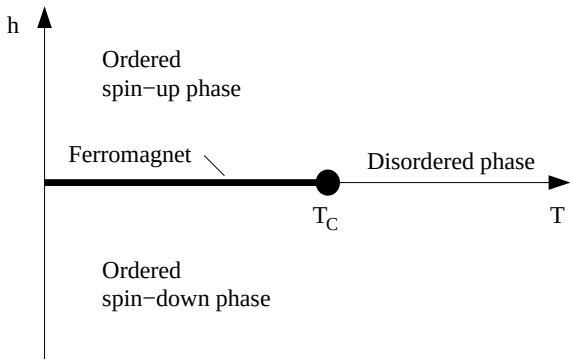

Figure 1.1: Phase diagram of the Ising model: the thicker line marks the first-order line and the dot indicates the second-order critical point.

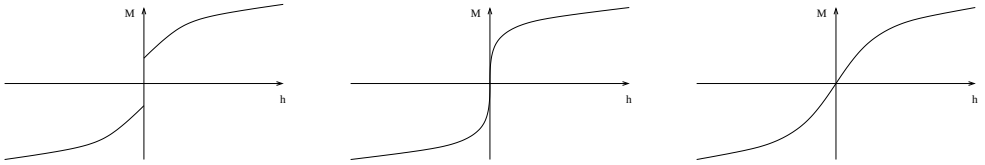

(a) $T < T_C$

There is a discontinuity in the value of the magnetisation at $h = 0$.

(b) $T = T_C$

M is a continuous function of h, but $\frac{\partial M}{\partial h}$ diverges at $h = 0$.

(c) $T > T_C$

$M(h)$ and $\frac{\partial M}{\partial h}$ are both continuous for all values of h.

Figure 1.2: Plots showing the dependence of the magnetisation M on the external magnetic field h.

Critical points also arise for other values of μ, and here the focus will be on the behaviour of the model when $h = 0$. When $T = 0$ the partition function is dominated by the ground state, which for $\mu < 2J$ is the configuration with all sites occupied, either with all spins up or all spins down, just as in the ordered phase of the Ising model. For $\mu > 2J$ the ground state is the configuration where all sites are vacant, corresponding to a non-magnetic phase. The magnetisation $M(h)$ is discontinuous at $\mu = 2J$ due to the shift between the ordered and non-magnetic phases, and so there is a critical point here signalling a first-order phase transition. This critical

point lies at one end of a line of such points that signal a first-order phase transition in the (μ, T) plane between ordered and disordered phases, and which extends until the phase transition becomes second-order. The point where this occurs is called the tricritical point. From the discussion of the Ising model, there is a critical point at $(\mu, T) \to (-\infty, T_C)$ lying at a second-order phase transition between the ordered and disordered phases, and this transition extends into the (μ, T) plane as a second-order critical line which meets the first-order critical line at the tricritical point. This phase behaviour is illustrated in the diagram below.

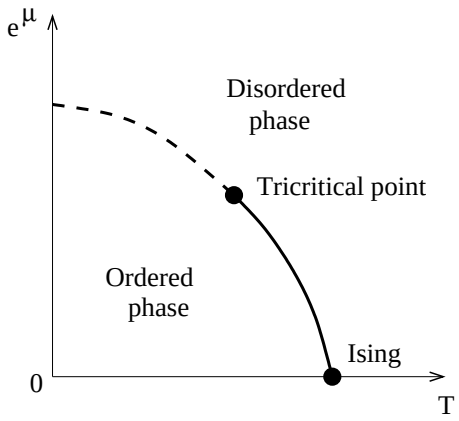

Figure 1.3: Phase diagram for the tricritical Ising model at $h = 0$.

1.2 The Renormalisation Group Flow

Close to a critical point, most thermodynamic variables have power-law dependence on the external variables. The exponents which appear in these power laws are called the critical exponents. In the example of the Ising model, critical exponents govern the power-law dependence of M and χ on T and h close to the point $T = T_C$, $h = 0$. The critical exponents depend only the parameters defining the universality class to which the system belongs, such as the number of dimensions and the symmetries of the Hamiltonian. This makes the study of critical points particularly interesting, but the infinite correlation length at second-order critical points makes them very difficult to analyse. It was for this reason that the renormalisation group (RG) method was developed, most notably by Wilson [7], in order to transform the system

to a simpler one whilst preserving the long-distance behaviour of the original system (see, for example [2–5, 8–11]).

The infinite correlation length at a critical point makes the system insensitive to scale transformations, and so a change in the length scale of the system can be considered. For magnetic systems this can be achieved in a simple way by implementing a block spin transformation. The premise of this is to begin with a regular lattice and divide it up into blocks, assigning to each block a spin; this spin is decided by the spins of the original lattice which lie inside that block. For example, figure 1.4 shows a lattice divided into three by three blocks, with the new lattice sites lying at the centre of each block.

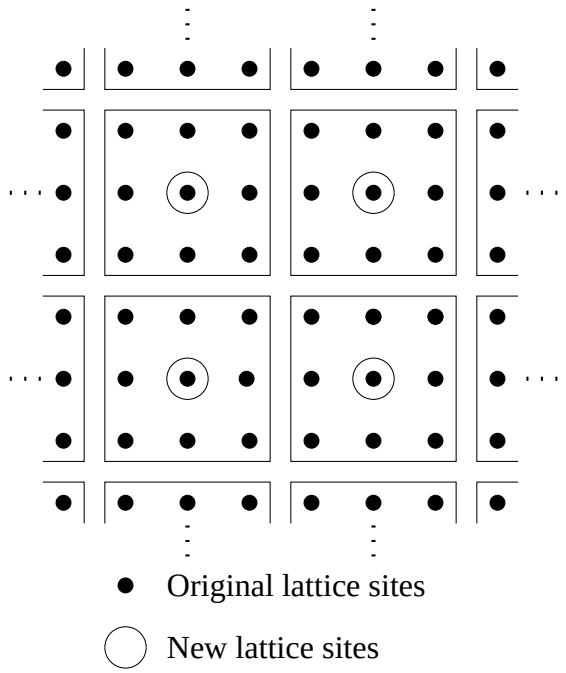

Figure 1.4: Block transformation of a lattice using 3×3 blocks.

The Hamiltonian for the system is then expressed in terms of these new spins. A rescaling has taken place during this process as follows: if the original lattice spacing is a and the lattice is broken up into identically sized blocks of length b, then the new lattice spacing after the transformation is ab. To maintain the original spatial density of lattice sites, a rescaling must be performed on the spatial distances, $x \to x/b$, and hence the correlation length is scaled in the same way, $\xi \to \xi/b$. In practice this involves a re-summation in the taking of the trace in the

partition function, resulting in the partition function being re-expressed in terms of a transformed Hamiltonian defined via the new spins. This can be seen in the example of the one-dimensional Ising model. Consider the situation of a closed chain of n spins, for which the partition function is

$$Z = \sum_{\{\sigma_i = \pm 1\}} \exp\left[\sum_{i=1}^{n} \left\{K + J\sigma_i\sigma_{i+1} + \tfrac{1}{2}h\left(\sigma_i + \sigma_{i+1}\right)\right\}\right]. \tag{1.2.1}$$

Here $K = 0$, but is included because it will be non-zero after the transformation. β is assumed to have been absorbed into the couplings and for simplicity n is taken to be even, with $\sigma_{n+1} = \sigma_1$. The lattice is divided up into blocks of two neighbouring original lattice sites, and each block is represented by the left-hand site in each block, that is σ_i with i odd. Therefore, the σ_i with even i should be summed over first in (1.2.1). Initially summing only over σ_2 leads to

$$Z = \sum_{\sigma_1, \sigma_3, \sigma_4, \cdots, \sigma_n} \left(\exp(2K) 2\cosh\left(J(\sigma_1\sigma_3) + h\right) \exp\left(\frac{h}{2}(\sigma_1 + \sigma_3)\right) \times \prod_{i=3}^{n} \exp\left\{K + J\sigma_i\sigma_{i+1} + \tfrac{1}{2}h\left(\sigma_i + \sigma_{i+1}\right)\right\} \right) \tag{1.2.2}$$

and so after the summation has been carried out for all even i

$$Z = \sum_{\sigma_j,\, j\ odd} \prod_{j=1}^{n/2} \exp(2K) 2\cosh\left(J(\sigma_{2j-1}\sigma_{2j+1}) + h\right) \exp\left(\frac{h}{2}(\sigma_{2j-1} + \sigma_{2j+1})\right). \tag{1.2.3}$$

Relabelling σ_i for i odd as the new lattice sites σ'_i produces the renormalised partition function

$$Z = \sum_{\sigma'_i} \prod_{i=1}^{n/2} \exp(2K) 2\cosh\left(J(\sigma'_i\sigma'_{i+1}) + h\right) \exp\left(\frac{h}{2}(\sigma'_i + \sigma'_{i+1})\right). \tag{1.2.4}$$

The renormalised partition function is expected to indicate that the renormalised theory behaves in a similar way to the original one. In this case the initial Hamiltonian was a nearest-neighbour Hamiltonian, so short-distance interactions are expected to dominate the Hamiltonian in the new partition function. In fact it can

again be written in a nearest-neighbour form. Setting

$$Z = \sum_{\{\sigma'_j=\pm 1\}} \exp\left[\sum_{i=1}^{n/2} \left\{K' + J'\sigma'_i\sigma'_{i+1} + \tfrac{1}{2}h'\left(\sigma'_i + \sigma'_{i+1}\right)\right\}\right] \tag{1.2.5}$$

$$= \sum_{\{\sigma'_j=\pm 1\}} \prod_{i=1}^{n/2} \exp\left\{K' + J'\sigma'_i\sigma'_{i+1} + \tfrac{1}{2}h'\left(\sigma'_i + \sigma'_{i+1}\right)\right\} \tag{1.2.6}$$

and equating the factors in the products in (1.2.4) and (1.2.6) for all possible values of σ'_i and σ'_{i+1}, it is possible to solve for K', J' and h' to see that the renormalised partition function can indeed be expressed via a nearest-neighbour Hamiltonian.

The above process demonstrates how renormalisation leads to the Hamiltonian being expressed in terms of new couplings. The renormalisation group transformation can therefore be thought of as an operator R acting on the space of all possible couplings $\{K_i\}$. If the transformation is applied repeatedly, then the resulting flow in the set of couplings is known as the renormalisation group flow. If at some point the set of couplings is such that $R\{K_i^*\} = \{K_i^*\}$ then $\{K_i^*\}$ is a fixed point of this flow. Since $\xi \to \xi/b$ under the renormalisation group transformation, ξ must be infinite or zero at the fixed point, and the focus will be on the $\xi = \infty$ case as this corresponds to the system being at a critical point. Working back along a flow ending at such a critical fixed point, ξ must always be infinite and so the system is at a critical point at all points in the flow.

Studying the effect of the renormalisation group transformation on points close to a fixed point allows a picture to be formed of the renormalisation group flows in the region surrounding this fixed point. Assuming R is differentiable at $\{K_i^*\}$ and defining $R(K_i) = K'_i$, R can be linearised close to the fixed point so that

$$R\left(K_i\right) = R\left(K_i^*\right) + \sum_j R'\left(K^*\right)\left(K_j - K_j^*\right) \tag{1.2.7}$$

$$\Rightarrow K'_i = K_i^* + \sum_j \left.\frac{\partial K'_i}{\partial K_j}\right|_{K=K^*} \left(K_j - K_j^*\right). \tag{1.2.8}$$

Treating K_i and K'_i as the components of vectors K and K' and $\left.\frac{\partial K'_i}{\partial K_j}\right|_{K^*}$ as a matrix

M, and writing $K_i = K_i^* + \delta K_i$ and $K_i' = K_i^* + \delta K_i'$, the above becomes

$$\delta K' = M\,\delta K. \tag{1.2.9}$$

Assuming M possesses a complete set of eigenvectors ψ_a and eigenvalues λ_a, δK and $\delta K'$ can be expanded in terms of the eigenvectors so that

$$\delta K = \sum_a u_a \psi_a \quad \text{and} \quad \delta K' = \sum_a u_a' \psi_a \tag{1.2.10}$$

and so by (1.2.9)

$$\delta K' = M\,\delta K = \sum_a u_a \lambda_a \psi_a. \tag{1.2.11}$$

Therefore, $u_a' = \lambda_a u_a$, and repeated (say n) applications of the transformation close to the fixed point gives $u_a^{(n)} = (\lambda_a)^n\, u_a$. The quantities u_a are coordinates of the eigenbasis, and are known as the scaling variables, and defining $\lambda_a = b^{y_a}$, the y_a are known as the renormalisation group eigenvalues. The value of y_a therefore determines the effect of the renormalisation group transformation on the coordinate associated to the eigenvector ψ_a, thereby showing whether the renormalisation group flow is towards or away from the fixed point in this direction. If $y_a > 0$ then the renormalisation group flow is away from the fixed point, and u_a is known as a relevant variable, whereas if $y_a < 0$ the flow is towards the fixed point and u_a is an irrelevant variable, as depicted in figure 1.5. If $y_a = 0$ then u_a is called a marginal

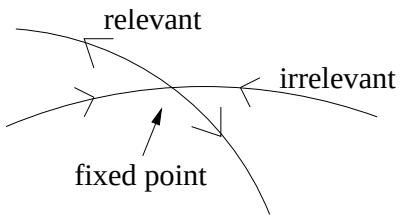

Figure 1.5: RG flows close to a fixed point with one relevant direction and one irrelevant direction associated to it.

variable, since in the linearised regime it does not have a significant effect.

The eigenvectors associated to the irrelevant scaling variables provide a basis for a hyper-surface on which all points are attracted to the given fixed point. All

renormalisation group flows on the surface therefore end at the fixed point, so each point is a critical point and the surface is known as the critical surface. Each point on the critical surface of a particular fixed point belongs to the same universality class as the fixed point. This means that the long distance behaviour of a theory at each point on the critical surface will be governed by that of the fixed point.

In cases where the parameter space has more than one critical fixed point, renormalisation group flows can follow trajectories between them. These occur when, once the theory has been shifted slightly away from the initial fixed point in a relevant direction, the renormalisation group flow takes the theory to another fixed point, with respect to which the direction of the flow is irrelevant. The initial and final fixed points are known as the UV and IR fixed points, respectively. In such cases there is a crossover phenomenon determined by a crossover scale. Moving along the RG flow the theory is initially controlled by the UV fixed point, in the sense that correlation functions over distances up to the scale set by the crossover scale behave as at the UV fixed point. There is then a transition period, after which the theory is controlled by the IR fixed point. Another possibility is that an RG flow might pass close to a number of fixed points. In this case there is a series of crossovers, and the theory is controlled by each fixed point in turn. Such behaviour will be seen when the staircase model is introduced in chapter 4.

In the tricritical Ising model, a flow in a certain relevant direction away from the tricritical fixed point takes the theory to the Ising fixed point. So, the theory is initially controlled by the tricritical fixed point, and then after a crossover period is controlled by the Ising fixed point. If the theory is initially shifted away from the tricritical fixed point in the opposite direction from that just described then the correlation length becomes finite, and so in this case the crossover is from the tricritical fixed point to a massive theory. The two flows just described are depicted in figure 1.6.

Conjugate to each scaling variable u_a is a local field ϕ_a of scaling dimension x_a, where in d dimensions $x_a + y_a = d$. These are known as the scaling fields, and close

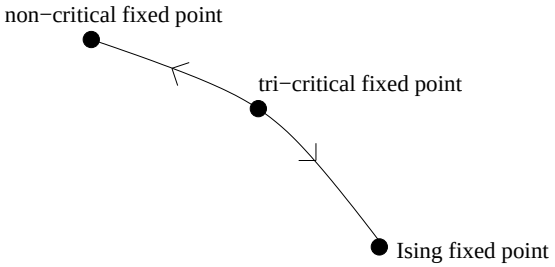

Figure 1.6: RG flows between fixed points in the tricritical Ising model.

to a fixed point the Hamiltonian can be written as

$$H = \sum_a \sum_r u_a \phi_a(r). \tag{1.2.12}$$

The scaling fields are themselves described as relevant, marginal or irrelevant, depending on the scaling variable to which they are conjugate. These fields will have an important role in the perturbation of conformal field theories which will be described later.

The link with conformal field theory (CFT) arises from local scale invariance. The lattice set-up and the block-spin transformations used the discussion above resulted in the Hamiltonian at a fixed point having global scale invariance. However, block-spin transformations can also be considered that do not have a constant block size b, but instead use one that depends on the position within the lattice $b(r)$, such as that depicted in figure 1.7). As long as $b(r)$ varies smoothly and slowly

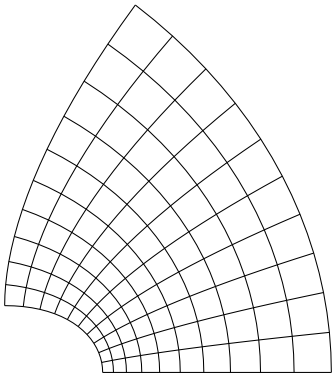

Figure 1.7: A lattice transformed by a non-constant block-spin transformation.

enough with r, then in the neighbourhood of a particular lattice cell at $\hat{r}$, the transformation will be the same as if the whole lattice was transformed by constant block-size $b(\hat{r})$. Therefore, as long as the Hamiltonian only includes short-distance interactions, the Hamiltonian will transform in the same way as for a constant block size, and will have the same fixed point. The renormalisation group transformation is now a local rescaling, and such transformations are members of the set of conformal transformations.

In the rest of this thesis, RG flows will be viewed in the context of quantum field theory, so it is the continuum limit of these lattice theories that is important. Assume now that the lattice has spacing a (up until this point the spacing has been taken to equal one). In taking the continuum limit, the lattice spacing must be taken to zero in such a way that the correlation length remains large. This can be achieved by considering a theory close to the critical surface. Here the correlation length ξ (measured in lattice units) is very large, and diverges as the critical surface is approached. As this is the case, it makes sense to measure distances in units of the physical correlation length $\xi_{phys} = a\xi$. From this perspective, ξ_{phys} is held fixed meaning that the lattice spacing a becomes variable and tends to zero as $\xi \to \infty$ in such a way that $a\xi$ remains fixed and finite. So, the continuum limit arises as the limit of a series of models defined on increasingly fine lattices, as the critical surface is approached.

1.3 Conformal Field Theory

The conformal group [9, 10, 12, 13] is the group of coordinate transformations that leave the metric unchanged up to a scale factor. In three or more dimensions this is the group of global translations, dilations (scale transformations) and rotations, plus the special conformal transformations which transform the coordinates as

$$x^\mu \to \frac{x^\mu - a^\mu x^2}{1 - 2a.x + a^2x^2}. \tag{1.3.1}$$

However, in two dimensions the group is much bigger, in fact infinite dimensional, and it is this that makes two-dimensional conformally invariant theories so interesting. In two-dimensional Euclidean space the line element is $ds^2 = dx^2 + dy^2$. This can be re-expressed using $z = x + iy$ and $\bar{z} = x - iy$ so that $ds^2 = dzd\bar{z}$. Under a transformation $z \to f(z, \bar{z})$, $\bar{z} \to \bar{f}(z, \bar{z})$

$$ds^2 = dzd\bar{z} \to df d\bar{f} = \left(\frac{\partial f}{\partial z}dz + \frac{\partial f}{\partial \bar{z}}d\bar{z}\right)\left(\frac{\partial \bar{f}}{\partial z}dz + \frac{\partial \bar{f}}{\partial \bar{z}}d\bar{z}\right). \tag{1.3.2}$$

For this transformation to be conformal it must satisfy $df d\bar{f} = \Lambda(z, \bar{z})dzd\bar{z}$, which holds if $f = f(z)$ and $\bar{f} = \bar{f}(\bar{z})$, or alternatively if $f = f(\bar{z})$ and $\bar{f} = \bar{f}(z)$. It is conventional to take the former case, so that f and $\bar{f}$ are respectively holomorphic and anti-holomorphic. These functions form an infinite set of transformations. They are not necessarily invertible, and are therefore known as local conformal transformations. The transformations are generated by the operators

$$l_n = -z^{n+1}\partial_z \qquad \bar{l}_n = -\bar{z}^{n+1}\partial_{\bar{z}} \tag{1.3.3}$$

which form the elements of the Witt algebra

$$[l_n, l_m] = (n-m)l_{n+m} \quad \left[\bar{l}_n, \bar{l}_m\right] = (n-m)\bar{l}_{n+m} \quad \left[l_n, \bar{l}_m\right] = 0. \tag{1.3.4}$$

l_{-1}, l_0 and l_1 form a finite sub-algebra and generate the global conformal transformations corresponding to the transformations present in higher dimensions: l_{-1}, $l_0 + \bar{l}_0$, $l_0 - \bar{l}_0$ and l_1 respectively generate the translations, dilations, rotations and

special conformal translations.

In order to study conformally invariant field theories, the way fields transform under conformal transformations must be determined. Primary fields are of particular importance, and these transform as

$$\phi'(w,\bar{w}) = \left(\frac{dw}{dz}\right)^{-h}\left(\frac{d\bar{w}}{d\bar{z}}\right)^{-\bar{h}}\phi(z,\bar{z}) \tag{1.3.5}$$

under any conformal transformation $z \to w(z)$, $\bar{z} \to \bar{w}(\bar{z})$. h and $\bar{h}$ are the conformal and anti-conformal dimensions of the field and are defined via the scaling dimension Δ and spin s as

$$h = \tfrac{1}{2}(\Delta + s) \qquad \bar{h} = \tfrac{1}{2}(\Delta - s). \tag{1.3.6}$$

A field obeying (1.3.5) for some but not all conformal transformations is called quasi-primary. The energy-momentum tensor, the tensor made up of the conserved currents due to constant spacetime translations, is such a field. Returning briefly to d dimensions, the change of action under a general coordinate transformation $x^\mu \to x^\mu + \epsilon^\mu(\mathbf{x})$ is

$$\delta S = \int d^d x T^{\mu\nu}\partial_\mu \epsilon_\nu. \tag{1.3.7}$$

If rotational invariance is assumed then $T^{\mu\nu}$ is symmetric. (1.3.7) can then be written as

$$\delta S = \tfrac{1}{2}\int d^d x T^{\mu\nu}\left(\partial_\mu\epsilon_\nu + \partial_\nu\epsilon_\mu\right). \tag{1.3.8}$$

The bracketed part of this can be re-written using the fact that under an infinitesimal coordinate transformation, the metric transforms as $g_{\mu\nu} \to g_{\mu\nu} - (\partial_\mu\epsilon_\nu + \partial_\nu\epsilon_\mu)$. Requiring this to be a conformal transformation requires that $\partial_\mu\epsilon_\nu + \partial_\nu\epsilon_\mu = \alpha(x)g_{\mu\nu}$ with α some function of x, and taking the trace of both sides of this gives $\alpha(x) = 2\partial_\rho\epsilon^\rho/d$. So under a conformal transformation the change in the action is

$$\delta S = \frac{1}{d}\int d^d x T^\mu_\mu \partial_\nu \epsilon^\nu. \tag{1.3.9}$$

The trace of the energy-momentum tensor must therefore vanish in conformally invariant theories. For a two-dimensional conformal field theory in the $(z,\bar{z})$ coor-

dinates, the tracelessness and symmetry of $T_{\mu\nu}$ fix $T_{z\bar{z}} = T_{\bar{z}z} = 0$. The conservation of the energy-momentum tensor $\partial^\mu T_{\mu\nu} = 0$ then becomes

$$\partial_z T_{\bar{z}z} + \partial_{\bar{z}} T_{zz} = 0 \Rightarrow \partial_{\bar{z}} T_{zz} = 0 \tag{1.3.10}$$

$$\text{and} \qquad \partial_z T_{\bar{z}\bar{z}} + \partial_{\bar{z}} T_{z\bar{z}} = 0 \Rightarrow \partial_z \bar{T}_{\bar{z}\bar{z}} = 0 \tag{1.3.11}$$

and this leads to the natural definition $T_{zz} = T(z)$ and $T_{\bar{z}\bar{z}} = \bar{T}(\bar{z})$.

To study conformal symmetry in quantum field theory the behaviour of correlation functions must be considered. Under a conformal transformation $z \to w(z)$, $\bar{z} \to \bar{w}(\bar{z})$ the correlation functions of primary fields transform as

$$\langle \phi_1(w_1, \bar{w}_1)\phi_2(w_2, \bar{w}_2) \cdots \phi_n(w_n, \bar{w}_n)\rangle = \tag{1.3.12}$$
$$\prod_{i=1}^{n} \left(\frac{dw}{dz}\right)^{-h_i}_{w=w_i} \left(\frac{d\bar{w}}{d\bar{z}}\right)^{-\bar{h}_i}_{\bar{w}=\bar{w}_i} \langle \phi_1(z_1, \bar{z}_1)\phi_2(z_2, \bar{z}_2) \cdots \phi_n(z_n, \bar{z}_n)\rangle.$$

The form of the two-point and three-point correlation functions can then be fixed by considering the restrictions placed on (1.3.12) when $w(z)$ is one of the global conformal transformations, which leads to the conclusion

$$\langle \phi_1(z_1, \bar{z_1})\phi_2(z_2, \bar{z}_2)\rangle = \begin{cases} \frac{C_{12}}{(z_1 - z_2)^{2h}(\bar{z}_1 - \bar{z}_2)^{2\bar{h}}} & \text{if } h_1 = h_2 = h, \bar{h}_1 = \bar{h}_2 = \bar{h} \\ 0 & \text{otherwise} \end{cases} \tag{1.3.13}$$

$$\langle \phi_1(z_1, \bar{z}_1)\phi_2(z_2\bar{z}_2)\phi_3(z_3, \bar{z}_3)\rangle = \frac{C_{123}}{z_{12}^{h_1+h_2-h_3} z_{23}^{h_2+h_3-h_1} z_{13}^{h_3+h_1-h_2} \bar{z}_{12}^{\bar{h}_1+\bar{h}_2-\bar{h}_3} \bar{z}_{23}^{\bar{h}_2+\bar{h}_3-\bar{h}_1} \bar{z}_{13}^{\bar{h}_3+\bar{h}_1-\bar{h}_2}}. \tag{1.3.14}$$

where C_{12} and C_{123} are constants and $z_{ij} = z_i - z_j$. Information about correlation functions is often encoded using the operator product expansion (OPE). This expresses the product of two fields at points z and w respectively as an expansion in powers of $(z - w)$, the coefficients of which are fields which are non-singular at $z = w$. The product of fields, and hence the expansion, only has meaning when considered inside a correlation function; the presence in the expansion of negative powers of $(z - w)$ makes manifest the singular behaviour which generally appears

in correlation functions involving fields at the same position. OPEs simplify the task of evaluating the correlation functions of a theory since correlators of strings of operators can be reduced down to two point functions, the forms of which are known.

The OPEs involving the fields which arise from the energy-momentum tensor are of particular interest. The non-regular part of its correlation function with a string of primary fields is given by the Ward identity [14]

$$\langle T(z)\phi_1(z_1)\cdots\phi_n(z_n)\rangle = \sum_{i=1}^{n}\left\{\frac{h_i}{(z-z_i)^2}+\frac{1}{z-z_i}\frac{\partial}{\partial z_i}\right\}\langle\phi_1(z_1)\cdots\phi_n(z_n)\rangle \quad (1.3.15)$$

with a similar identity holding for $\bar{T}(\bar{z})$. The OPE of $T(z)$ with a single primary field of conformal dimensions $(h,\bar{h})$ is then

$$T(z)\phi(w,\bar{w}) = \frac{h}{(z-w)^2}\phi(w,\bar{w})+\frac{1}{z-w}\partial_w\phi(w,\bar{w})+ \text{ regular terms.} \quad (1.3.16)$$

The OPE of $T(z)$ with itself is

$$T(z)T(w) = \frac{c}{2(z-w)^4}+\frac{2T(w)}{(z-w)^2}+\frac{\partial_w T(w)}{z-w}+ \text{ regular terms} \quad (1.3.17)$$

so that

$$\langle T(z)T(0)\rangle = \frac{c}{2z^4}. \quad (1.3.18)$$

c is known as the central charge or the conformal anomaly, and its importance will be discussed later.

The fields inside a correlation function must be time-ordered. A particularly illuminating way to decide the time direction is radial quantisation. Starting from Minkowski space with real coordinates (x,t), the spatial direction x is compactified so that spacetime becomes a cylinder with the spatial direction running along the circumference of length L. This is then analytically continued into Euclidean space, so that the coordinates on the cylinder are defined to be $w = x+it$. The conformal map $z(w) = \exp(-2\pi wi/L)$ then maps this onto the complex plane, so that time is now measured by the radial distance from the origin, and at fixed time the distance

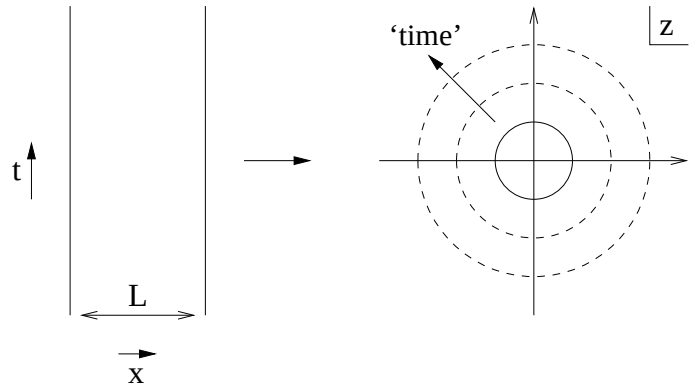

Figure 1.8: Radial quantisation: time flows in the radial direction.

x is measured by the distance around the circle of radius $\exp(2\pi t/L)$ centred on the origin. This is depicted in figure 1.8.

A field $\phi(z,\bar{z})$ with conformal dimension $(h,\bar{h})$ can now be expanded in modes as

$$\phi(z,\bar{z}) = \sum_{m\in\mathbb{Z}}\sum_{n\in\mathbb{Z}} z^{-m-h}\bar{z}^{-n-\bar{h}}\phi_{m,n}. \tag{1.3.19}$$

The energy-momentum fields $T(z)$ and $\bar{T}(\bar{z})$ have conformal dimensions $(2,0)$ and $(0,2)$ respectively and so

$$\begin{aligned} T(z) &= \sum_{n\in\mathbb{Z}} z^{-n-2}L_n \qquad \text{with} \qquad L_n = \frac{1}{2\pi i}\oint dz\, z^{n+1}T(z) \\ \text{and} \qquad \bar{T}(z) &= \sum_{n\in\mathbb{Z}} \bar{z}^{-n-2}\bar{L}_n \qquad \text{with} \qquad \bar{L}_n = -\frac{1}{2\pi i}\oint d\bar{z}\, \bar{z}^{n+1}\bar{T}(\bar{z}). \end{aligned} \tag{1.3.20}$$

The L_n and $\bar{L}_n$'s are the generators of conformal transformations on the Hilbert space of the quantum theory. The algebra they obey is called the Virasoro algebra and is derived using (1.3.17) and (1.3.20) to be

$$[L_n, L_m] = (n-m)L_{n+m} + \frac{c}{12}n(n^2-1)\delta_{n+m,0} \tag{1.3.21}$$

$$\left[\bar{L}_n, \bar{L}_m\right] = (n-m)\bar{L}_{n+m} + \frac{c}{12}n(n^2-1)\delta_{n+m,0} \tag{1.3.22}$$

$$\left[L_n, \bar{L}_m\right] = 0. \tag{1.3.23}$$

As in the Witt algebra, the global conformal transformations are generated by L_{-1},

L_0 and L_1 and as before, dilations are generated by $L_0 + \bar{L}_0$. In the complex plane, the effect of a dilation by a factor α is $z \to \alpha z$, which scales the radial distance and so corresponds to a time translation. It is therefore natural to associate $L_0 + \bar{L}_0$ with the Hamiltonian. The quantum states making up the Hilbert space are eigenstates of this Hamiltonian. It is natural to assume the existence of a vacuum state $|0\rangle$ which is invariant under the global conformal transformations, and hence annihilated by L_{-1}, L_0, L_1, $\bar{L}_{-1}$, $\bar{L}_0$ and $\bar{L}_1$. In fact, assuming $T(z)|0\rangle$ and $\bar{T}(\bar{z})|0\rangle$ are well-defined as $z, \bar{z} \to 0$, the definitions of the conformal generators imply that

$$L_n|0\rangle = 0 \qquad \text{and} \qquad \bar{L}_n|0\rangle = 0 \quad \forall\, n \geq -1. \tag{1.3.24}$$

Other states are created by acting with fields (now viewed as operators) on the vacuum state. In terms of 'in' and 'out' states, corresponding to $t = -\infty$ and $t = +\infty$ respectively, the in states are viewed as being those created by fields at $z = 0$, $\bar{z} = 0$ acting on the vacuum state, $|\phi_{in}\rangle = \lim_{z,\bar{z}\to 0} \phi(z, \bar{z})|0\rangle$. The out state is the hermitian conjugate of this, where conjugation is defined as $\phi^\dagger(z, \bar{z}) = z^{-2h}\bar{z}^{-2\bar{h}}\phi(\frac{1}{\bar{z}}, \frac{1}{z})$ with $\phi(z, \bar{z})$ assumed to be quasi-primary. This leads to the out state being defined as $\langle\phi_{out}| = \langle 0| \lim_{w,\bar{w}\to\infty} w^{2h}\bar{w}^{2\bar{h}}\phi(w, \bar{w})$.

Let ϕ now be a primary field of conformal dimensions $(h, \bar{h})$ and define the in state it creates as

$$|h, \bar{h}\rangle = \phi(0, 0)|0\rangle. \tag{1.3.25}$$

Then from the definition of the conformal generators and the OPE of the energy-momentum fields with a primary field,

$$L_0|h, \bar{h}\rangle = h|h, \bar{h}\rangle \qquad \text{and} \qquad \bar{L}_0|h, \bar{h}\rangle = \bar{h}|h, \bar{h}\rangle \tag{1.3.26}$$

making $|h, \bar{h}\rangle$ an eigenstate of the Hamiltonian. In addition,

$$L_n|h, \bar{h}\rangle = 0 \qquad \text{and} \qquad \bar{L}_n|h, \bar{h}\rangle = 0 \qquad \text{for} \qquad n > 0. \tag{1.3.27}$$

Using the Virasoro relations,

$$L_0(L_n|h,\bar{h}\rangle) = (h-n)L_n|h,\bar{h}\rangle. \tag{1.3.28}$$

So, since acting with L_0 produces the conformal dimension of a state, the operators L_{-n} for $n > 0$ act as raising operators, creating excited states. The general form of an excited state is then given by $L_{-m_1}L_{-m_2}\cdots L_{-m_n}|h,\bar{h}\rangle$ with $m_n \geq m_{n-1} \geq \cdots \geq m_1 \geq 1$. These states are called descendants of $|h,\bar{h}\rangle$. Such a state has eigenvalue $h + m_1 + m_2 + \cdots + m_n$ of L_0, and the number $N = m_1 + m_2 + \cdots + m_n$ is defined as the level of the descendant. $|h,\bar{h}\rangle$ and its descendants form a closed subset of the Hilbert space with respect to the Virasoro generators, which means they form a representation of the Virasoro algebra. This is called a Verma module.

Excited states can also be thought of as descendant fields acting on the vacuum state. If the descendant field is defined as

$$\phi^{-n}(z) = (L_{-n}\phi)(z) = \frac{1}{2\pi i}\oint_z dw \frac{1}{(w-z)^{n-1}} T(w)\phi(z) \tag{1.3.29}$$

then

$$L_{-n}|h,\bar{h}\rangle = \phi^{-n}(0)|0\rangle. \tag{1.3.30}$$

A primary field ϕ and its descendants make up a conformal family $[\phi]$. The operator product expansion of two fields contains in its general form fields arising from all conformal families. However, not all of these will actually appear; the information about which conformal families can occur in an OPE is encoded in the fusion rules

$$\phi_a \times \phi_b = \sum_k N_{ab}^c \phi_c \tag{1.3.31}$$

where ϕ_i denotes a primary field and all members of its conformal family, and the fusion coefficients N_{ab}^c are non-negative integers.

In general the field-content of a theory is made up of an infinite set of conformal families. However, this set can be restricted by the presence of null fields $\chi(z)$. Null fields arise from states $|\chi\rangle$ which are linear combinations of descendant states but which themselves satisfy $L_n|\chi\rangle = 0 \;\forall\; n > 0$ so that they act as a highest-weight

state of a sub-module of the Verma module of which they are part, thus making the representation reducible. They are orthogonal to all states in the original Verma module, including themselves, and hence have zero norm. These properties mean that no information is lost by setting $|\chi\rangle = 0$, and doing so makes the representation irreducible. From the field viewpoint, the analogue of the orthogonality property is the vanishing of the correlation function of the null field with any other string of fields. A null field is a descendant field; using (1.3.29) and the Ward identity (1.3.15), a correlation function involving a descendant field can be rewritten in terms of differential operators acting on the correlation function involving the corresponding primary field. Therefore, a correlation function involving a primary field whose conformal family includes a null field will satisfy a partial differential equation (PDE). These PDEs impose constraints which have the effect of truncating the operator algebra. For certain values of the conformal dimension h there exists an infinite number of null fields and the effect of the truncation is that the number of conformal families becomes finite. Such theories are called the minimal models and are labelled by positive coprime integers p and p' and denoted $M(p,p')$. In terms of these labels the central charge is

$$c = 1 - \frac{6(p-p')^2}{pp'}, \tag{1.3.32}$$

so that $c < 1$, and the conformal dimensions of the primary fields are

$$h = h_{r,s} = \frac{(pr - p's)^2 - (p-p')^2}{4pp'}, \quad 1 \leq r < p' \quad \text{and} \quad 1 \leq s < p. \tag{1.3.33}$$

The above has the symmetry $h_{r,s} = h_{p'-r,p-s}$ and so the corresponding primary fields satisfy $\phi_{(r,s)} = \phi_{(p'-r,p-s)}$ meaning that there are $(p-1)(p'-1)/2$ distinct primary fields, and hence conformal families, in the theory. The possible conformal weights are often tabulated, forming the entries of the so-called Kac table.

Amongst these theories are the unitary minimal models, the representations of which contain no states of negative norm. Using the Virasoro algebra the norm of

a basic descendant state is

$$\langle h|L_n L_{-n}|h\rangle = \left(2nh + \frac{c}{12}n(n^2-1)\right)\langle h|h\rangle \tag{1.3.34}$$

and so a unitary theory must have $2nh + \frac{c}{12}n(n^2-1) \geq 0$ for all $n \geq 0$. c must be non-negative, otherwise the condition is not satisfied for large enough n. In addition, the condition for $n = 1$ requires that $h \geq 0$, so that the primary fields of a unitary model must have non-negative conformal dimension. Finding unitary minimal models therefore amounts to considering which values of p and p' make (1.3.33) non-negative, and in particular this must hold when $(pr - p's)^2$ takes its smallest possible value. The restrictions on r and s mean that $pr - p's$ can never equal zero. However, since p and p' are coprime there exist $1 \leq \rho < p'$ and $1 \leq \sigma < p$ such that $p\rho - p'\sigma = 1$. So the smallest possible value taken by the conformal dimension is $h = (1-(p-p')^2)/4pp'$, which is only non-negative if $|p-p'|=1$. The unitary minimal model with $(p,p') = (m+1,m)$ is denoted $\mathcal{M}_m$, and for the $c \geq 0$ unitarity condition to also be satisfied and the model to be non-trivial m must be greater than or equal to three.

The partition function for the minimal models can be written in a particularly simple form. This can be seen by considering a conformal field theory on a torus. For a torus with modular parameter τ, defined in the complex plane as having vertices $(0, 1, \tau, 1+\tau)$ with opposite edges identified, the partition function can be expressed in terms of the Hamiltonian and momentum operators that arise in radial quantisation. This is possible because radial quantisation corresponds to a theory defined on a cylinder, from which a torus can be created by sewing together the ends. It was seen earlier that time translations are generated by the dilation operator $L_0 + \bar{L}_0$, and in fact the Hamiltonian is $H = 2\pi(L_0 + \bar{L}_0) - \pi c/6$. Spatial translations correspond to rotations centred on the origin, and therefore the momentum operator is proportional to $L_0 - \bar{L}_0$, in fact $P = 2\pi(L_0 - \bar{L}_0)$. The torus partition function is

$$Z(\tau,\bar{\tau}) = \mathrm{Tr} e^{-\mathrm{Im}\tau H + i\mathrm{Re}\tau P} \tag{1.3.35}$$

which on defining $q = \exp(2\pi i\tau)$ becomes

$$Z(\tau, \bar{\tau}) = \mathrm{Tr}\, q^{L_0 - c/24} \bar{q}^{\bar{L}_0 - c/24}. \tag{1.3.36}$$

The Hilbert space for the theory is defined as

$$\mathcal{H} = \bigoplus_{h,\bar{h}} n_{h,\bar{h}} V_h \otimes \bar{V}_{\bar{h}} \tag{1.3.37}$$

where V_h and $\bar{V}_{\bar{h}}$ are the Verma modules arising from the action of the holomorphic and anti-holomorphic generators respectively on a state corresponding to a primary field of dimensions $(h, \bar{h})$. The $n_{h,\bar{h}}$ are non-negative integers determining which Verma modules appear in the Hilbert space. In view of this decomposition of the Hilbert space, the partition function can be rewritten as

$$Z(\tau, \bar{\tau}) = \sum_{h,\bar{h}} n_{h,\bar{h}} \chi_h(q) \chi_{\bar{h}}(\bar{q}), \tag{1.3.38}$$

where χ, known as the character of a Verma module, encodes the degeneracy $d_h(N)$ at each level of a conformal family and is defined as

$$\chi_h(q) = \sum_N d_h(N) q^{h+N-c/24}. \tag{1.3.39}$$

A torus with modular parameter τ is invariant under the action of the maps $S : \tau \to -1/\tau$ and $T : \tau \to \tau + 1$. The partition function of a theory on the torus should therefore be invariant under these transformations, and this constrains which representations contribute to the partition function. In particular, invariance under $S(\tau)$ restricts the values that can be taken by the $n_{h,\bar{h}}$. Under this transformation the characters χ and $\bar{\chi}$ obey

$$\chi_h\left(e^{-2\pi i/\tau}\right) = \sum_{h'} S_h^{h'} \chi_{h'}\left(e^{2\pi i\tau}\right) \tag{1.3.40}$$

with the matrix S determined by the model in question. For a minimal model

$M(p,p')$, the element of S for $h = h_{a,b}$ and $h' = h_{c,d}$ is

$$S_h^{h'} = 2\sqrt{\frac{2}{pp'}}(-1)^{1+bc+ad}\sin\left(\frac{\pi acp}{p'}\right)\sin\left(\frac{\pi bdp'}{p}\right). \tag{1.3.41}$$

This matrix is symmetric and orthogonal. Its orthogonality means that it preserves the inner product of vectors, and hence the partition function

$$Z(\tau,\bar{\tau}) = \sum_{h,\bar{h}} \chi_h(q)\chi_h(\bar{q}) \tag{1.3.42}$$

is invariant under S, defining $n_{h,\bar{h}} = \delta_{h,\bar{h}}$. The modular transformation T demands that $h - \bar{h} \in \mathbb{Z}$ and this is clearly satisfied here. A partition function of the above form is therefore known as a diagonal modular invariant.

Some of the minimal models describe the statistical models already discussed. The simplest unitary minimal model is $M(4,3) = \mathcal{M}_3$. This has three distinct primary fields, with conformal dimensions $h_{1,1} = 0$, $h_{1,2} = 1/16$ and $h_{1,3} = 1/2$, and central charge $c = 1/2$. This matches the operator content of the critical two-dimensional Ising model, which consists of the identity operator of dimensions $(0,0)$ and two local scaling operators, σ of dimensions $(1/16, 1/16)$ and ϵ of dimensions $(1/2, 1/2)$. σ and ϵ are continuum versions of the terms appearing in the lattice Hamiltonian, with σ corresponding to σ_i and ϵ to the nearest-neighbour term $\sigma_i\sigma_j$. A similar correspondence between primary fields and operators exists between the next minimal model in the series, $M(5,4) = \mathcal{M}_4$ with central charge $c = 7/10$, and the tricritical Ising model.

Chapter 2

Integrability Away From Criticality

2.1 Perturbed Conformal Field Theory

The tools described in the previous two sections can now be used to consider two-dimensional field theories away from the renormalisation group fixed point described by a conformal field theory. This can be achieved by considering a perturbed conformal field theory (PCFT), where the original CFT is perturbed in a relevant direction with the respect to the fixed point it describes. It is then possible to consider the renormalisation group flow of such a theory. This section will consist of a review of Alexander Zamolodchikov's work on this subject [15] (see also [10]).

The construction of the perturbed theory means that the original CFT is the UV limit of the resulting field theory, and as such governs the structure its field content. The action of the field theory is described by the perturbation of the original conformal field theory by one of its relevant fields. A field with conformal dimensions $(h, \bar{h})$ is relevant if its scaling dimension $\Delta = h + \bar{h}$ satisfies $\Delta < 2$. A spinless field is chosen so that the theory is rotation invariant, and so $h = \bar{h}$ and the field is relevant if $h < 1$. The focus will be on unitary theories; these have $h \geq 0$ meaning that all such fields are primary. The perturbation of the action by such a

relevant, spinless, primary field ϕ is then given as

$$S_{PCFT} = S_{CFT} + \lambda \int \phi(x)\, d^2x. \tag{2.1.1}$$

λ is a coupling constant which indicates the distance of the perturbation away from the fixed point and is taken to be zero at the fixed point itself. It must have dimension $(\text{mass})^{2-2h}$ for the action to be dimensionless.

An important property to maintain as the theory is perturbed away from the fixed point is that of integrability (it will be seen in section 2.2 that in the case of massive field theory this leads to simple scattering behaviour). A theory is integrable if it has an infinite number of commuting conserved charges which arise as integrals of conserved densities. In a CFT, the energy momentum tensor is such a conserved density since

$$\partial_{\bar{z}} T = 0. \tag{2.1.2}$$

The associated charge is then

$$Q_1 = \oint \frac{T(z)}{z^n} dz \qquad n \in \mathbb{Z}. \tag{2.1.3}$$

Since T is holomorphic, this integral is equal to $2\pi i\, \partial_z^{n-1} T(z)/(n-1)!$ and this result is independent of the choice of closed contour. In particular, if the contour is chosen to be a circle centred on the origin then the value of the integral is independent of the radius of the circle. In radial quantisation, a circle centred on the origin represents a particular time slice, and therefore Q_1 is a conserved charge. $T(z)$ is a conformal descendant of the identity operator since by (1.3.29)

$$(L_{-2}\mathbb{I})(z) = \frac{1}{2\pi i} \oint_z dw \frac{1}{(w-z)} T(w) = T(z). \tag{2.1.4}$$

Further conserved charges arise from considering other descendants of the identity operator. The action of a Virasoro operator L_{-n} with $n \geq 2$ is

$$(L_{-n}\mathbb{I})(z) = \frac{1}{2\pi i} \oint_z dw \frac{1}{(w-z)^{n-1}} T(w) = \frac{1}{(n-2)!} \partial_z^{n-2} T(z). \tag{2.1.5}$$

and a general descendant of the form $(L_{-k_1}L_{-k_2}\cdots L_{-k_n}\mathbb{I})(z)$, $k_i \geq 1$ is a combination of powers of $T(z)$ and its derivatives. The set of such fields is not linearly independent because fields such as (2.1.5) are total derivatives, and therefore since L_{-1} acts as $\frac{\partial}{\partial z}$ they also emerge as a field of the form

$$\alpha(L_{-1}L_{-l_1}L_{-l_2}\cdots L_{-l_m}\mathbb{I})(z). \tag{2.1.6}$$

with α some multiplicative factor. In order to restrict to a linearly independent set, only fields made up of elements of the form

$$(L_{-k_1}L_{-k_2}\cdots L_{-k_n}\mathbb{I})(z) \qquad k_1 \geq 2,\ k_i \geq 1 \text{ for } i \neq 1 \tag{2.1.7}$$

are considered. The space of such fields is labelled as Ω, and decomposes into spaces of fields at each level as $\Omega = \bigoplus_{s=0}^{\infty} \Omega_s$. Since the identity field has conformal dimensions $(0,0)$, a descendant at level N has dimensions $(N,0)$, and (1.3.6) implies that N is equal to the spin of the field. The descendants described above can therefore be denoted by $T_s^{(a)}$, where s is the spin, and a distinguishes between the various descendants at a particular level. Their relation to $T(z)$ means that the $T_s^{(a)}$ are all holomorphic, satisfying

$$\partial_{\bar{z}} T_s^{(a)} = 0, \tag{2.1.8}$$

and can be integrated to give an infinite set of conserved charges

$$Q_{s,n}^{(a)} = \oint \frac{T_s^{(a)}}{z^n} dz \qquad n \in \mathbb{Z}. \tag{2.1.9}$$

In order for the perturbed theory to be integrable, at least some of these conserved charges must survive away from the fixed point described by the CFT. The $T_s^{(a)}$ are no longer conserved in the perturbed theory and the former conservation equations become

$$\partial_{\bar{z}} T_s^{(a)} = \lambda R_{s-1}^{(a,1)} + \cdots + \lambda^n R_{s-1}^{(a,n)} \tag{2.1.10}$$

where the $R_{s-1}^{(a,n)}$ are local fields in the perturbed theory. The left hand side has dimensions $(s,1)$ and λ has dimensions $(1-h, 1-h)$ for perturbing field ϕ of di-

mensions (h, h) (these left and right dimensions have the same relation to spin and scaling dimension as the conformal dimensions did in the CFT), so $R^{(a,n)}_{s-1}$ must have dimensions $(s - n(1-h), 1 - n(1-h))$. This indicates that for $s > 1$ $R^{(a,n)}_{s-1}$ is the perturbed theory version of a descendant of a relevant primary field of dimensions $(1-n(1-h), 1-n(1-h))$. Since $h < 1$ due to ϕ being relevant, $n(1-h) > 1$ for large enough n and the right dimension of $R^{(a,n)}_{s-1}$ becomes negative. However, since it is a unitary CFT that is being perturbed, no fields can have negative dimensions and so the right hand side of (2.1.10) involves a finite number of terms. Furthermore, $n > 1$ implies that $1 - n(1-h) < h$, so assuming that ϕ is the most relevant field (the field of smallest dimension bar the identity) then $1 - n(1-h)$ must equal zero. So for an $n > 1$ term to exist in (2.1.10) h must have the form

$$h = 1 - \frac{1}{n} \tag{2.1.11}$$

and $R^{(a,n)}_{s-1}$ is a level $s-1$ descendant of the identity field. For the $n = 1$ term, $R^{(a,1)}_{s-1}$ has dimensions $(s - 1 + h, h)$ making it a level $s - 1$ descendant of ϕ. The space of such fields, along with its decomposition into spaces at each level, is denoted by $\Phi = \bigoplus_{s=0}^{\infty} \Phi_s$.

Assuming first that (2.1.11) is not satisfied and only the $n = 1$ term appears in (2.1.10), then

$$\partial_{\bar{z}} T^{(a)}_s = \lambda R^{(a,1)}_{s-1}. \tag{2.1.12}$$

Zamolodchikov [15] defined operators D_n, $n \in \mathbb{Z}$ which define the action of $\partial_{\bar{z}}$ on the $T^{(a)}_s(z, \bar{z})$ in the perturbed theory. These operators act on elements of Ω as

$$D_n T^{(a)}_s(z, \bar{z}) = \frac{1}{2\pi i} \oint_z \phi(w, \bar{z})(w - z)^n T^{(a)}_s dw \tag{2.1.13}$$

and have the following properties

$$\partial_{\bar{z}} = -\lambda D_0, \tag{2.1.14}$$

$$D_{-n-1}\mathbb{I} = \frac{1}{n!} L^n_{-1}\phi(z, \bar{z}) = \frac{1}{n!}\partial^n_z \phi(z, \bar{z}) \qquad \text{and} \tag{2.1.15}$$

$$[L_n, D_m] = -((1-h)(n+1) + m) D_{n+m}. \tag{2.1.16}$$

Then, for example,

$$\partial_{\bar{z}} T(z,\bar{z}) = -\lambda D_0 L_{-2}\mathbb{I} = \lambda(1-h)D_{-2}\mathbb{I} = \lambda(1-h)\partial_z\phi(z,\bar{z}). \tag{2.1.17}$$

Identifying $\lambda(h-1)\phi(z,\bar{z})$ with $T_{\bar{z}z} = -\Theta$, this is the conservation equation for the energy-momentum tensor in the perturbed theory (cf 1.3.11))

$$\partial_{\bar{z}} T = \partial_z \Theta. \tag{2.1.18}$$

Considering the one-form

$$\alpha = T dz + \Theta d\bar{z}, \tag{2.1.19}$$

$d\alpha = 0$ by the continuity equation and so α is a closed form. An integral of α between two points is therefore independent of the particular contour chosen, so that an integral over a closed contour is equal to zero. In particular this means that integrals over circular contours around the origin

$$\oint T dz + \Theta d\bar{z} \tag{2.1.20}$$

are always equal to zero, making such integrals conserved charges in radial quantisation.

So one conserved quantity has been found for the perturbed theory, but since the energy-momentum tensor is expected to be conserved in any field theory the real question is whether there are other conserved quantities. The D_n algebra demonstrates that not all the derivatives $\partial_{\bar{z}} T_s^{(a)}(z,\bar{z})$ can be expressed as total derivatives with respect to z. However, Zamolodchikov showed that the existence of some conserved quantities can be determined by counting the dimensions of the spaces Ω_s and Φ_s [15]. The properties of (2.1.12) already discussed mean that $\partial_{\bar{z}}$ maps from Ω_s to Φ_{s-1}. Define $\hat{\Phi}_s$ to be the space of those fields in Φ_s which are not total ∂_z derivatives, and Π_s to be the projection operation from Φ_s onto $\hat{\Phi}_s$. Then if

$$\Pi_{s-1}\partial_{\bar{z}} T_s = 0, \tag{2.1.21}$$

$\partial_{\bar{z}} T_s$ can only equal one of the total ∂_z derivative fields in Φ_{s-1}. A conservation equation of the form

$$\partial_{\bar{z}} T_s = \partial_z \Theta_{s-2}, \qquad \Theta_{s-2} \in \Phi_{s-2} \tag{2.1.22}$$

therefore exists if the linear map $\Pi_{s-1}\partial_{\bar{z}}$ has a kernel of non-zero dimension. Zamolodchikov's counting argument, which identifies when such a kernel occurs, relies on the property that a linear map $A : X \to Y$ satisfies the equation

$$\dim(\ker A) + \dim(\mathrm{im} A) = \dim(X). \tag{2.1.23}$$

This means that $\ker(\Pi_{s-1}\partial_{\bar{z}})$ has non-zero dimension if $\dim(\Omega_s) > \dim(\mathrm{im}(\Pi_{s-1}\partial_{\bar{z}}))$. This is certainly true if $\dim(\Omega_s) > \dim(\hat{\Phi}_{s-1})$, and this requirement is the key element of Zamolodchikov's counting argument.

Zamolodchikov noted that if ϕ lives in a Virasoro representation which includes null fields, then the null field equations can provide the extra relations between descendent fields necessary for conservation equations to exist. Null fields occur when a primary field has dimension

$$h_{r,s} = \frac{1}{24}(c-1) + \frac{1}{4}(r\alpha_+ + s\alpha_-)^2 \tag{2.1.24}$$

where

$$\alpha_\pm = \frac{\sqrt{1-c} \pm \sqrt{25-c}}{\sqrt{24}}. \tag{2.1.25}$$

This dimension is real for $c < 1$. $\phi_{(1,3)}$, i.e. the field with dimension $h_{1,3}$, is a relevant field in this regime, and so $\phi = \phi_{(1,3)}$ is a natural example to consider. This satisfies the null field equation

$$\left(L_{-3} - \frac{2}{h+2} L_{-1}L_{-2} + \frac{1}{(h+1)(h+2)} L_{-1}^3\right) \phi_{(1,3)} = 0. \tag{2.1.26}$$

Consider $T_4(z,\bar{z}) = (L_{-2}L_{-2}\mathbb{I})(z,\bar{z})$. Using the D_n operators this satisfies

$$\partial_{\bar{z}} T_4 = \lambda(1-h)\left(2L_{-2}L_{-1} + \frac{h-3}{6} L_{-1}^3\right)\phi. \tag{2.1.27}$$

Using the null field equation and the Virasoro algebra this can be expressed as

$$\partial_{\bar{z}} T_4 = \lambda \left(\frac{1-h}{h+2} \right) \partial_z \left(2hL_{-2} + \frac{(h-2)(h-1)(h+3)}{6(h+1)} L_{-1}^2 \right) \phi_{(1,3)} \tag{2.1.28}$$

which is a conservation equation. From the counting argument viewpoint, this arose because $\dim(\Omega_4) = 1$ (since T_4 is its only linearly independent field) and $\dim(\hat{\Phi}_3) = 0$ (due to the null field equation). Hence $\Pi_{s-1}\partial_{\bar{z}}$ has a kernel of non-zero dimension. It has been seen above that conservation equations exist for a theory with perturbing field $\phi_{(1,3)}$ for T_2 and T_4, and Zamolodchikov used the counting argument to show that such equations also exist for T_6 and T_8 and therefore conjectured that the T_s for all even, positive values of s give rise to conserved quantities

$$\oint T_s dz + \Theta_{s-2} d\bar{z}. \tag{2.1.29}$$

As was discussed earlier, the minimal models are special cases of theories involving null fields. However, one has to be careful when applying the above assumptions to the minimal models. This is because the central charge c is rational in these models, and so there is the possibility of (2.1.11) being satisfied meaning that an extra term of the form $\lambda^n R_{s-1}^{(a,n)}$ (which will be a level $s-1$ descendent of the identity field) must be added to (2.1.12). For a unitary minimal model $\mathcal{M}_m$, $\phi_{(1,3)}$ has dimension $h_{1,3} = 1 - \frac{2}{m+1}$, which has the form of (2.1.11) for odd values of m. The dimension of Ω_r for $r = 1$, 3 ,5 and 7 is zero meaning that $R_{s-1}^{(a,n)}$ must be a total ∂_z derivative for $s - 1 = 1$, 3, 5 and 7 and so conservation equations for T_2, T_4, T_6 and T_8 still exist. Zamolodchikov conjectured that this is in fact true for T_s for all even s.

2.1.1 The c-theorem

In order to study the RG flow of perturbed CFTs, Zamolodchikov defined the c-function [16], which encodes the position of a theory along the RG flow from a fixed point. His c-theorem states that a renormalisable theory with couplings $\{\lambda_j\}$ and positive-definite Hermitian product possesses a function $C(\{\lambda_j\})$ of the RG couplings, which is

i) non-increasing along the direction of the RG flows

ii) stationary only at fixed points

iii) equal at a fixed point to the central charge of the theory describing the fixed point.

The proof of this [5,10,12,16] uses the energy-momentum tensor $T_{\mu\nu}$. As before, the components of the energy-momentum tensor are labelled as

$$T_{zz} = T \quad T_{\bar{z}\bar{z}} = \bar{T} \quad T_{z\bar{z}} = T_{\bar{z}z} = -\Theta. \tag{2.1.30}$$

The conservation of the energy-momentum tensor, $\partial^\mu T_{\mu\nu} = 0$ then implies that

$$\partial_{\bar{z}} T - \partial_z \Theta = 0 \quad \text{and} \tag{2.1.31}$$

$$\partial_z \bar{T} - \partial_{\bar{z}} \Theta = 0. \tag{2.1.32}$$

The two-point functions for these components have the form

$$\langle T(z,\bar{z})T(0,0)\rangle = \frac{F(z\bar{z})}{z^4} \tag{2.1.33}$$

$$\langle \Theta(z,\bar{z})T(0,0)\rangle = \langle T(z,\bar{z})\Theta(0,0)\rangle = \frac{G(z\bar{z})}{z^3\bar{z}} \tag{2.1.34}$$

$$\langle \Theta(z,\bar{z})\Theta(0,0)\rangle = \frac{H(z\bar{z})}{z^2\bar{z}^2} \tag{2.1.35}$$

Taking the correlation function of (2.1.31) with $T(0,0)$ and with $\Theta(0,0)$ gives

$$z\bar{z}F'(z\bar{z}) - z\bar{z}G'(z\bar{z}) + 3G(z\bar{z}) = 0 \quad \text{and} \tag{2.1.36}$$

$$z\bar{z}G'(z\bar{z}) - G(z\bar{z}) - z\bar{z}H'(z\bar{z}) + 2H(z\bar{z}) = 0. \tag{2.1.37}$$

Eliminating G from this leads to

$$z\bar{z}F'(z\bar{z}) + 2z\bar{z}G'(z\bar{z}) - 3z\bar{z}H'(z\bar{z}) + 6H = 0 \tag{2.1.38}$$

so defining

$$C = 2F + 4G - 6H \tag{2.1.39}$$

gives

$$z\bar{z}C'(z\bar{z}) = -12H(z\bar{z}). \tag{2.1.40}$$

By positivity $H \geq 0$, so $C'(z\bar{z}) \leq 0$. Therefore, C is a non-increasing function of $R = \sqrt{z\bar{z}}$, at some fixed values of the RG couplings $\{\lambda_j\}$. Since C is dimensionless, this is equivalent to it being non-increasing along the RG trajectory at fixed R. Therefore, defining $C(\{\lambda_j\}) \equiv C(1, \{\lambda_j\})$ gives a quantity that is a function of the RG couplings that is non-increasing along the RG trajectories. Furthermore, C is stationary only at fixed points, since this only occurs when H and therefore Θ are equal to zero. Finally, at a fixed point $H = G = 0$ and $F = c/2$ by (1.3.18), so the definition of C (2.1.39) implies that $C = c$. So $C(\{\lambda_j\})$ satisfies all the requirements of Zamolodchikov's theorem.

Zamolodchikov analysed the c-function for the perturbation of a unitary minimal model $\mathcal{M}_m$ by the relevant operator $\phi_{(1,3)}$

$$S_{pert} = S_{\mathcal{M}_m} + \lambda \int \phi_{(1,3)}(x) d^2x, \tag{2.1.41}$$

with $\lambda > 0$. For $m \gg 1$, the IR limit of the RG flow was found to be another fixed point, with c-function value $c_{IR} = 1 - \frac{6}{m(m-1)}$, equal to that of the minimal model $\mathcal{M}_{m-1}$. It was shown in [17] that the only unitary CFTs with $c < 1$ are the unitary minimal models. So, at least for $m \gg 1$, the IR fixed point of the RG flow from $\mathcal{M}_m$ can be identified with $\mathcal{M}_{m-1}$. Zamolodchikov also showed that in the IR limit, the perturbing operator becomes $\phi^{(m-1)}_{(3,1)}$. This has the dimension $1 + 2/(m-1)$ and so is an irrelevant operator, explaining the flow into $\mathcal{M}_{m-1}$. The field theory which describes this interpolating flow between $\mathcal{M}_m$ and $\mathcal{M}_{m-1}$ is denoted by $\mathcal{M}A^{(+)}_m$. Although Alexander Zamolodchikov's proof was given for $m \gg 1$, evidence that such flows exist for all $m > 3$ emerges when Alexei Zamolodchikov's thermodynamic Bethe ansatz approach is applied to the $\mathcal{M}A^{(+)}_m$ theories [18], and this will be discussed further in section 2.3.

2.2 The S-matrix

The previous section demonstrated how a theory that lies on a renormalisation group flow in a relevant direction away from a fixed point can be considered as a perturbation of that fixed point. However, to fully define a theory in this manner is very complicated as quantities are expressed as sums of an infinite number of terms. An alternative description of such theories can be found by recalling the fact that in a flow between UV and IR fixed points, each point in the flow except the UV fixed point itself is controlled by the IR fixed point, as was described in section 1.2. If this IR fixed point is non-critical then this means that the theory can be described by a massive field theory. Moving from Euclidean space to Minkowski space, the asymptotic states of the theory can be interpreted as collections of particles whose scattering is described by the S-matrix [19–22].

The S-matrix S is a unitary matrix which given a basis of asymptotic states $|in\rangle$ for $t \to -\infty$ and $|out\rangle$ for $t \to \infty$ maps between the in-basis and the out-basis:

$$|in\rangle = S|out\rangle. \tag{2.2.1}$$

Combined with the unitarity of the matrix, this allows the scattering amplitude between an initial state expressed via the in-basis and a final state expressed via the out-basis to be given entirely in terms of the in-basis or the out-basis:

$$\begin{aligned} Amplitude = \langle final, out|initial, in\rangle &= \langle final, in|S|initial, in\rangle \\ &= \langle final, out|S|initial, out\rangle. \end{aligned} \tag{2.2.2}$$

The existence of conserved charges has several important consequences in the scattering theory. Before investigating this further, some notation must be established. Working in light-cone coordinates, the momentum of a particle of mass m is

$$(p, \bar{p}) = (p^0 + p^1, p^0 - p^1) \tag{2.2.3}$$

so that when the particle is on-shell $p\bar{p} = m^2$. p and $\bar{p}$ can be expressed in terms of

the rapidity θ of the particle as

$$p = me^{\theta} \qquad \bar{p} = me^{-\theta}. \tag{2.2.4}$$

Multi-particle asymptotic states are distinguished by the types a_i and rapidities θ_i of the particles involved. An n-particle state is written as

$$|A_{a_1}(\theta_1)A_{a_2}(\theta_2)\cdots A_{a_n}(\theta_n)\rangle_{\substack{in\\out}}. \tag{2.2.5}$$

Physically, since an in-state is defined as having no further interactions for $t \to -\infty$ the particle with the greatest rapidity must be the left-most particle, and that with the smallest rapidity must be right-most. The opposite is true for out-states, which have no further interactions for $t \to \infty$. This can be represented by taking the $A_{a_i}(\theta)$ symbols outside the bra-ket notation and requiring that they do not commute. The in- and out-states are then represented by

$$\text{in:} \quad A_{a_1}(\theta_1)A_{a_2}(\theta_2)\cdots A_{a_n}(\theta_m) \quad \theta_1 > \theta_2 > \cdots > \theta_m \tag{2.2.6}$$

$$\text{out:} \quad A_{b_1}(\theta'_1)A_{b_2}(\theta'_2)\cdots A_{b_n}(\theta'_n) \quad \theta'_1 < \theta'_2 < \cdots < \theta'_n \tag{2.2.7}$$

so that the position of the $A_{a_i}(\theta)$'s represents the physical position of the particle. The action of the S-matrix is then

$$A_{a_1}(\theta_1)A_{a_2}(\theta_2)\cdots A_{a_m}(\theta_m) = \sum_{n=m}^{\infty} \sum_{\theta'_1<\cdots<\theta'_n} S^{b_1\cdots b_n}_{a_1\cdots a_m}(\theta_1,\cdots,\theta_m;\theta'_1,\cdots,\theta'_n)\, A_{b_1}(\theta'_1)A_{b_2}(\theta'_2)\cdots A_{b_n}(\theta'_n) \tag{2.2.8}$$

with $\theta_1 > \theta_2 > \cdots > \theta_m$.

The energy-momentum operator acts on states as

$$P|A_a(\theta)\rangle = m_a e^{\theta}|A_a(\theta)\rangle \quad \text{and} \quad \bar{P}|A_a(\theta)\rangle = m_a e^{-\theta}|A_a(\theta)\rangle. \tag{2.2.9}$$

If the theory contains additional conserved quantities then these are taken to cor-

respond to operators Q_s which are assumed to be simultaneously diagonalised with respect to the basis of asymptotic states. These operators are then defined to act on asymptotic states as

$$Q_s|A_a(\theta)\rangle = q_a^{(s)} e^{s\theta}|A_a(\theta)\rangle. \tag{2.2.10}$$

Comparing with (2.2.9), the energy-momentum operators are taken to be $Q_1 = P$ and $Q_{-1} = \bar{P}$. As in section 2.1 only those conserved quantities which are local conserved charges will be considered, i.e. those which arise as integrals of local conserved densities. Since multi-particle asymptotic states are viewed as a collection well-separated wavepackets, this means that the action of Q_s is additive

$$\begin{aligned} Q_s|A_{a_1}(\theta_1)A_{a_2}(\theta_2)\cdots A_{a_n}(\theta_n)\rangle = \\ \left(q_{a_1}^{(s)} e^{s\theta_1} + q_{a_2}^{(s)} e^{s\theta_2} + \cdots q_{a_n}^{(s)} e^{s\theta_n}\right)|A_{a_1}(\theta_1)A_{a_2}(\theta_2)\cdots A_{a_n}(\theta_n)\rangle. \end{aligned} \tag{2.2.11}$$

Conservation of such a charge means that given an initial state which is an eigenstate of Q_s with some eigenvalue as above, the final state must be a superposition of states for which all states in the superposition have that same eigenvalue. Applying this to an $m \to n$ scattering process with the in- and out-states given by (2.2.6) and (2.2.7) results in the condition

$$q_{a_1}^{(s)} e^{s\theta_1} + q_{a_2}^{(s)} e^{s\theta_2} + \cdots q_{a_m}^{(s)} e^{s\theta_m} = q_{b_1}^{(s)} e^{s\theta'_1} + q_{b_2}^{(s)} e^{s\theta'_2} + \cdots q_{b_n}^{(s)} e^{s\theta'_n}. \tag{2.2.12}$$

If the theory has conserved charges for an infinite number of values of s then an infinite number of such equations exist. For all these to be satisfied for generic θ_i, the left-hand side must be exactly the same as the right hand side in each case so that m must equal n and

$$\theta_i = \theta'_i \quad \text{and} \quad q_{a_i}^{(s)} = q_{b_i}^{(s)}, \quad i = 1, \cdots, m \tag{2.2.13}$$

(up to a possible re-ordering of the final rapidities). $q_{a_i}^{(s)} = q_{b_i}^{(s)}$ does not necessarily imply that a_i equals b_i, just that the conserved charges do not distinguish between the particle types in question. Therefore, when an infinite number of conserved quantities exist, scattering cannot lead to particle production, so all processes have

the form $n \to n$. In addition, the initial and final sets of rapidities and hence the initial and final sets of momenta must be equal. This means that if there is no degeneracy in the masses of the particles then the S-matrix is diagonal.

Further consequences of the existence of conserved charges can be found by using the fact that the initial and final states can be viewed as collections of well-separated particles, which means that it is sufficient to consider the effect of the charge operators on single-particle wave-functions. Such a wave function in position space is given by

$$\psi(x^1) \propto \int_{-\infty}^{\infty} e^{-a^2(p^1-\tilde{p})^2} e^{ip^1(x^1-\tilde{x})} dp^1 \tag{2.2.14}$$

with a being the spread of the wave-packet and $\tilde{x}$ and $\tilde{p}$ the particle's approximate position and momentum respectively. Consider acting on this with some operator A which has the effect of giving the wave-function a momentum-dependent phase-factor:

$$A\psi = \tilde{\psi} \propto \int_{-\infty}^{\infty} e^{-a^2(p^1-\tilde{p})^2} e^{ip^1(x^1-\tilde{x})} e^{-i\phi(p^1)} dp^1. \tag{2.2.15}$$

Since the greatest contribution to the integral comes at $p^1 \approx \tilde{p}$ it makes sense to expand $\phi(p^1)$ in powers of $p^1 - \tilde{p}$, $\phi(p^1) \approx \phi(\tilde{p}) + (p^1 - \tilde{p})\phi'(\tilde{p})$ so that

$$\tilde{\psi} \propto \int_{-\infty}^{\infty} e^{-a^2(p^1-\tilde{p})^2} e^{ip^1(x^1-\tilde{x}-\phi'(\tilde{p}))} dp^1. \tag{2.2.16}$$

The approximate position of the wave-packet has now shifted to $\tilde{x} + \phi'(\tilde{p})$ whilst the approximate momentum remains unchanged. In a similar fashion, considering a multi-particle state of well-separated particles as a product of single-particle wave-functions the action of the operator will give a phase which depends on all of the momenta. Expanding this phase as a multi-variable function with the expansion centred on the approximate values of each of the momenta leads to a shift in the position of each particle.

The action of certain charge operators can have this position-shifting effect. Assume that there exist conserved charge operators P_s which act on one-particle and well-separated multi-particle states as $(P_1)^s$, with P_1 being the spatial part of the energy-momentum operator. When acting on a one-particle state with spatial momentum p^1 this operator has the eigenvalue $(p^1)^s$. So, acting on the one-particle

wave function with $\exp(-i\xi P_s)$ produces a phase factor $\exp(-i\xi(p^1)^s)$, which corresponds to a shift in the position of the particle by $s\xi(p^1)^{s-1}$. For $s = 1$ this is in line with the momentum operator generating constant spatial translations. For a multi-particle state consisting of a set of particles with momenta p_i^1, the operator P_s shifts each position by $s\xi(p^1)_i^{s-1}$. So for a theory containing these conserved charges there exist operators which shift the positions of the wavepackets in the well-separated initial and final states.

The conservation of charge means that all charge operators Q_s commute with the S-matrix. This means that acting with $\exp(-i\xi P_s)$ on both the initial and final states leaves the scattering amplitude of a process unchanged, since

$$\langle final|e^{i\xi P_s} S e^{-i\xi P_s}|initial\rangle = \langle final|S|initial\rangle. \tag{2.2.17}$$

The charge operators can therefore be used to shift the positions of the particles in the initial and final states without affecting the amplitude. This property means that for an integrable theory in $1+1$ dimensions the S-matrix for an $n \to n$ scattering process can be factorised into 2-particle S-matrices. To see this, first consider $3 \to 3$ particle scattering, for which the possible processes are shown in Fig.2.1. Inspection of figures 2.1a) and 2.1c) shows that these processes are composed of

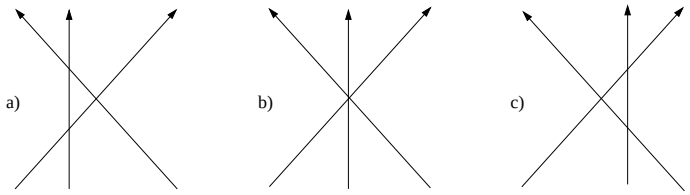

Figure 2.1: $3 \to 3$ scattering processes.

two-particle interactions and so their amplitudes factorise into products of amplitudes of $2 \to 2$ processes. Although this is not immediately obvious for figure 2.1b), the position-shifting properties of charge operators discussed above mean that this process can be transformed to process 2.1a) or 2.1c) without changing the amplitude. The amplitude for process 2.1b) therefore factorises into $2 \to 2$ processes. Since this factorisation occurs for all possible processes the full S-matrix factorises into a product of two-particle S-matrices. For processes involving larger numbers of particles

the same arguments can be applied, so that with appropriate position-shifting by the charge operators all amplitudes can be seen to factorise into $2 \to 2$ processes. This property is unique to $1+1$ dimensional systems, because only there will particles of different rapidities always collide, allowing this position-shifting argument to be applied.

For integrable theories in 1+1 dimensions the problem of finding the full S-matrix is therefore reduced to finding the 2-particle S-matrices, defined by

$$A_a(\theta_1)A_b(\theta_2) = S_{ab}^{cd}(\theta_1 - \theta_2)A_d(\theta_2)A_c(\theta_1) \tag{2.2.18}$$

with $\theta_1 > \theta_2$, as shown in Fig.2.2. S only depends on the difference of the rapidi-

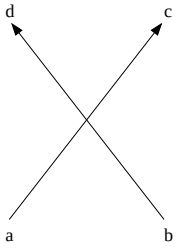

Figure 2.2: 2-particle scattering

ties because the S-matrix is Lorentz invariant and Lorentz transformations translate rapidities by a constant. The 2-particle problem itself is reduced by various restrictions on the form of such S-matrices. Firstly this is restricted by the symmetries which are assumed for the theories in question:

$$\text{Parity:} \qquad S_{ab}^{cd}(\theta) = S_{ba}^{dc}(\theta) \tag{2.2.19}$$

$$\text{Charge conjugation symmetry :} \qquad S_{ab}^{cd}(\theta) = S_{\bar{a}\bar{b}}^{\bar{c}\bar{d}}(\theta) \tag{2.2.20}$$

$$\text{Time-reversal symmetry :} \qquad S_{ab}^{cd}(\theta) = S_{dc}^{ba}(\theta). \tag{2.2.21}$$

Further conditions arise from real analyticity, which requires that $S(\theta)$ is real when θ is purely imaginary, unitarity

$$S_{ab}^{ef}(\theta)S_{ef}^{cd}(-\theta) = \delta_a^c\delta_b^d \tag{2.2.22}$$

and crossing symmetry, which is the symmetry arising when an incoming particle is instead viewed as an outgoing particle

$$S_{ab}^{cd}(\theta) = S_{a\bar{d}}^{c\bar{b}}(i\pi - \theta). \tag{2.2.23}$$

In addition, returning to the $3 \to 3$ processes, the existence of infinitely many conserved charges also shows that the amplitudes of the processes 2.1a) and 2.1c) are the same. Since this is true for any initial and final sets of rapidities, the S-matrix elements for the two processes must be equal, and this results in the Yang-Baxter equation

$$S_{a_1a_2}^{\beta\alpha}(\theta_{12})S_{\beta a_3}^{b_1\gamma}(\theta_{13})S_{\alpha\gamma}^{b_2b_3}(\theta_{23}) = S_{a_2a_3}^{\beta\gamma}(\theta_{23})S_{a_1\gamma}^{\alpha b_3}(\theta_{13})S_{\alpha\beta}^{b_1b_2}(\theta_{12}) \tag{2.2.24}$$

where θ_{ij} denotes $\theta_i - \theta_j$.

These conditions simplify for diagonal theories, which are those for which $a = c$ and $b = d$ in $S_{ab}^{cd}(\theta)$. Such S-matrices need only be denoted by two indices $S_{ab}(\theta)$. In this case the crossing and unitarity conditions simplify and the Yang-Baxter equation becomes trivial. The removal of this constraint makes it harder to determine what the S-matrix should be for a particular theory. However, bound states can be easily handled in diagonal theories, and considering these provides additional constraints on the form of the S-matrix. This approach was pioneered by Alexander Zamolodchikov [15, 23]. Bound states can be identified by considering the pole structure of the S-matrix. A bound state corresponding to a pole in the S-matrix element $S_{ij}(\theta_{12})$ at $\theta_{12} = \chi_{ij}^k$ is seen as a particle of type k emerging from the fusion of particles of type a and b and existing for some macroscopic time before splitting again as shown in Fig.2.3. The existence of such a bound state makes it possible to find further S-matrix elements using the bootstrap principle. This is achieved by considering another particle l interacting with these particles. The ability of the conserved charge operators to shift the positions of the particles in the initial and final states means that the amplitude for l to interact with i and j before they fuse is the same as for l to interact with k, so that the interaction with l takes place after

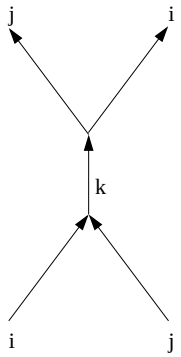

Figure 2.3: Bound state

the fusion. This results in the S-matrix bootstrap equation

$$S_{lk}(\theta) = S_{li}(\theta - i\pi + \chi^j_{ki})S_{lj}(\theta + i\pi - \chi^i_{jk}) \tag{2.2.25}$$

Given an initial proposal for an S-matrix element with a pole indicating a bound state, this equation can be used to find an S-matrix element for the particle corresponding to that bound state. If this new element itself has a pole corresponding to a bound state, then the process can be repeated, and so on. The equation can therefore be used iteratively to find all S-matrix elements. If a finite number of particles emerge then this suggests that the initial proposal was correct.

2.3 The Thermodynamic Bethe Ansatz

The methods described for finding the exact S-matrix rely on the theory in question being defined on a space of infinite volume, since only there can particles become sufficiently well-separated so as to be viewed as free particles when they are not interacting. However, it is also important to be able to consider theories defined on a finite space; by varying the size of the space a theory can be considered at different points along its RG flow. Through the Thermodynamic Bethe Ansatz (TBA) [24, 25] it is possible to use the exact infinite-volume S-matrix to find the exact energy spectrum of a theory, whatever the size of the space on which it is defined. The focus will be on finding the ground state energy for a theory defined on a torus formed from a cylinder of length L and circumference R, as in figure 2.4.

As a simple example, consider a theory involving only a single type of massive particle. There are two ways of writing the partition function of a theory defined

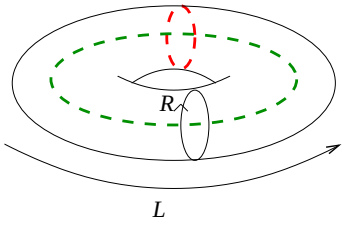

Figure 2.4: Torus. Green and red dotted lines indicate different ways of viewing the Hilbert space.

on a torus, depending on what is taken as the time direction. This corresponds to whether states are viewed as living along the 'R' direction or the 'L' direction, and the two possibilities for the space occupied by states at a fixed time are demonstrated by the red and green lines in figure 2.4. The 'red-type' and 'green-type' states are defined as belonging to Hilbert spaces $\mathcal{H}_R$ and $\mathcal{H}_L$, respectively, and contribute to Hamiltonians H_R and H_L.

Consider the limit where $L \to \infty$ but R remains finite. From the H_R viewpoint the ground state is dominant, so denoting the ground state energy by $E(R)$ the dominant term in the partition function is

$$Z(R, L) \sim e^{-E(R)L}. \tag{2.3.1}$$

On the other hand, since R remains finite all states contribute when the partition function is formed from H_L:

$$Z(R, L) = \mathrm{Tr}_{\mathcal{H}_L}\left[e^{-RH_L}\right]. \tag{2.3.2}$$

Since $L \to \infty$, from this viewpoint the spatial dimension occupied by the states is infinite, allowing the exact S-matrix to be found. In such a situation the asymptotic Bethe ansatz can be used. This quantises the allowed momenta of particles, and arises when periodicity conditions are applied to the 'time'-direction in the N-particle wave-function. For an N-particle state the ansatz is

$$e^{ip_i L}\Pi_{j\neq i}S(\theta_i - \theta_j) = 1, \qquad i = 1 \cdots N. \tag{2.3.3}$$

After defining $S(\theta) = \exp(i\chi(\theta))$ and taking logarithms this becomes

$$mL\sinh(\theta_i) + \sum_{j\neq i}\chi(\theta_i - \theta_j) = 2\pi n_i, \qquad i = 1 \cdots N,\ n_i \in \mathbb{Z}. \tag{2.3.4}$$

The integers $\{n_i\}$ determine the allowed rapidities $\{\theta_i\}$ and hence characterise a state. The focus here is on fermionic-type particles, so all the rapidities must be different and therefore so must the n_i's.

As $L \to \infty$ the system is dominated by states for which N is large and in addition the rapidities in the set $\{\theta_i\}$ for each state become closer together. It therefore makes sense in this limit to refer to the density of allowed rapidities rather than the explicit set $\{\theta_i\}$. The density $\rho_1(\theta)$ is defined so that in a rapidity interval $\Delta\theta$ there are $n = \rho_1(\theta)\Delta\theta$ allowed rapidities. (2.3.4) can then be rewritten as

$$mL\sinh(\theta_i) + \int_{\mathbb{R}}\chi(\theta_i - \theta')\rho_1(\theta')d\theta' = 2\pi n_i. \tag{2.3.5}$$

Considering some particular set of integers $\{n_i\}$, in an interval $\Delta\theta$ there will be values of θ that are not allowed in this state, but would be allowed for some other choice of the n_i's. These unfilled θ_i's are described as holes. The total density of particles and holes is labelled as $\rho(\theta)$, so that there are $n' = \rho(\theta)\Delta\theta$ occupied and

unoccupied θ_i's in the interval $\Delta\theta$. With a view to writing the above condition in terms of $\rho(\theta)$ a strictly increasing function $J(\theta)$ is defined as in [26]

$$J(\theta) = mL\sinh(\theta) + \int_{\mathbb{R}} \chi(\theta - \theta')\rho_1(\theta')d\theta'. \tag{2.3.6}$$

Comparing this with (2.3.5) implies that $J(\theta)/(2\pi) = n_i$ when $\theta = \theta_i$. If in an interval $\Delta\theta$ $J(\theta)$ is equal to an integer a certain number of times, then a value of θ for which this integer belongs to the set $\{n_i\}$ under consideration corresponds to the rapidity of a particle. If the integer is not in $\{n_i\}$ then this θ corresponds to a hole. The number of particles and holes appearing in a given interval therefore corresponds to the number of times $J(\theta)$ is equal to an integer in that interval. So since $J(\theta)$ is strictly increasing, $\rho(\theta) = (1/2\pi)dJ(\theta)/d\theta$, and therefore

$$2\pi\rho(\theta) = mL\cosh(\theta) + 2\pi\int_{\mathbb{R}} \phi(\theta - \theta')\rho_1(\theta')d\theta' \tag{2.3.7}$$

where

$$\phi(\theta) = \frac{1}{2\pi}\frac{d\chi(\theta)}{d\theta} = -\frac{i}{2\pi}\frac{d\ln S(\theta)}{d\theta}. \tag{2.3.8}$$

Given a density $\rho(\theta)$, different particle rapidity sets $\{\theta_i\}$ can result in the same particle density $\rho_1(\theta)$, and this freedom must be quantified in order to write the partition function as a sum over the densities. The number of such possibilities in an interval $\Delta\theta$ is the number of ways of choosing n rapidities from the set of n' possibilities, which is

$$\frac{n'!}{n!(n'-n)!}. \tag{2.3.9}$$

Multiplying together the number of possibilities arising in each interval $\Delta\theta$ gives the total number of possible rearrangements over the full extent of θ, denoted by $\mathcal{N}$.

The partition function (2.3.2) can now be re-expressed as

$$Z(R, L) = \sum_{\rho,\rho_1} \mathcal{N}(\rho, \rho_1)e^{-RH_L}. \tag{2.3.10}$$

Defining $\mathcal{S}(\rho, \rho_1) = \ln \mathcal{N}(\rho, \rho_1)$ this can be written as

$$Z(R, L) = \sum_{\rho, \rho_1} e^{-RH_L + \mathcal{S}(\rho, \rho_1)}. \tag{2.3.11}$$

In terms of the particle density, the Hamiltonian H_L is

$$H_L = \int_{\mathbb{R}} m \cosh\theta \rho_1(\theta) d\theta \tag{2.3.12}$$

and using Stirling's formula

$$\mathcal{S}(\rho, \rho_1) = \int \left(\rho \ln \rho - \rho_1 \ln \rho_1 - (\rho - \rho_1) \ln(\rho - \rho_1)\right) d\theta. \tag{2.3.13}$$

Denoting the free energy density by $f(\rho, \rho_1)$,

$$-RLf(\rho, \rho_1) = -RH_L + \mathcal{S}(\rho, \rho_1) \tag{2.3.14}$$

so that the dominant term in the partition function comes from the configuration (ρ, ρ_1) which minimises $f(\rho, \rho_1)$. Performing the extremisation and imposing the constraint (2.3.7) results in the condition

$$\varepsilon(\theta) = mR\cosh(\theta) - \int_{\mathbb{R}} \phi(\theta - \theta') \ln\left(1 + e^{-\varepsilon(\theta')}\right) d\theta \tag{2.3.15}$$

where $\varepsilon(\theta)$ is called the pseudoenergy and is defined via

$$e^{-\varepsilon} = \frac{\rho_1}{\rho - \rho_1}. \tag{2.3.16}$$

(2.3.15) is the TBA equation for a theory with a single massive particle.

The resulting expression for the free energy is

$$-RLf(\rho, \rho_1) = \frac{1}{2\pi} \int_{\mathbb{R}} mL\cosh(\theta) \ln\left(1 + e^{-\varepsilon(\theta)}\right) d\theta. \tag{2.3.17}$$

This can now be compared to the other approach to calculating the partition function (2.3.1). The exponent of the dominant term there is $-E(R)L$, so equating this with

(2.3.17) gives

$$E(R) = -\frac{1}{2\pi}\int_{\mathbb{R}} m\cosh(\theta)\ln\left(1+e^{-\varepsilon(\theta)}\right)d\theta. \tag{2.3.18}$$

Therefore, through the TBA equation (2.3.15), the ground state energy of a theory defined on a system of finite compact spatial dimension R can be calculated from the exact infinite-volume S-matrix.

TBA equations can also be found for theories with massless particles. Although the scattering of such particles cannot be determined by the techniques described in the previous section, it is still possible to propose S-matrices based on the expected behaviour of the particles involved [27]. Zamolodchikov [18] did this in order to find TBA equations to describe the $\mathcal{M}A_m^{(+)}$ theories introduced in section 2.1. These interpolate between the minimal models $\mathcal{M}_m$ and $\mathcal{M}_{m-1}$, so that the UV and IR limits of $\mathcal{M}A_m^{(+)}$ are both CFTs. The ground state energy of a CFT defined on a cylinder (or equivalently a torus), with states living on the circumference and time propagating along the length of the cylinder, is known to be $E(R) = -c\pi/6R$. This relationship between the ground state energy and the central charge suggests the definition of a function $c_{eff}(r)$,where $r = mR$, known as the effective central charge, which is defined at all points along the RG flow as

$$c_{eff}(r) = \frac{-6RE(R)}{\pi} \tag{2.3.19}$$

and coincides with the central charge at points where the theory is described by a CFT. Note that although it is built on a similar premise, this function differs in definition from the c-function described in section 2.1.1. The value of this function can indicate which CFTs are appearing in an RG flow, and where this information is already known, provides a test for the UV and IR ground state energy results emerging from the TBA calculations.

$\mathcal{M}A_4^{(+)}$ interpolates between the tricritical Ising model $\mathcal{M}_4$ ($c = 7/10$) and the Ising model $\mathcal{M}_3$ ($c = 1/2$). The theory contains a single massless particle. Right-moving particles, i.e. those with momentum p equal to energy E, are treated separately from left-moving particles, which have $p = -E$. Their momentum can be parametrised by starting with the expression for momentum for a massive particle

with rapidity β, $p = m\sinh\beta$, and setting $\beta = \theta + \theta_1$ for the right-movers and $\beta = \theta - \theta_1$ for the left-movers. Then taking the limit $m \to 0$ and $\theta_1 \to \infty$ in such a way that $M = me^{\theta_1}$ stays finite leads to the following expressions for the momentum of the right- and left-movers:

$$p_R = \tfrac{1}{2}Me^{\theta} \qquad \text{and} \qquad p_L = -\tfrac{1}{2}Me^{-\theta}. \tag{2.3.20}$$

M has dimensions of mass and determines the crossover between the UV and IR theories. Note that now in the two cases zero momentum corresponds to $\theta \to \mp\infty$, respectively. Zamolodchikov found that left-left and right-right scattering is trivial, and that the right-left scattering between particles of rapidities θ and θ' is described by the S-matrix

$$S_{RL}(\theta - \theta') = S(\theta - \theta') = -\tanh\left(\frac{\theta - \theta'}{2} - \frac{i\pi}{4}\right) \tag{2.3.21}$$

(with left-right scattering satisfying $S_{RL}(\theta - \theta')S_{LR}(\theta' - \theta) = 1$).

The TBA equations can then be derived by using the same process as before but giving the left- and right-movers separate density functions. This leads to the system of TBA equations

$$\begin{aligned}\varepsilon_1(\theta) =& \tfrac{1}{2}MRe^{\theta} - \int_{\mathbb{R}} \phi(\theta - \theta')L_2(\theta')d\theta' \\ \varepsilon_2(\theta) =& \tfrac{1}{2}MRe^{-\theta} - \int_{\mathbb{R}} \phi(\theta - \theta')L_1(\theta')d\theta'\end{aligned} \tag{2.3.22}$$

where

$$L_a(\theta) = \ln\left(1 + e^{-\varepsilon_a(\theta)}\right) \quad \text{for } i = 1, 2 \tag{2.3.23}$$

and

$$\phi(\theta) = -\frac{i}{2\pi}\frac{d\ln S(\theta)}{d\theta} = \frac{1}{2\pi\cosh\theta}. \tag{2.3.24}$$

The ground state energy is [18]

$$E(R) = \frac{-M}{4\pi}\int_{\mathbb{R}} \left(e^{\theta}L_1(\theta) + e^{-\theta}L_2(\theta)\right)d\theta \tag{2.3.25}$$

and in the UV and IR limits can be calculated exactly with the results

$$E(R \to 0) = \frac{-7\pi}{60R} \tag{2.3.26}$$

$$E(R \to \infty) = -\frac{\pi}{12R}, \tag{2.3.27}$$

in agreement with the results from CFT.

Zamolodchikov also proposed TBA equations for $\mathcal{M}A_m^{(+)}$ for all $m > 3$, as systems of $m-2$ integral equations [18]:

$$\varepsilon_1(\theta) = \tfrac{1}{2}MRe^{\theta} - \int_{\mathbb{R}} \phi(\theta - \theta')L_2(\theta')d\theta' \tag{2.3.28}$$

$$\varepsilon_a(\theta) = -\int_{\mathbb{R}} \phi(\theta - \theta') \left(L_{a-1}(\theta') + L_{a+1}(\theta')\right) d\theta' \quad a = 2, 3, \cdots m-3 \tag{2.3.29}$$

$$\varepsilon_{m-2}(\theta) = \tfrac{1}{2}MRe^{-\theta} - \int_{\mathbb{R}} \phi(\theta - \theta')L_{m-3}(\theta')d\theta'. \tag{2.3.30}$$

The ground state energy is given by

$$E(R) = -\frac{M}{4\pi} \int_{\mathbb{R}} \left(e^{\theta}L_1(\theta) + e^{-\theta}L_{m-2}(\theta)\right) d\theta \tag{2.3.31}$$

which in the UV limit becomes

$$E(R \to 0) = -\frac{\pi}{6R}\left(1 - \frac{6}{m(m+1)}\right) \tag{2.3.32}$$

and in the IR limit is

$$E(R \to \infty) = -\frac{\pi}{6R}\left(1 - \frac{6}{(m-1)m}\right). \tag{2.3.33}$$

These are in line with the central charge values of $c = 1 - \frac{6}{m(m+1)}$ for a minimal model $\mathcal{M}_m$. The method used to evaluate the ground state energy (via the effective central charge $c_{eff}(r)$) will be discussed in detail in section 4.1.

It will be seen in the following chapters that these TBA systems emerge in certain limits of a massive diagonal scattering theory known as the staircase model, where the standard concepts of the S-matrix apply. A more detailed discussion of the behaviour of these pseudoenergies and the calculation of the ground state energy

will be made in this context in chapter 4.

Chapter 3

Integrable Theories with Boundaries

3.1 Boundary Conformal Field Theory

The focus of this chapter is to introduce how the concepts of conformal field theories and their perturbations already discussed can be adapted and extended to theories living on a space with boundaries [9, 10, 13, 28–30]. For such a theory to be conformally invariant, the boundary conditions must be invariant under conformal transformations as well as the bulk theory. Such boundary conditions are found by considering coordinates parallel and perpendicular to the boundary and demanding that the parallel/perpendicular component of the energy-momentum tensor vanishes on the boundary.

Consider a theory defined on a right cylinder of finite length, formed by identifying the vertical sides of a rectangle in the upper half complex plane. A rectangle with vertices 0, R, iL and $R+iL$ corresponds to a cylinder of length L and circumference R. Imposing boundary conditions a and b on the lower and upper horizontal sides of the rectangle respectively translates to the circles at the bottom and top of the cylinder having these conditions. As in section 2.3, the partition function for this theory can be found in two different ways, depending on what is taken as the 'time' direction on the cylinder, which of course affects the form of the Hamiltonian. In both cases, coordinate transformations are applied which are similar to that used

in formulating radial quantisation. Firstly, time is taken to travel in the compacti-

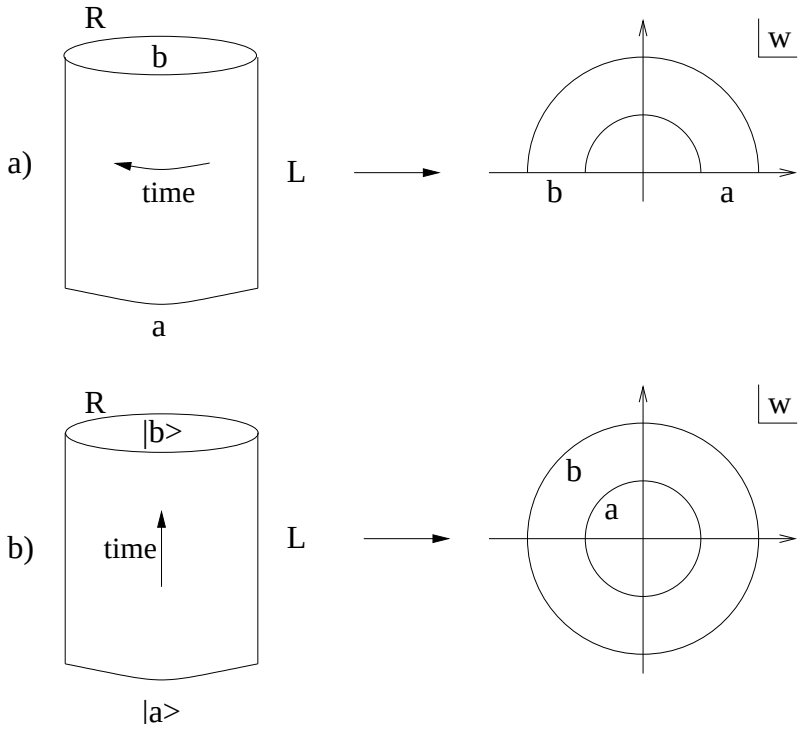

Figure 3.1: Set-up for cylinder partition function: a) time direction around the cylinder b) time direction along the cylinder.

fied direction around the cylinder, corresponding to the horizontal direction on the rectangle. The map $w(z) = \exp(\pi z/L)$ takes the rectangle to a half-annulus on the upper half of the complex plane, with the a boundary forming the end of the annulus on the positive real axis, and the b boundary doing likewise on the negative real axis. The time direction is now the radial direction on the plane, as depicted in figure 3.1a. This is the same set-up as for radial quantisation in the previous section, but because the space under consideration is now the upper half plane the Hamiltonian is defined slightly differently. To see this, consider a theory defined on the full upper half of the complex plane, with boundary condition a on the full positive real axis and boundary condition b on the negative real axis. Such a change in boundary condition is viewed as the effect of a boundary condition changing field $\phi_{(ab)}(z)$ inserted at the origin. In this set-up, the conformal boundary condition on the energy momentum tensor is

$$T(z) = \bar{T}(\bar{z}) \tag{3.1.1}$$

on the boundary (which is equivalent to $T_{xy} = 0$). This allows the dilation operator on the upper half plane to be written as

$$D = L_0 = \frac{1}{2\pi i} \oint zT(z)dz. \tag{3.1.2}$$

The other Virasoro operators are defined similarly, and there is only one Virasoro algebra in contrast to the two that exist for a theory on the full complex plane. This dilation operator therefore generates time translations on the half-annulus so applies to the theory on the finite cylinder. The Hamiltonian is related to the above dilation operator and is defined as

$$H_{ab}^{strip} = \frac{\pi}{L}\left(L_0 - \frac{c}{24}\right) \tag{3.1.3}$$

so that the partition function is

$$Z_{ab}(R, L) = \mathrm{Tr}\, e^{-RH_{ab}} \tag{3.1.4}$$

and in terms of characters

$$Z_{ab}(R, L) = \sum_h n_{ab}^h \chi_h(e^{-\pi R/L}). \tag{3.1.5}$$

The other option is to take the time direction to be along the length of the cylinder (and in the vertical direction on the rectangle). From this viewpoint the partition function is the propagation of the system from boundary state $|a\rangle$ at the bottom of the cylinder to boundary state $|b\rangle$ at the top of the cylinder. Then at each point in time the theory is defined on a circle, and so the partition function is

$$Z_{ab}(R, L) = \langle a|e^{-LH^{circle}}|b\rangle. \tag{3.1.6}$$

In this case it makes sense to map the rectangle to a full annulus on the complex plane via the map $w(z) = e^{-2\pi iz/R}$ so that the a and b boundaries respectively lie on the inner and outer concentric circles which form the edges of the annulus, as shown in figure 3.1b. On the full plane, as for radial quantisation, there are two Virasoro

algebras, leading to the Hamiltonian on the circle being defined as

$$H^{circle} = \frac{2\pi}{R}\left(L_0 + \bar{L}_0 - \frac{c}{12}\right). \tag{3.1.7}$$

For a boundary on a circle, the conformal boundary condition corresponds to the following condition on a boundary state $|a\rangle$

$$\left(L_n - \bar{L}_{-n}\right)|a\rangle = 0. \tag{3.1.8}$$

Note that the $n = 0$ condition implies that $h = \bar{h}$ for $|a\rangle$. A basis of boundary states satisfying the above condition is given by the Ishibashi states [31]. For a minimal model, there is a basis state for each Verma module, and so they are labelled by the highest weight of each representation, and denoted $|h\rangle\rangle$. They are defined in terms of orthonormal bases of each level of both the holomorphic and anti-holomorphic Virasoro representations. Given a level of dimension $d_h(N)$, such a basis is denoted as $|h, N; i\rangle$ for V_h and $\overline{|h, N; i\rangle}$ for $\bar{V}_h$,where $1 \leq i \leq d_h(N)$. The Ishibashi states are then defined as

$$|h\rangle\rangle = \sum_{N=0}^{\infty}\sum_{j=1}^{d_h(N)} |h, N; j\rangle \otimes \overline{|h, N; j\rangle} \tag{3.1.9}$$

which means that

$$\langle\langle h'|e^{-LH^{circle}}|h\rangle\rangle = \delta_{h,h'}\sum_{N=0}^{\infty}\sum_{j=1}^{d_h(N)} e^{-4\pi L(h+N-c/24)/R} \tag{3.1.10}$$

$$= \delta_{h,h'}\chi_h\left(e^{-4\pi L/R}\right). \tag{3.1.11}$$

The physical boundary states are expanded in terms of the Ishibashi states as

$$|a\rangle = \sum_h g_a^h |h\rangle\rangle, \tag{3.1.12}$$

defining $g_a^h = \langle\langle h|a\rangle$. In this notation the partition function (3.1.6) is

$$Z_{ab}(R, L) = \sum_h g_a^h g_b^h \chi_h\left(e^{-4\pi L/R}\right). \tag{3.1.13}$$

The partition functions that emerge from the different time-direction viewpoints must be equal. Using the modular transformation rule for the characters (1.3.40), the partition function expression (3.1.5) can be written as

$$Z_{ab}(R,L) = \sum_{h,h'} n_{ab}^{h} S_{h}^{h'} \chi_{h'}\left(e^{-4\pi L/R}\right) \tag{3.1.14}$$

where n_{ab}^{h} is the number of copies of the representation of highest weight h appearing in the spectrum of H_{ab}. On imposing linear independence of the characters, equality of the partition functions (3.1.5) and (3.1.6) becomes the Cardy condition

$$g_a^h g_b^h = \sum_{h'} n_{ab}^{h'} S_{h'}^{h}. \tag{3.1.15}$$

When certain choices are made for the coefficients n_{ab}^{h} there is a one-to-one map between Virasoro representations and allowed boundary states. Denoting these states $|h'\rangle$ and defining

$$g_{h'}^{h} = \frac{S_{h'}^{h}}{\sqrt{S_0^h}}, \tag{3.1.16}$$

the Cardy condition holds when $n_{h'0}^{h} = \delta_{h,h'}$ and $n_{h'h''}^{h} = \sum_j S_{h'}^{j} S_{h''}^{j} S_{j}^{h} / S_0^j$. The first condition indicates that only the representation $h = 0$ appears in the spectrum of the Hamiltonian for the $(a,b) = (0,0)$ boundary condition, and that the spectrum of $H_{h',0}$ is the $h = h'$ representation. The second condition is the same expression as the Verlinde formula for the fusion coefficients N_{ab}^{c} on the torus, and so the coefficients n_{ab}^{h} are equal to the fusion coefficients. Since the fusion coefficients are indexed by the highest weights of the Virasoro representations, this confirms their correspondence with the allowed boundary states. In the minimal models $\mathcal{M}_{p,p'}$, the highest weights take their labels from the Kac table, and so a boundary state corresponding to $h_{r,s}$ is labelled as (r,s). Since $h_{r,s} = h_{p'-r,p-s}$, the corresponding boundary conditions are identified with one another

$$(r,s) \equiv (p'-r, p-s). \tag{3.1.17}$$

The fusion coefficients appear here due to the action of boundary changing op-

erators. Consider a theory defined on a vertical strip, with time moving upwards. Take the left-hand boundary to have boundary condition 0 until time t_0 and then boundary condition a thereafter, and the right-hand boundary to have condition b always. Up until t_0, the fact that $n_{0b}^h = \delta_{b,h}$ means that only states in the representation of highest weight b can propagate. However, after $t = t_0$, states belonging to other representations can propagate, and the number of copies of the representation of highest weight c is given by n_{ab}^c. However, since the change in boundary condition is realised by a boundary changing operator $\phi_{(0a)}$, this process can also be viewed as the action of the operator on the propagating states. Since states emerge as the action of fields on the vacuum state, the action of the boundary changing operator can be expressed via the operator algebra. From this viewpoint, the number of copies of a particular representation c is given by the fusion coefficients N_{ab}^c.

The leading term in the partition function is the contribution from the ground state. This term dominates in the thermodynamic limit $L/R \to \infty$ so that (3.1.6) becomes

$$Z_{ab} \sim \langle a|0\rangle\langle 0|b\rangle e^{\pi Lc/6R}, \tag{3.1.18}$$

where $|0\rangle$ is the bulk ground state. For Ishibashi states $\langle 0|h\rangle\rangle = \delta_{0h}$ so

$$\langle a|0\rangle = g_a^0 \equiv g_a, \tag{3.1.19}$$

where g_a is known as the g-function for boundary condition a. This was first introduced by Affleck and Ludwig [32]; it is described as the ground-state degeneracy and its logarithm as the boundary entropy. This is because the calculation of the entropy $\mathcal{S}_{ab}$ from (3.1.18) produces

$$\mathcal{S}_{ab} \sim \frac{\pi cL}{3R} + \ln\langle a|0\rangle + \ln\langle b|0\rangle \tag{3.1.20}$$

and so $\ln g_a$ is the contribution to the entropy from the boundary a. For a minimal model $\mathcal{M}_{p,p'}$ the g-function for a boundary corresponding to highest weight $h = h_{a_1,a_2}$

is found from (1.3.41) to be

$$g_{(a_1,a_2)} = \frac{\left(\frac{8}{pp'}\right)^{1/4}(-1)^{1+a_1+a_2}\sin\left(\frac{\pi a_1 p}{p'}\right)\sin\left(\frac{\pi a_2 p'}{p}\right)}{\sqrt{-\sin\left(\frac{\pi p}{p'}\right)\sin\left(\frac{\pi p'}{p}\right)}}. \tag{3.1.21}$$

The g-function encodes the boundary conditions of a conformal field theory, just as the central charge encodes the bulk theory. This suggests that it would be interesting to consider an off-critical version of the g-function, which would coincide with the critical g-function at fixed points, just as the effective central charge agrees with the central charge when the bulk theory is conformal. This subject will be discussed in section 3.3, but first the concept of considering a boundary conformal field theory away from a fixed point will be made more concrete.

3.2 Perturbed Boundary Conformal Field Theory

To consider perturbed conformal theories defined on spaces with boundaries, it must be determined how integrability can be preserved when such a theory is perturbed away from the boundary conformal field theory (BCFT) fixed point, just as was done in section 2.1 for a CFT defined on a space without boundaries. This was investigated by Ghoshal and Zamolodchikov in [33] (see also [34]). To study this, consider a theory defined on the left half of the Euclidean plane, $x \leq 0$, $-\infty < y < \infty$ so that the y-axis forms a boundary and y is taken to be the time direction. Now, in addition to a perturbation of the bulk theory, a perturbation of the boundary can also be considered. In terms of bulk and boundary couplings λ and μ and relevant bulk and boundary fields $\phi(x,y)$ and $\psi(x)$ the perturbed action is written as [33]

$$S_{PBCFT} = S_{BCFT} + \lambda\int_{-\infty}^{\infty} dy \int_{-\infty}^{0} \phi(x,y)\,dx + \mu\int_{-\infty}^{\infty}\psi(y)\,dy. \tag{3.2.1}$$

For integrability to survive, it needs to be checked that an infinite number of conserved charges exist when a boundary is present. These turn out to be slightly amended versions of the conserved charges found in the case of the pure bulk perturbation which were described in section 2.1. Symmetry considerations mean that

the perturbed theory should have the following condition at the boundary

$$T_{xy}\,|_{x=0} = \frac{d}{dy}b(y) \tag{3.2.2}$$

for some local field $b(y)$. This is the perturbed theory version of the condition (3.1.1) for boundaries in a conformal field theory. If this condition holds then it is possible to find conserved quantities for the theory.

To introduce this, the conservation of the Hamiltonian at the boundary of the perturbed theory will first be considered (which must hold for any time-translation invariant theory). As was discussed in the previous section, in the perturbed theory there are the continuity equations, (2.1.18) and its anti-holomorphic counterpart

$$\partial_{\bar{z}}T = \partial_z\Theta \qquad \text{and} \qquad \partial_z\bar{T} = \partial_{\bar{z}}\Theta \tag{3.2.3}$$

which give rise to path-independent integrals

$$P_1(C) = \int_C (Tdz + \Theta d\bar{z}) \qquad \text{and} \qquad \bar{P}_1(C) = \int_C \left(\bar{T}d\bar{z} + \Theta dz\right) \tag{3.2.4}$$

that equal zero when the contour C is closed, as long as there are no other operators inside the contour. This can be used to show the existence of a conserved quantity in the left-half (x, y) plane. Consider the contour $C = C_{x1} + C_y + C_{x2}$ shown in figure 3.2. which is taken to be closed at $x \to -\infty$. Consider adding together P_1

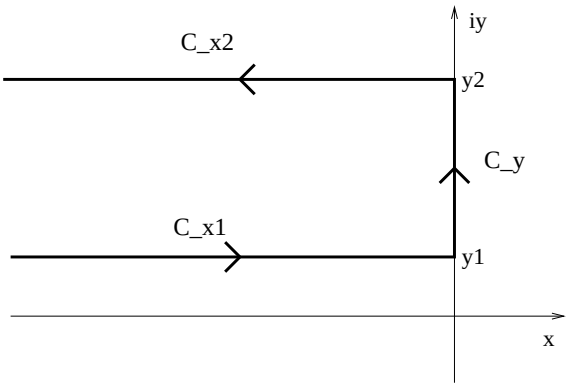

Figure 3.2: Contour $C = C_{x_1} + C_y + C_{x_2}$.

and $\bar{P}_1$. Both equal zero for a closed contour and so

$$P_1(C) + \bar{P}_1(C) = 0. \tag{3.2.5}$$

Now consider the part of this integral where the contour runs up the imaginary y-axis between y_1 and y_2, denoted C_y.

$$P_1(C_y) + \bar{P}_1(C_y) = i \int_{y_1}^{y_2} (T - \Theta - \bar{T} + \Theta) dy \tag{3.2.6}$$

and so noting that $T - \bar{T} = -iT_{xy}$, (3.2.2) implies that

$$P_1(C_y) + \bar{P}_1(C_y) = b(y_2) - b(y_1). \tag{3.2.7}$$

So, by (3.2.5)

$$P_1(C_{x_1}) + \bar{P}_1(C_{x_1}) - b(y_1) = -(P_1(C_{x_2}) + \bar{P}_1(C_{x_2})) - b(y_2). \tag{3.2.8}$$

This means that

$$H_B = \int_{-\infty}^{0} (T(x,y) + \bar{T}(x,y) + 2\Theta(x,y)) dx - b(y) \tag{3.2.9}$$

is independent of y. It is therefore a conserved quantity, identified with the Hamiltonian of the perturbed boundary theory, which exists if the boundary perturbation is such that (3.2.2) holds.

A similar method can be followed to find conserved quantities at the boundary from the other bulk conserved densities. For a theory with a pure bulk perturbation, these conserved densities were seen to obey the equations (2.1.22)

$$\partial_{\bar{z}} T_s = \partial_z \Theta_{s-2} \qquad \text{and} \qquad \partial_z \bar{T}_s = \partial_{\bar{z}} \bar{\Theta}_{s-2}. \tag{3.2.10}$$

Following the same pattern as above it makes sense to require at the boundary that

$$i \left(T_s - \Theta_{s-2} - \bar{T}_s + \bar{\Theta}_{s-2} \right) |_{x=0} = \frac{d}{dy} b_{s-1}(y), \tag{3.2.11}$$

where $b_{s-1}(y)$ can be any local field defined on the boundary, since then the quantity

$$H_B^{(s)} = \int_{-\infty}^{0} dx \left(T_s(x,y) + \Theta_{s-2}(x,y) + \bar{T}_s(x,y) + \bar{\Theta}_{s-2}(x,y)\right) - b_{s-1}(y) \quad (3.2.12)$$

is independent of y and hence is conserved. So, for the perturbed theory to be integrable the perturbing boundary field must be such that an infinite number of these conserved quantities (3.2.12) exist.

Ghoshal and Zamolodchikov [33] proposed that this is the case for a unitary minimal model perturbed by bulk and boundary perturbing fields $\phi_{(1,3)}$ and $\psi_{(1,3)}$ respectively. As was described earlier in this section, for a pure bulk perturbation by $\phi_{(1,3)}$ there are an infinite number of conserved charges T_s with s even [15]. When a boundary perturbation is added, for integrability to survive (3.2.11) must be satisfied for some field $b_{s-1}(y)$ by each pair $(T_s, \bar{T}_s)$. Indications that this is the case can be found by considering the situation $\lambda = 0$, $\mu \neq 0$, where the perturbation is purely by the boundary field $\psi_{(1,3)}$. Since the bulk theory is not perturbed, Θ_{s-2} and $\bar{\Theta}_{s-2}$ both equal zero, and so a field $b_{s-1}(y)$ must be found that satisfies

$$i\left(T_s - \bar{T}_s\right)|_{x=0} = \frac{d}{dy} b_{s-1}(y). \quad (3.2.13)$$

For the energy-momentum tensor T_2 this can be seen by considering the $x \to 0$ limit of the following correlation function in the perturbed theory

$$\langle (T(y+ix) - \bar{T}(y-ix))X \rangle_{CFT + \mu \int_{-\infty}^{\infty} \psi_{(1,3)}(y)\, dy}, \quad (3.2.14)$$

where X is a string of fields sitting away from the boundary. Using the Gell-Mann-Low formula this can be rewritten as a correlation function in the non-perturbed theory

$$\frac{\langle (T(y+ix) - \bar{T}(y-ix))X e^{-\mu \int_{-\infty}^{\infty} \psi_{(1,3)}(y')\, dy'} \rangle_{CFT}}{\langle e^{-\mu \int_{-\infty}^{\infty} \psi_{(1,3)}(y')\, dy'} \rangle_{CFT}}. \quad (3.2.15)$$

In the $x \to 0$ limit this is controlled by terms with the integrand

$$\mu (T(y-ix) - \bar{T}(y+ix)) \psi_{(1,3)}(y') \quad (3.2.16)$$

which using (1.3.16) has the operator product expansion

$$\mu\left(\frac{h_{1,3}}{(y+ix-y')^2}-\frac{h_{1,3}}{(y-ix-y')^2}+\frac{1}{y+ix-y'}\frac{\partial}{\partial y'}-\frac{1}{y-ix-y'}\frac{\partial}{\partial y'}\right)\psi_{(1,3)}(y'). \tag{3.2.17}$$

Since such terms appear as integrands, the rule

$$\lim_{\varepsilon\to 0}\int\left(\frac{f(x)}{x+i\varepsilon}-\frac{f(x)}{x-i\varepsilon}\right)dx=-2i\pi\int f(x)\delta(x)dx \tag{3.2.18}$$

(see for example [35]) can be used so that

$$\lim_{x\to 0}(T(y-ix)-\bar{T}(y+ix))=-2i\pi\mu\left(h_{1,3}\delta'(y-y')+\delta(y-y')\frac{\partial}{\partial y'}\right)\psi_{(1,3)}(y'). \tag{3.2.19}$$

Then (3.2.13) is satisfied at $s=2$ by taking

$$b_1(y)=2\pi\mu(1-h_{1,3})\psi_{(1,3)}(y). \tag{3.2.20}$$

Similar methods can be used to find b_{s-1} for each T_s so that, at least to the first order in μ, (3.2.13) is satisfied for all s even.

3.3 The Off-Critical g-function

In section 2.3 it was seen how the effective central charge allows the identification of minimal models appearing as fixed points in RG flows. The g-function that was introduced towards the end of section 3.1 encodes the boundary conditions of a CFT, and just as the central charge was generalised to the effective central charge, it is natural to extend the idea of the g-function to all points along the RG flow, so that it coincides with the expected CFT values at fixed points. Such a function then encodes the boundary behaviour of a theory both at and away from fixed points.

Boundary quantum field theories are defined not only by how particles scatter off one another, but also by how the particles scatter off the boundaries. Therefore, in addition to the bulk S-matrix, reflection factors must be defined for such theories. The focus will be on theories where the scattering of a particle off the boundary is

elastic, so that the rapidity of the particle is unaffected. The reflection factor for a particle of type a scattering off a boundary with boundary condition α is denoted in terms of its rapidity as $R_\alpha^{(a)}(\theta)$. As for the bulk S-matrix, it satisfies unitarity, crossing symmetry and bootstrap equations [33], which take the form:

$$R_a(\theta)R_a(-\theta) = 1, \tag{3.3.1}$$

$$R_a(\theta)R_{\bar{a}}(\theta - i\pi) = S_{aa}(2\theta) \tag{3.3.2}$$

$$R_{\bar{c}}(\theta) = R_a\left(\theta + iU_{ac}^b\right) R_b\left(\theta - i\bar{U}_{bc}^a\right) S_{ab}\left(2\theta + i\bar{U}_{ac}^b - i\bar{U}_{bc}^a\right), \tag{3.3.3}$$

where U_{ab}^c corresponds to a pole in the reflection factor, indicating a bound state.

Expressions for the exact g-function for certain integrable field theories have been found in terms of the S-matrix and reflection factors of the theory, and the pseudoenergies solving the periodic TBA equations for that theory (as introduced in section 2.3). For a massive diagonal integrable theory with N types of particle, the g-function for boundary condition α was found by Dorey et al. in [36, 37] to be

$$\begin{aligned}\ln g_\alpha(r) = &\\ &\frac{1}{2}\sum_{n=1}^{\infty}\frac{1}{n}\sum_{a_1=1}^{N}\cdots\sum_{a_n=1}^{N}\int_{\mathbb{R}_n}\prod_{i=1}^{n}\frac{d\theta_i}{1+e^{\varepsilon_{a_i}(\theta_i)}}\phi_{a_1a_2}(\theta_1+\theta_2)\phi_{a_2a_3}(\theta_2-\theta_3)\cdots\phi_{a_na_1}(\theta_n-\theta_1)\\ &+\tfrac{1}{2}\sum_{a=1}^{N}\int_{\mathbb{R}}d\theta\left(\phi_\alpha^{(a)}(\theta)-\tfrac{1}{2}\delta(\theta)-\phi_{aa}(2\theta)\right)\ln\left(1+e^{-\varepsilon_a(\theta)}\right),\end{aligned} \tag{3.3.4}$$

where

$$\phi_{ab}(\theta) = -\frac{1}{2\pi}\frac{d}{d\theta}\ln S_{ab}(\theta) \qquad \text{and} \qquad \phi_\alpha^{(a)}(\theta) = -\frac{i}{2\pi}\frac{d}{d\theta}\ln R_\alpha^{(a)}(\theta). \tag{3.3.5}$$

As before, $r = mR$, where the theory is defined on a cylinder of circumference R with a boundary at one end. Note, however, that the pseudoenergies which appear in the g-function expressions are those satisfying the TBA equations defined on the torus. The second line of this formula was originally proposed as the full g-function expression by LeClair et al. [38]. It had the expected dependence on the boundary parameter (which appears in the reflection factor), but failed to produce the correct

bulk dependence. Dorey et al. [36] resolved this by proposing the addition of the infinite sum term. Starting with the case of a single particle type this arose from working initially in the IR and considering the contributions to the partition function and hence to the g-function from all possible particle number configurations. They then found the full result valid for all values of r by rewriting the expressions found in terms of TBA quantities, and showed that this expression had both the correct UV behaviour and agreement at each particle-number order with the expected IR terms. This led to the single particle-type version of the above formula (3.3.4), and the latter emerged as a generalisation of this case. An alternative approach was taken by Woynarovich [39] whose approach was to evaluate the g-function through its definition as the $\mathcal{O}(1)$ contribution to the free energy (see (3.1.18)), which he found by considering the partition function expressed in terms of the saddle point solution of the free energy and the fluctuations around it. This was only partially successful, but in [40] Pozsgay used an adapted version of this method to successfully reproduce the above equations. The key feature of this approach is that the infinite sum term arises from the Fredholm determinants of certain integral operators which are defined in terms of the S-matrix and the TBA pseudoenergies.

An expression has also been found for the $\mathcal{M}A_4^{(+)}$ theory (the TBA system of which was described in section 2.3), which has massless bulk degrees of freedom even in the far IR limit. For this theory the exact g-function is [41]

$$\begin{aligned}\ln g(r) &= \ln g_0(r) + \ln g_b(r) \\ &= \ln g_0(r) + \ln g_{b1}(r) + \ln g_{b2}(r) + \ln g_{b3}(r)\end{aligned} \tag{3.3.6}$$

where

$$\ln g_0 = \sum_{j=1}^{\infty} \frac{1}{2j-1} \int \frac{d\theta_1}{1+e^{\varepsilon(\theta_1)}} \cdots \frac{d\theta_{2j-1}}{1+e^{\varepsilon(\theta_{2j-1})}} \phi(\theta_1+\theta_2)\phi(\theta_2+\theta_3)\cdots\phi(\theta_{2j-1}+\theta_1) \tag{3.3.7}$$

$$\ln g_{b1} = -\tfrac{1}{2}\ln 2 \tag{3.3.8}$$

$$\ln g_{b2} = \int \Big(\phi_{\left(\frac{3}{4}\right)}(\theta) - \phi(2\theta)\Big) L(\theta) d\theta \tag{3.3.9}$$

$$\ln g_{b3} = \int \phi(\theta-\theta_b) L(\theta) d\theta. \tag{3.3.10}$$

Here $\phi(\theta) = \frac{1}{2\pi\cosh(\theta)}$ and $\phi_{(3/4)}(\theta)$ is defined using the block notation

$$(x)(\theta) = \frac{\sinh\left(\frac{\theta}{2} + \frac{i\pi x}{2}\right)}{\sinh\left(\frac{\theta}{2} - \frac{i\pi x}{2}\right)}, \qquad \phi_{(x)}(\theta) = -\frac{i}{2\pi}\frac{d}{d\theta}\ln(x)(\theta) = \frac{-\sin(\pi x)/(2\pi)}{\cosh(\theta)-\cos(\pi x)}, \tag{3.3.11}$$

and $\varepsilon(\theta)$ satisfies

$$\varepsilon(\theta) = \tfrac{1}{2} r e^{\theta} - \int_{\mathbb{R}} \phi(\theta+\theta') L(\theta') d\theta', \tag{3.3.12}$$

which is equivalent to the TBA equations (2.3.22) upon setting $\varepsilon(\theta) = \varepsilon_1(\theta)$ and employing the symmetry $\varepsilon_1(\theta) = \varepsilon_2(-\theta)$. Further flows arise when $\frac{1}{2}\ln 2$ is added to $\ln g_b$. This result was also reproduced by Pozsgay [40] using the same method as in the massive diagonal case.

The situation for the interpolating theories $\mathcal{M}A_m^{(+)}$ with $m > 4$ is expected to be more complex since unlike $\mathcal{M}A_4^{(+)}$, these theories are non-diagonal. The following chapters will explore how a massive diagonal theory known as the staircase model can be used to probe these models.

Chapter 4

Introduction to the Staircase Model

4.1 The Bulk Theory

The staircase model was first introduced by Al.B. Zamolodchikov in [42]. It will be seen that this model is strongly linked to the collection of flows $\mathcal{M}_m \to \mathcal{M}_{m-1}$ discussed in the previous chapters. The staircase model involves a single massive particle of mass M and its S-matrix is

$$S(\theta) = \frac{\sinh\theta - i\cosh\theta_0}{\sinh\theta + i\cosh\theta_0} = \tanh\left(\frac{\theta-\theta_0}{2} - \frac{i\pi}{4}\right)\tanh\left(\frac{\theta+\theta_0}{2} - \frac{i\pi}{4}\right) \tag{4.1.1}$$

where θ_0 is a real parameter. One of the original motivations for studying this theory is its connection with the sinh-Gordon model. This an integrable theory with S-matrix

$$S_{shG(\theta)} = \frac{\sinh\theta - i\sin\gamma}{\sinh\theta + i\sin\gamma} \tag{4.1.2}$$

for real coupling constant γ. The staircase model emerges when γ is analytically continued to complex values of the form $\gamma = \pi/2 + i\theta_0$.

Since the theory involves a single massive particle, from equation (2.3.15) the TBA equation for the staircase model on a circle of circumference R is

$$\varepsilon(\theta) = r\cosh\theta - \int_{\mathbb{R}} \phi_S(\theta-\theta')L(\theta')d\theta' \tag{4.1.3}$$

where $r = mR$. Defining

$$\phi(\theta) = \frac{1}{2\pi \cosh(\theta)} \tag{4.1.4}$$

the staircase model kernel is

$$\phi_S(\theta) = -\frac{i}{2\pi}\frac{d}{d\theta} \ln S(\theta) = \phi(\theta - \theta_0) + \phi(\theta + \theta_0). \tag{4.1.5}$$

so that the TBA can also be written as

$$\varepsilon(\theta) = r \cosh\theta - \int_{\mathbb{R}} \phi(\theta - \theta') \left(L(\theta' + \theta_0) + L(\theta' - \theta_0)\right) d\theta'. \tag{4.1.6}$$

The function $\phi(\theta)$ has its support close to $\theta = 0$ so $\phi_S(\theta)$ is localised about $\theta = \pm\theta_0$, as shown in the figure below.

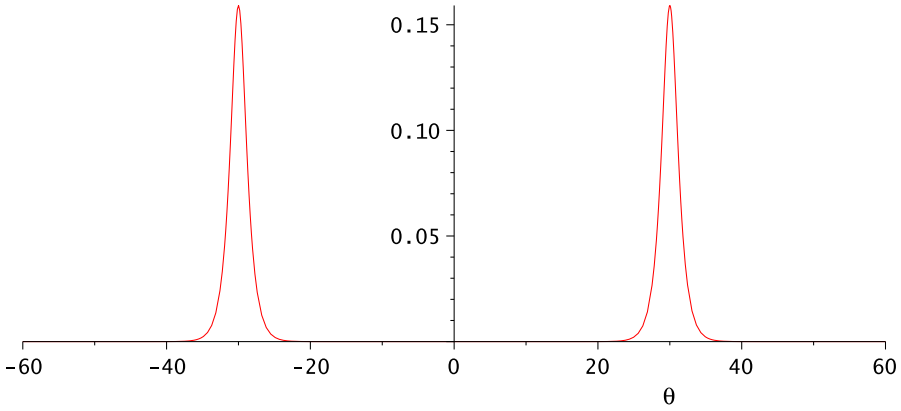

Figure 4.1: The staircase kernel $\phi_S(\theta)$ with $\theta_0 = 30$.

The integral of $\phi(\theta)$ is

$$\int_{\mathbb{R}} \phi(\theta) d\theta = \tfrac{1}{2}. \tag{4.1.7}$$

To study the form of the pseudoenergy $\varepsilon(\theta)$ the terms of the TBA equation must be considered as r and θ vary, following [42] and [43]. The driving term for the equation is $r\cosh(\theta)$, and the form of $\varepsilon(\theta)$ depends on the size of this term. When $re^{\theta} \gg 1$ or $re^{-\theta} \gg 1$ the TBA equation is dominated by the driving term. $\ln(1 + e^{-\varepsilon(\theta)})$ therefore experiences double-exponential decay in these θ-regions so that $L(\theta) \sim 0$ for $\theta \gg \ln(1/r)$ and $\theta \ll -\ln(1/r)$. These regions overlap for $r > 1$, so for $r \to \infty$ $L(\theta) = 0$ for all values of θ. As r decreases towards $r = 1$, both $\ln(1/r)$

and $-\ln(1/r)$ tend towards zero and $L(\theta)$ has a small non-zero region centred around $\theta = 0$. For $r < 1$, $L(\theta)$ becomes significant in the regions around $|\theta| = \ln(1/r)$ where $r\cosh(\theta)$ is of order 1. For $|\theta| < \ln(1/r)$ the driving term becomes small and the TBA is instead dominated by the convolution term involving $\phi(\theta)$ and $L(\theta)$. So, for $r < 1$, $L(\theta)$ is zero for $|\theta| \gg \ln(1/r)$ and then becomes non-zero, taking the form of a kink, for $|\theta| \approx \ln(1/r)$ before becoming constant again (but not necessarily zero) as $|\theta|$ decreases further and the driving term becomes insignificant.

However, this is not the full story for $|\theta| < \ln(1/r)$. The presence of θ_0 in the kernel means that the TBA equation couples $\varepsilon(\theta)$ to $\varepsilon(\theta + \theta_0)$ and $\varepsilon(\theta - \theta_0)$, and so the kinks centred on $\theta = \pm\ln(1/r)$ affect the form of $L(\theta)$ for $|\theta| < \ln(1/r)$ (the form is unaffected outside this region because there the driving term dominates). The form of the $L(\theta)$ as r varies depends on the number of integer multiples n of θ_0 that fit within the interval $[-\ln(1/r), \ln(1/r)]$. The behaviour at some particular value of n can be considered by working in the limit where $\theta_0, \ln(1/r) \to \infty$ in such a way that

$$(m-3)\theta_0 \ll 2\ln(1/r) \ll (m-2)\theta_0. \tag{4.1.8}$$

As will become apparent later, the labelling of the integers here is to aid the identification with the minimal models $\mathcal{M}_m$. The regions $\theta < \ln(1/r) - n\theta_0$ and $\theta > -\ln(1/r) + n\theta_0$ cannot be coupled to either the left or right hand kinks, so $L(\theta)$ is constant in these regions. However, for $\theta \approx -\ln(1/r) + k\theta_0$ or $\theta \approx \ln(1/r) - k\theta_0$ for $k \leq n \in \mathbb{Z}$, $L(\theta)$ is coupled to the left and right-hand kinks respectively, and the picture becomes more complicated.

The form of $L(\theta)$ becomes more clear when the derivative $L'(\theta)$ is considered. So far it is known that as θ increases through the region $\theta < \ln(1/r) - n\theta_0$, $L'(\theta)$ is initially zero, and then becomes non-zero around $\theta = -\ln(1/r)$ while $L(\theta)$ takes the form of a kink, before returning to zero as $L(\theta)$ becomes constant. The same pattern occurs as θ decreases through the region $\theta > -\ln(1/r) + n\theta_0$. Differentiating the TBA equation (4.1.6) (using $d\phi(\theta - \theta')/d\theta = -d\phi(\theta - \theta')/d\theta'$ and integration by parts to get the second term) gives

$$\varepsilon'(\theta) = r\sinh\theta - \int_{\mathbb{R}} \phi(\theta - \theta')\left(L'(\theta' + \theta_0) + L'(\theta' - \theta_0)\right) d\theta'. \tag{4.1.9}$$

Noting also that

$$L'(\theta) = \frac{-\varepsilon' e^{-\varepsilon(\theta)}}{1 + e^{-\varepsilon(\theta)}} \tag{4.1.10}$$

the above equation couples $L'(\theta)$ to $L'(\theta \pm \theta_0)$, and hence to $L'(\theta \pm 2\theta_0)$ and so on. For $|\theta| < \ln(1/r)$ the $\sinh(\theta)$ term can be ignored, so using the localised nature of $\phi(\theta)$ it is clear from the equation that $L'(\theta)$ will be zero at all points except in the regions around $\mp \ln(1/r) \pm k\theta_0$, $k \in 0, \cdots, n$. So there are kinks at $-\ln(1/r) + k\theta_0$ and at $\ln(1/r) - k\theta_0$ for all $k \in 1, \cdots, n$ which are 'descendants' of the 'seed' kinks at $\theta \approx \pm \ln(1/r)$.

The form of $L(\theta)$ changes as the value of r decreases and $\ln(1/r)$ increases. At points where $2\ln(1/r)$ is equal to an integer multiple of θ_0 the form of $L(\theta)$ undergoes a transition after which each of the two seed kinks will have one more descendant. So every time $\lfloor 2\ln(1/r)/\theta_0 \rfloor$ increases by one the number of kinks increases by two. For $(m-3)\theta_0 \ll 2\ln(1/r) \ll (m-2)\theta_0$ there are a total of $2m-4$ kinks, which are labelled from right to left as as K_i, $i = 1 \cdots 2m-4$. Between each pair of consecutive kinks there are near-constant plateaux, and including the $L(\theta) = 0$ plateaux to the left of K_{2m-4} and to the right of K_1 there are $2m-3$ such plateaux. The value of θ at the centre of the non-zero plateau immediately to the left of K_i is

$$z_i = \frac{(m-2-i)\theta_0}{2} \qquad i = 1 \cdots 2m-5 \tag{4.1.11}$$

and z_0 and z_{2m-4} are taken to indicate some arbitrary values lying in the right and left hand zero-valued plateaux respectively. The widths of the non-zero plateaux alternate: defining $\alpha = 2\ln(1/r) - (m-3)\theta_0$, α satisfies $0 \ll \alpha \ll \theta_0$, and then the plateaux centred on z_i for i odd have width α and those with i even have width $\theta_0 - \alpha$. The values of $\varepsilon(\theta)$ and $L(\theta)$ on the plateaux are labelled by ε_i and L_i for $i = 0 \cdots 2m-4$. The form of $L(\theta)$ for various values of r is shown in figure 4.2.

It is the effect of this behaviour on the effective central charge that gives the theory its staircase nature. The effective central charge $c_{eff}(r)$ is

$$c_{eff}(r) = \frac{3}{\pi^2} \int_{\mathbb{R}} r \cosh(\theta) L(\theta) d\theta. \tag{4.1.12}$$

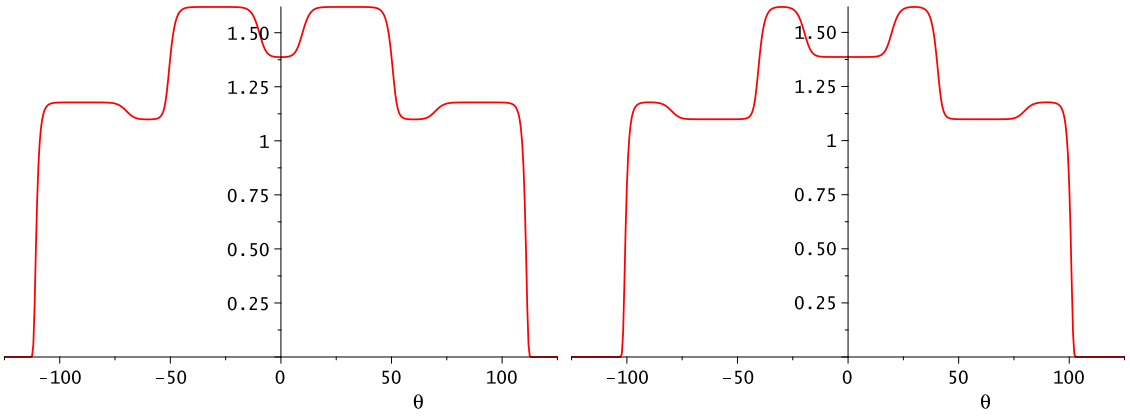

(a) $\ln r = -110$ (b) $\ln r = -100$

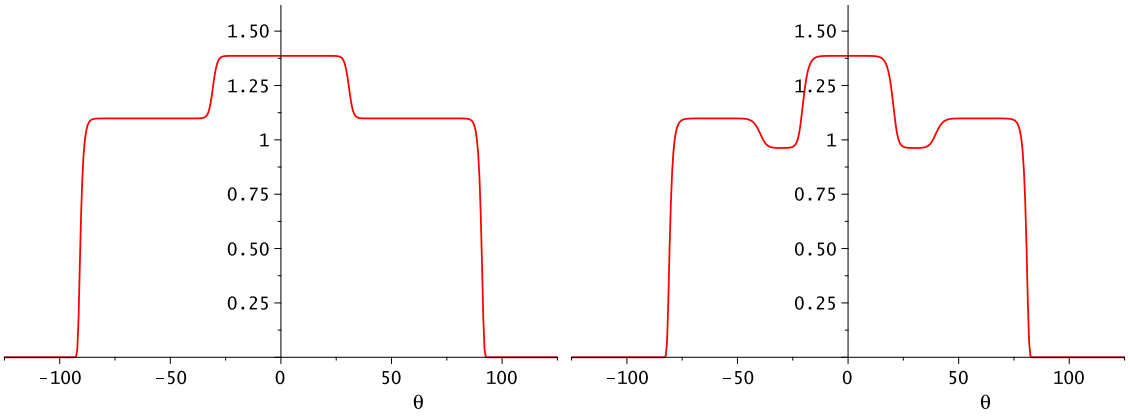

(c) $\ln r = -90$ (d) $\ln r = -80$

Figure 4.2: Plots of $L(\theta)$ at $\ln r = -110, -100, -90$ and -80. As will be described in the main text, the theory passes close to each of the unitary minimal models $\mathcal{M}_m$ in turn as r varies. Here, for the first two plots the theory is close to $\mathcal{M}_6$. The third then shows $L(\theta)$ when the theory is in the crossover period between $\mathcal{M}_6$ and $\mathcal{M}_5$, and for the final plot the theory is close to $\mathcal{M}_5$.

The plot in figure 4.3 shows how, for sufficiently large θ_0, the value of $c_{eff}(r)$ passes through a series of plateaux as r varies, the values of which are those of the central charges of the unitary minimal models

$$c_{\mathcal{M}_m} = 1 - \frac{6}{m(m+1)}. \tag{4.1.13}$$

To see more explicitly why this should be the case, $c_{eff}(r)$ can be decomposed as

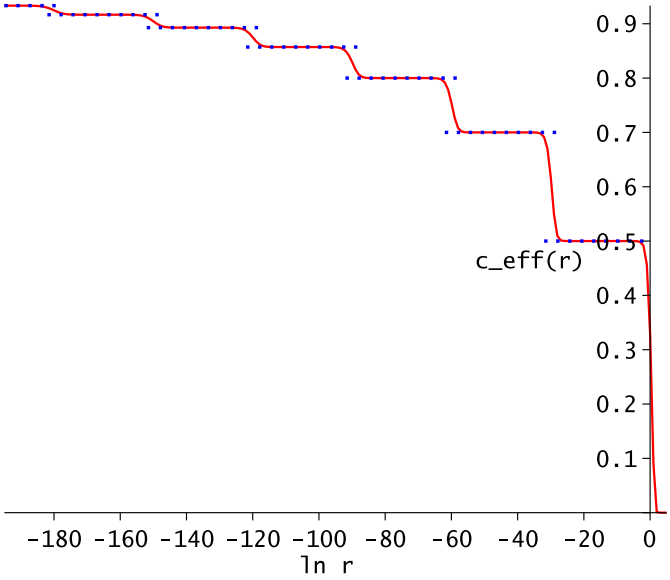

Figure 4.3: Plot of $c_{eff}(r)$ for $r = -195 \cdots 5$. The blue dotted lines show the values of the central charges of the minimal models $\mathcal{M}_m$ for $m = 3 \cdots 9$ moving from right to left.

$c_{eff}(r) = c_+ + c_-$, with

$$c_+ = \frac{3}{2\pi^2} \int_{-\infty}^{\infty} re^{\theta} L(\theta) d\theta \tag{4.1.14}$$

$$c_- = \frac{3}{2\pi^2} \int_{-\infty}^{\infty} re^{-\theta} L(\theta) d\theta, \tag{4.1.15}$$

where $c_+ = c_-$ by the symmetry of $L(\theta)$. Since $L(\theta) \sim 0$ for $|\theta| \gg \ln(1/r)$, $re^{\theta}/2 \sim 0$ for $\theta \ll \ln(1/r)$ and $re^{-\theta}/2 \sim 0$ for $\theta \gg -\ln(1/r)$, the domains of integration can be restricted to K_1 for c_+ and K_{2m-4} for c_-. The methods used in [43] can now be followed to find c_{eff} entirely in terms of $\varepsilon(\theta)$ and $L(\theta)$. The TBA equation (4.1.6) is first differentiated with respect to θ, then multiplied by $L(\theta)$ before being integrated over the kink K_i to give

$$A^i = C^i - B^i_+ - B^i_- \tag{4.1.16}$$

where

$$A^i = \int_{K_i} d\theta\, \varepsilon'(\theta) L(\theta) \tag{4.1.17}$$

$$B^i_{\pm} = \int_{K_i} d\theta \int_{\mathbb{R}} d\theta'\, \phi'(\theta - \theta') L(\theta' \pm \theta_0) L(\theta) \tag{4.1.18}$$

$$C^i = \int_{K_i} d\theta\, r \sinh\theta L(\theta). \tag{4.1.19}$$

Also

$$r\sinh\theta = \frac{r}{2}\left(e^{\theta} - e^{-\theta}\right) \sim \begin{cases} \frac{re^{\theta}}{2} & \text{for} \quad \theta \in K_1 \\ 0 & \text{for} \quad \theta \in K_2, \cdots, K_{2m-5} \\ \frac{-re^{-\theta}}{2} & \text{for} \quad \theta \in K_{2m-4} \end{cases} \tag{4.1.20}$$

so

$$\frac{3}{\pi^2}\int_{K_i} r\sinh\theta L(\theta) d\theta = \delta_{i,1} c_+ - \delta_{i,2m-4} c_-. \tag{4.1.21}$$

Therefore, focussing on the $i = 1$ part of (4.1.20) gives

$$\frac{\pi^2}{3} c_+ = A^1 + B^1_+ + B^1_-. \tag{4.1.22}$$

This can be manipulated using the following result from [43]

$$\int_{K_i} d\theta f' * P(\theta)Q(\theta) = -\int_{K_i} d\theta f' * Q(\theta)P(\theta) + \left(\int_{-\infty}^{\infty} d\theta f(\theta)\right)\left[P(\theta)Q(\theta)\right]_{z_i}^{z_{i-1}} \tag{4.1.23}$$

where

$$\alpha * \beta(\theta) = \int_{\mathbb{R}} d\theta' \alpha(\theta - \theta')\beta(\theta'), \tag{4.1.24}$$

$f(\theta)$ is an even function with its support concentrated at the origin, and $P(\theta)$ and $Q(\theta)$ vary slowly with respect to the scale of the support of f close to z_{i-1} and z_i. In the case in question, $\phi(\theta)$ has the properties of $f(\theta)$ and $L(\theta)$ behaves like $P(\theta)$

and $Q(\theta)$. So

$$\int_{K_i} d\theta \int_{\mathbb{R}} d\theta' \, \phi'(\theta-\theta') L(\theta' \pm \theta_0) L(\theta) \tag{4.1.25}$$

$$= -\int_{K_i} d\theta \int_{\mathbb{R}} d\theta' \, \phi'(\theta-\theta') L(\theta') L(\theta \pm \theta_0) + \left(\int_{-\infty}^{\infty} d\theta \, \phi(\theta) \right) \left[L(\theta) L(\theta \pm \theta_0) \right]_{z_i}^{z_{i-1}} \tag{4.1.26}$$

$$= -\int_{K_{i\mp 2}} d\theta \int_{\mathbb{R}} d\theta' \, \phi'(\theta-\theta') L(\theta' \mp \theta_0) L(\theta) + \tfrac{1}{2} \left[L(\theta) L(\theta \pm \theta_0) \right]_{z_i}^{z_{i-1}} . \tag{4.1.27}$$

Both variables are shifted by $\pm\theta_0$ in going from the second to the third lines, and $K_i \pm \theta_0 = K_{i\mp 2}$ is used. Therefore,

$$B_{\pm}^{i} = -B_{\mp}^{i\mp 2} + \tfrac{1}{2} \left[L(\theta) L(\theta \pm \theta_0) \right]_{z_i}^{z_{i-1}} \tag{4.1.28}$$

Since $B_{-}^{-1} = 0$ and $\left[L(\theta) L(\theta + \theta_0) \right]_{z_1}^{z_0} = 0$ this means that $B_{+}^{1} = 0$, so applying (4.1.28) to (4.1.22)

$$\frac{\pi^2}{3} c_+ = A^1 - B_{+}^{3} + \tfrac{1}{2} \left[L(\theta) L(\theta - \theta_0) \right]_{z_1}^{z_0} . \tag{4.1.29}$$

From (4.1.16) $B_{+}^{3} = -A^3 - B_{-}^{3}$, and then from (4.1.28) $B_{-}^{3} = -B_{+}^{5} + \frac{1}{2} \left[L(\theta) L(\theta - \theta_0) \right]_{z_3}^{z_2}$, and so on, resulting in

$$\frac{\pi^2}{3} c_+ = \sum_{j=1}^{m-2} \left(A^{2j-1} + \tfrac{1}{2} \left[L(\theta) L(\theta - \theta_0) \right]_{z_{2j-1}}^{z_{2j-2}} \right) . \tag{4.1.30}$$

Also

$$\left[L(\theta) L(\theta - \theta_0) \right]_{z_{2j-1}}^{z_{2j-2}} = L(z_{2j-2}) L(z_{2j-2} - \theta_0) - L(z_{2j-1}) L(z_{2j-1} - \theta_0) \tag{4.1.31}$$

$$= L(z_{2j} + \theta_0) L(z_{2j}) - L(z_{2j+1} + \theta_0) L(z_{2j+1}) \tag{4.1.32}$$

$$= \left[L(\theta) L(\theta + \theta_0) \right]_{z_{2j+1}}^{z_{2j}} \tag{4.1.33}$$

so

$$\frac{\pi^2}{3} c_+ = \sum_{j=1}^{m-2} \left(A^{2j-1} + \frac{1}{4} \left[L(\theta) \left(L(\theta + \theta_0) + L(\theta - \theta_0) \right) \right]_{z_{2j-1}}^{z_{2j-2}} \right) , \tag{4.1.34}$$

using $[L(\theta)L(\theta+\theta_0)]_{z_1}^{z_0} = 0 = [L(\theta)L(\theta-\theta_0)]_{z_{2m-5}}^{z_{2m-6}}$. Revisiting the TBA equation (4.1.6) and setting $\theta = z_i$, $i = 1, \cdots, 2m-5$ gives

$$\varepsilon(z_i) = \varepsilon_i = -\tfrac{1}{2}\left(L(z_i+\theta_0) + L(z_i-\theta_0)\right). \tag{4.1.35}$$

The surface term in the expression for c_+ only involves these particular values of θ, so (4.1.34) becomes

$$\frac{\pi^2}{3}c_+ = \sum_{j=1}^{m-2}\left(\int_{K_{2j-1}} \varepsilon'(\theta)L(\theta)d\theta - \frac{1}{2}\left[L(\theta)\varepsilon(\theta)\right]_{z_{2j-1}}^{z_{2j-2}}\right). \tag{4.1.36}$$

Changing the variable twice,

$$\int_{K_{2j-1}} \varepsilon'(\theta)L(\theta)d\theta = \int_{\varepsilon_{2j-1}}^{\varepsilon_{2j-2}} \ln(1+e^{-\varepsilon})d\varepsilon \tag{4.1.37}$$

$$= -\int_{-e^{-\varepsilon_{2j-1}}}^{-e^{-\varepsilon_{2j-2}}} \frac{\ln(1-u)}{u}du \tag{4.1.38}$$

$$= \mathrm{Li}_2\left(-e^{-\varepsilon_{2j-2}}\right) - \mathrm{Li}_2\left(-e^{-\varepsilon_{2j-1}}\right), \tag{4.1.39}$$

where $\mathrm{Li}_2(x)$ is the dilogarithm function defined as

$$\mathrm{Li}_2(x) = \int_x^0 \frac{\ln(1-u)}{u}du. \tag{4.1.40}$$

This expression can be simplified further by introducing new notation for the plateau values

$$e^{-\varepsilon_i} = \begin{cases} x_{(i+3)/2} & \text{for } i \text{ odd} \\ y_{(i+2)/2} & \text{for } i \text{ even} \end{cases} \tag{4.1.41}$$

so that the non-zero plateau values of $L(\theta)$ are

$$\ln(1+x_a) \quad \text{for} \quad z_{2a-3} - \alpha/2 \ll \theta \ll z_{2a-3} + \alpha/2\,, \quad a = 2\ldots m-1 \qquad \text{and} \tag{4.1.42}$$

$$\ln(1+y_a) \quad \text{for} \quad z_{2a-2} - (\theta_0-\alpha)/2 \ll \theta \ll z_{2a-2} + (\theta_0-\alpha)/2\,, \quad a = 2\ldots m-2, \tag{4.1.43}$$

where α is defined in the discussion immediately after (4.1.11) as

$$\alpha = 2\ln(1/r) - (m-3)\theta_0, \tag{4.1.44}$$

and the plateaux form the sequence

$$\{\ln(1+x_{m-1}), \ln(1+y_{m-2}), \ln(1+x_{m-2}), \cdots, \ln(1+y_2), \ln(1+x_2))\}. \tag{4.1.45}$$

The x_a and y_a can be evaluated from the TBA equation, as this couples each x_a plateau to all other x_a plateaux, and similarly for the y_a plateaux:

$$x_a = \sqrt{(1+x_{a-1})(1+x_{a+1})} \quad a = 2\cdots m-1 \tag{4.1.46}$$

$$y_a = \sqrt{(1+y_{a-1})(1+y_{a+1})} \quad a = 2\cdots m-2. \tag{4.1.47}$$

The solution to these equations is [44]

$$1+x_a = \frac{\sin^2\left(\frac{\pi a}{m+1}\right)}{\sin^2\left(\frac{\pi}{m+1}\right)}, \quad 1+y_a = \frac{\sin^2\left(\frac{\pi a}{m}\right)}{\sin^2\left(\frac{\pi}{m}\right)}. \tag{4.1.48}$$

From (4.1.48), $\ln(1+x_1) = \ln(1+y_1) = 0 = \ln(1+y_{m-1}) = \ln(1+x_m)$, and so since $L(\theta)$ is zero for $\theta \ll -\ln(1/r)$ and $\theta \gg \ln(1/r)$, these constants can be added to the sequence (4.1.45) in their natural places. Note that $x_a = x_{m+1-a}$ and $y_a = y_{m-a}$, which reflects the more general symmetry $L(\theta) = L(-\theta)$. These plateau values are approximate, becoming exact when the limit $\theta_0 \to \infty$ is taken in such a way that $-(m-2)\theta_0/2 \ll \ln r \ll -(m-3)\theta_0/2$. In the following sections these values will be described as the plateau values of $L(\theta)$, and the caveat that they only become exact in such a limit will be left implicit.

Returning to the calculation of c_+, Li_2 is related to the Rogers dilogarithm $\mathcal{L}(x)$ function by

$$\mathcal{L}\left(\frac{x}{1+x}\right) = -\mathrm{Li}_2(-x) - \tfrac{1}{2}\ln(1+x)\ln(x) \tag{4.1.49}$$

so on including the surface term

$$c_+ = \frac{3}{\pi^2}\sum_{j=1}^{m-2}\left(\mathcal{L}\left(\frac{x_{j+1}}{1+x_{j+1}}\right) - \mathcal{L}\left(\frac{y_j}{1+y_j}\right)\right). \tag{4.1.50}$$

This can be evaluated using various sum rules for the Rogers dilogarithm [45]:

$$\sum_{k=2}^{n-2}\mathcal{L}\left(\frac{\sin^2\frac{\pi}{n}}{\sin^2\frac{k\pi}{n}}\right) = \frac{\pi^2(n-3)}{3n} \tag{4.1.51}$$

$$\mathcal{L}(x) + \mathcal{L}(1-x) = \frac{\pi^2}{6} \tag{4.1.52}$$

$$\mathcal{L}(1) = \frac{\pi^2}{6} \tag{4.1.53}$$

$$\mathcal{L}(0) = 0. \tag{4.1.54}$$

Combining these gives

$$\sum_{j=1}^{m-2}\mathcal{L}\left(\frac{x_{j+1}}{1+x_{j+1}}\right) = \frac{\pi^2(m-2)}{6} - \frac{\pi^2(m-2)}{3(m+1)} \tag{4.1.55}$$

$$\sum_{j=1}^{m-2}\mathcal{L}\left(\frac{y_j}{1+y_j}\right) = \frac{\pi^2(m-2)}{6} - \frac{\pi^2(m-3)}{3m} - \frac{\pi^2}{6} \tag{4.1.56}$$

which leads to

$$c_{eff} = 2c_+ = 1 - \frac{6}{m(m+1)}. \tag{4.1.57}$$

This is equal to the central charge for the minimal model $\mathcal{M}_m$. So, for $(m-3)\theta_0 \ll 2\ln(1/r) \ll (m-2)\theta_0$, the theory is close to the minimal model $\mathcal{M}_m$, and as r increases, the transition from $\mathcal{M}_m$ to $\mathcal{M}_{m-1}$ occurs at $\ln(r) \approx -(m-3)\theta_0/2$. Therefore, as r varies from 0 to ∞, $c_{eff}(r)$ descends a staircase, with the steps made up of the central charges c_m of the minimal models $\mathcal{M}_m$. The RG flow of the staircase model therefore begins in the UV at a fixed point described by the model $M_{m\to\infty}$, and then flows close to a series of fixed points made up of the minimal models M_m, before flowing to a massive theory in the IR limit. This interpretation is supported by perturbative work done for $m \gg 1$ [46]. The behaviour just described is depicted in figure 4.4.

Another important property of the staircase model that has emerged here is

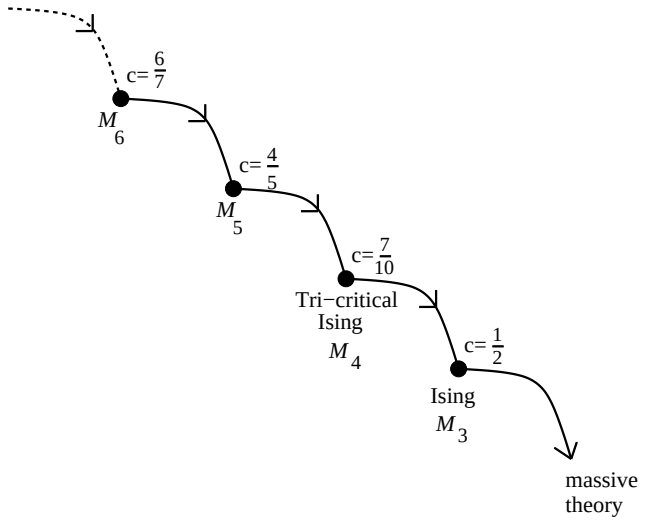

Figure 4.4: Depiction of the flow in the bulk theory of the staircase model.

that the plateau values x_a and y_a when $(m-3)\theta_0 \ll 2\ln(1/r) \ll (m-2)\theta_0$ are the same as those that appear in the UV of the $\mathcal{M}A_m^{(+)}$ models [18, 44]. Coupled with the matching of the central charge values, this indicates that in this limit the TBA equation for the staircase model decouples into the $\mathcal{M}A_m^{(+)}$ equations. This will be explored in more detail in section 5.3.

4.2 The Staircase Model with Boundaries

The focus of the next chapter will be to analyse this theory when it is defined on a space with boundaries using the g-function, as introduced in section 3.3. Since the staircase model is a massive diagonal theory the expression for its exact g-function should be given by the formula (3.3.4), with the particle number N set to one. One further piece of information that is needed to write down an expression for the g-function is the reflection factor for this theory. Since the staircase model S-matrix arose from analytic continuation from the sinh-Gordon model, it seems natural to perform the same analytic continuation on the reflection factor of that model. The reflection factor for the boundary sinh-Gordon model with no additional boundary degrees of freedom [47] follows from that of the first sine-Gordon breather which was found in [48]. This involves the two parameters that determine the integrable

boundary conditions in the boundary sine- and sinh-Gordon models [33]. After continuing the sinh-Gordon bulk coupling the staircase model reflection factor is found to be

$$R(\theta) = \frac{(\frac{1}{2})(\frac{3}{4} - \frac{i\theta_0}{2\pi})(\frac{3}{4} + \frac{i\theta_0}{2\pi})}{(\frac{1}{2} - \frac{E}{2})(\frac{1}{2} + \frac{E}{2})(\frac{1}{2} - \frac{F}{2})(\frac{1}{2} + \frac{F}{2})}, \tag{4.2.1}$$

using the same block notation as before (3.3.11). E and F are related to the two original boundary parameters of the sinh-Gordon model. They often take real values in the sinh-Gordon model, but just as the bulk coupling was analytically continued, in the staircase model it will be interesting to consider the boundary parameters at complex values for which real-analyticity is preserved. The staircase model boundary parameters are therefore taken to be real parameters θ_{b1} and θ_{b2} defined via

$$E = \frac{2i\theta_{b1}}{\pi}\ , \qquad F = \frac{2i\theta_{b2}}{\pi}. \tag{4.2.2}$$

Using (3.3.4), the logarithm of the g-function is then [1]

$$\ln g(r) = \ln g_0(r) + \ln g_b(r) \tag{4.2.3}$$

where

$$\ln g_0(r) = \sum_{n=1}^{\infty} \frac{1}{2n} \int_{\mathbb{R}^n} \frac{d\theta_1}{1+e^{\varepsilon(\theta_1)}} \cdots \frac{d\theta_n}{1+e^{\varepsilon(\theta_n)}} \phi_S(\theta_1+\theta_2)\phi_S(\theta_2-\theta_3)\cdots\phi_S(\theta_n-\theta_1) \tag{4.2.4}$$

and

$$\ln g_b(r) = \frac{1}{2}\int_{\mathbb{R}} d\theta \left(\phi_b(\theta) - \phi_S(2\theta) - \tfrac{1}{2}\,\delta(\theta)\right) L(\theta). \tag{4.2.5}$$

Here $\varepsilon(\theta)$ solves the TBA equation (4.1.3), $\phi_S(\theta)$ is the bulk kernel defined in (4.1.5), and $\phi_b(\theta)$ is the boundary kernel which expressed in the block notation (3.3.11) is

$$\begin{aligned} \phi_b(\theta) &= -\frac{i}{2\pi}\frac{d}{d\theta}\ln R(\theta) \\ &= -\phi(\theta) + \phi_{(\frac{3}{4})}(\theta - \tfrac{1}{2}\theta_0) + \phi_{(\frac{3}{4})}(\theta + \tfrac{1}{2}\theta_0) \\ &\qquad + \phi(\theta-\theta_{b1}) + \phi(\theta+\theta_{b1}) + \phi(\theta-\theta_{b2}) + \phi(\theta+\theta_{b2})\,. \end{aligned} \tag{4.2.6}$$

The properties

$$(a+b)(\theta)(a-b)(\theta) = (a)(\theta + i\pi b)(a)(\theta - i\pi b) \tag{4.2.7}$$

and

$$\phi_{(\frac{1}{2})}(\theta) = -\frac{1}{2\pi\cosh(\theta)} = -\phi(\theta) \tag{4.2.8}$$

are used in defining the above. Like $\phi(\theta)$, the function $\phi_{(3/4)}(\theta)$ has its support close to $\theta = 0$, as can be seen in figure 4.5. and its integral is

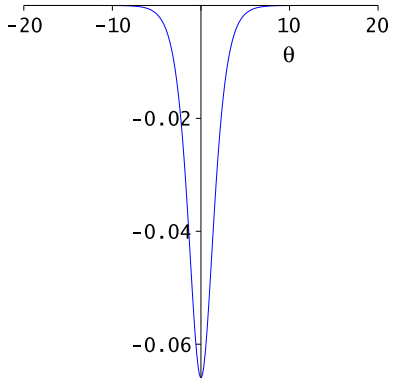

Figure 4.5: Plot of $\phi_{(3/4)}(\theta)$

$$\int_{\mathbb{R}} \phi_{(3/4)}(\theta)d\theta = -\frac{1}{4}. \tag{4.2.9}$$

Collecting together the boundary parameter-dependent terms and those with explicit θ_0-dependence, $\ln g_b$ splits naturally into three new terms as $\ln g_b = \ln g_{b1} + \ln g_{b2} + \ln g_{b3}$, with

$$\ln g_{b1} = \frac{1}{2}\int_{\mathbb{R}} d\theta \left(-\phi(\theta) - \tfrac{1}{2}\delta(\theta)\right) L(\theta)\,, \tag{4.2.10}$$

$$\ln g_{b2} = \frac{1}{2}\int_{\mathbb{R}} d\theta \left(\phi_{(\frac{3}{4})}(\theta - \tfrac{1}{2}\theta_0) + \phi_{(\frac{3}{4})}(\theta + \tfrac{1}{2}\theta_0) - \phi(2\theta - \theta_0) - \phi(2\theta + \theta_0)\right) L(\theta)\,, \tag{4.2.11}$$

$$\ln g_{b3} = \frac{1}{2}\int_{\mathbb{R}} d\theta \left(\phi(\theta - \theta_{b1}) + \phi(\theta + \theta_{b1}) + \phi(\theta - \theta_{b2}) + \phi(\theta + \theta_{b2})\right) L(\theta)\,. \tag{4.2.12}$$

As was discussed in the previous section, $L(\theta)$ is made up of a series of plateaux,

with the number of plateaux depending on the number of integer multiples of θ_0 in the interval $[-\ln(1/r), \ln(1/r)]$, so that the form of $L(\theta)$ varies with r. Coupled with the localised nature of $\phi(\theta)$ and $\phi_{(3/4)}(\theta)$, this means that in the large-θ_0 limit the g-function itself passes through a series of plateaux as r varies. The dependence on $L(\theta)$ and $\varepsilon(\theta)$ means that the plateaux of the g-function occur when the bulk theory is close to a minimal model (although as will be described below, boundary crossovers can occur while the bulk theory stays close to the same minimal model, meaning that $g(r)$ can visit more than one plateau value while $c_{eff}(r)$ remains on the same step). This means that each plateau of the g-function is expected to correspond to the conformal g-function value of either a single Cardy boundary condition or a superposition of them. From (3.1.21), the g-function value of a Cardy boundary condition (a, b) in the unitary minimal model $\mathcal{M}_m$ is

$$g(m, a, b) = \left(\frac{8}{m(m+1)}\right)^{\frac{1}{4}} \frac{\sin(\frac{a\pi}{m})\sin(\frac{b\pi}{m+1})}{\sqrt{\sin(\frac{\pi}{m})\sin(\frac{\pi}{m+1})}}, \tag{4.2.13}$$

with the g-function for a superposition of n boundary conditions $(a_1, b_1)\&(a_2, b_2)\&\cdots\&(a_n, b_n)$ being

$$g(m, (a_1, b_1)\&(a_2, b_2)\&\cdots\&(a_n, b_n)) = \sum_{i=1}^{n} g(m, a_i, b_i). \tag{4.2.14}$$

In the following sections rules will be developed that use the flow in the g-function to identify each pair of boundary parameters $(\theta_{b1}, \theta_{b2})$ with a series of conformal boundary conditions as r varies. In addition, by focussing on pairs of consecutive 'steps' in the staircase model, exact equations will be derived for the g-function of the $\mathcal{M}A_m^{(+)}$ models. The next section demonstrates how this can be done for the final 'step' of the staircase model, as the bulk theory flows from $\mathcal{M}_4$ to $\mathcal{M}_3$.

Chapter 5

The Staircase Model g-function

5.1 Warm-up Example: $\mathcal{M}A_4^{(+)}$

The focus of this warm-up example is to show how equations for the exact g-function of the boundary version of the interpolating theory $\mathcal{M}A_4^{(+)}$ can be extracted from the staircase model g-function, and will give a more detailed derivation of the results of Dorey, Rim and Tateo [41] which were discussed in section 3.3. $\mathcal{M}A_4^{(+)}$ interpolates between the minimal models $\mathcal{M}_4$ and $\mathcal{M}_3$ in the bulk, so the only values of r that are of interest when considering how this theory might emerge from the staircase model are those for which the bulk theory comes close to or moves between these minimal models. From (4.1.57), the effective central charge of the staircase model is close to 7/10 when $\theta_0/2 \ll \ln(1/r) \ll \theta_0$ and 1/2 when $0 \ll \ln(1/r) \ll \theta_0/2$, so as $\ln(1/r)$ decreases through the domain

$$0 \ll \ln(1/r) \ll \theta_0, \tag{5.1.1}$$

the bulk theory moves from the vicinity of the minimal model $\mathcal{M}_4$ to that of $\mathcal{M}_3$, with the crossover occurring at $\ln(1/r) \approx \theta_0/2$. In order for $\mathcal{M}A_4^{(+)}$ to be described exactly, the staircase model must be 're-focussed' about $\ln(1/r) = \theta_0/2$, with θ_0 taken to infinity so that whatever the value of r, it is impossible for the theory to reach either the 'step' above $\mathcal{M}_4$, i.e. $\mathcal{M}_5$, or the massive theory which forms the IR limit of the staircase model. A new variable $\hat{r}$ must also be defined, which

when varied from zero to infinity moves the theory along the full RG flow of $\mathcal{M}A_4^{(+)}$. Formally, this is achieved by defining

$$\ln r = -\theta_0/2 + \ln \hat{r} \tag{5.1.2}$$

and taking a double-scaling limit where $\hat{r}$ is initially held finite while the limit $\theta_0 \to \infty$ is taken, after which $\ln \hat{r}$ is allowed to vary over the full real line. Note that the bulk crossover occurs at $\ln \hat{r} \approx 0$.

Turning now to the form of the pseudoenergy $\varepsilon(\theta)$, the figure below shows the form $L(\theta)$ at values of r for which the bulk theory is close to $\mathcal{M}_4$ and $\mathcal{M}_3$, and during the transition between them. It is natural to divide $L(\theta)$ into two mirror-

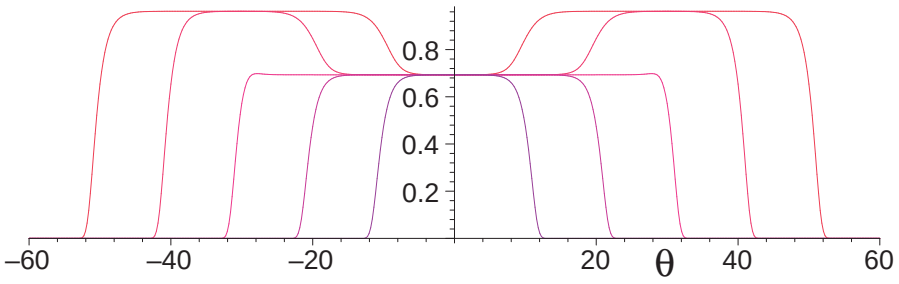

Figure 5.1: Plots of $L(\theta)$ produced with $\theta_0 = 60$. From the highest to lowest curves the values of r are $\ln r = -50$, -40, -30, -20 and -10. When $\ln r = -50$ and $\ln r = -40$ the bulk theory is close to $\mathcal{M}_4$, the bulk crossover from $\mathcal{M}_4$ to $\mathcal{M}_3$ occurs when $\ln r \approx -30$, and when $\ln r = -20$ and $\ln r = -10$ the bulk theory is close to $\mathcal{M}_3$.

image parts, centred on $\theta_0/2$ and $-\theta_0/2$, which become infinitely separated as the limit $\theta_0 \to \infty$ is taken. By holding θ finite as this limit is taken, each of these two parts can be 'tracked' as $\theta_0 \to \infty$ by defining the following functions

$$\varepsilon_1(\theta) = \lim_{\theta_0 \to \infty} \varepsilon\left(\theta + \frac{\theta_0}{2}\right) \quad \text{and} \quad \varepsilon_2(\theta) = \lim_{\theta_0 \to \infty} \varepsilon\left(\theta - \frac{\theta_0}{2}\right) \tag{5.1.3}$$

which clearly satisfy $\varepsilon_1(\theta) = \varepsilon_2(-\theta)$. θ is only allowed to vary over the full real line

once the limit has been taken. Similarly

$$\begin{aligned} L_1(\theta) &= \ln(1+e^{\varepsilon_1(\theta)}) = \lim_{\theta_0\to\infty} L\left(\theta+\frac{\theta_0}{2}\right) \quad \text{and} \\ L_2(\theta) &= \ln(1+e^{\varepsilon_2(\theta)}) = \lim_{\theta_0\to\infty} L\left(\theta-\frac{\theta_0}{2}\right). \end{aligned} \tag{5.1.4}$$

Using (5.1.2), in the double-scaling limit the staircase TBA (4.1.6) can be re-expressed in terms of these new functions as

$$\begin{aligned} \varepsilon_1(\theta) &= \lim_{\theta_0\to\infty} \tfrac{1}{2}\hat{r}e^{-\theta_0/2}\left(e^{\theta+\theta_0/2}+e^{-(\theta+\theta_0/2)}\right) \\ &\quad - \int_{\mathbb{R}} \phi\left(\theta+\frac{\theta_0}{2}-\theta'\right)\left(L(\theta'+\theta_0)+L(\theta'-\theta_0)\right)d\theta' \\ &= \lim_{\theta_0\to\infty}\left(\tfrac{1}{2}\hat{r}\left(e^{\theta}+e^{-(\theta+\theta_0)}\right) - \int_{\mathbb{R}} \phi\left(\theta-\theta'\right)\left(L\left(\theta'+\frac{3\theta_0}{2}\right)+L\left(\theta'-\frac{\theta_0}{2}\right)\right)d\theta'\right) \end{aligned} \tag{5.1.5}$$

and

$$\begin{aligned} \varepsilon_2(\theta) &= \lim_{\theta_0\to\infty} \tfrac{1}{2}\hat{r}e^{-\theta_0/2}\left(e^{\theta-\theta_0/2}+e^{-(\theta-\theta_0/2)}\right) \\ &\quad - \int_{\mathbb{R}} \phi\left(\theta-\frac{\theta_0}{2}-\theta'\right)\left(L(\theta'+\theta_0)+L(\theta'-\theta_0)\right)d\theta' \\ &= \lim_{\theta_0\to\infty}\left(\tfrac{1}{2}\hat{r}\left(e^{\theta-\theta_0}+e^{-\theta}\right) - \int_{\mathbb{R}} \phi\left(\theta-\theta'\right)\left(L\left(\theta'+\frac{\theta_0}{2}\right)+L\left(\theta'-\frac{3\theta_0}{2}\right)\right)d\theta'\right). \end{aligned} \tag{5.1.6}$$

Since θ is kept finite as the $\theta_0 \to \infty$ limit is taken, the second exponential term vanishes in (5.1.5) and the first vanishes in (5.1.6). $\theta = \pm 3\theta_0/2$ lie outside the non-zero region of $L(\theta)$ in the relevant part of the staircase model, so in the $\theta_0 \to \infty$ limit the terms involving $L\left(\theta' \pm 3\theta_0/2\right)$ equal zero. After combining these observations with (5.1.4), and allowing θ to vary over the full real line, (5.1.5) and (5.1.6) become the coupled pair of equations

$$\varepsilon_1(\theta) = \tfrac{1}{2}\hat{r}e^{\theta} - \int_{\mathbb{R}} \phi(\theta-\theta')L_2(\theta')d\theta' \tag{5.1.7}$$

$$\varepsilon_2(\theta) = \tfrac{1}{2}\hat{r}e^{-\theta} - \int_{\mathbb{R}} \phi(\theta-\theta')L_1(\theta')d\theta'. \tag{5.1.8}$$

This is the TBA system for $\mathcal{M}A_4^{(+)}$ that was introduced in section 2.3, in equation (2.3.22). Plots of these functions at various values of $\hat{r}$ are shown in the figures below, and it is apparent that given some value of $\hat{r}$, $L_1(\theta)$ and $L_2(\theta)$ can be appropriately shifted and glued together to form the staircase $L(\theta)$ at $\ln r = \ln \hat{r} - 30$.

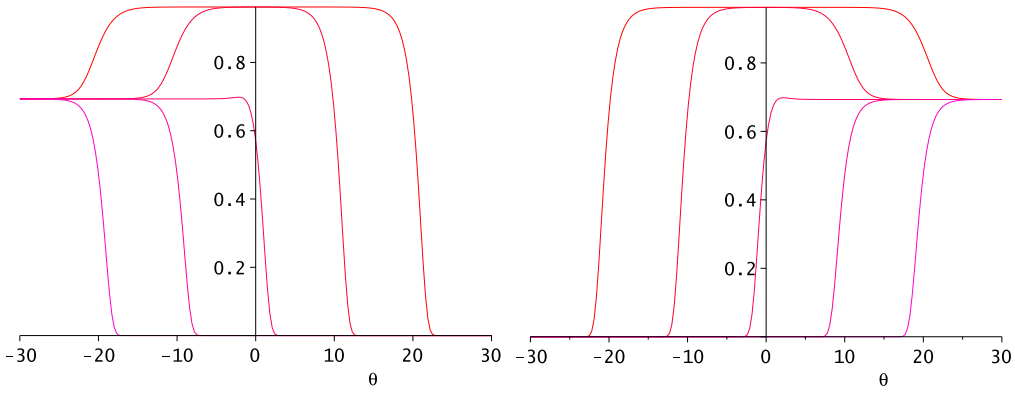

(a) $L_1(\theta)$ (b) $L_2(\theta)$

Figure 5.2: Plots of $L_1(\theta)$ and $L_2(\theta)$ at $\ln \hat{r} = -20, -10, 0, 10, 20$, where for $\ln \hat{r} = 20$ $L_1(\theta)$ has a kink close to $\theta = -20$ and $L_2(\theta)$ has a kink close to $\theta = 20$, etc.

The behaviour of these equations in the UV ($\hat{r} \ll 1$) and IR ($\hat{r} \gg 1$) limits gives a simple example of how the plateaux values of $L(\theta)$ given in (4.1.48) emerge. To begin with, set $\hat{r} \ll 1$, so that the theory is described by $\mathcal{M}_4$. When $\theta \gg \ln(1/\hat{r})$, $\varepsilon_1(\theta)$ (5.1.7) is dominated by the driving term $\hat{r}\exp(\theta)$ and so tends to infinity, meaning that $L_1(\theta) \approx 0$. This corresponds to the y_1 plateau in (4.1.48) at $m = 4$. Turning to (5.1.8), the driving term tends to zero for these values of θ, and so since $L_1(\theta)$ also vanishes here, $\varepsilon_2(\theta) = 0$ and $L_2(\theta) = \ln 2$, corresponding to the value of the y_2 plateau in (4.1.48). The symmetry between $\varepsilon_1(\theta)$ and $\varepsilon_2(\theta)$ means that when $\theta \ll -\ln(1/\hat{r})$ this behaviour is switched, with the plateaux values becoming $L_1(\theta) = \ln 2$ and $L_2(\theta) = 0$, corresponding to the y_2 and y_3 plateaux in (4.1.48) respectively. For $|\theta| \ll \ln(1/\hat{r})$, the driving term can be neglected in each equation, leaving a pair of simultaneous equations in $\exp(-\varepsilon_1(\theta))$ and $\exp(-\varepsilon_2(\theta))$ which solve to show that both $L_1(\theta)$ and $L_2(\theta)$ have a plateau of value $\ln((3+\sqrt{5})/2)$ for these values of θ. These plateaux correspond to the x_2 and x_3 plateaux at $m = 4$. When $\hat{r} \gg 1$, $\varepsilon_1(\theta)$ is dominated by the driving term for $\theta \gg -\ln \hat{r}$, so that $L_1(\theta)$ vanishes for these values of θ, and by symmetry $L_2(\theta)$ vanishes for $\theta \ll \ln \hat{r}$. There is now

no value of θ for which neither $L_1(\theta)$ nor $L_2(\theta)$ vanishes, and so the only non-zero values of $L_{1,2}(\theta)$ are $L_1(\theta) = \ln 2$ for $\theta \ll -\ln \hat{r}$ and $L_2(\theta) = \ln 2$ for $\theta \gg \ln \hat{r}$. These plateau values line up with the y_1, x_2 and y_2 plateaux that emerge from (4.1.48) at $\mathcal{M}_3$. The plateau values in the UV and IR limits are summarised below:

$$\begin{array}{lccc}
\hat{r} \ll 1 & & L_1(\theta) & L_2(\theta) \\
& \theta \gg \ln(1/\hat{r}) & 0 & \ln 2 \\
& -\ln(1/\hat{r}) \ll \theta \ll \ln(1/\hat{r}) & \ln\left(\frac{3+\sqrt{5}}{2}\right) & \ln\left(\frac{3+\sqrt{5}}{2}\right) \\
& \theta \ll -\ln(1/\hat{r}) & \ln 2 & 0 \\
\hat{r} \gg 1 & & & \\
& \theta \gg \ln \hat{r} & 0 & \ln 2 \\
& -\ln \hat{r} \ll \theta \ll \ln \hat{r} & 0 & 0 \\
& \theta \ll -\ln \hat{r} & \ln 2 & 0
\end{array} \quad . \tag{5.1.9}$$

As was discussed for the full staircase model, the sizes of these plateaux change as $\hat{r}$ varies. Focussing on $L_1(\theta)$, in the far UV ($\hat{r} \to 0$) limit, the widths of the plateaux of height 0 and $\ln 2$ tend to zero, while the width of the central plateaux tends to infinity. As $\hat{r}$ increases from zero, the central plateau shrinks allowing the width of the other two to increase in size, until at $\hat{r} = 1$ the central plateau has shrunk to zero so that $L_1(\theta)$ consists of a plateau of value $\ln 2$ for negative values of θ, and a zero-valued plateau for positive values of θ, with a kink between the two centred on $\theta \approx 0$. This is the point at which the crossover between $\mathcal{M}_4$ and $\mathcal{M}_3$ occurs. As $\hat{r}$ continues to increase, the kink between the two plateaux shifts in the direction of decreasing θ, until in the far IR ($\hat{r} \to \infty$) limit it goes off to minus infinity. The behaviour of $L_2(\theta)$ is that of $L_1(\theta)$ reflected in the line $\theta = 0$.

By working in the double-scaling limit defined above (5.1.2), an exact equation for the $\mathcal{M}A_4^{(+)}$ g-function can be derived from the formulae for the staircase g-function (4.2.4)-(4.2.12) in terms of the pseudoenergies $\varepsilon_1(\theta)$ and $\varepsilon_2(\theta)$. Beginning with $\ln g_0$, the analysis is made simpler if the symmetry of $\phi_S(\theta)$ and $\varepsilon(\theta)$ is used to

rewrite (4.2.4) as

$$\ln g_0(\hat{r}) = \sum_{n=1}^{\infty} \frac{1}{2n} \int_{\mathbb{R}^n} \frac{d\theta_1}{1+e^{\varepsilon(\theta_1)}} \cdots \frac{d\theta_n}{1+e^{\varepsilon(\theta_n)}} \phi_S(\theta_1-\theta_2)\phi_S(\theta_2-\theta_3)\cdots\phi_S(\theta_n+\theta_1) \tag{5.1.10}$$

where the $n=1$ term is

$$\tfrac{1}{2}\int_{\mathbb{R}} \frac{d\theta}{1+e^{\varepsilon(\theta)}}\phi_S(2\theta). \tag{5.1.11}$$

Using the definition of $\phi_S(\theta)$ (4.1.5), each product of n $\phi_S(\theta)$ factors appearing in the integrands in (5.1.10) can be expanded into a sum of 2^n terms of the form

$$\phi(\theta_1-\theta_2-\alpha_1\theta_0)\phi(\theta_2-\theta_3-\alpha_2\theta_0)\cdots\phi(\theta_n+\theta_1-\alpha_n\theta_0) \tag{5.1.12}$$

with $\alpha_i = \pm 1$. Since $\phi(\theta)$ has its support close to $\theta = 0$, each such term is only non-zero in a sub-region of $\mathbb{R}^n$. The value of (5.1.10) is therefore dependent on the value of the measure factor $1/(1+\exp(\varepsilon(\theta_i)))$ at each coordinate θ_i of the sub-regions (where for now the single staircase pseudoenergy $\varepsilon(\theta)$ is used). Since $L(\theta) = \ln(1+\exp(-\varepsilon(\theta)))$ is equal to zero for $|\theta| \gg \ln(1/r)$, $\exp(-\varepsilon(\theta)) = 0$ and $1/(1+\exp(\varepsilon(\theta))) \to 0$ for these values of θ, so for the product of measure factors to be non-zero in a particular sub-region, each coordinate θ_i in that sub-region must satisfy $|\theta_i| \ll \ln(1/r)$. Given $\{\alpha_1, \cdots, \alpha_n\}$, the corresponding sub-region is centred on $(\tilde{\theta}_1, \tilde{\theta}_2, \cdots, \tilde{\theta}_n)$, satisfying

$$\begin{aligned} \tilde{\theta_1} - \tilde{\theta}_2 &= \alpha_1\theta_0 \\ \tilde{\theta}_2 - \tilde{\theta}_3 &= \alpha_2\theta_0 \\ &\vdots \\ \tilde{\theta}_n + \tilde{\theta}_1 &= \alpha_n\theta_0. \end{aligned} \tag{5.1.13}$$

The only solutions to this occur when the $\tilde{\theta}_i$ are integer or half integer multiples of θ_0. The only such values of $\tilde{\theta}_i$ for which $1/(1+\exp(\varepsilon(\tilde{\theta}_i)))$ is non-zero are $\tilde{\theta}_i = 0$ and $\tilde{\theta}_i = \pm\theta_0/2$. It is clear from inspection of (5.1.13) that the only solutions involving

these values occur when n is odd and are

$$(\tilde{\theta}_1, \tilde{\theta}_2, \cdots, \tilde{\theta}_n) = (\pm\theta_0/2, \mp\theta_0/2, \pm\theta_0/2, \cdots, \pm\theta_0/2), \tag{5.1.14}$$

corresponding to

$$(\alpha_1, \alpha_2, \cdots, \alpha_n) = (\pm 1, \mp 1, \pm 1, \cdots, \pm 1) \tag{5.1.15}$$

respectively. In the double-scaling limit (5.1.2), $\varepsilon(\theta)$ is described by $\varepsilon_1(\theta - \theta_0/2)$ in the region around $\theta = \theta_0/2$ and by $\varepsilon_2(\theta + \theta_0/2)$ around $\theta = -\theta_0/2$. So, when $\theta_i \approx \pm\theta_0/2$, the measure factors $1/(1+\exp(-\varepsilon(\theta_i)))$ in (5.1.10) can be replaced by $1/(1+\exp(-\varepsilon_1(\theta_i - \theta_0/2)))$ or $1/(1+\exp(-\varepsilon_2(\theta_i + \theta_0/2)))$ respectively. Denoting the measure factors $1/(1+\exp(\varepsilon_{1,2}(\theta)))$ by $\chi_{1,2}(\theta)$, the integrand in the n^{th} term in $\ln g_0(\hat{r})$ is

$$\begin{aligned}
&\chi_1(\theta_1 - \frac{\theta_0}{2})\chi_2(\theta_2 + \frac{\theta_0}{2}) \cdots \chi_1(\theta_n - \frac{\theta_0}{2}) \times \\
&\qquad \phi(\theta_1 - \theta_2 - \theta_0)\phi(\theta_2 - \theta_3 + \theta_0) \cdots \phi(\theta_n + \theta_1 - \theta_0) + \\
&\chi_2(\theta_1 + \frac{\theta_0}{2})\chi_1(\theta_2 - \frac{\theta_0}{2}) \cdots \chi_2(\theta_n + \frac{\theta_0}{2}) \times \\
&\qquad \phi(\theta_1 - \theta_2 + \theta_0)\phi(\theta_2 - \theta_3 - \theta_0) \cdots \phi(\theta_n + \theta_1 + \theta_0)
\end{aligned} \tag{5.1.16}$$

which upon changing the variables and using the symmetry $\varepsilon_1(\theta) = \varepsilon_2(-\theta)$ gives the expression for $\ln g_0(\hat{r})$ to be

$$\ln g_0(\hat{r}) = \sum_{\substack{n=1 \\ n\ odd}}^{\infty} \frac{1}{n} \int_{\mathbb{R}^n} \frac{d\theta_1}{1+e^{\varepsilon_1(\theta_1)}} \frac{d\theta_2}{1+e^{\varepsilon_1(\theta_2)}} \cdots \frac{d\theta_n}{1+e^{\varepsilon_1(\theta_n)}} \phi(\theta_1+\theta_2)\phi(\theta_2+\theta_3) \cdots \phi(\theta_n+\theta_1). \tag{5.1.17}$$

The other terms in $\ln g(r)$ are simpler. Using again the localised behaviour of $\phi(\theta)$, $\ln g_{b1}$ (4.2.10) is determined by $L(\theta \approx 0)$, which in the double scaling limit is equal to $L_1(\theta \to -\infty) = L_2(\theta \to \infty)$. As can be seen from (5.1.9), this has constant value $\ln 2$ throughout the RG flow and so can be taken outside the integral in (4.2.10) so that

$$\ln g_{b1}(\hat{r}) = -\tfrac{1}{2} \ln 2. \tag{5.1.18}$$

$\ln g_{b2}$ (4.2.11) is governed by $\theta \approx \pm\theta_0/2$ so can be re-expressed in terms of $\varepsilon_1(\theta)$

and $\varepsilon_2(\theta)$ as

$$\begin{aligned}\ln g_{b2}(\hat{r}) =& \tfrac{1}{2}\int_{\mathbb{R}} d\theta \left(\phi_{(3/4)}(\theta-\frac{\theta_0}{2}) - \phi(2\theta-\theta_0)\right) L_1(\theta-\frac{\theta_0}{2}) + \\ & \tfrac{1}{2}\int_{\mathbb{R}} d\theta \left(\phi_{(3/4)}(\theta+\frac{\theta_0}{2}) - \phi(2\theta+\theta_0)\right) L_2(\theta+\frac{\theta_0}{2}) \\ =& \int_{\mathbb{R}} d\theta \left(\phi_{(3/4)}(\theta) - \phi(2\theta)\right) L_1(\theta) \end{aligned} \tag{5.1.19}$$

where $L_1(\theta) = L_2(-\theta)$ and the fact that $\phi(\theta)$ and $\phi_{(3/4)}(\theta)$ are even have been used in reaching the final step.

The behaviour of $\ln g_{b3}$ (4.2.12) is governed by $L(\theta \approx \pm\theta_{b1})$ and $L(\theta \approx \pm\theta_{b2})$. (4.2.12) is symmetric with respect to a sign change of either or both of the boundary parameters, $\theta_{b1} \to -\theta_{b1}$ and $\theta_{b2} \to -\theta_{b2}$, and so θ_{b1} and θ_{b2} can be taken to be non-negative without loss of generality. In the double-scaling limit, the boundary parameters can be treated by defining

$$\theta_{b1,b2} = \frac{\theta_0}{2} + \hat{\theta}_{b1,b2}, \tag{5.1.20}$$

where $\hat{\theta}_{b1,b2}$ are held fixed while the $\theta_0 \to \infty$ limit is taken, and afterwards are allowed to take all real values. Then $L(\theta \approx \theta_{b1,b2}) = L_1(\theta \approx \hat{\theta}_{b1,b2})$ and $L(\theta \approx -\theta_{b1,b2}) = L_2(\theta \approx -\hat{\theta}_{b1,b2})$ so that $\ln g_{b3}$ becomes

$$\ln g_{b3}(\hat{r}) = \frac{1}{2}\int_{\mathbb{R}} d\theta \left\{ \left(\phi(\theta-\hat{\theta}_{b1}) + \phi(\theta-\hat{\theta}_{b2})\right) L_1(\theta) + \left(\phi(\theta+\hat{\theta}_{b1}) + \phi(\theta+\hat{\theta}_{b2})\right) L_2(\theta) \right\} \tag{5.1.21}$$

$$= \int_{\mathbb{R}} d\theta \left(\phi(\theta-\hat{\theta}_{b1}) + \phi(\theta-\hat{\theta}_{b2})\right) L_1(\theta) \tag{5.1.22}$$

using $L_1(\theta) = L_2(-\theta)$.

So, the expressions (5.1.17), (5.1.18), (5.1.19) and (5.1.22), make up the g-function $\ln g(\hat{r}) = \ln g_0(\hat{r}) + \ln g_{b1}(\hat{r}) + \ln g_{b2}(\hat{r}) + \ln g_{b3}(\hat{r})$ for $\mathcal{M}A_4^{(+)}$. When $\hat{\theta}_{b2}$ (or equivalently $\hat{\theta}_{b1}$) is taken to plus or minus infinity before $\hat{r}$ is varied, these equations reduce to the single boundary parameter results of Dorey et al. [41] which were reported in section 3.3. The plots in figure 5.3 show some examples of the behaviour of the g-function at various values of the boundary parameters. The horizontal lines

indicate the conformal g-function values of certain Cardy boundary conditions (a, b) or their superpositions at $\mathcal{M}_4$ and $\mathcal{M}_3$ ((4.2.13),(4.2.14)), and their agreement with the values of plateaux of $\ln g(\hat{r})$ is clear from the plots.

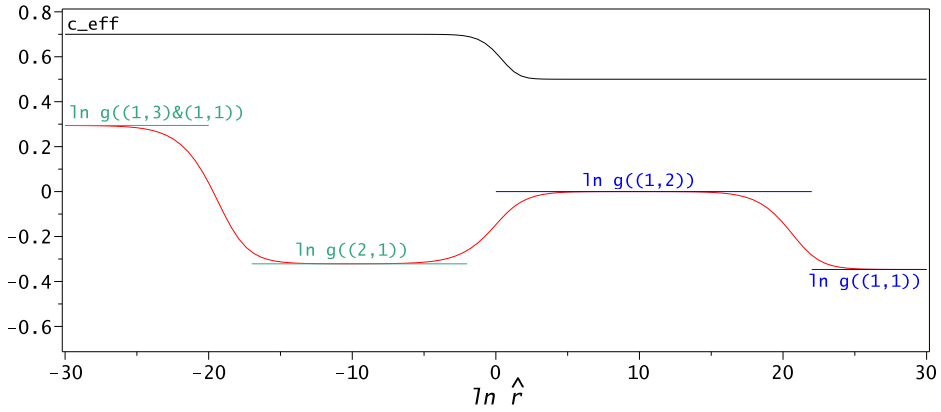

(a) $\hat{\theta}_{b1} = 20$, $\hat{\theta}_{b2} = -20$

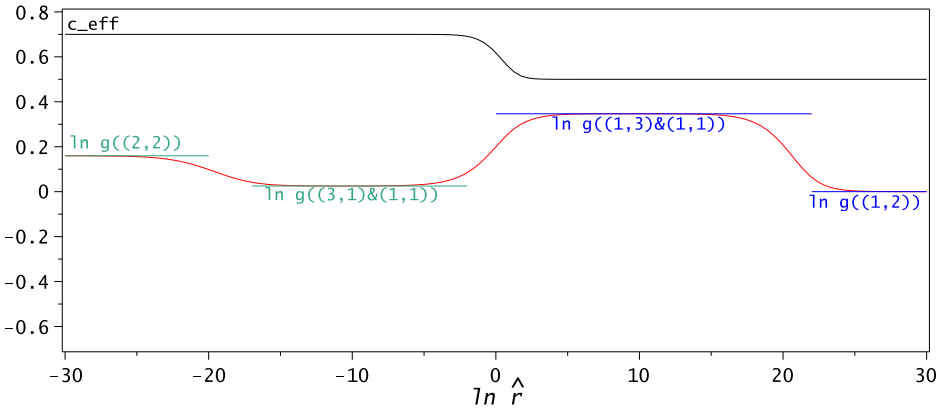

(b) $\hat{\theta}_{b1} = -20$, $\hat{\theta}_{b2} = -40$

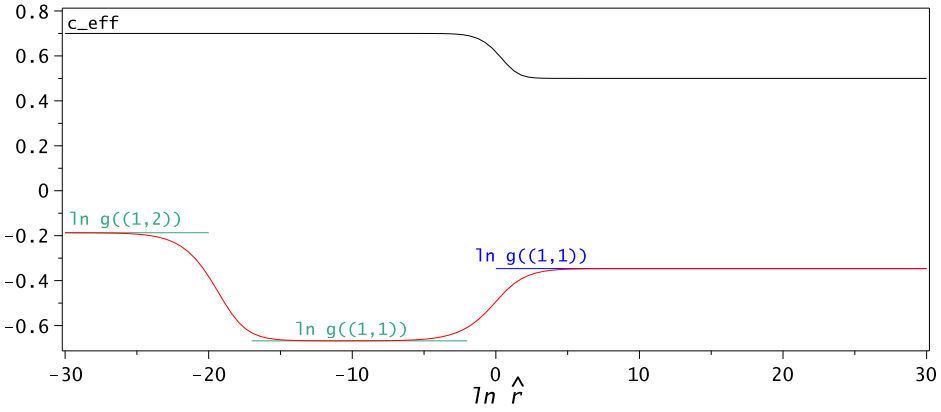

(c) $\hat{\theta}_{b1} = 20$, $\hat{\theta}_{b2} = 40$

Figure 5.3: Flow of $\ln g(\hat{r})$ for $\ln \hat{r} = -30 \cdots 30$ at various values of the boundary parameters $\hat{\theta}_{b1}$ and $\hat{\theta}_{b2}$.

To determine in general which boundary conditions appear and the flows that occur between them, the UV and IR limits of the value of the g-function must be studied. Beginning with $\ln g_0(\hat{r})$, the products of $\phi(\theta_i + \theta_j)$ have their support close to $\theta_i = 0$ for $i = 1, \cdots, n$ so (5.1.17) is governed by $\varepsilon_1(\theta \approx 0)$. In the far UV limit ($\hat{r} \to 0$), $\exp(-\varepsilon_1(\theta \approx 0)) = (1+\sqrt{5})/2$ so that $\ln g_0(\hat{r})$ becomes

$$\begin{aligned}
&\lim_{\hat{r}\to 0} \ln\, g_0(\hat{r}) = \\
&\sum_{\substack{n=1 \\ n\ odd}}^{\infty} \frac{1}{n} \left(\frac{\sqrt{5}-1}{2}\right)^n \int_{\mathbb{R}^n} d\theta_1 d\theta_2 \cdots d\theta_n \phi(\theta_1+\theta_2)\phi(\theta_2+\theta_3)\cdots\phi(\theta_n+\theta_1) \\
=&\sum_{\substack{n=1 \\ n\ odd}}^{\infty} \frac{1}{n\, 2^{n+1}} \left(\frac{\sqrt{5}-1}{2}\right)^n \\
=&\frac{1}{4} \ln\left(1+\frac{2}{\sqrt{5}}\right)
\end{aligned} \tag{5.1.23}$$

where (4.1.7) has been used. In the far IR limit ($\hat{r} \to \infty$), $\exp(-\varepsilon_1(\theta \approx 0)) \to 0$ and so $1/(1+\exp(\varepsilon_1(\theta \approx 0))) \to 0$ and $\lim_{\hat{r}\to\infty} \ln g_0(\hat{r})$ vanishes.

$\ln g_{b1}$ is constant throughout $\mathcal{M}A_4^{(+)}$, so it is equal to $-\frac{1}{2}\ln 2$ in both the UV and IR limits. $\ln g_{b2}(\hat{r})$ is controlled by $L_1(\theta \approx 0)$ and so taking the UV and IR values of this from (5.1.9) gives

$$\lim_{\hat{r}\to 0} \ln g_{b2}(\hat{r}) = -\tfrac{1}{2} \ln \frac{3+\sqrt{5}}{2} \tag{5.1.24}$$

$$\lim_{\hat{r}\to \infty} \ln g_{b2}(\hat{r}) = 0. \tag{5.1.25}$$

$\ln g_{b3}(\hat{r})$ depends on $L_1(\theta \approx \hat{\theta}_{b1})$ and $L_1(\theta \approx \hat{\theta}_{b2})$. Beginning with the simplest cases, if $\hat{\theta}_{b1} \to \infty$ before $\hat{r}$ is varied then from (5.1.9) $L_1(\hat{\theta}_{b1}) = 0$ for all values of $\hat{r}$, and if $\hat{\theta}_{b1} \to -\infty$ then $L_1(\hat{\theta}_{b1}) = \ln 2$ for all values of $\hat{r}$. If $\hat{\theta}_{b1} = 0$ then $L_1(\hat{\theta}_{b1}) = \ln((3+\sqrt{5})/2)$ for $\hat{r} \to 0$, but then changes value during the bulk transition from $\mathcal{M}_4$ to $\mathcal{M}_3$, becoming $L_1(\hat{\theta}_{b1}) = 0$ for $\hat{r} \to \infty$. For finite, non-zero values of $\hat{\theta}_{b1}$ the situation is more complicated. In this case, in the far UV limit the central plateau of $L_1(\theta)$ has infinite width and so $L_1(\hat{\theta}_{b1}) \approx \ln((3+\sqrt{5})/2)$ for all finite values of $\hat{\theta}_{b1}$. As $\ln(1/\hat{r})$ decreases this plateau shrinks, and $L_1(\hat{\theta}_{b1})$ moves off this plateau while the bulk is still close to $\mathcal{M}_4$, corresponding to a boundary flow within

this minimal model. For $\hat{\theta}_{b1} > 0$ a transition in the value of $L_1(\hat{\theta}_{b1})$ occurs at $\ln(1/\hat{r}) \approx \hat{\theta}_{b1}$, after which $L_1(\theta \approx \hat{\theta}_{b1}) \approx 0$. There are no further transitions in this case, and $L_1(\theta \approx \hat{\theta}_{b1})$ remains zero into the far IR limit ($\hat{r} \to \infty$). For $\hat{\theta}_{b1} < 0$ the transition occurs at $\ln(1/\hat{r}) \approx -\hat{\theta}_{b1}$, after which $L_1(\theta \approx \hat{\theta}_{b1}) \approx \ln 2$. After the bulk transition at $\ln(1/\hat{r}) \approx 1$, $L_1(\theta \approx \hat{\theta}_{b1})$ keeps this value until the point where $\ln(1/\hat{r}) = \hat{\theta}_{b1}$, after which $L_1(\theta \approx \hat{\theta}_{b1}) \approx 0$ and there are no further transitions. The same rules apply for $\hat{\theta}_{b2}$.

At the values of $\hat{r}$ for which both $\hat{\theta}_{b1}$ and $\hat{\theta}_{b2}$ lie on plateaux of $L_1(\theta)$, $L_1(\hat{\theta}_{b1})$ and $L_1(\hat{\theta}_{b2})$ can be pulled outside the integral in (5.1.22) to give

$$\ln g_{b3}(\hat{r}) = \tfrac{1}{2}\left(L_1(\hat{\theta}_{b1}) + L_1(\hat{\theta}_{b2})\right). \tag{5.1.26}$$

The possible plateau values of $\ln g(\hat{r})$ can then be found by adding this to the expressions for $\ln g_0(\hat{r})$, $\ln g_{b1}(\hat{r})$ and $\ln g_{b2}(\hat{r})$ in the UV and IR limits, and these values can then be identified with boundary conditions using (4.2.13). The tables below give the boundary condition identified for each possible pair of plateau values $L_1(\hat{\theta}_{b1})$ and $L_1(\hat{\theta}_{b2})$; the first table is for the UV limit, where the theory is close to $\mathcal{M}_4$, and the second is for the IR limit where it is close to $\mathcal{M}_3$.

$\mathcal{M}_4$:

$L(\hat{\theta}_{b1})$	$L(\hat{\theta}_{b2})$	$\ln g$	Boundary condition
0	0	$\frac{1}{4}\ln\frac{5-\sqrt{5}}{40}$	$(1,1) = (+)$
$\ln\frac{3+\sqrt{5}}{2}$	0	$\frac{1}{4}\ln\frac{5+2\sqrt{5}}{20}$	$(1,2) = (0+)$
$\ln 2$	0	$\frac{1}{4}\ln\frac{5-\sqrt{5}}{10}$	$(2,1) = (0)$
$\ln\frac{3+\sqrt{5}}{2}$	$\ln 2$	$\frac{1}{4}\ln\frac{5+2\sqrt{5}}{5}$	$(2,2) = (d)$
$\ln\frac{3+\sqrt{5}}{2}$	$\ln\frac{3+\sqrt{5}}{2}$	$\frac{1}{4}\ln\frac{65+29\sqrt{5}}{40}$	$(1,3)\&(1,1) = (-0)\&(+)$
$\ln 2$	$\ln 2$	$\frac{1}{4}\ln\frac{2(5-\sqrt{5})}{5}$	$(3,1)\&(1,1) = (+)\&(-)$.

(5.1.27)

$\mathcal{M}_3$:

$$\begin{array}{ccccc} L(\hat{\theta}_{b1}) & L(\hat{\theta}_{b2}) & \ln g(r) & \text{Boundary condition} \\ 0 & 0 & -\frac{1}{2}\ln 2 & (1,1)=(+) \\ \ln 2 & 0 & 0 & (1,2)=(f) \\ \ln 2 & \ln 2 & \frac{1}{2}\ln 2 & (1,3)\&(1,1)=(+)\&(-). \end{array} \tag{5.1.28}$$

The boundary condition labels $(+)$, $(-)$, (0), $(0+)$, (-0) and (d) in (5.1.27) and $(+)$, $(-)$ and (f) in (5.1.28) are the standard labels for boundary conditions in the tricritical Ising model (described by $\mathcal{M}_4$) and the Ising model (described by $\mathcal{M}_3$) respectively.

Combining these identifications with the movement between plateau values described above results in the network of flows shown in figure 5.4, where the top layer represents flows within $\mathcal{M}_4$, the bottom layer represents those within $\mathcal{M}_3$, and the vertical flows represent the flows that occur during the bulk transition around $\ln(1/\hat{r}) = 0$. It should be noted here that the identification of g-function values

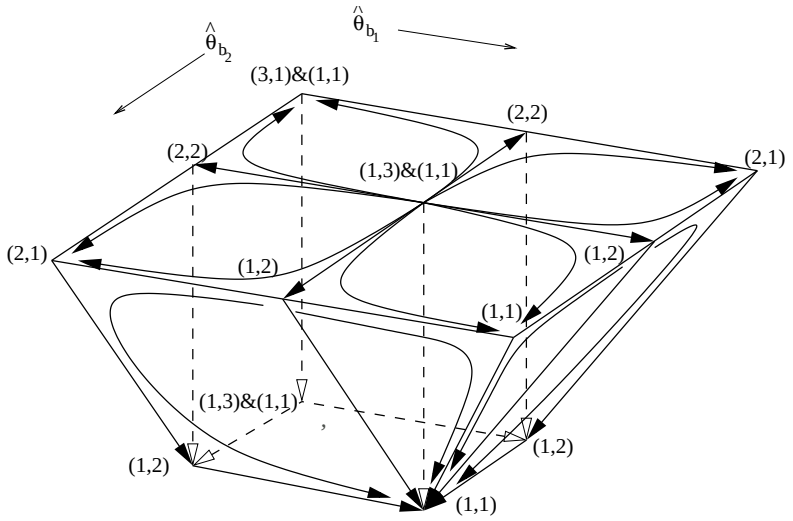

Figure 5.4: Flows between boundary conditions in the $\mathcal{M}A_4^{(+)}$ interpolating theory.

with boundary conditions in (5.1.27) and (5.1.27) is not unique, because ambiguities arise due to the symmetries of the conformal g-function (4.2.13). Firstly, there is the equivalence of the boundary conditions (a, b) and $(m - a, m + 1 - b)$ which

was first discussed around (3.1.17). The only ambiguity resulting from this is that there is a choice in the labelling of the boundary conditions appearing in the table above. However, the symmetries

$$g(m,a,b) = g(m,m-a,b) \quad \text{and} \quad g(m,a,b) = g(m,a,m+1-b) \tag{5.1.29}$$

do result in ambiguities as to the actual physical boundary condition that occurs. The boundary condition $(m-a,b)$ will be referred to as the spin-flip conjugate of (a,b). In the Ising model this arises from the symmetry of the g-function under the $\mathbb{Z}_2$ flip from the $(+)$ to $(-)$ boundary conditions, and an analogue of this symmetry exists in the higher unitary minimal models. In the original staircase g-function $\ln g(r)$, these symmetries arise from the fact that $L(\theta)$ is even so that

$$\ln g(r,\theta_{b1},\theta_{b2}) = \ln g(r,\theta_{b1},-\theta_{b2}) = \ln g(r,-\theta_{b1},\theta_{b2}). \tag{5.1.30}$$

In terms of the double-scaling limit g-function, $\ln g(\hat{r})$ is unchanged if both $\hat{\theta}_{b_i} \to -\hat{\theta}_{b_i}$ and $L_1(\theta) \to L_2(\theta)$.

However, there are good indications that the correct boundary condition identifications have been made. The boundary flows found in [49] and [50] for the tricritical Ising model match those along the edges of the $\mathcal{M}_4$ level of figure 5.4, and the flows at the $\mathcal{M}_3$ level match those which occur in the Ising model (see, for example, [32] and [51]). Furthermore, the combinations of these with the bulk flows agree with those found in [52] in the case of one boundary parameter. It will be seen in chapter 6.2 that a version of the g-function involving an excited bulk state can be used to check the identification of the boundary conditions, but for now they will be assumed to be correct. The conjugate boundary conditions can be incorporated by allowing θ_{b1} and θ_{b2} to take negative values, so that if $(\theta_{b1},\theta_{b2})$ is identified with (a,b) then $(\theta_{b1},-\theta_{b2})$ is identified with $(m-a,b)$, and in the case of the superposition the conjugate of each boundary condition in the superposition is taken.

5.2 The Full Staircase

The focus is now widened to the study of g-function flows in the full staircase model, such as those plotted in figure 5.5. The results appearing here and in the next chapter were reported in [1]. The aim of this section is to find the flows between boundary conditions that occur during the full RG flow of the staircase model. To achieve this, Cardy boundary conditions (or superpositions) must be identified with configurations of boundary parameters $(\theta_{b1}, \theta_{b2})$ in the staircase g-function, whenever the bulk theory passes close to each of the unitary minimal models $\mathcal{M}_m$, and the flows induced by either pure boundary transitions or those coinciding with bulk transitions must be determined, just as was done for the $\mathcal{M}_4 \to \mathcal{M}_3$ flows in the previous section. The derivation of exact g-function equations for flows between consecutive minimal models $\mathcal{M}_m$ and $\mathcal{M}_{m-1}$, i.e. those described by the interpolating theories $\mathcal{M}A_m^{(+)}$, will be left to the section 5.3.

The first task is to establish the value of each term in the g-function $\ln g(r) = \ln g_0(r) + \ln g_{b1}(r) + \ln g_{b2}(r) + \ln g_{b3}(r)$ when it is close to a minimal model $\mathcal{M}_m$, i.e. for $(m-3)\theta_0/2 \ll \ln(1/r) \ll (m-2)\theta_0/2$.

5.2.1 $\ln g_0(r)$

As in the warm-up case, the most complex term to treat is $\ln g_0(r)$

$$\ln g_0(r) = \sum_{n=1}^{\infty} \frac{1}{2n} \int_{\mathbb{R}^n} \frac{d\theta_1}{1+e^{\varepsilon(\theta_1)}} \cdots \frac{d\theta_n}{1+e^{\varepsilon(\theta_n)}} \phi_S(\theta_1-\theta_2)\phi_S(\theta_2-\theta_3)\cdots\phi_S(\theta_n+\theta_1), \tag{5.2.1}$$

and as was described in the warm-up case, the 'double-bump' form of $\phi_S(\theta)$ means that the value of $\ln g_0(r)$ is determined by sub-regions of $\mathbb{R}^n$ centred on $(\tilde{\theta}_1, \tilde{\theta}_2, \cdots, \tilde{\theta}_n)$,

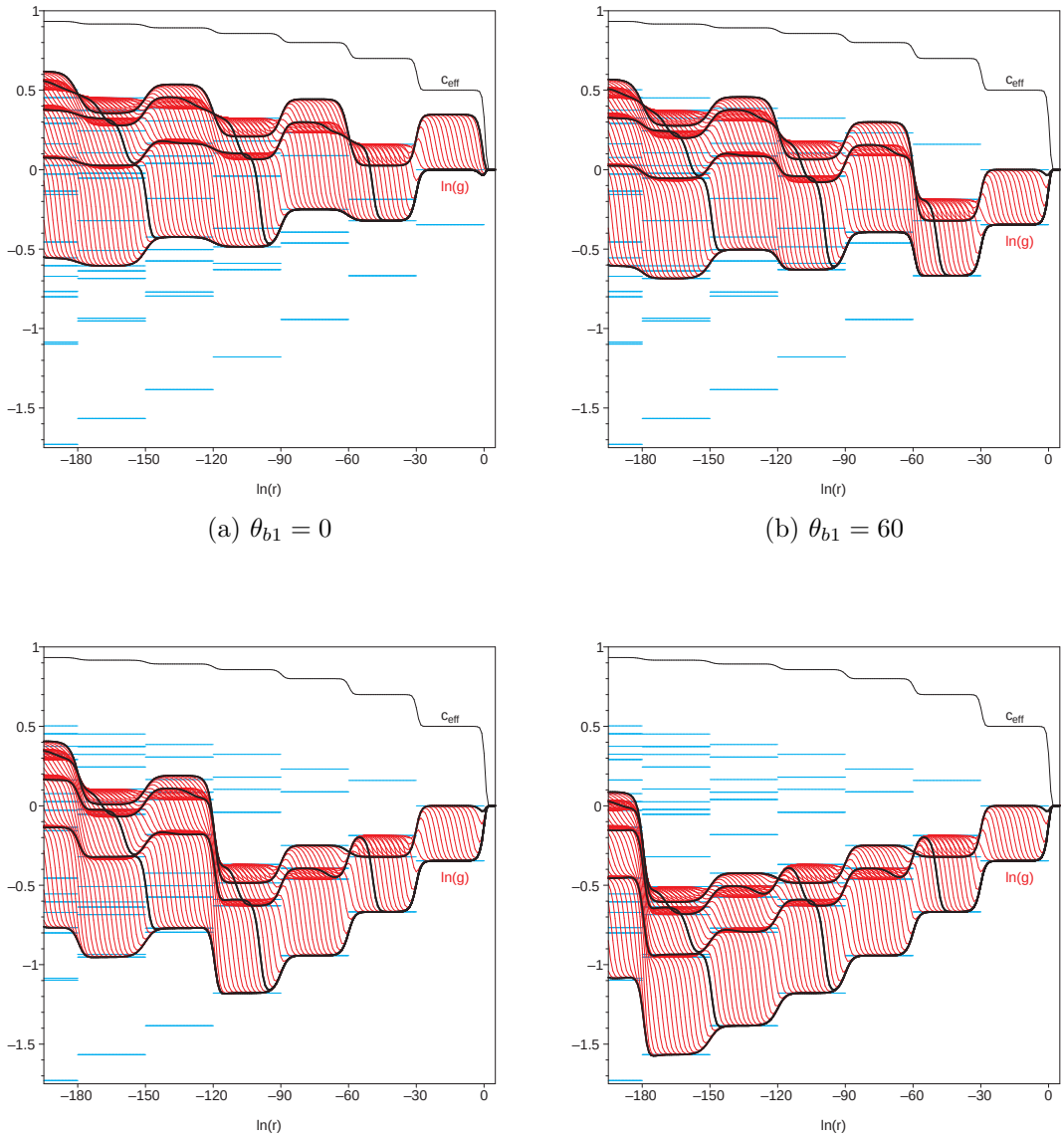

(a) $\theta_{b1} = 0$ (b) $\theta_{b1} = 60$

(c) $\theta_{b1} = 120$ (d) $\theta_{b1} = 180$

Figure 5.5: Plots of the logarithm of the staircase g-function flows at four different values of θ_{b1}. θ_0 is set to 60, and the collection of curves in each plot emerge as θ_{b2} ranges from 0 to 200 in steps of 2. The five highlighted flows in each plot are $\theta_{b2} = 200$, 150, 100, 50 and 0, with $\theta_{b2} = 200$ producing the lowest-lying of these, and reading from left to right, this is joined by the other flows in decreasing numerical order. The plateau values of c_{eff} indicate that the bulk passes close to the minimal models $\mathcal{M}_9$ down to $\mathcal{M}_3$ for these values of r, and the logarithms of the conformal g-function values (4.2.13) of the Cardy boundary conditions at each of these minimal models are indicated by the short light blue horizontal lines. Those g-function plateaux that do not coincide with these lines correspond to superpositions of these boundary conditions.

which satisfy

$$\begin{pmatrix} 1 & -1 & 0 & 0 & \cdots & 0 & 0 \\ 0 & 1 & -1 & 0 & \cdots & 0 & 0 \\ 0 & 0 & 1 & -1 & \cdots & 0 & 0 \\ . & . & . & . & . & . & . \\ . & . & . & . & . & . & . \\ 0 & 0 & 0 & 0 & \cdots & 1 & -1 \\ 1 & 0 & 0 & 0 & \cdots & 0 & 1 \end{pmatrix} \begin{pmatrix} \tilde{\theta}_1 \\ \tilde{\theta}_2 \\ \tilde{\theta}_3 \\ . \\ . \\ . \\ \tilde{\theta}_n \end{pmatrix} = \theta_0 \begin{pmatrix} \alpha_1 \\ \alpha_2 \\ \alpha_3 \\ . \\ . \\ . \\ \alpha_n \end{pmatrix} \tag{5.2.2}$$

where $\alpha_i = \pm 1,\ i = 1 \cdots n$. Inverting this gives

$$\begin{pmatrix} \tilde{\theta}_1 \\ \tilde{\theta}_2 \\ . \\ . \\ . \\ \tilde{\theta}_n \end{pmatrix} = \tfrac{1}{2}\theta_0 \begin{pmatrix} 1 & 1 & 1 & \cdots & 1 & 1 \\ -1 & 1 & 1 & \cdots & 1 & 1 \\ -1 & -1 & 1 & \cdots & 1 & 1 \\ . & . & . & . & . & \\ . & . & . & . & . & \\ -1 & -1 & -1 & \cdots & -1 & 1 \end{pmatrix} \begin{pmatrix} \alpha_1 \\ \alpha_2 \\ . \\ . \\ . \\ \alpha_n \end{pmatrix} \tag{5.2.3}$$

from which it is clear that when n is odd each $\tilde{\theta}_i$ is a half integer multiple of θ_0, and when n is even the $\tilde{\theta}_i$'s are integer multiples of θ_0. Therefore, if $L(\tilde{\theta}_i)$ is non-zero then $\tilde{\theta}_i$ lies at the centre of a plateau of $L(\theta)$ when $(m-3)\theta_0/2 \ll \ln(1/r) \ll (m-2)\theta_0/2$. In particular, the centres of the non-zero x-type plateaux are

$$\{-(m-3)\theta_0/2, -(m-5)\theta_0/2, \cdots, (m-5)\theta_0/2, (m-3)\theta_0/2\}, \tag{5.2.4}$$

which are integer multiples of θ_0 for m odd and half integer multiples of $\theta_0/2$ for m even. The centres of the non-zero y-type plateaux are

$$\{-(m-4)\theta_0/2, -(m-6)\theta_0/2, \cdots, (m-6)\theta_0/2, (m-4)\theta_0/2\}, \tag{5.2.5}$$

which are half integer multiples of θ_0 for m odd and integer multiples for m even. So, when $m+n$ is odd each $\tilde{\theta}_i$ lies at the centre of an x-type plateau, and when

$m+n$ is even each $\tilde{\theta}_i$ lies at the centre of a y-type plateau.

Hence for $(m-3)\theta_0/2 \ll \ln(1/r) \ll (m-2)\theta_0/2$, $L(\theta)$ and therefore the measure factors $\frac{1}{1+\exp(\varepsilon(\theta))}$ can be approximated by the plateau values x_a and y_a (4.1.48) in each of the sub-regions centred on $(\tilde{\theta}_1, \tilde{\theta}_2, \cdots, \tilde{\theta}_n)$. Given $(\alpha_1, \cdots, \alpha_n)$, the corresponding term in $\ln g_0(r)$ is

$$\begin{aligned}
&\frac{1}{1+e^{\varepsilon(\tilde{\theta}_1)}} \cdots \frac{1}{1+e^{\varepsilon(\tilde{\theta}_n)}} \times \\
&\qquad \int_{\mathbb{R}^n} d\theta_1 \cdots d\theta_n \phi(\theta_1 - \theta_2 - \alpha_1\theta_0)\phi(\theta_2 - \theta_3 - \alpha_2\theta_0) \cdots \phi(\theta_n + \theta_1 - \alpha_n\theta_0) \\
\approx &\frac{1}{2^{n+1}} \frac{1}{1+e^{\varepsilon(\tilde{\theta}_1)}} \cdots \frac{1}{1+e^{\varepsilon(\tilde{\theta}_n)}}.
\end{aligned} \tag{5.2.6}$$

This becomes exact when the limit $\theta_0 \to \infty$ is taken in such a way that $\hat{r}$ remains within the above domain. From now on '$\approx$' will be replaced with '$=$' in such calculations, with the caveat that true equality only holds in this limit. In the warm-up case (where only $\mathcal{M}_3$ and $\mathcal{M}_4$ appeared) only relatively few terms of above form were non-zero. However, as m increases, the number of integer and half integer multiples of θ_0 for which $L(\theta)$ is non-zero increases, and so do the number of non-zero terms of the form (5.2.6). Nevertheless, it is possible to formulate an expression for the terms of the sum in $\ln g_0(r)$, by splitting the sum in $\ln g_0(r)$ into two terms, $\ln g_A(r)$ consisting of those terms where $m+n$ is odd, and $\ln g_B(r)$ consisting of those terms for which $m+n$ is even.

First, consider the situation when $m+n$ is odd. Here the non-zero terms of the form (5.2.6) correspond to the sub-regions for which

$$\frac{1}{1+e^{\varepsilon(\tilde{\theta}_i)}} = \frac{x_a}{1+x_a}, \qquad a \in \{2, \cdots, m-1\} \tag{5.2.7}$$

for each $\tilde{\theta}_i$. Using (5.2.2), there are restrictions on the values taken by consecutive $1/(1+\exp(\varepsilon(\tilde{\theta}_i)))$ terms in (5.2.6):

$$\begin{aligned}
&\frac{1}{1+e^{\varepsilon(\tilde{\theta}_i)}} = \frac{x_a}{1+x_a} \quad \text{for} \quad i = 1, \cdots, n-1 \\
\Rightarrow \quad &\frac{1}{1+e^{\varepsilon(\tilde{\theta}_{i+1})}} = \frac{x_{a+1}}{1+x_{a+1}} \quad \text{or} \quad \frac{1}{1+e^{\varepsilon(\tilde{\theta}_{i+1})}} = \frac{x_{a-1}}{1+x_{a-1}}
\end{aligned} \tag{5.2.8}$$

with only the former option allowed if $a = 2$ and only the latter if $a = m - 1$. There is also the additional constraint that

$$\frac{1}{1+e^{\varepsilon(\tilde{\theta}_1)}} = \frac{x_a}{1+x_a} \quad \Rightarrow \quad \frac{1}{1+e^{\varepsilon(\tilde{\theta}_n)}} = \frac{x_{m-a+1\pm1}}{1+x_{m-a+1\pm1}} \tag{5.2.9}$$

where only the '$-$' choice is allowed for $a = 2$ and only the '$+$' choice for $a = m - 1$.

Each term in the sum in $\ln g_0(r)$ is itself a sum of all possible terms of the form (5.2.6) obeying these rules at a particular value of n, so that for $n = k$ it is a sum of sequences of measure factors of length k. It is possible to construct a matrix which when taken to the k^{th} power has entries that reproduce these sequences. Consider an $r \times r$ matrix A, the entries of which satisfy

$$\begin{aligned} A_{i,i-1} &= A_{i,i+1}, \\ A_{ij} &= 0 \quad \text{for} \quad j \neq i-1 \ \text{ or } \ i+1. \end{aligned} \tag{5.2.10}$$

If this matrix is taken to the power k then the (i, j) entry is

$$\left(A^k\right)_{ij} = A_{il_1}A_{l_1l_2}\cdots A_{l_{k-2}l_{k-1}}A_{l_{k-1}j}. \tag{5.2.11}$$

Assigning the same value to each non-zero element within a particular row, then the form of A means that if an element of one of the above sequences with non-zero value has the row s value, then the next element in the sequence must either have the row $s - 1$ or row $s + 1$ value (with suitable restrictions if $s = 1$ or $s = r$). This is the same restriction as that on consecutive terms in the sequences of measure factors in (5.2.6). So, setting $r = m - 2$ and the entries of A to be equal to

$$A = \begin{pmatrix} 0 & \frac{x_2}{1+x_2} & 0 & 0 & \cdots & 0 & 0 & 0 \\ \frac{x_3}{1+x_3} & 0 & \frac{x_3}{1+x_3} & 0 & \cdots & 0 & 0 & 0 \\ 0 & \frac{x_4}{1+x_4} & 0 & \frac{x_4}{1+x_4} & \cdots & 0 & 0 & 0 \\ \vdots & & \vdots & & & \vdots & & \vdots \\ 0 & 0 & 0 & 0 & \cdots & 0 & \frac{x_{m-1}}{1+x_{m-1}} & 0 \end{pmatrix}, \tag{5.2.12}$$

the entries of A^k are then made up of all the possible sequences of $x_a/(1 + x_a)$ of

length k obeying the constraint given in (5.2.8). It is noted here for later use that due to the property $x_a = x_{m+1-a}$, the entries of A satisfy

$$A_{ij} = A_{m-1-i,m-1-j}. \tag{5.2.13}$$

It now remains to determine which of these entries obey the constraint (5.2.9) between the initial and final elements of the sequence of measure factors. This amounts to restricting the terms (5.2.11) to those with

$$A_{l_{k-1}j} = A_{m-1-i\pm1,j}. \tag{5.2.14}$$

where only the '$-$' sign is allowed for $i = 1$ and only the '$+$' sign for $i = m-2$.

Consider first the '$+$' choice. Then for $i = 2$, the only non-zero term occurs when $j = m-i-1 = m-3$, and for $i = 3, \cdots, m-2$ there are two choices, $j = m-i\pm1$. In each case,

$$A_{m-i,j} = \frac{x_{m-i+1}}{1+x_{m-i+1}}. \tag{5.2.15}$$

Although there is a choice in the value of j for $i \neq 2$, this has no impact on the preceding terms in the sequence, and so for $a = 4, \cdots, m-1$, each sequence of measure factors beginning with $x_a/(1+x_a)$ and satisfying the '$+$' part of the constraint (5.2.9) appear twice in A^k. So, to reproduce each sequence of measure factors satisfying the '$+$' part of the constraint (5.2.9) once and only once, $j = m-i-1$ must be chosen so that the relevant elements of A^k are those of the form

$$\left(A^k\right)_{ij} = A_{il_1}A_{l_1l_2}\cdots A_{l_{k-2}l_{k-1}}A_{m-i,m-i-1} \quad i = 2, \cdots, m-2. \tag{5.2.16}$$

where for now the Einstein summation convention has been dropped on i.

Similarly, if the '$-$' sign is chosen in (5.2.14) then for $i = m-3$ the only non-zero term appears when $j = m-2-(m-3)+1 = 2$. For $i = 1, \cdots, m-4$ there are two choices, $j = m-2-i\pm1$. In each case

$$A_{m-i-2,j} = \frac{x_{m-i-1}}{1+x_{m-i-1}} \tag{5.2.17}$$

so here the sequences of measure factors beginning with $x_a/(1+x_a)$ for $a = 2, \cdots, m-3$ and satisfying the '$-$' part of the constraint (5.2.9) appears twice in A^k. As before, the choice $j = m-1-i$ can be made so that the set of elements of A^k of the form

$$\left(A^k\right)_{ij} = A_{il_1}A_{l_1l_2}\cdots A_{l_{k-2}l_{k-1}}A_{m-i-2,m-i-1} \quad i = 1, \cdots, m-3 \tag{5.2.18}$$

contains each sequence of measure factors satisfying the '$-$' part of the constraint (5.2.9) once and only once.

Conversely, if $j = m-i-1$ in (5.2.11) then the only possible values of l_{k-1} are $l_{k-1} = m-3$ for $i = 1$, $l_{k-1} = m-i$ or $l_{k-1} = m-i-2$ for $i = 2, \cdots, m-3$, and $l_{k-1} = 2$ for $i = m-2$. The set of such elements of A^k is the union of the two sets (5.2.16) and (5.2.18) found above. The k^{th} term of $\ln g_A(r)$ is the sum of the elements of these sets so, reintroducing the summation convention, for $(m-3)\theta_0/2 \ll \ln(1/r) \ll (m-2)\theta_0/2$,

$$\ln g_A(r) = \sum_{\substack{n\geq 1 \\ m+n\ odd}} \frac{1}{2n}\frac{1}{2^{n+1}} A_{il_1}A_{l_1l_2}\cdots A_{l_{n-2}l_{n-1}}A_{l_{n-1},m-i-1}. \tag{5.2.19}$$

The sum of matrix elements here is the sum of the anti-diagonal elements of A^n, known as the anti-trace of A^n. So

$$\ln g_A(r) = \sum_{\substack{n\geq 1 \\ m+n\ odd}} \frac{1}{2n}\frac{1}{2^{n+1}} \mathrm{antiTr}(A^n), \tag{5.2.20}$$

where defining the $N \times N$ matrix J_N to have elements

$$(J_N)_{ij} = \delta_{i,N+1-j}, \tag{5.2.21}$$

the anti-trace can be expressed using J_{m-2} as

$$\mathrm{antiTr}(A^k) = \mathrm{Tr}(A^k J_{m-2}). \tag{5.2.22}$$

Turning to the situation where $m+n$ is even, the non-zero terms in $\ln g_B(r)$

correspond to those sub-regions for which

$$\frac{1}{1+e^{\varepsilon(\tilde{\theta}_i)}} = \frac{y_a}{1+y_a}, \qquad a \in \{2, \cdots, m-2\} \tag{5.2.23}$$

for each $\tilde{\theta}_i$. A similar constraint to the $m+n$ odd case exists on the values of the measure factors for consecutive $\tilde{\theta}_i$'s:

$$\begin{aligned} &\frac{1}{1+e^{\varepsilon(\tilde{\theta}_i)}} = \frac{y_a}{1+y_a} \quad \text{for} \quad i = 1, \cdots n \Rightarrow \\ &\frac{1}{1+e^{\varepsilon(\tilde{\theta}_{i+1})}} = \frac{y_{a+1}}{1+y_{a+1}} \quad \text{or} \quad \frac{1}{1+e^{\varepsilon(\tilde{\theta}_{i+1})}} = \frac{y_{a-1}}{1+y_{a-1}} \end{aligned} \tag{5.2.24}$$

with only the former option allowed if $a = 2$ and only the latter if $a = m-2$. So, the relevant sequences again appear as elements of powers of a matrix of the form (5.2.10), which in this case is an $m-3 \times m-3$ matrix B defined as

$$B = \begin{pmatrix} 0 & \frac{y_2}{1+y_2} & 0 & 0 & \cdots & 0 & 0 & 0 \\ \frac{y_3}{1+y_3} & 0 & \frac{y_3}{1+y_3} & 0 & \cdots & 0 & 0 & 0 \\ 0 & \frac{y_4}{1+y_4} & 0 & \frac{y_4}{1+y_4} & \cdots & 0 & 0 & 0 \\ \vdots & & \vdots & & & \vdots & & \vdots \\ 0 & 0 & 0 & 0 & \cdots & 0 & \frac{y_{m-2}}{1+y_{m-2}} & 0 \end{pmatrix} \tag{5.2.25}$$

There is also the additional constraint that

$$\frac{1}{1+e^{\varepsilon(\tilde{\theta}_1)}} = \frac{y_a}{1+y_a} \quad \Rightarrow \quad \frac{1}{1+e^{\varepsilon(\tilde{\theta}_n)}} = \frac{y_{m-a\pm1}}{1+y_{m-a\pm1}} \tag{5.2.26}$$

where only the '$-$' choice is allowed for $a = 2$ and only the '$+$' choice for $a = m-2$. This is the same form of constraint as in the $m+n$ odd case, just with m replaced with $m-1$, and since the y-plateaux at $\mathcal{M}_m$ have the same values as the x-type plateaux at $\mathcal{M}_{m-1}$, matrix B is just the same as matrix A with $m \to m-1$. The same conclusions can therefore be drawn and the allowed sequences of measure factors appear as the terms of the anti-trace of B^k:

$$\ln g_B(r) = \sum_{\substack{n \geq 1 \\ m+n \text{ even}}} \frac{1}{2n} \frac{1}{2^{n+1}} \text{antiTr}(B^n). \tag{5.2.27}$$

Now what remains is to evaluate $\ln g_A(r)$ and $\ln g_B(r)$ using the known values of $\{x_a\}$ and $\{y_a\}$ (4.1.48). To achieve this the anti-trace of the powers of matrices that appear in these expressions is rewritten in terms of the trace of powers of (slightly manipulated) matrices, which allows these expressions to be evaluated using the eigenvalues of the matrices in question. It suffices to derive this for the $m+n$ odd case, since the $m+n$ even case follows upon shifting $m \to m-1$. The situation depends on whether m is even or odd.

If m is even then

$$\ln g_A(r) = \sum_{\substack{n\geq 1\\ n\ odd}} \frac{1}{2n}\frac{1}{2^{n+1}}\mathrm{antiTr}(A^n) = \sum_{\substack{n\geq 1\\ n\ odd}} \frac{1}{2n}\frac{1}{2^{n+1}}\mathrm{Tr}(A^n J_{m-2}) \tag{5.2.28}$$

The property (5.2.13) leads to the observation

$$(J_{m-2}AJ_{m-2})_{ik} = (J_{m-2})_{ij_1}A_{j_1j_2}(J_{m-2})_{j_2k} = \delta_{i,m-1-j_1}A_{j_1j_2}\delta_{j_2,m-1-k} \tag{5.2.29}$$

$$= A_{m-1-i,m-1-k} = A_{ik}. \tag{5.2.30}$$

This means that for n odd

$$A^n J_{m-2} = A(J_{m-2}AJ_{m-2})A(J_{m-2}AJ_{m-2})A\cdots(J_{m-2}AJ_{m-2})AJ_{m-2} = (AJ_{m-2})^n \tag{5.2.31}$$

so that using the identity

$$\sum_{n=1}^{\infty}\frac{1}{n}\mathrm{Tr}M^n = -\mathrm{Tr}\ln(I-M) = -\ln\mathrm{Det}(I-M) \tag{5.2.32}$$

(5.2.28) becomes

$$\ln g_A(r) = \frac{1}{4}\sum_{\substack{n\geq 1\\ n\ odd}}\frac{1}{n}\mathrm{Tr}(\tfrac{1}{2}AJ_{m-2})^n \tag{5.2.33}$$

$$= \frac{1}{8}\ln\frac{\mathrm{Det}(I+\frac{1}{2}AJ_{m-2})}{\mathrm{Det}(I-\frac{1}{2}AJ_{m-2})}. \tag{5.2.34}$$

To find the eigenvalues of AJ_{m-2}, note that the matrix A can be written as

$$A_{ij} = l_{ij}\frac{x_{i+1}}{1+x_{i+1}} \tag{5.2.35}$$

where l_{ij} is the incidence matrix of the A_{m-2} Dynkin diagram. The transpose of this matrix appears in [18] where the eigenvalues are given as

$$\lambda_k = 2\cos\left(\frac{\pi k}{m+1}\right), \quad k = 2, 3, \cdots, m-1, \tag{5.2.36}$$

so these are also the eigenvalues of A. The eigenvectors ψ_k of A have the property

$$J_{m-2}\psi_k = (-1)^k\psi_k. \tag{5.2.37}$$

Therefore, the eigenvalues of AJ_{m-2} are $\mu_k = (-1)^k\lambda_k$, that is

$$\{\mu_k\} = \{2\cos\frac{2\pi}{m+1}, 2\cos\frac{4\pi}{m+1}, \cdots, 2\cos\frac{(m-2)\pi}{m+1}\}, \quad \text{all with multiplicity two.} \tag{5.2.38}$$

So

$$\frac{\mathrm{Det}\left(1+\frac{1}{2}AJ_{m-2}\right)}{\mathrm{Det}\left(1-\frac{1}{2}AJ_{m-2}\right)} = \frac{\cos^4\frac{\pi}{m+1}\cos^4\frac{2\pi}{m+1}\cdots\cos^4\frac{(m-2)\pi}{2(m+1)}}{\sin^4\frac{\pi}{m+1}\sin^4\frac{2\pi}{m+1}\cdots\sin^4\frac{(m-2)\pi}{2(m+1)}}. \tag{5.2.39}$$

This can be simplified using the well-known trigonometric identities

$$\cos\frac{\pi}{n}\cos\frac{2\pi}{n}\cdots\cos\frac{(n-1)\pi}{2n} = \frac{1}{2^{(n-1)/2}} \quad \text{for } n \text{ odd}, \tag{5.2.40}$$

and

$$\sin\frac{\pi}{n}\sin\frac{2\pi}{n}\cdots\sin\frac{(n-1)\pi}{n} = \frac{n}{2^{n-1}} \tag{5.2.41}$$

which implies

$$\sin^2\frac{\pi}{n}\sin^2\frac{2\pi}{n}\cdots\sin^2\frac{(n-1)\pi}{2n} = \frac{n}{2^{n-1}} \quad \text{for } n \text{ odd}. \tag{5.2.42}$$

Then $\ln g_A(r)$ becomes

$$\ln g_A(r) = \frac{1}{8}\ln\left(\frac{1}{(m+1)^2}\frac{\sin^4\frac{m\pi}{2(m+1)}}{\cos^4\frac{m\pi}{2(m+1)}}\right) = \frac{1}{8}\ln\left(\frac{4}{m+1}\frac{\sin^4\frac{m\pi}{2(m+1)}}{\sin^2\frac{\pi}{m+1}}\right)^2 \quad \text{for m even.} \tag{5.2.43}$$

If m is odd then

$$\ln g_A(r) = \sum_{\substack{n>1\\ n\ even}} \frac{1}{2n}\frac{1}{2^{n+1}}\mathrm{antiTr}(A^n) = \sum_{\substack{n>1\\ n\ even}} \frac{1}{2n}\frac{1}{2^{n+1}}\mathrm{Tr}(A^n J_{m-2}). \tag{5.2.44}$$

(5.2.31) no longer holds, but it is still possible to re-express (5.2.44) as the trace over powers of certain matrices. To see this, consider the matrix A_2, defined as the $(m-2)\times(m-2)$ matrix that only differs from A in the elements

$$(A_2)_{\frac{m-1}{2},\frac{m-3}{2}} = (A_2)_{\frac{m-1}{2},\frac{m+1}{2}} = 0. \tag{5.2.45}$$

Then it can be shown that

$$\mathrm{Tr}(A^n J_{m-2}) = \mathrm{Tr}(A^n - A_2^n) \tag{5.2.46}$$

for all m odd. Since each entry A_{ij} of A is proportional to the entry l_{ij} of the incidence matrix of the A_{m-2} Dynkin diagram, the non-zero terms in

$$\mathrm{Tr}(A^n J_{m-2}) = A_{il_1}A_{l_1l_2}\cdots A_{l_{n-2}l_{n-1}}A_{l_{n-1},m-i-1}, \tag{5.2.47}$$

can be pictured as a weighted path on the A_{m-2} Dynkin diagram, made up of steps between neighbouring nodes and starting at node i and finishing at the conjugate node $m-i-1$. The terms of $\mathrm{Tr}(A^n)$ and $\mathrm{Tr}(A_2^n)$ can be interpreted as weighted paths on the same Dynkin diagram, but this time starting and finishing on the same node i. Since m is odd, the paths in both cases must be made up of an even number of steps, so this interpretation makes it clear that both sides of (5.2.47) vanish for n odd. So n can be assumed to be even, which in any case are the values of interest for m odd.

Starting with the left hand side of (5.2.46) and dropping the summation conven-

tion, if a particular term

$$A_{il_1}A_{l_1l_2}\cdots A_{l_{n-2}l_{n-1}}A_{l_{n-1},m-i-1} \tag{5.2.48}$$

in (5.2.47) has $i < \frac{m-1}{2}$, then using (5.2.10) the sequence must contain the element $A_{\frac{m-1}{2}\frac{m+1}{2}}$ at least once. Suppose that the final time it appears is at $A_{l_rl_{r+1}}$. Using (5.2.13), the value of (5.2.48) is unchanged if each index $l_s > l_r$ is replaced by its conjugate $m-1-l_s$ (note that $\frac{m-1}{2}$ is self-conjugate). In particular, the final element in the sequence is now $A_{m-l_{n-1}-1,i}$. So, each term in trace of A^nJ_{m-2} with $i < \frac{m-1}{2}$ is equal to a term in the trace of A^n where the element $A_{\frac{m-1}{2}\frac{m-3}{2}}$ appears at least once. Similarly, if $i > \frac{m-1}{2}$ then $A_{\frac{m-1}{2}\frac{m-3}{2}}$ must be present in (5.2.48). Taking the conjugates of the indices after the final appearance of this element again equates each such term in the trace of A^nJ_{m-2} with a term in the trace of A^n, this time with the property that the element $A_{\frac{m-1}{2}\frac{m+1}{2}}$ appears at least once. Finally, if $i = \frac{m-1}{2}$ in (5.2.48) then $m-i-1 = \frac{m-1}{2}$ and so the term is already a term in the trace of A^n. By similar conjugation of indices the converse property follows that any term in $\mathrm{Tr}(A^n)$ which contains $A_{\frac{m-1}{2}\frac{m+1}{2}}$ or $A_{\frac{m-1}{2}\frac{m-3}{2}}$ at least once is equal to a term in $\mathrm{Tr}(A^nJ_{m-2})$. Therefore, $\mathrm{Tr}(A^nJ_{m-2})$ is equal to the sum of the terms of $\mathrm{Tr}(A^n)$ that contain $A_{\frac{m-1}{2}\frac{m+1}{2}}$ or $A_{\frac{m-1}{2}\frac{m-3}{2}}$ at least once.

Turning to the right hand side of (5.2.46), it follows from the definition of A_2 (5.2.45) that $\mathrm{Tr}(A_2)^n$ is equal to the sum of those terms of $\mathrm{Tr}(A^n)$ which contain neither $A_{\frac{m-1}{2}\frac{m+1}{2}}$ nor $A_{\frac{m-1}{2}\frac{m-3}{2}}$. So, $\mathrm{Tr}(A^n-(A_2)^n)$ consists of those terms of $\mathrm{Tr}(A^n)$ that contain either $A_{\frac{m-1}{2}\frac{m+1}{2}}$ or $A_{\frac{m-1}{2}\frac{m-3}{2}}$ at least once. These are exactly the terms that make up $\mathrm{Tr}(A^nJ_{m-2})$, so the identity (5.2.46) holds. So, using (5.2.32)

$$\ln g_A(r) = \frac{1}{4}\sum_{\substack{n>1\\ n\ even}}\frac{1}{n}\mathrm{Tr}\left(\left(\tfrac{1}{2}A\right)^n-\left(\tfrac{1}{2}A_2\right)^n\right) \tag{5.2.49}$$

$$= \frac{1}{8}\ln\frac{\mathrm{Det}\left(I-\frac{1}{4}\left(A_2\right)^2\right)}{\mathrm{Det}\left(I-\frac{1}{4}\left(A\right)^2\right)}. \tag{5.2.50}$$

In order to evaluate this, the characteristic equation and eigenvalues of A_2 must be determined. To find these, first note that the only non-zero entry on the middle row of $(A_2-\lambda I)$ is $-\lambda$ in the central column. So, expanding about the middle

row, $\mathrm{Det}(A_2 - \lambda I)$ is equal to $-\lambda$ multiplied by the determinant of a block diagonal matrix, with the blocks consisting of the upper-left- and lower-right-most $\frac{m-3}{2} \times \frac{m-3}{2}$ submatrices of $A - \lambda I$. Labelling these submatrices as $P - \lambda I$ and $Q - \lambda I$, the characteristic equation of A_2 is

$$-\lambda \,\mathrm{Det}(P - \lambda I)\,\mathrm{Det}(Q - \lambda I) = 0 \tag{5.2.51}$$

and the problem reduces to finding the eigenvalues of the submatrices P and Q of A.

These can be found from considerations of the form of the eigenvectors ψ_k of A for $k = \{3, 5, 7, \cdots m-2\}$. Since m is odd, the property (5.2.37) of the eigenvectors means that the central component of each ψ_k with k odd is zero, and that $(\psi_k)_i = -(\psi_k)_{m-1-i}$. With these properties, the linear independence of the ψ_k's implies the linear independence of the vectors ξ_k formed from the first $(m-3)/2$ elements of each ψ_k with k odd. Since the central element of each ψ_k with k odd is zero-valued, the first $(m-3)/2$ entries of the vector $A\psi_k = \lambda_k \psi_k$ are equal to the entries of the vector $P\xi_k$, so that $P\xi_k = \lambda_k \xi_k$. So the eigenvalues of P are λ_k for k odd, and the symmetries of the matrix A mean that Q has these same eigenvalues. So, in addition to 0, there are $(m-3)/2$ further eigenvalues of A_2, each with multiplicity 2, with values

$$\xi_k = 2\cos\Big(\frac{\pi k}{m+1}\Big)\,, \qquad k = 3, 5 \ldots m{-}2\,. \tag{5.2.52}$$

If $m+1 = 2 \bmod 4$ the A_2 itself is not fully diagonalisable. However, only the values of the eigenvalues and their algebraic multiplicities are needed to evaluate $\ln g_A(r)$, which becomes

$$\begin{aligned}\ln g_A(r) = \frac{1}{8}\ln\frac{\mathrm{Det}\left(I - \frac{1}{4}\left(A_2\right)^2\right)}{\mathrm{Det}\left(I - \frac{1}{4}\left(A\right)^2\right)} &= \frac{1}{8}\ln\frac{\sin^4\frac{3\pi}{m+1}\sin^4\frac{5\pi}{m+1}\cdots\sin^4\frac{(m-2)\pi}{m+1}}{\sin^2\frac{2\pi}{m+1}\sin^2\frac{3\pi}{m+1}\cdots\sin^2\frac{(m-1)\pi}{m+1}} \\ &= \frac{1}{8}\ln\frac{\sin^2\frac{3\pi}{m+1}\sin^2\frac{5\pi}{m+1}\cdots\sin^2\frac{(m-2)\pi}{m+1}}{\sin^2\frac{2\pi}{m+1}\sin^2\frac{4\pi}{m+1}\cdots\sin^2\frac{(m-1)\pi}{m+1}}\,.\end{aligned} \tag{5.2.53}$$

The identity (5.2.41) at $n = (m+1)/2$ becomes

$$\sin\frac{2\pi}{m+1}\sin\frac{4\pi}{m+1}\cdots\sin\frac{(m-1)\pi}{m+1} = \frac{m+1}{2^{(m+1)/2}} \tag{5.2.54}$$

and dividing the identity at $n = (m+1)$ by this gives

$$\sin\frac{\pi}{m+1}\sin\frac{3\pi}{m+1}\sin\frac{5\pi}{m+1}\cdots\sin\frac{m\pi}{m+1} = \frac{\left(\frac{m+1}{2^m}\right)}{\left(\frac{m+1}{2^{(m+1)/2}}\right)} \tag{5.2.55}$$

so that

$$\ln g_A(r) = \frac{1}{8}\ln\left(\frac{2}{(m+1)\sin^2\frac{\pi}{m+1}}\right)^2 \quad \text{for m odd.} \tag{5.2.56}$$

As was noted earlier,

$$\ln g_B(r)|_{\mathcal{M}_m} = \ln g_A(r)|_{\mathcal{M}_{m-1}}. \tag{5.2.57}$$

So, if m is even then $m-1$ is odd and $\ln g_B(r)$ is given by (5.2.56) with $m \to m-1$:

$$\ln g_B(r) = \frac{1}{8}\ln\left(\frac{2}{m\sin^2\frac{\pi}{m}}\right)^2. \tag{5.2.58}$$

Adding this to $\ln g_A$ for m even (5.2.43) gives $\ln g_0(r)$:

$$\ln g_0(r) = \ln g_A(r) + \ln g_B(r) \tag{5.2.59}$$

$$= \ln\left(\left(\frac{8}{m(m+1)}\right)^{\frac{1}{4}}\frac{\sin\frac{m\pi}{2(m+1)}}{\sqrt{\sin\frac{\pi}{m}\sin\frac{\pi}{m+1}}}\right) \qquad \text{for m even.} \tag{5.2.60}$$

When m is odd $\ln g_B(r)$ is given by (5.2.43) with $m \to m-1$ so

$$\ln g_B(r) = \frac{1}{8}\ln\left(\frac{4}{m}\frac{\sin^4\frac{(m-1)\pi}{2m}}{\sin^2\frac{\pi}{m}}\right)^2 \tag{5.2.61}$$

and

$$\ln g_0(r) = \ln g_A(r) + \ln g_B(r) \tag{5.2.62}$$

$$= \ln \left(\left(\frac{8}{m(m+1)} \right)^{\frac{1}{4}} \frac{\sin \frac{(m-1)\pi}{2m}}{\sqrt{\sin \frac{\pi}{m} \sin \frac{\pi}{m+1}}} \right) \qquad \text{for m odd.} \tag{5.2.63}$$

5.2.2 $\ln g_{b1}(r)$ and $\ln g_{b2}(r)$

The derivations of the values of $\ln g_{b1}$ and $\ln g_{b2}$ when the bulk theory is close to $\mathcal{M}_m$ are much simpler. Looking at the expressions (4.2.10) and (4.2.11) for $\ln g_{b1}$ and $\ln g_{b2}$, the localised nature of $\phi(\theta)$ and $\phi_{(3/4)}(\theta)$ means that the only parts of $L(\theta)$ that contribute to $\ln g_{b1}$ and $\ln g_{b2}$ are $L(\theta \approx 0)$ and $L(\theta \approx \theta_0/2) = L(\theta \approx -\theta_0/2)$ respectively. As can be seen from (5.2.4) and (5.2.5), when the bulk theory is close to a minimal model $\theta = 0$ lies the centre of the central plateau of $L(\theta)$, which has the value $\ln(1 + x_{(m+1)/2})$ or $\ln(1 + y_{m/2})$ depending on whether m is odd or even, respectively. $\theta = \theta_0/2$ lies at the centre of the first plateau to the right of this, the value of which is $\ln(1 + y_{(m-1)/2})$ for m odd and $\ln(1 + x_{m/2})$ for m even. So while the bulk theory stays close to $\mathcal{M}_m$, $L(\theta)$ is approximately constant close to these values of θ and so can be pulled outside the integrals and evaluated using the plateau values given by (4.1.48) and the integral results (4.1.7) and (4.2.9):

$$\ln g_{b1}(r) = -\tfrac{1}{2} L(0) = \begin{cases} -\frac{1}{2} \ln(1+x_{(m+1)/2}) = -\frac{1}{2} \ln \left(\dfrac{1}{\sin^2 \frac{\pi}{m+1}} \right) & \text{for } m \text{ odd} \qquad (5.2.64) \\ -\frac{1}{2} \ln(1+y_{m/2}) = -\frac{1}{2} \ln \left(\dfrac{1}{\sin^2 \frac{\pi}{m}} \right) & \text{for } m \text{ even} \qquad (5.2.65) \end{cases}$$

and

$$\ln g_{b2}(r) = -\tfrac{1}{2}L\left(\tfrac{1}{2}\theta_0\right) = \begin{cases} -\frac{1}{2}\ln(1+y_{(m-1)/2}) = -\frac{1}{2}\ln\left(\dfrac{\sin^2\frac{(m-1)\pi}{2m}}{\sin^2\frac{\pi}{m}}\right) & \text{for } m \text{ odd} \quad (5.2.66) \\ -\frac{1}{2}\ln(1+x_{m/2}) = -\frac{1}{2}\ln\left(\dfrac{\sin^2\frac{m\pi}{2(m+1)}}{\sin^2\frac{\pi}{m+1}}\right) & \text{for } m \text{ even}\,. \quad (5.2.67) \end{cases}$$

When $\ln g_0$, $\ln g_{b1}$ and $\ln g_{b2}$ are summed, the pieces which differ depending on whether m is odd or even cancel, giving

$$\ln g_0 + \ln g_{b1} + \ln g_{b2} = \ln\left(\left(\frac{8}{m(m+1)}\right)^{\frac{1}{4}}\sqrt{\sin\frac{\pi}{m}\sin\frac{\pi}{m+1}}\right) \forall\, m \geq 3. \quad (5.2.68)$$

As can be seen from (4.2.13), this is the equal to $\ln g(m,1,1) = \ln g(m,m{-}1,1)$, the logarithm of the g-function value of the conformal boundary condition associated with the bulk vacuum field or its conjugate. These are the boundary conditions with the smallest conformal g-function value, and the reason why this emerges becomes apparent once $\ln g_{b3}$ is analysed.

5.2.3 Adding in $\ln g_{b3}(r)$

Using the same reasoning as for $\ln g_{b1}$ and $\ln g_{b2}$, the behaviour of $\ln g_{b3}$ depends on $L(\theta \approx \theta_{b1}) = L(\theta \approx -\theta_{b1})$ and $L(\theta \approx \theta_{b2}) = L(\theta \approx -\theta_{b2})$. Since θ_{b1} and θ_{b2} can take any real value, they will not always lie at the centre of plateaux of $L(\theta)$, and so it is possible for $\ln g_{b3}$ to undergo pure boundary transitions as r varies through the domain $(m-3)\theta_0/2 \ll \ln(1/r) \ll (m-2)\theta_0/2$, that is while the bulk model remains close to $\mathcal{M}_m$. Suppose that for a certain value of r, θ_{b1} and θ_{b2} both lie on plateaux of $L(\theta)$, so that each lie within one of the x- and y-type intervals (4.1.42) and (4.1.43). Then as before the factors of $L(\theta)$ can be pulled outside the integrals, giving

$$\ln g_{b3}(r) = \tfrac{1}{2}\left(L\left(\theta_{b1}\right) + L\left(\theta_{b2}\right)\right). \quad (5.2.69)$$

For small changes in r, θ_{b1} and θ_{b2} will remain on their respective plateaux, so the value of $\ln g_{b3}(r)$ will be unaffected. So, adding this to the other terms of the logarithm of the g-function gives rise to a plateau of $\ln g(r)$, like those seen in figure 5.5.

Given a pair of boundary parameters $(\theta_{b1}, \theta_{b2})$, the task now is to identify particular boundary conditions with plateau values of $\ln g(r)$, just as was done in the warm-up case in section 5.1. When $|\theta_{b1}| \gg \ln(1/r)$ and $|\theta_{b2}| \gg \ln(1/r)$ both $L(\theta_{b1})$ and $L(\theta_{b2})$ are effectively zero and the logarithm of the g-function is independent of the boundary parameters and is equal to $\ln g_0 + \ln g_{b1} + \ln g_{b2}$. Since $\ln g_{b3}$ is always non-negative this is the lowest possible value of $\ln g(r)$ within each $\mathcal{M}_m$, which explains the identification made above of $\ln g_0 + \ln g_{b1} + \ln g_{b2}$ with the boundary conditions with the lowest conformal g-function, $(1,1)$ or $(m-1,1)$.

If $|\theta_{b1}| \ll \ln(1/r)$ then $L(\theta_{b1})$ becomes non-zero and different boundary conditions emerge, and the same applies to θ_{b2}. Then on a plateau of $\ln g(r)$, each choice of a pair of boundary parameters $(\theta_{b1}, \theta_{b2})$ corresponds to two (possibly equal) plateau values of $L(\theta)$, with each taking the form of

$$\ln(1+x_a) \quad a = 1 \cdots m \tag{5.2.70}$$

$$\text{or} \quad \ln(1+y_a) \quad a = 1 \cdots m-1, \tag{5.2.71}$$

from which the logarithm of the g-function can be calculated using (5.2.68) and (5.2.69). Given a pair of plateau values, the following rules allow the identification of either a single Cardy boundary condition or a superposition of the latter which has this g-function value:

$L(\theta_{b1})$	$L(\theta_{b2})$	Boundary condition
$\ln(1+x_a)$	$\ln(1+y_b)$	$[x_a, y_b] \equiv (b, a)$
$\ln(1+x_p)$	$\ln(1+x_q)$	$[x_p, x_q] \equiv (1, \lvert p-q\rvert+1)\&(1, \lvert p-q\rvert+3)\&\cdots\&(1, m-\lvert p+q-m-1\rvert)$
$\ln(1+y_r)$	$\ln(1+y_s)$	$[y_r, y_s] \equiv (\lvert r-s\rvert+1, 1)\&(\lvert r-s\rvert+3, 1)\&\cdots\&(m-1-\lvert r+s-m\rvert, 1)$

(5.2.72)

In the above, θ_{b1} and θ_{b2} are allowed to take both positive and negative values, with the same result holding for $\theta_{b1} \leftrightarrow \theta_{b2}$. These rules have the property that sending

$\theta_{b_i} \to -\theta_{b_i}$ has the effect of conjugating the corresponding plateau index, which seems a natural assumption to make. This will be explored further in section 6.2. To see how these results arise, $\ln g(r)$ must be calculated by evaluating $\ln g_{b3}$ (5.2.69) using the $L(\theta)$ plateau values (4.1.48) and adding this to the other parts of $\ln g(r)$ (5.2.68). For the $[x_a, y_b]$ case this gives the result

$$\ln g(r) = \ln \left(\left(\frac{8}{m(m+1)} \right)^{\frac{1}{4}} \frac{\sin(\frac{a\pi}{m+1}) \sin(\frac{b\pi}{m})}{\sqrt{\sin(\frac{\pi}{m+1}) \sin(\frac{\pi}{m})}} \right) \tag{5.2.73}$$

which can immediately be seen to equal $\ln g(m, b, a)$ as defined in (4.2.13). The other two cases are slightly more complicated.

For plateau values $[x_p, x_q]$

$$\ln g(r) = \ln \left(\left(\frac{8}{m(m+1)} \right)^{\frac{1}{4}} \frac{\sin(\frac{p\pi}{m+1}) \sin(\frac{q\pi}{m+1}) \sqrt{\sin \frac{\pi}{m}}}{\sin^{3/2} \frac{\pi}{m+1}} \right). \tag{5.2.74}$$

To see that the proposed superposition of boundary conditions has this same g-function value, the conformal g-function values of each boundary condition making up the superposition are added together giving

$$\begin{aligned} &\ln \left[g(m, 1, |p-q|+1) + g(m, 1, |p-q|+3) + \cdots + g(m, 1, m-|p+q-m-1|) \right] \\ &= \ln \left[\left(\frac{8}{m(m+1)} \right)^{\frac{1}{4}} \sqrt{\frac{\sin \frac{\pi}{m}}{\sin \frac{\pi}{m+1}}} \right. \\ &\qquad \left. \times \left(\sin \left(\frac{(|p-q|+1)\pi}{m+1} \right) + \cdots + \sin \left(\frac{(m-|p+q-m-1|)\pi}{m+1} \right) \right) \right]. \end{aligned} \tag{5.2.75}$$

Equality with (5.2.74) emerges upon using the identity [53]

$$\sum_{k=0}^{n-1} \sin(\alpha + k\beta) = \sin \left(\alpha + \frac{n-1}{2} \beta \right) \sin \frac{n\beta}{2} \operatorname{cosec} \frac{\beta}{2}. \tag{5.2.76}$$

This same identity can be used to show the equality between the $\ln g(r)$ result for the $[y_r, y_s]$ plateaux

$$\ln g = \left(\frac{8}{m(m+1)} \right)^{\frac{1}{4}} \frac{\sin(\frac{r\pi}{m}) \sin(\frac{s\pi}{m}) \sqrt{\sin \frac{\pi}{m+1}}}{\sin^{3/2} \frac{\pi}{m}} \tag{5.2.77}$$

and the conformal result for the proposed superposition

$$\begin{aligned}
&\ln\left[g(m,|r{-}s|{+}1,1)+g(m,|r{-}s|{+}3,1)+\cdots+g(m,m{-}1{-}|r{+}s{-}m|,1)\right]\\
&=\ln\left[\left(\frac{8}{m(m+1)}\right)^{\frac{1}{4}}\sqrt{\frac{\sin\frac{\pi}{m+1}}{\sin\frac{\pi}{m}}}\right.\\
&\qquad\left.\times\left(\sin\left(\frac{(|r{-}s|{+}1)\pi}{m}\right)+\cdots+\sin\left(\frac{(m{-}1{-}|r{+}s{-}m|)\pi}{m}\right)\right)\right]. \qquad (5.2.78)
\end{aligned}$$

Although the above rules are successful in assigning a boundary condition with the correct g-function value to a pair of plateau values, as in the warm-up example there is still some ambiguity due to the $\mathbb{Z}_2$ spin-flip symmetry of the g-function. In terms of $L(\theta)$, these symmetries arise from the fact that $L(\theta)$ is even so that $x_a = x_{m+1-a}$ and $y_b = y_{m-b}$, which means that the same g-function value arises for each of the four choices $(\pm\theta_{b1}, \pm\theta_{b2})$. This means the $[x_a, y_b]$ plateau configuration in the g-function could be identified with the boundary condition $(m-a, b)$ rather than (a, b). There is even greater freedom when the g-function equals that of a superposition of boundary conditions, because then each one of these boundary conditions (a, b) can be individually exchanged for its spin-flip conjugate whilst leaving the g-function of the superposition unchanged. It is possible that this ambiguity could be resolved by considering the RG flows of inner products not only between boundary states and the bulk ground state as has been done in defining the g-function so far, but also between boundary states and excited bulk states. This will be explored further in section 6.2. Further ambiguities can arise from more 'accidental' equalities between the g-functions of different boundary conditions, and appear as additional equalities in the set of g-function values for all possible superpositions of Cardy boundary conditions. For example, $g(5,1,3) = 2g(5,1,1)$, so that the g-function is unable to distinguish between the $(1,3)$ and $(1,1)\&(1,1)$ boundary conditions in $\mathcal{M}_5$. However, modulo the spin-flip ambiguities, the identifications between plateau values and boundary conditions given in (5.2.72) are the only set of rules that have been found to work consistently for all minimal models $\mathcal{M}_m$. Furthermore, the boundary conditions that emerge line up with those appearing in [52] (see also [54]), where the perturbation of a minimal model with boundary described by a single

boundary parameter were considered. The rules given in (5.2.72) will therefore be assumed to be correct, and the spin-flip ambiguity will be left implicit.

Now that all the g-function plateaux in the staircase model have been identified with conformal boundary conditions, it remains to determine what flows occur between these as r varies for particular values of the boundary parameters. The pure boundary flows that occur while the bulk theory is close to a minimal model must be identified, along with those that coincide with bulk transitions. Once again, this is all governed by the form of $L(\theta)$ as r varies. As can be seen from the discussion of the plateaux of $L(\theta)$ in section 4.1 ((4.1.42), (4.1.43)), if the bulk theory is initially close to $\mathcal{M}_m$ then as $\ln(1/r)$ ranges from $(m-2)\theta_0/2$ down to $(m-3)\theta_0/2$ the x-type plateaux decrease in width down to 0, while the widths of the y-type plateaux start at 0 and increase. At $\ln(1/r) = (m-3)\theta_0/2$ the crossover from $\mathcal{M}_m$ to $\mathcal{M}_{m-1}$ occurs, and the y-type plateaux of $\mathcal{M}_m$ become the x-type plateaux of $\mathcal{M}_{m-1}$. New y-type plateaux appear as $\ln(1/r)$ decreases further, whose centres coincide with those of the $\mathcal{M}_m$ x-type plateaux.

The simplest situation occurs once $\ln(1/r) < |\theta_{b_i}|$ for $i = 1, 2$, since then, as was described earlier, $\ln g(r)$ becomes independent of the boundary parameters so the only transitions are bulk transitions. The g-function here is equal to that of the $(1,1)$ boundary condition whenever the bulk theory is close to a minimal model, so the boundary condition flow is simply through the $(1,1)$ boundary conditions of the minimal models appearing in the flow of the bulk theory for $\ln(1/r) < |\theta_{b_i}|$. If both θ_{b1} and θ_{b2} are sent to infinity before r is varied then $\ln(1/r) < \theta_{b1}$ and $\ln(1/r) < \theta_{b2}$ for all values of r and the full g-function flow consists solely of the $(1,1)$ boundary condition of each successive minimal model. Since this flow arises when $\ln g_{b3}$ is zero, the fact that $\ln g_{b3}$ is non-negative for all values of r means that this flow provides a lower bound on the g-function at each value of r. This is seen in figure 5.5a, where for $\ln r > -180$ the lowest-lying flow is through plateaux corresponding to the $(1,1)$ boundary conditions of the minimal models from $\mathcal{M}_8$ down to $\mathcal{M}_3$.

When $|\theta_{b1}| < \ln(1/r)$ or $|\theta_{b2}| < \ln(1/r)$ the boundary transitions do not necessarily coincide with the bulk transitions. Transitions in the value of $L(\theta_{b_i})$ for $i = 1, 2$ and hence in the value of $\ln g(r)$ occur whenever r is such that either θ_{b1}

or θ_{b2} (or both) lies on a kink between the $L(\theta)$ plateaux, i.e. somewhere between the intervals (4.1.42) and (4.1.43). The presence of both θ_{b_i} and $-\theta_{b_i}$ for $i = 1, 2$, coupled with the symmetry of $L(\theta)$ means that transitions caused by descendants of the left and right hand seed kinks of $L(\theta)$ occur at the same values of r. For θ_{b_i} positive, boundary crossovers associated with θ_{b_i} therefore occur when r satisfies

$$\ln(1/r) - k\theta_0 = \theta_{b_i} \quad \Rightarrow \quad \ln(r) = -k\theta_0 - \theta_{b_i}\,, \quad k = 0, 1, \ldots \tag{5.2.79}$$

or

$$\ln(1/r) - k\theta_0 = -\theta_{b_i} \quad \Rightarrow \quad \ln(r) = -k\theta_0 + \theta_{b_i}\,, \quad k = A, A{+}1, \ldots \tag{5.2.80}$$

where $A = \lceil 2\theta_{b_i}/\theta_0 \rceil$, the smallest integer greater than or equal to $2\theta_{b_i}/\theta_0$ (this restriction on the value of k is due to the fact a transition involving θ_{b_i} can only occur if $|\theta_{b_i}| < \ln(1/r)$). Similar rules hold for θ_{b_i} negative, but with the signs before θ_{b_i} switched.

To treat the cases where $|\theta_{b_i}| < \ln(1/r)$, consider first the values of r for which the theory is close to the minimal model $\mathcal{M}_m$, $(m-3)\theta_0/2 \ll \ln(1/r) \ll (m-2)\theta_0/2$. The simplest case here occurs if a boundary parameter satisfies $\theta_{b_i} = \gamma\theta_0/2$ for $\gamma \in \mathbb{Z}$, so that while the theory is close to $\mathcal{M}_m$ the parameter sits at the centre of an x- or y-type plateau of $L(\theta)$, and so $L(\theta)$ and therefore $\ln g(r)$ are constant for these values of r. In both of these cases there are no pure boundary transitions associated to the parameter in question; all the boundary transitions coincide with the bulk transition since it is at this point that the x-type plateaux vanish and are replaced by the $\mathcal{M}_{m-1}$ y-type plateaux, and the $\mathcal{M}_m$ y-type plateaux are re-identified as the $\mathcal{M}_{m-1}$ x-type plateaux. This is the case for θ_{b1} in the plots in figure 5.5; all the boundary transitions that occur while the bulk is close to a minimal model are induced by θ_{b2}.

If $\theta_{b_i} \neq \gamma\theta_0/2$ then as r ranges through $(m-3)\theta_0/2 \ll \ln(1/r) \ll (m-2)\theta_0/2$, θ_{b_i} lies initially at some non-central point of an $\mathcal{M}_m$ x-type plateau. Then as $\ln(1/r)$ decreases, at some point $L(\theta_{b_i})$ will undergo a transition after which θ_{b_i} lies on an $\mathcal{M}_m$ y-type plateau, thus effecting a flow between g-function values corresponding

to different boundary conditions. The value of r for which the transition occurs depends on the distance of the boundary parameter from the centre of the relevant x-type plateau, and the particular y-type plateau that θ_{b_i} moves to depends on whether it lies to the left or right of the centre of the x-type plateau.

To consider this in more detail, assume that θ_{b1} initially lies on the $\ln(1+x_r)$ plateau of $L(\theta)$, with θ_{b2} on the $\ln(1+x_s)$ plateau, so that $\theta_{b1} \in [z_{2r-3}-\theta_0/2, z_{2r-3}+\theta_0/2]$ and $\theta_{b2} \in [z_{2s-3}-\theta_0/2, z_{2s-3}+\theta_0/2]$. These plateaux are centred on z_{2r-3} and z_{2s-3} respectively (4.1.11). Assuming that neither parameter coincides with the centre of its x-type plateau, then if $\theta_{b1} > z_{2r-3}$ $L(\theta_{b1})$ moves to the $\ln(1+y_{r-1})$ plateau after the boundary transition, whereas if $\theta_{b1} < z_{2r-3}$ it moves to the $\ln(1+y_r)$ plateau. Replacing r with s, the same rules apply for θ_{b2}. Which transition occurs first depends on the distance of each boundary parameter from the centre of their respective x-type plateaux. If $|\theta_{b1} - z_{2r-3}| > |\theta_{b2} - z_{2s-3}|$ then the θ_{b1} transition occurs first as $\ln(1/r)$ decreases. If the opposite is true then the θ_{b2} transition precedes the θ_{b1} one, and if they are equal then the transitions happen at exactly the same value of r.

Let us assume initially that the values of θ_{b1} and θ_{b2} are such that neither lie at the centre of a plateau, and that their distances from the centres of their respective x-type plateau are sufficiently different from one another for the $L(\theta_{b1})$ transition to be effectively complete before the $L(\theta_{b2})$ transition begins, or vice versa. Then while the bulk theory stays close to $\mathcal{M}_m$, the set of possible flows starting from the plateau configuration $L(\theta_{b1}) = \ln(1+x_r)$, $L(\theta_{b2}) = \ln(1+x_s)$ is

$$\begin{array}{ccccc}
[y_r, y_s] & \longleftarrow & [x_r, y_s] & \longrightarrow & [y_{r-1}, y_s] \\
\uparrow & & \uparrow & & \uparrow \\
[y_r, x_s] & \longleftarrow & [x_r, x_s] & \longrightarrow & [y_{r-1}, x_s] \\
\downarrow & & \downarrow & & \downarrow \\
[y_r, y_{s-1}] & \longleftarrow & [x_r, y_{s-1}] & \longrightarrow & [y_{r-1}, y_{s-1}]
\end{array} . \tag{5.2.81}$$

The set of flows arising from all possible boundary parameter pairs $(\theta_{b1}, \theta_{b2})$ is then the union of such diagrams. θ_{b1} and θ_{b2} will again be allowed to take all real values satisfying the above conditions, both positive and negative. The full diagram is

then made up of interlocking 3×3 blocks of the form (5.2.81), with the plateau configurations at the centre of each forming the set $\{[x_r, x_s] |\, r, s \in 2, \cdots, m-1\}$.

As an example, let us consider $\mathcal{M}_5$. Then there are nine possible $[x_r, x_s]$ starting points for the flows, and the union of the resulting blocks of flows produces a 7×7 grid. The figure below shows the lower ($\theta_{b2} > 0$) part of this:

$$
\begin{array}{ccccccccccccc}
\vdots & & \vdots & & \vdots & & \vdots & & \vdots & & \vdots & & \vdots \\
{[y_4, x_3]} & \longleftarrow & {[x_4, x_3]} & \longrightarrow & {[y_3, x_3]} & \longleftarrow & {[x_3, x_3]} & \longrightarrow & {[y_2, x_3]} & \longleftarrow & {[x_2, x_3]} & \longrightarrow & {[y_1, x_3]} \\
\downarrow & & \downarrow & & \downarrow & & \downarrow & & \downarrow & & \downarrow & & \downarrow \\
{[y_4, y_2]} & \longleftarrow & {[x_4, y_2]} & \longrightarrow & {[y_3, y_2]} & \longleftarrow & {[x_3, y_2]} & \longrightarrow & {[y_2, y_2]} & \longleftarrow & {[x_2, y_2]} & \longrightarrow & {[y_1, y_2]} \\
\uparrow & & \uparrow & & \uparrow & & \uparrow & & \uparrow & & \uparrow & & \uparrow \\
{[y_4, x_2]} & \longleftarrow & {[x_4, x_2]} & \longrightarrow & {[y_3, x_2]} & \longleftarrow & {[x_3, x_2]} & \longrightarrow & {[y_2, x_2]} & \longleftarrow & {[x_2, x_2]} & \longrightarrow & {[y_1, x_2]} \\
\downarrow & & \downarrow & & \downarrow & & \downarrow & & \downarrow & & \downarrow & & \downarrow \\
{[y_4, y_1]} & \longleftarrow & {[x_4, y_1]} & \longrightarrow & {[y_3, y_1]} & \longleftarrow & {[x_3, y_1]} & \longrightarrow & {[y_2, y_1]} & \longleftarrow & {[x_2, y_1]} & \longrightarrow & {[y_1, y_1]}
\end{array}
\tag{5.2.82}
$$

As is clear from the above, boundary conditions corresponding to plateau values of the form $[x_r, x_s]$ behave as sources in the network of flows for each $\mathcal{M}_m$, whereas those corresponding to $[y_r, y_s]$ act as sinks.

The rules given in (5.2.72) can be used to convert the plateau configurations to specific boundary conditions, modulo the $\mathbb{Z}_2$ ambiguity described earlier, and the result in the $\mathcal{M}_5$ case is shown in figure 5.6. In this figure, the requirement that the θ_{b1} and θ_{b2} transitions be well-separated has been removed and this has introduced additional flows: the flows depicted by straight diagonal arrows arise when θ_{b1} and θ_{b2} are exactly the same distance from the centres of their respective x-type plateaux, so the transitions occur simultaneously; the curved flows occur when the θ_{b1} transition begins before the θ_{b2} transition is complete, or vice versa. Note that reflection in the lines $\theta_{b1} = \theta_{b2}$ and $\theta_{b1} = -\theta_{b2}$ maps a boundary condition to itself, whereas reflection in the line $\theta_{b1} = 0$ sends a boundary condition to its

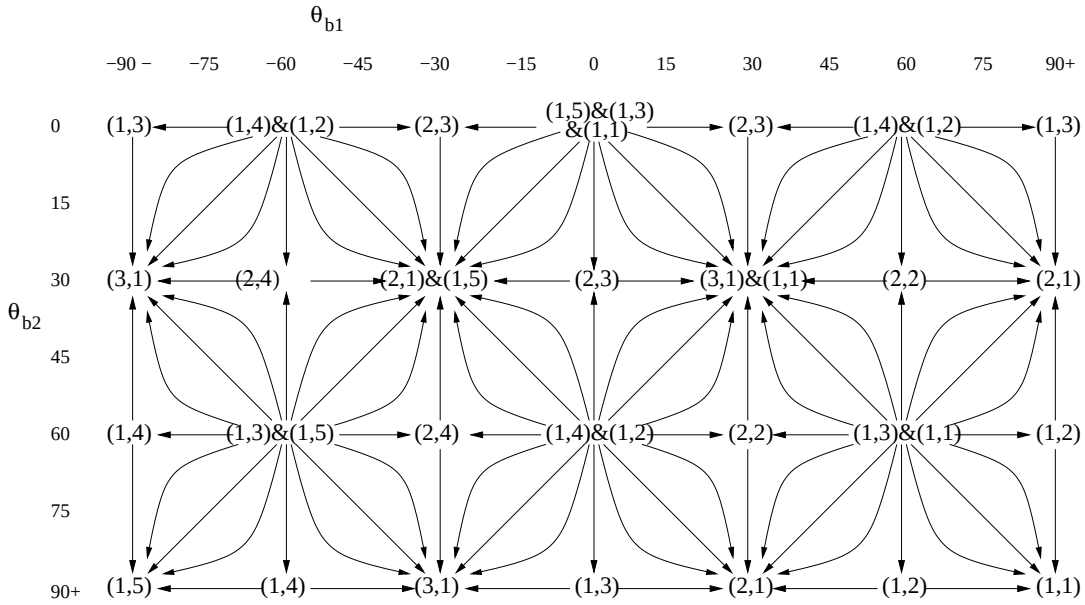

Figure 5.6: A diagram showing the pure boundary flows that occur when the bulk theory is close to $\mathcal{M}_5$, for various values of θ_{b1} and θ_{b2}, where $\theta_0 = 60$.

spin-flip conjugate.

To complete the picture of the flows between boundary conditions, the flows that coincide with the bulk transitions also need to be studied. The bulk flow from $\mathcal{M}_m$ to $\mathcal{M}_{m-1}$ occurs as $\ln(1/r)$ decreases through a region centred on $\ln(1/r) = (m-3)\theta_0/2$, and the g-function during this period is again governed by the form of $L(\theta)$. As has already been discussed, as $\ln(1/r)$ approaches $(m-3)\theta_0/2$ the widths of the x-type plateaux shrink to zero while the y-type plateaux increase in size. After the crossover at $\ln(1/r) = (m-3)\theta_0/2$, the plateaux which were y-type while the bulk theory was close to $\mathcal{M}_m$ become the x-type plateaux for $\mathcal{M}_{m-1}$:

$$\ln(1+y_a)|_{\mathcal{M}_m} \to \ln(1+x_a)|_{\mathcal{M}_{m-1}}, \qquad a = 1, \cdots, m-1. \tag{5.2.83}$$

As can be seen from (4.1.48), $y_a|_{\mathcal{M}_m} = x_a|_{\mathcal{M}_{m-1}}$ and so the transition leaves the values of these plateaux are unchanged. However, their different interpretations within their respective minimal models means that in the context of the g-function they are associated with different boundary conditions, and this will be explored in greater detail below. As $\ln(1/r)$ decreases beyond the transition point, new y-type

plateaux emerge whose centres coincide with those of the $\mathcal{M}_m$ x-type plateaux, and whose heights can be found by evaluating (4.1.48) at $\mathcal{M}_{m-1}$ with $a = 1, \cdots, m-2$.

As the bulk theory transition occurs, the set of possible boundary conditions changes from those allowed in $\mathcal{M}_m$ to those allowed in $\mathcal{M}_{m-1}$, and so the g-function describes a flow from an $\mathcal{M}_m$ boundary condition to an $\mathcal{M}_{m-1}$ one. These boundary flows can be determined by considering the $\mathcal{M}_m$ and $\mathcal{M}_{m-1}$ plateaux of $L(\theta)$ on which the boundary parameters lie immediately before and after the transition. Suppose for now that both $|\theta_{b1}| \leq (m-3)\theta_0/2$ and $|\theta_{b2}| \leq (m-3)\theta_0/2$, so that $L(\theta_{b1})$ and $L(\theta_{b2})$ are both non-zero at the point where the transition from $\mathcal{M}_m$ to $\mathcal{M}_{m-1}$ takes place. The possible configurations in this situation fall into three categories:

(i) If

$$\theta_{b1}, \theta_{b2} \neq (m-3)\theta_0/2 - k\theta_0\,, \qquad k = 0, 1, \ldots m-3. \tag{5.2.84}$$

then neither θ_{b1} nor θ_{b2} lies at the centre of an x-type plateau of $\mathcal{M}_m$ as the bulk transition is approached. Then θ_{b1} and θ_{b2} have either been positioned at the centre of y-type plateaux for the whole period where the bulk theory is close to $\mathcal{M}_m$, or they have each initially been on an x-type plateau, and then moved to a y-type plateau as r has varied through the $\mathcal{M}_m$ range. In either case, both θ_{b1} and θ_{b2} lie on y-type plateaux once $\ln r$ is such that the bulk transition takes place. As described above, the bulk transition does not change the value of these plateaux, but after it they are re-interpreted as x-type plateaux. Taking

$$\begin{aligned}
&\theta_{b1} \in ((m-3)\theta_0/2-(r-1)\theta_0\,,\ (m-3)\theta_0/2-(r-2)\theta_0) \quad \text{and} \\
&\theta_{b2} \in ((m-3)\theta_0/2-(s-1)\theta_0\,,\ (m-3)\theta_0/2-(s-2)\theta_0),
\end{aligned}$$

the corresponding pair of plateau values immediately prior to the transition is $[y_r, y_s]|_{\mathcal{M}_m}$, which according to (5.2.83) flows to $[x_r, x_s]|_{\mathcal{M}_{m-1}}$ during the bulk transition. Such flows therefore begin at 'sinks' in the network of pure-boundary flows for $\mathcal{M}_m$ and end at 'sources' in the network for $\mathcal{M}_{m-1}$.

Translating the plateau values to Cardy boundary conditions using the rules

given in (5.2.72) produces the flow

$$\begin{array}{ll} (f,1)\,\&\,(f{+}2,1)\,\&\,\cdots\,\&\,(g,1) & \mathcal{M}_m \\ \downarrow & \\ (1,f)\,\&\,(1,f{+}2)\,\&\,\cdots\,\&\,(1,g) & \mathcal{M}_{m-1} \end{array} \tag{5.2.85}$$

where

$$f = |r{-}s|{+}1\ , \quad g = m{-}1{-}|r{+}s{-}m| \quad \text{and} \quad 2 \leq r,s \leq m{-}2\,. \tag{5.2.86}$$

The symmetry $[y_r, y_s] = [y_{m-r}, y_{m-s}]$ and the $\theta_{b1} \leftrightarrow \theta_{b2}$ symmetry of the g-function (which means that $[y_r, y_s]$ is equivalent to $[y_s, y_r]$) allow r and s to be restricted to

$$2 \leq r \leq s \leq m-2, \quad r+s \leq m \tag{5.2.87}$$

whilst still giving rise to the full set of flows of the type (5.2.85). Applying these restrictions to f and g gives

$$1 \leq f < g \leq m-1\,, \quad f-g \in 2\mathbb{Z}. \tag{5.2.88}$$

(ii) If one of θ_{b1} or θ_{b2} lies at the centre of an x-type plateau of $\mathcal{M}_m$ prior to the bulk transition then since the centres of the plateaux are fixed while the bulk is close to $\mathcal{M}_m$, the boundary parameter remains on this plateau right up to the point where the transition occurs. Then after the transition y-type plateaux emerge with the same centres as the $\mathcal{M}_m$ x-type plateaux, so the boundary parameter now lies at the centre of a new $\mathcal{M}_{m-1}$ y-type plateau. Without loss of generality, let us assume that it is θ_{b1} for which this is the case. Then with

$$\theta_{b1} = (m-3)\theta_0/2 - (s{-}2)\theta_0 \quad 2 \leq s \leq m{-}1 \tag{5.2.89}$$

and

$$\theta_{b2} \in ((m{-}3)\theta_0/2{-}(r{-}1)\theta_0\,,\,(m{-}3)\theta_0/2{-}(r{-}2)\theta_0), \quad r = 2\cdots m-1, \tag{5.2.90}$$

θ_{b1} originally lies at the centre of the $\ln(1+x_s)|_{\mathcal{M}_m}$ plateau and after the transition ends up at the centre of the $\ln(1+y_{s-1})|_{\mathcal{M}_{m-1}}$ plateau, whereas θ_{b2} behaves as in case i), and in the process of the transition moves from $\ln(1+y_r)|_{\mathcal{M}_m}$ to $\ln(1+x_r)|_{\mathcal{M}_{m-1}}$. The flow is then $[x_s, y_r]_{\mathcal{M}_m} \to [y_{s-1}, x_r]_{\mathcal{M}_{m-1}}$ which on converting to Cardy boundary conditions using the rules (5.2.72) becomes

$$\begin{array}{ccc} (r,s) & \mathcal{M}_m & \\ \downarrow & , & 2\le r\le m-2\,,\quad 2\le s\le m-1\,. \\ (s-1,r) & \mathcal{M}_{m-1} & \end{array} \tag{5.2.91}$$

(iii) If

$$\theta_{b1} = (m-3)\theta_0/2 - (r-2)\theta_0, \quad 2\le r\le m-1 \quad \text{and} \tag{5.2.92}$$

$$\theta_{b2} = (m-3)\theta_0/2 - (s-2)\theta_0, \quad 2\le s\le m-1 \tag{5.2.93}$$

then both boundary parameters lie at the centres of x-type plateaux prior to the transition. The flow in the plateau values induced by the bulk transition is then $[x_r, x_s]_{\mathcal{M}_m} \to [y_{r-1}, y_{s-1}]_{\mathcal{M}_{m-1}}$, so this time 'sources' in the $\mathcal{M}_m$ flow network flow to 'sinks' in the $\mathcal{M}_{m-1}$ network. This corresponds to the following flow in Cardy boundary conditions:

$$\begin{array}{cc} (1,f)\,\&\,(1,f+2)\,\&\,\cdots\,\&\,(1,g) & \mathcal{M}_m \\ \downarrow & \\ (f,1)\,\&\,(f+2,1)\,\&\,\cdots\,\&\,(g-2,1) & \mathcal{M}_{m-1} \end{array} \tag{5.2.94}$$

where now

$$f = |r-s|+1\,,\quad g = m-|r+s-m-1| \quad \text{and} \quad 2\le r,s\le m-1\,. \tag{5.2.95}$$

The symmetries used in case (i) can again be used to reduce the domains of r and s while still producing all possible flows. This time the restrictions amount to

$2 \leq r \leq s \leq m-1$ and $r+s \leq m+1$ which in terms of f and g corresponds to

$$1 \leq f < g \leq m\,, \quad f-g \in 2\mathbb{Z}\,. \tag{5.2.96}$$

To get a complete set of rules for the boundary flows induced by the bulk transition, the situation where either one or both boundary parameters satisfy $|\theta_{b_i}| > (m-3)\theta_0/2$ must be included. In this case, one or both of $L(\theta_{b2})$ and $L(\theta_{b2})$ has become equal to zero before the transition occurs, and so just remains zero during and after the transition. Recalling that $\ln(1+x_1)|_{\mathcal{M}_m}$, $\ln(1+x_m)|_{\mathcal{M}_m}$, $\ln(1+y_1)|_{\mathcal{M}_m}$ and $\ln(1+y_{m-1})|_{\mathcal{M}_m}$ are all equal to zero, by careful choice of the labelling of the zero-valued plateaux it is possible to incorporate the situations that arise here into the rules already formulated.

(i) If both $L(\theta_{b1})$ and $L(\theta_{b2})$ equal zero before the transition, or if $L(\theta_{b1}) = 0$ and θ_{b2} lies away from the centre of a non-zero x-type plateau (or vice versa), then by labelling the flow(s) on the zero-valued plateaux as $y_1 \to x_1$ or $y_{m-1} \to x_{m-1}$ these flows can be incorporated into case (i) by extending the r and s domains to allow $r, s = 1, m-1$. This corresponds to allowing f to equal g in the flows of the form (5.2.85), so that now

$$1 \leq f \leq g \leq m-1\,, \quad f-g \in 2\mathbb{Z}\,. \tag{5.2.97}$$

The choices $f = g = 1$ and $f = g = m-1$ in (5.2.85) produce the flows

$$\begin{aligned} (1,1)|_{\mathcal{M}_m} &\to (1,1)|_{\mathcal{M}_{m-1}} \quad \text{and} \\ (m-1,1)|_{\mathcal{M}_m} &\to (1,m-1)|_{\mathcal{M}_{m-1}}. \end{aligned} \tag{5.2.98}$$

These (f,g) values correspond to the situation where $\ln g_{b3} = 0$. The logarithm of the g-function is then $\ln g_0 + \ln g_{b1} + \ln g_{b2}$, which equals $\ln g(m,1,1) = \ln g(m,m-1,1)$ when the bulk is close to a minimal model, as seen in (5.2.68). Recalling the symmetry $(a,b)|\mathcal{M}_m = (m-a, m+1-b)|\mathcal{M}_m$, it is clear that the flows in (5.2.98) are in agreement with this.

(ii) The final situation to consider is where $|\theta_{b2}| > (m-3)\theta_0/2$ while θ_{b1} lies at the centre of an x-type plateau, say $\theta_{b1} = (m-3)\theta_0/2 - (s-2)\theta_0$, $2 \leq s \leq m-1$. Then, labelling the flows between the zero-valued plateaux as before, the flow induced by the bulk transition is either $[x_s, y_1]|_{\mathcal{M}_m} \to [y_{s-1}, x_1]|_{\mathcal{M}_{m-1}}$ or $[x_s, y_{m-1}]|_{\mathcal{M}_m} \to [y_{s-1}, x_{m-1}]|_{\mathcal{M}_{m-1}}$ with $2 \leq s \leq m-1$. The flow therefore fits into case (ii) if the domain of r is extended to allow $r = 1$ and $r = m-1$, so that the flows appearing in (5.2.91) can occur for

$$1 \leq r \leq m-1\,, \quad 2 \leq s \leq m-1\,. \tag{5.2.99}$$

Combining these rules for the bulk transitions with the networks of flows at each minimal model (such as that depicted for $\mathcal{M}_5$ in (5.2.82)) describes all the flows that can occur as $\ln(1/r)$ decreases through the staircase model and passes close to the series of minimal models $\mathcal{M}_m$. In the cases where the flows between consecutive minimal models are induced by only one boundary parameter, say θ_{b1} (which occurs when $\ln g(r)$ is independent of θ_{b2} or when θ_{b2} sits at the centre of an $\mathcal{M}_m$ y-type plateau), then the flows seen agree with those found perturbatively by Fredenhagen et al. [52] in the single parameter case. To conclude this section, some examples of combined sequences flows are shown in figures 5.7 and 5.8 for θ_{b1} equal to 180 and 60 respectively, at various values of θ_{b2}. An important feature of these diagrams is the matching of the parts below and including $\mathcal{M}_4$. This is also apparent in figure 5.5, where plot 5.5b matches plot 5.5c for $\ln r > -60$, and plot 5.5c matches plot 5.5d for $\ln r > -120$, and is due to the fact that $L(\theta_{b1})$ equals zero for $\ln r \gg -\theta_{b1}$ so that $\ln g(r)$ is independent of θ_{b1} for these values of r.

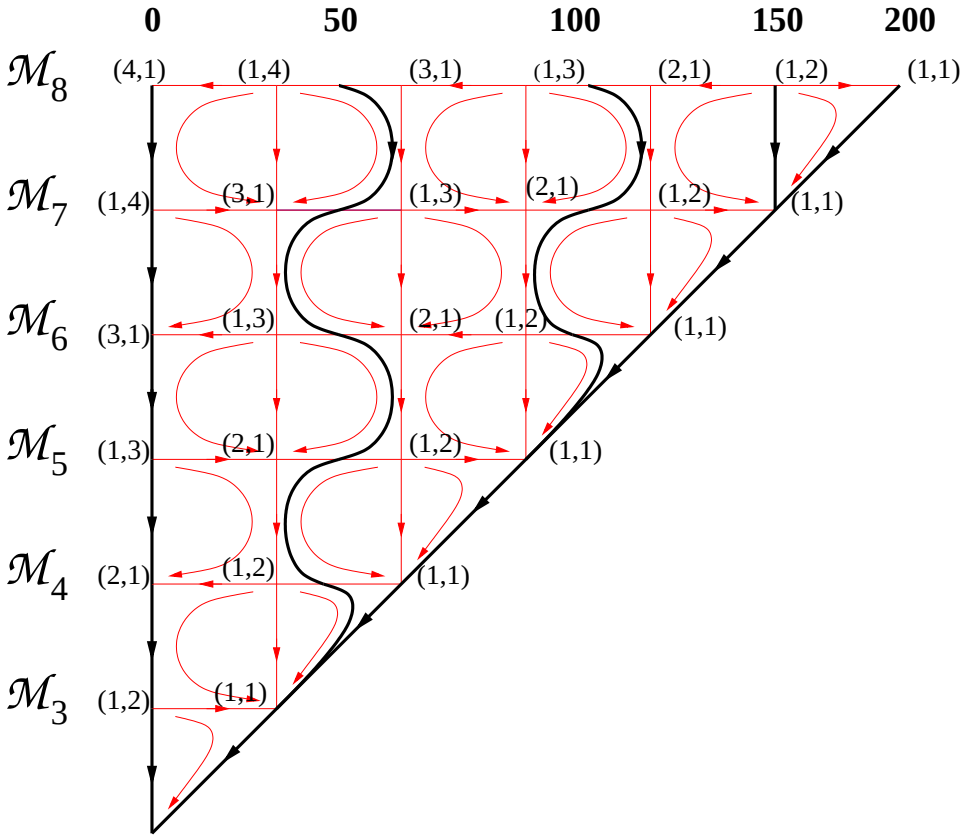

Figure 5.7: A diagram of the flows between boundary conditions for $\theta_{b1} = 180$ as the bulk theory flows close to the series of minimal models $\mathcal{M}_8 \to \cdots \to \mathcal{M}_3$. The horizontal direction shows flows within a particular minimal model, and the vertical direction shows flows occurring during the bulk transitions. The flows here correspond to the g-function plots in figure 5.5d, and the same flows have been highlighted in both figures.

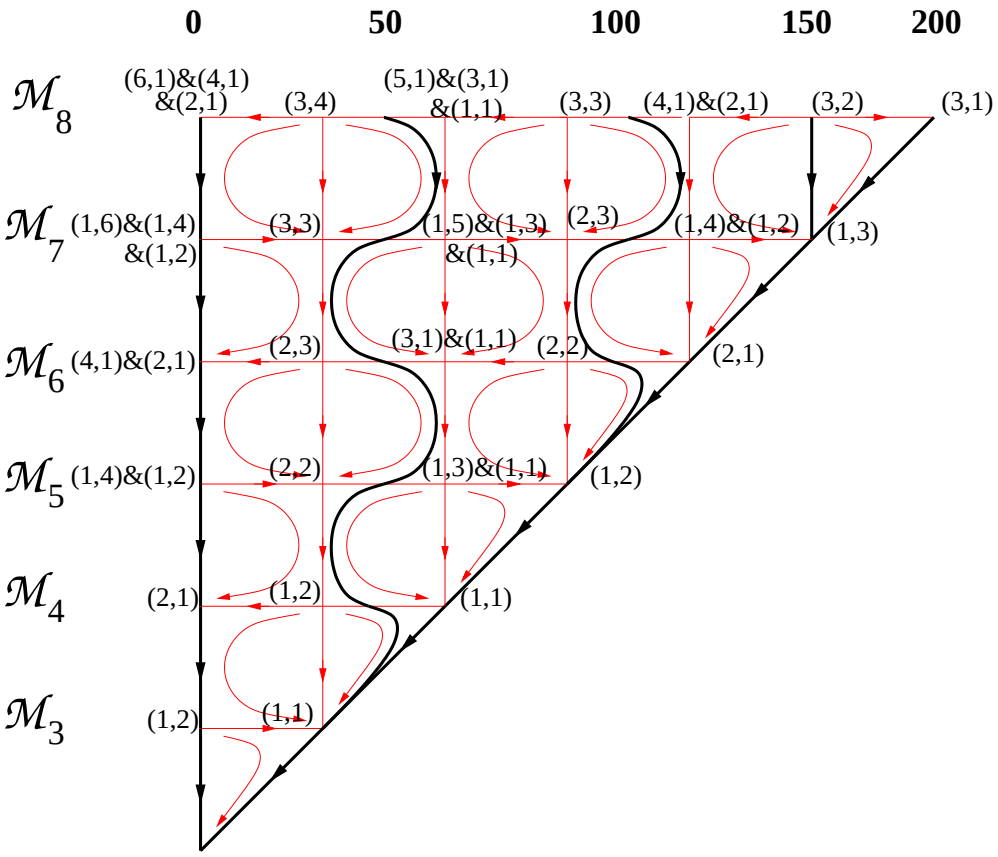

Figure 5.8: A diagram of boundary conditions flows for $\theta_{b1} = 60$, corresponding to the g-function plots in figure 5.5b, with the same highlighted flows.

5.3 The $\mathcal{M}A_m^{(+)}$ g-function

The boundary condition flows found in the previous section can also be obtained in a more formal way by finding exact equations for the g-function of the theories $\mathcal{M}A_m^{(+)}$ with $m > 3$, which interpolate between the minimal models $\mathcal{M}_m$ and $\mathcal{M}_{m-1}$. As was done for $\mathcal{M}A_4^{(+)}$ warm-up case in section 5.1, this is achieved by taking a suitable double-scaling limit that focusses in on the relevant section of the staircase. For $\mathcal{M}A_m^{(+)}$ this limit is taken by defining

$$\ln(r) = -(m-3)\theta_0/2 + \ln(\hat{r}) \tag{5.3.1}$$

and holding $\ln \hat{r}$ finite while the limit $\theta_0 \to \infty$ is taken, before allowing $\ln \hat{r}$ to vary from $-\infty$ to ∞ so that as $\hat{r}$ ranges from 0 to ∞, the bulk theory flows from $\mathcal{M}_m$ to $\mathcal{M}_{m-1}$. As in the warm-up case, holding θ finite until after the $\theta_0 \to \infty$ limit is taken and defining

$$\varepsilon_a(\theta) = \lim_{\theta_0 \to \infty} \varepsilon(\theta + (m-1-2a)\theta_0/2), \qquad a = 1 \cdots m-2 \tag{5.3.2}$$

allows each section of the staircase pseudoenergy $\varepsilon(\theta)$ centred on $(m-1-2a)\theta_0/2$ to be tracked as the $\theta_0 \to \infty$ is taken. Following the method used for $\mathcal{M}A_4^{(+)}$, substituting these definitions along with (5.3.1) into the staircase TBA (4.1.3) leads to the coupled TBA system

$$\begin{aligned}
\epsilon_1(\theta) &= \frac{1}{2}\hat{r}\, e^{\theta} - \int_{\mathbb{R}} \phi(\theta-\theta') L_2(\theta')\, d\theta' \\
\epsilon_a(\theta) &= -\int_{\mathbb{R}} \phi(\theta-\theta')(L_{a-1}(\theta') + L_{a+1}(\theta'))\, d\theta' \qquad a = 2 \ldots m-3 \\
\epsilon_{m-2}(\theta) &= \frac{1}{2}\hat{r}\, e^{-\theta} - \int_{\mathbb{R}} \phi(\theta-\theta') L_{m-3}(\theta')\, d\theta'
\end{aligned} \tag{5.3.3}$$

where $L_a(\theta) = \ln(1 + e^{-\epsilon_a(\theta)})$. This is the same system of equations as was proposed for $\mathcal{M}A_m^{(+)}$ by Al.B. Zamolodchikov in [18]. The effective central charge becomes

$$c_{\text{eff}}(\hat{r}) = \frac{3\hat{r}}{2\pi^2} \int_{\mathbb{R}} (e^{\theta} L_1(\theta) + e^{-\theta} L_{m-2}(\theta))\, d\theta \tag{5.3.4}$$

and moves from c_m at $\hat{r} = 0$ to c_{m-1} at $\hat{r} \to \infty$ as the bulk theory flows from $\mathcal{M}_m$ to $\mathcal{M}_{m-1}$. In terms of the x- and y-type plateaux of $\varepsilon(\theta)$ the plateaux of $\varepsilon_a(\theta)$ when the bulk theory is close to $\mathcal{M}_m$ ($\hat{r} \ll 1$) and $\mathcal{M}_{m-1}$ ($\hat{r} \gg 1$) are

$$\begin{array}{lcc} \hat{r} \ll 1 & & L_a(\theta) \\ & \theta \gg \ln(1/\hat{r}) & \ln\left(1 + y_a|_{\mathcal{M}_m}\right) \\ & -\ln(1/\hat{r}) \ll \theta \ll \ln(1/\hat{r}) & \ln\left(1 + x_{a+1}|_{\mathcal{M}_m}\right) \\ & \theta \ll -\ln(1/\hat{r}) & \ln\left(1 + y_{a+1}|_{\mathcal{M}_m}\right) \\ \hat{r} \gg 1 & & \\ & \theta \gg \ln \hat{r} & \ln\left(1 + x_a|_{\mathcal{M}_{m-1}}\right) \\ & -\ln \hat{r} \ll \theta \ll \ln \hat{r} & \ln\left(1 + y_a|_{\mathcal{M}_{m-1}}\right) \\ & \theta \ll -\ln \hat{r} & \ln\left(1 + x_{a+1}|_{\mathcal{M}_{m-1}}\right). \end{array} \tag{5.3.5}$$

The matching between the $\varepsilon_a(\theta)$ pseudoenergies and the staircase pseudoenergy $\varepsilon(\theta)$ can be seen by comparing plots of $L_a(\theta)$ to the corresponding sections of $L(\theta)$ at appropriate values of r and $\hat{r}$. For example, figure 5.9 shows $L_1(\theta)$, $L_2(\theta)$ and $L_3(\theta)$ for $\mathcal{M}A_5^{(+)}$, plotted at various values of $\ln(\hat{r})$. Figure 5.10 shows $L(\theta)$ plotted at the corresponding values of $\ln(r) = \ln(\hat{r}) - \theta_0$ (with $\theta_0 = 60$), and it is clear that $L_1(\theta)$, $L_2(\theta)$ and $L_3(\theta)$ match the $\theta > 30$, $-30 < \theta < 30$ and $\theta < -30$ parts of $L(\theta)$, respectively.

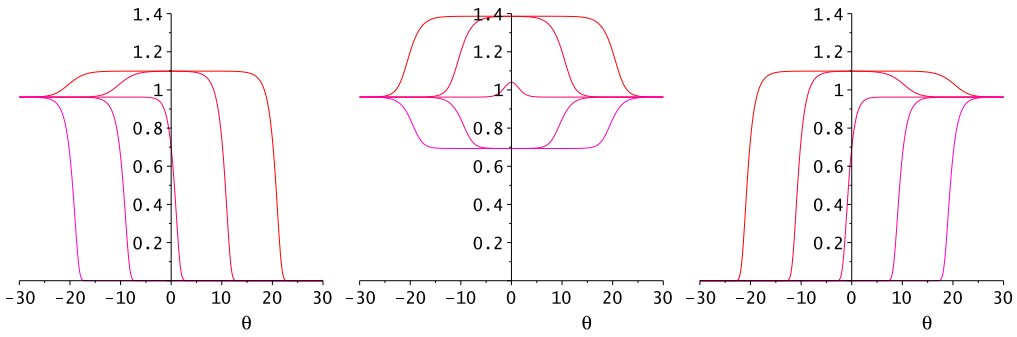

(a) $L_1(\theta)$ (b) $L_2(\theta)$ (c) $L_3(\theta)$

Figure 5.9: Plots of $L_1(\theta)$, $L_2(\theta)$ and $L_3(\theta)$ for $\mathcal{M}A_5^{(+)}$. The sequence of curves from the highest to lowest lying correspond to $\ln(\hat{r}) = -20, -10, 0, 10$ and 20 in each case. The bulk crossover from $\mathcal{M}_5$ to $\mathcal{M}_4$ occurs at $\ln(\hat{r}) = 0$.

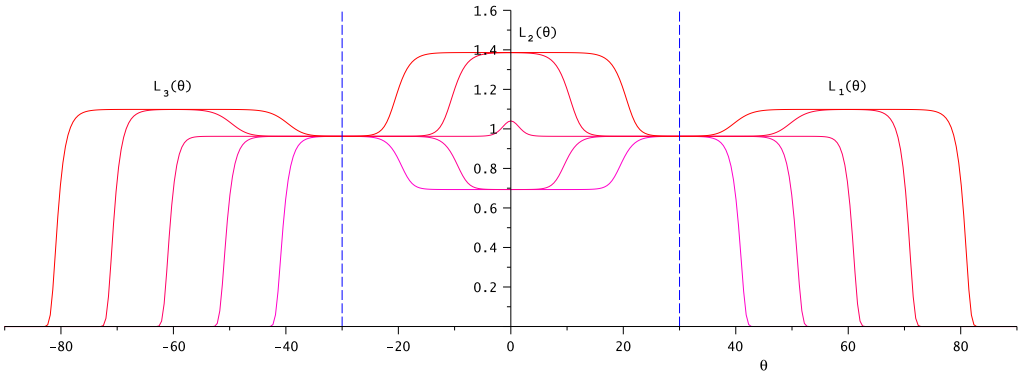

Figure 5.10: Plots of $L(\theta)$ at $\ln r = -80, -70, -60, -50$ and -40, moving from the highest to lowest lying curves. The dotted vertical lines divide the plots into the sections that correspond to the plots of $L_1(\theta)$, $L_2(\theta)$ and $L_3(\theta)$ above. The bulk crossover from $\mathcal{M}_5$ to $\mathcal{M}_4$ occurs at $\ln(\hat{r}) = -60$.

The task now is to re-express the staircase g-function

$$\ln g(r) = \ln g_0(r) + \ln g_{b1}(r) + \ln g_{b2}(r) + \ln g_{b3}(r)$$

(as defined in (4.2.4) and (4.2.10)-(4.2.12)) in the double scaling limit (5.3.1) in terms of the $\varepsilon_a(\theta)$, in order to find an exact expression for the g-function at $\mathcal{M}A_m^{(+)}$. The analysis in the previous section of where each part of the staircase g-function has its support was independent of the value of r and so still holds here. However, the conclusions drawn there as to the actual value of the g-function are only valid while the theory is close to $\mathcal{M}_m$, so form only the UV limit of the g-function in $\mathcal{M}A_m^{(+)}$. Hence a careful analysis is needed of each part of the g-function to determine how it behaves for all values of $\hat{r}$.

As was discussed in the previous section, the staircase $\ln g_0$ is given by

$$\ln g_0(r) = \sum_{n=1}^{\infty} \frac{1}{2n} \int_{\mathbb{R}^n} \frac{d\theta_1}{1+e^{\varepsilon(\theta_1)}} \cdots \frac{d\theta_n}{1+e^{\varepsilon(\theta_n)}} \phi_S(\theta_1-\theta_2)\phi_S(\theta_2-\theta_3)\cdots\phi_S(\theta_n+\theta_1) \tag{5.3.6}$$

which for each n is made up of 2^n terms of the form

$$\int_{\mathbb{R}^n} \frac{d\theta_1}{1+e^{\varepsilon(\theta_1)}} \cdots \frac{d\theta_n}{1+e^{\varepsilon(\theta_n)}} \phi(\theta_1-\theta_2-\alpha_1\theta_0)\phi(\theta_2-\theta_3-\alpha_2\theta_0)\cdots\phi(\theta_n+\theta_1-\alpha_n\theta_0) \tag{5.3.7}$$

with $\alpha_i = \pm 1$. The support of such integrals was found in the previous section, independent of r, to be sub-regions of $\mathbb{R}^n$ which were centred on coordinates $(\tilde{\theta}_1, \tilde{\theta}_2, \cdots, \tilde{\theta}_n)$ satisfying the restrictions (5.1.13) on consecutive $\tilde{\theta}_i$'s. These $\tilde{\theta}_i$'s turned out to be elements of the sets

$$\{-(m-3)\theta_0/2, -(m-5)\theta_0/2, \cdots, (m-5)\theta_0/2, (m-3)\theta_0/2\} \qquad \text{for } m+n \text{ odd}, \tag{5.3.8}$$

$$\{-(m-4)\theta_0/2, -(m-6)\theta_0/2, \cdots, (m-6)\theta_0/2, (m-4)\theta_0/2\} \qquad \text{for } m+n \text{ even}. \tag{5.3.9}$$

The behaviour of the measure factors $\frac{1}{1+\exp(\varepsilon(\theta_i))}$ needs to be determined around these values of θ_i, for all $\hat{r} \in \mathbb{R}^+$. Following the pattern in the previous section, $\ln g_0$ will be split into two terms $\ln g_0(\hat{r}) = \ln g'_A(\hat{r}) + \ln g'_B(\hat{r})$, with $\ln g'_A$ comprising of those terms for which $m+n$ is odd, and the terms of $\ln g'_B$ being those for which $m+n$ is even. The UV limits of $\ln g'_A(\hat{r})$ and $\ln g'_B(\hat{r})$ are given by $\ln g_A$ (5.2.20) and $\ln g_B$ (5.2.27) respectively.

Turning first to $\ln g'_B$, for $\hat{r} \ll 1$ the values of $\tilde{\theta}_i$ (5.3.9) sit at the centres of y-type plateaux of $\mathcal{M}_m$. Since the $\mathcal{M}_m$ y-type plateaux grow in width as $\hat{r}$ increases and the crossover is approached, and plateaux of these values survive the bulk transition and are simply re-identified as x-type plateaux at $\mathcal{M}_{m-1}$, $L(\theta)$ is constant for values of θ close to each $\tilde{\theta}_i$ for all $\hat{r} \in \mathbb{R}^+$, and therefore the measure factor $\frac{1}{1+\exp(\varepsilon(\theta))}$ is also constant close to these values. So $\ln g'_B$ is equal to $\ln g_B$ and from (5.2.61) and (5.2.58):

$$\ln g'_B|_{\mathcal{M}A_m^{(+)}} = \begin{cases} \ln\left(\left(\frac{4}{m}\right)^{\frac{1}{4}} \frac{\sin\frac{(m-1)\pi}{2m}}{\sqrt{\sin\frac{\pi}{m}}}\right) & \text{for } m \text{ odd} \qquad (5.3.10) \\ \ln\left(\left(\frac{2}{m}\right)^{\frac{1}{4}} \frac{1}{\sqrt{\sin\frac{\pi}{m}}}\right) & \text{for } m \text{ even}\,. \qquad (5.3.11) \end{cases}$$

In contrast, the terms of $\ln g'_A$ are not constant throughout $\mathcal{M}A_m^{(+)}$. Here the sub-regions of $\mathbb{R}^n$ in question are centred on coordinates $\tilde{\theta}_i$ that all have the form $\tilde{\theta}_i = (m-2a+1)\theta_0/2$, $a = 2 \cdots m-1$, so that the $\tilde{\theta}_i$'s (5.3.8) sit at the centres

of x-type plateaux of $\mathcal{M}_m$ for $\hat{r} \ll 1$, but the value of $L(\tilde{\theta}_i)$ changes as the bulk transition occurs and the x-type plateaux vanish and are replaced by new y-type plateaux with the same centres for $\hat{r} \gg 1$. So, the measure factors $\frac{1}{1+\exp(\varepsilon(\theta))}$ cannot always be expressed in terms of the x-type plateaux as was done for $\ln g_A$, while the theory was close to $\mathcal{M}_m$ (5.2.7). Nevertheless, it is still possible to find an exact expression for these terms of $\ln g_0$ for $\mathcal{M}A_m^{(+)}$. Around this value of θ, the staircase pseudoenergy $\varepsilon(\theta)$ is described by $\varepsilon_{a-1}(\theta \approx 0)$, so each factor $\frac{1}{1+\exp(\varepsilon(\theta_i))}$ can be replaced by $\frac{1}{1+\exp(\varepsilon_{a-1}(\theta_i-(m-2a+1)\theta_0/2))}$ in $\ln g_0$ so that (5.3.7) becomes

$$\int_{\mathbb{R}^n} \frac{d\theta_1}{1+e^{\epsilon_{a_1-1}(\theta_1-(m-2a_1+1)\theta_0/2)}} \cdots \frac{d\theta_n}{1+e^{\epsilon_{a_n-1}(\theta_n-(m-2a_n+1)\theta_0/2)}} \times \\ \phi(\theta_1-\theta_2-\alpha_1\theta_0)\phi(\theta_2-\theta_3-\alpha_2\theta_0)\cdots\phi(\theta_n+\theta_1-\alpha_n\theta_0) \tag{5.3.12}$$

with a_i for $i = 1, \cdots, n$ determined by $\{\alpha_i\}$. The restrictions on the values of consecutive $\tilde{\theta}_i$'s (5.1.13) mean that after a change of variables

$$\theta_i \to \theta_i + \frac{m-2a_i+1}{2}\theta_0 \tag{5.3.13}$$

such a term becomes

$$\int_{\mathbb{R}^n} \frac{d\theta_1}{1+e^{\epsilon_{a_1-1}(\theta_1)}} \cdots \frac{d\theta_n}{1+e^{\epsilon_{a_n-1}(\theta_n)}} \phi(\theta_1-\theta_2)\phi(\theta_2-\theta_3)\cdots\phi(\theta_n+\theta_1). \tag{5.3.14}$$

Furthermore, the restrictions (5.1.13) mean that for $i = 1 \cdots n-1$, $\frac{1}{1+e^{\epsilon_{a-1}(\theta_i)}}$ must be followed by $\frac{1}{1+e^{\epsilon_a(\theta_{i+1})}}$ or $\frac{1}{1+e^{\epsilon_{a-2}(\theta_{i+1})}}$, and also that if the sequence of measure factors begins with $\frac{1}{1+e^{\epsilon_{a-1}(\theta_1)}}$ it must end with $\frac{1}{1+e^{\epsilon_{m-a-1}(\theta_n)}}$ or $\frac{1}{1+e^{\epsilon_{m-a+1}(\theta_n)}}$ (with only the former applying to $a = 2$ and only the latter to $a = m-1$). The UV limits of these agree with the constraints (5.2.8) and (5.2.9) that appeared in the previous section, and the allowed sequences of measure factors for $\mathcal{M}A_m^{(+)}$ have the same form as those that appeared for the theory close $\mathcal{M}_m$, just with each factor of $\frac{x_a}{1+x_a}$ replaced with $\frac{1}{1+e^{\epsilon_{a-1}(\theta_i)}}$. The steps in the previous section which enabled the identification of the allowed sequences of terms with the anti-trace of products of a matrix depended only on the relationship between the terms in the sequences, not the value of the elements themselves. So, the same reasoning can be applied here

and after defining the $(m-2)\times(m-2)$ matrix $A'(\theta)$ to be

$$A'(\theta)=\begin{pmatrix} 0 & \frac{1}{1+e^{\epsilon_1(\theta)}} & 0 & 0 & \cdots & 0 & 0 & 0 \\ \frac{1}{1+e^{\epsilon_2(\theta)}} & 0 & \frac{1}{1+e^{\epsilon_2(\theta)}} & 0 & \cdots & 0 & 0 & 0 \\ 0 & \frac{1}{1+e^{\epsilon_3(\theta)}} & 0 & \frac{1}{1+e^{\epsilon_3(\theta)}} & \cdots & 0 & 0 & 0 \\ \vdots & \vdots & \vdots & \vdots & & \vdots & \vdots & \vdots \\ 0 & 0 & 0 & 0 & \cdots & \frac{1}{1+e^{\epsilon_{m-3}(\theta)}} & 0 & \frac{1}{1+e^{\epsilon_{m-3}(\theta)}} \\ 0 & 0 & 0 & 0 & \cdots & 0 & \frac{1}{1+e^{\epsilon_{m-2}(\theta)}} & 0 \end{pmatrix}, \tag{5.3.15}$$

$\ln g'_A(\hat{r})$ can be expressed as

$$\ln g'_A(\hat{r}) \;=\; \sum_{\substack{n\geq 1\\ m+n \text{ odd}}} \frac{1}{2n}\int_{\mathbb{R}^n} \mathrm{antiTr}\big(\Pi_{i=1}^n A'(\theta_i)d\theta_i\big)\phi(\theta_1-\theta_2)\phi(\theta_2-\theta_3)\cdots\phi(\theta_{n-1}-\theta_n)\phi(\theta_n+\theta_1). \tag{5.3.16}$$

where if $n=1$ appears here, the corresponding term in the sum is

$$\tfrac{1}{2}\int_{\mathbb{R}} \mathrm{antiTr}(A'(\theta))\phi(2\theta)d\theta.$$

Expressions for $\ln g_{b1}(\hat{r})$ and $\ln g_{b2}(\hat{r})$ can similarly be derived by generalising the results of the previous section. $\ln g_{b1}(r)$ is governed by $L(\theta\approx 0)$, which for m even this has constant value $\ln(1+y_{m/2}|_{\mathcal{M}_m})$. For m odd $L(\theta\approx 0)$ is not constant, but is equal to $\ln(1+\exp(-\varepsilon_{(m-1)/2}(\theta\approx 0)))$. Therefore

$$\ln g_{b1}(\hat{r}) = \begin{cases} -\frac{1}{2}\displaystyle\int_{\mathbb{R}} d\theta\,\big(\phi(\theta)+\tfrac{1}{2}\delta(\theta)\big)\ln(1+e^{-\epsilon_{\frac{m-1}{2}}(\theta)}) & \text{for } m \text{ odd} \qquad (5.3.17) \\ -\frac{1}{2}\ln(1+y_{m/2}) & \text{for } m \text{ even.} \qquad (5.3.18) \end{cases}$$

Similarly, $\ln g_{b2}$ is governed by $L(\theta\approx\theta_0/2)$ which has constant value $\ln(1+y_{(m-1)/2}|_{\mathcal{M}_m})$ for m odd, but is non-constant for m even, equalling $\ln(1+\exp(-\varepsilon_{(m-2)/2}(\theta\approx 0)))$. So, $\varepsilon(\theta)$ in (4.2.11) can be replaced by $\varepsilon_{(m-2)/2}(\theta-\theta_0/2)$, and after a shift in variable

$\ln g_{b2}(\hat{r})$ is found to be

$$\ln g_{b2}(\hat{r}) = \begin{cases} -\frac{1}{2}\ln(1+y_{(m-1)/2}) & \text{for } m \text{ odd} \qquad (5.3.19) \\ \int_{\mathbb{R}} d\theta \big(\phi_{(\frac{3}{4})}(\theta) - \phi(2\theta)\big) \ln(1+e^{-\epsilon_{\frac{m-2}{2}}(\theta)}) & \text{for } m \text{ even}\,. \qquad (5.3.20) \end{cases}$$

The validity of these expressions can be checked by evaluating $\ln g_0(\hat{r}) + \ln g_{b1}(\hat{r}) + \ln g_{b2}(\hat{r})$ in the UV ($\hat{r} \to 0$) and IR ($\hat{r} \to \infty$) limits. In the previous section it was noted that if the boundary-dependent part of the g-function vanishes and the bulk theory is close to a minimal model $\mathcal{M}_m$ then the g-function equals that of the $(1,1)$ boundary condition. For $\mathcal{M}A_m^{(+)}$, in the UV limit the bulk theory is $\mathcal{M}_m$ and in the IR limit it is $\mathcal{M}_{m-1}$, so in each of these limits the boundary parameter-independent part of the g-function is expected to equal that of the $(1,1)$ boundary condition of the respective minimal models. For the UV limit, since the integrals in $\ln g_0(\hat{r})$ have their support close to $\theta_i = 0$ for all i, and the integrals in $\ln g_{b1}(\hat{r})$ for m odd and $\ln g_{b1}(\hat{r})$ for m even have their support close to $\theta = 0$, whenever $\exp(-\varepsilon_a(\theta))$ appears in each of these equations it can be replaced with $x_{a+1}|_{\mathcal{M}_m}$. These expressions then become the same as the results of the previous section, which is as expected since the calculations there were for the staircase model close to $\mathcal{M}_m$. Therefore for both m odd and m even $(\ln g_0 + \ln g_{b1} + \ln g_{b2})|_{\hat{r}=0}$ is given by (5.2.68):

$$(\ln g_0 + \ln g_{b1} + \ln g_{b2})|_{\hat{r}=0} = \ln\left(\left(\frac{8}{m(m+1)}\right)^{\frac{1}{4}} \sqrt{\sin\frac{\pi}{m}\sin\frac{\pi}{m+1}}\right) = \ln g(m,1,1). \qquad (5.3.21)$$

In the IR limit, the supports of the various integrals have the effect that each $\exp(-\varepsilon_a(\theta))$ term can be replaced by $y_a|_{\mathcal{M}_{m-1}}$. For $\ln g_0(\hat{r})$ this means that the

matrix $A'(\theta)$ becomes A'_{IR} where

$$A'_{IR} = \begin{pmatrix} 0 & \frac{y_1}{1+y_1}\big|_{\mathcal{M}_{m-1}} & 0 & \cdots & 0 & 0 \\ \frac{y_2}{1+y_2}\big|_{\mathcal{M}_{m-1}} & 0 & \frac{y_2}{1+y_2}\big|_{\mathcal{M}_{m-1}} & \cdots & 0 & 0 \\ 0 & \frac{y_3}{1+y_3}\big|_{\mathcal{M}_{m-1}} & 0 & \cdots & 0 & 0 \\ & \vdots & \vdots & \vdots & \vdots & \\ 0 & 0 & 0 & \cdots & 0 & \frac{y_{m-3}}{1+y_{m-3}}\big|_{\mathcal{M}_{m-1}} \\ 0 & 0 & 0 & \cdots & \frac{y_{m-2}}{1+y_{m-2}}\big|_{\mathcal{M}_{m-1}} & 0 \end{pmatrix} \tag{5.3.22}$$

and then

$$\ln g'_A(\hat{r}\to\infty) = \sum_{\substack{n\geq 1 \\ m+n \text{ odd}}} \frac{1}{n2^{n+2}} \operatorname{Tr}\left((A'_{\mathrm{IR}})^n J_{m-2}\right). \tag{5.3.23}$$

This can be evaluated by noting that the central $(m-4)\times(m-4)$ sub-matrix of A'_{IR} is equal to the matrix B (5.2.25) evaluated for $\mathcal{M}_{m-1}$. Since $y_1|_{\mathcal{M}_{m-1}}$ and $y_{m-2}|_{\mathcal{M}_{m-1}}$ equal zero, all the entries in the first and final rows of A'_{IR} are zero. This means that $(A'_{IR})^n$ also has only zero entries in its first and final rows, and that its central $(m-4)\times(m-4)$ sub-matrix is equal to $(B|_{\mathcal{M}_{m-1}})^n$. Therefore, the anti-trace of $(A'_{IR})^n$ is equal to that of $(B|_{\mathcal{M}_{m-1}})^n$ so that

$$\ln g'_A(\hat{r}\to\infty) = \sum_{\substack{n\geq 1 \\ (m-1)+n \text{ even}}} \frac{1}{n2^{n+2}} \operatorname{Tr}\left(\left(B|_{\mathcal{M}_{m-1}}\right)^n J_{m-4}\right) = \ln g_B|_{\mathcal{M}_{m-1}} \tag{5.3.24}$$

which using (5.2.58) and (5.2.61) is evaluated to be

$$\ln g'_A(\hat{r}\to\infty) = \begin{cases} \ln\left(\left(\frac{2}{m-1}\right)^{\frac{1}{4}} \frac{1}{\sqrt{\sin\frac{\pi}{m-1}}}\right) & \text{for } m \text{ odd} \qquad (5.3.25) \\ \ln\left(\left(\frac{4}{m-1}\right)^{\frac{1}{4}} \frac{\sin\frac{(m-2)\pi}{2(m-1)}}{\sqrt{\sin\frac{\pi}{m-1}}}\right) & \text{for } m \text{ even.} \qquad (5.3.26) \end{cases}$$

The $\exp(-\varepsilon_a(\theta))$ terms in $\ln g_{b1}(\hat{r})$ and $\ln g_{b2}(\hat{r})$ can similarly be replaced by

$y_a|_{\mathcal{M}_{m-1}}$ and evaluated using (4.1.48) at $\mathcal{M}_{m-1}$, so that

$$(\ln g_0 + \ln g_{b1} + \ln g_{b2})|_{\hat{r}\to\infty} = \tag{5.3.27}$$
$$\ln\left(\left(\frac{4}{m}\right)^{\frac{1}{4}}\sqrt{\sin\frac{\pi}{m}}\right) - \tfrac{1}{2}\ln\left(\frac{1}{\sin^2\left(\frac{\pi}{m-1}\right)}\right) + \ln\left(\left(\frac{2}{m-1}\right)^{\frac{1}{4}}\frac{1}{\sqrt{\sin\frac{\pi}{m-1}}}\right)$$
$$\text{for } m \text{ odd}$$

and

$$(\ln g_0 + \ln g_{b1} + \ln g_{b2})_{\hat{r}\to\infty} = \tag{5.3.28}$$
$$\ln\left(\left(\frac{2}{m}\right)^{\frac{1}{4}}\sqrt{\sin\frac{\pi}{m}}\right) - \tfrac{1}{2}\ln\left(\frac{\sin^2\left(\frac{(m-2)\pi}{2(m-1)}\right)}{\sin^2\left(\frac{\pi}{m-1}\right)}\right) + \ln\left(\left(\frac{4}{m-1}\right)^{\frac{1}{4}}\frac{\sin\left(\frac{(m-2)\pi}{2(m-1)}\right)}{\sqrt{\sin\frac{\pi}{m-1}}}\right)$$
$$\text{for } m \text{ even}$$

which both give the expected result

$$(\ln g_0+\ln g_{b1}+\ln g_{b2})|_{\hat{r}\to\infty} = \ln\left(\left(\frac{8}{m(m-1)}\right)^{\frac{1}{4}}\sqrt{\sin\frac{\pi}{m-1}\sin\frac{\pi}{m}}\right) = \ln g(m-1,1,1). \tag{5.3.29}$$

The final task is adapt the expression for $\ln g_{b3}(r)$ (4.2.12) for $\mathcal{M}A_m^{(+)}$. As in the warm-up example, the boundary parameters $(\theta_{b1}, \theta_{b2})$ need to be treated carefully in the double-scaling limit (5.3.1) to ensure that the g-function can still describe all possible boundary flows. This is achieved by picking two integers a_1 and a_2 from the set $\{0 \cdots m-1\}$ and defining $\hat{\theta}_{b1}$ and $\hat{\theta}_{b2}$ by

$$\theta_{b_i} = \tfrac{1}{2}(m-1-2a_i)\theta_0 + \hat{\theta}_{b_i} \tag{5.3.30}$$

for $i = 1, 2$, keeping $\hat{\theta}_{b1}$ and $\hat{\theta}_{b2}$ finite until after the $\theta_0 \to 0$ limit is taken, when they are then allowed to vary over all real values. This has the effect of restricting $L(\theta_{b1})$ and $L(\theta_{b2})$ to take the values of $\ln(1+e^{-\varepsilon_{a_1}(\theta)})$ and $\ln(1+e^{-\varepsilon_{a_2}(\theta)})$ respectively (which equal 0 if $a_i = 0$ or $m-1$). The full set of boundary flows is found by doing this for all pairs of integers (a_1, a_2) in turn.

In terms of the rescaled boundary parameters $\hat{\theta}_{b1}$ and $\hat{\theta}_{b2}$, $\ln g_{b3}$ (4.2.12) becomes

$$\begin{aligned}\ln g_{b3\ a_1a_2}(\hat{r},\hat{\theta}_{b1},\hat{\theta}_{b2}) &= \tfrac{1}{2}\sum_{i=1}^{2}\int_{\mathbb{R}} d\theta\big(\phi(\theta-\hat{\theta}_{b_i})\ln(1+e^{-\epsilon_{a_i}(\theta)})+\phi(\theta+\hat{\theta}_{b_i})\ln(1+e^{-\epsilon_{m-1-a_i}(\theta)})\big)\\ &= \sum_{i=1}^{2}\int_{\mathbb{R}} d\theta\,\phi(\theta-\hat{\theta}_{b_i})\ln(1+e^{-\epsilon_{a_i}(\theta)}) \qquad (5.3.31)\end{aligned}$$

where the symmetry $\epsilon_a(\theta)=\epsilon_{m-1-a}(-\theta)$ has been used.

The full exact expression for the $\mathcal{M}A_m^{(+)}$ g-function is found by adding the above to the expressions (5.3.10), (5.3.11) and (5.3.16)-(5.3.20) for $\ln g_0(\hat{r})$, $\ln g_{b1}(\hat{r})$ and $\ln g_{b2}(\hat{r})$. The results depend on whether m is odd or even, and consist of families of expressions indexed by a_1 and a_2 and dependent on $\hat{r}$ and the rescaled boundary parameters $\hat{\theta}_{b1}$ and $\hat{\theta}_{b2}$:

$$\begin{aligned}\ln g_{a_1a_2}(\hat{r},\hat{\theta}_{b1},\hat{\theta}_{b2}) &= \ln\left(\left(\frac{4}{m}\right)^{\frac{1}{4}}\sqrt{\sin\frac{\pi}{m}}\right)-\tfrac{1}{2}\int_{\mathbb{R}} d\theta\,\big(\phi(\theta)+\tfrac{1}{2}\delta(\theta)\big)\ln(1+e^{-\epsilon_{\frac{m-1}{2}}(\theta)})\\ &\quad+\ln g_A(\hat{r})+\ln g_{b3\ a_1a_2}(\hat{r},\hat{\theta}_{b1},\hat{\theta}_{b2}) \qquad \text{for } m \text{ odd;} \quad (5.3.32)\\ \ln g_{a_1a_2}(\hat{r},\hat{\theta}_{b1},\hat{\theta}_{b2}) &= \ln\left(\left(\frac{2}{m}\right)^{\frac{1}{4}}\sqrt{\sin\frac{\pi}{m}}\right)+\int_{\mathbb{R}} d\theta\Big(\phi_{(\frac{3}{4})}(\theta)-\phi(2\theta)\Big)\ln(1+e^{-\epsilon_{\frac{m-2}{2}}(\theta)})\\ &\quad+\ln g_A(\hat{r})+\ln g_{b3\ a_1a_2}(\hat{r},\hat{\theta}_{b1},\hat{\theta}_{b2}) \qquad \text{for } m \text{ even.} \quad (5.3.33)\end{aligned}$$

The constant term in each expression arises from adding the appropriate expression for $\ln g_B(\hat{r})$ ((5.3.10) for m odd or (5.3.11) for m even) to $\ln g_{b2}(\hat{r})$ (5.3.19) in the m odd case and $\ln g_{b1}(\hat{r})$ (5.3.18) in the m even case.

Some examples of the flows in the value of $\ln g(\hat{r})$ at $\mathcal{M}A_5^{(+)}$ are shown in the plots in figures 5.11 and 5.12 . Using the relationship (5.3.30) at $\theta_0 = 60$, the values of the $\hat{\theta}_{b1}$ and $\hat{\theta}_{b2}$ in figures 5.11a and 5.11c correspond to the staircase boundary parameters $(\theta_{b1},\theta_{b2}) = (60,50)$ and $(\theta_{b1},\theta_{b2}) = (100,50)$, respectively. Since the staircase model matches the $\mathcal{M}A_5^{(+)}$ flows for $-\frac{3\theta_0}{2} < \ln r < -\frac{\theta_0}{2}$, the flow in figure 5.11a matches the $-90 < \ln r < -30$ part of the highlighted $\theta_{b2} = 50$ flow in figure 5.5b. Also, since the staircase flow is independent of θ_{b1} for $\theta_{b1} > \ln\frac{1}{r}$, the flow in 5.11c matches the same part of the $\theta_{b2} = 50$ highlighted flow in figures 5.5c and

5.5d. The central plateaux in figures 5.11a and 5.11c fail to coincide fully with the conformal g-function values indicated by the horizontal lines. This is because having $\hat{\theta}_{b2} = -10$ positions this boundary parameter close to the centre of the central plateau of $L_1(\theta)$ on which it initially lies, meaning that the bulk transition begins before the 'pure' boundary transition at $\mathcal{M}_5$ is complete, and then the 'pure' boundary transition at $\mathcal{M}_4$ begins before the bulk transition is over. In figures 5.11b and 5.11d this problem is remedied by slightly increasing the size of $\hat{\theta}_{b2}$ so that the boundary and bulk transitions are sufficiently separated. All the plateaux of $\ln g(\hat{r})$ in these figures then coincide with the conformal values.

In each of flows in figure 5.11 only $L_1(\theta)$ contributed to $\ln g_{b3\ a_1a_2}(\hat{r}, \hat{\theta}_{b1}, \hat{\theta}_{b2})$; the plots in figure 5.12 show examples of flows where other pseudoenergies contribute. Each of the boundary condition flows appearing in these figures matches those predicted from the staircase model. This can be seen by considering the values of $L_{a_1}(\hat{\theta}_{b1})$ and $L_{a_2}(\hat{\theta}_{b2})$ at various points in the flow, and translating these into the x- and y-type plateaux of the staircase $L(\theta)$. The flows seen in the plots can then be checked against the rules given in (5.2.72). For example, the values of $L_2(\hat{\theta}_{b1} = 15)$ and $L_3(\hat{\theta}_{b2} = -15)$ correspond to the flow $[x_3, x_4]|_{\mathcal{M}_5} \to [y_2, y_4]|_{\mathcal{M}_5} \to [x_2, x_4]|_{\mathcal{M}_4} \to [y_2, x_4]|_{\mathcal{M}_4}$, which using (5.2.72) does indeed reproduce the flow in boundary conditions seen in figure 5.12a (after recalling that $(2,4)|_{\mathcal{M}_4} \cong (2,1)|_{\mathcal{M}_4}$).

For general $\mathcal{M}A_m^{(+)}$, for finite $\hat{\theta}_{b1}$ and $\hat{\theta}_{b2}$ the boundary flows encoded in (5.3.32) and (5.3.33) all begin in the UV at the $\mathcal{M}_m$ boundary condition corresponding to the $[x_{a_1+1}, x_{a_2+1}]$ plateau configuration. For $2 \leq a_1, a_2 \leq m-3$ the flows are those seen in figure 5.13. If $\hat{\theta}_{b1} = \hat{\theta}_{b2} = 0$ then the flow is the direct vertical flow from $[x_{a_1+1}, x_{a_2+1}]|_{\mathcal{M}_m}$ to $[y_{a_1}, y_{a_2}]$. Similar direct flows occur when one boundary parameter is zero and the other tends to plus or minus infinity, or when both tend to plus or minus infinity. For other, finite values of the rescaled boundary parameters, additional 'pure boundary' flows also occur as theory flows from its UV to its IR limits. If one or both of a_1 and a_2 equals 1 or $m-2$ then the flows truncate, just as the flow in figure 5.12b flowed straight to the $(1,1)$ boundary condition as the bulk theory flowed to $\mathcal{M}_4$. This behaviour is illustrated for the $a_1 = 1$, $2 \leq a_2 \leq m-3$ choice in figure 5.14 and the $a_1 = a_2 = 1$ choice in figure 5.15.

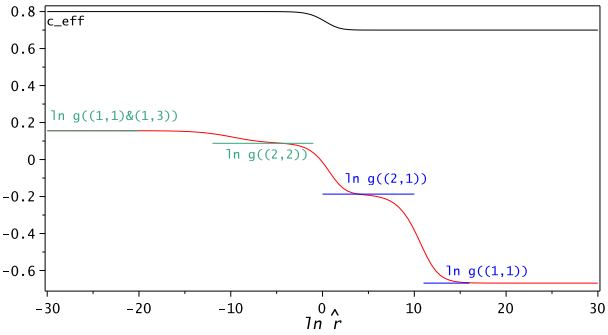

(a) $a_1 = 1$, $a_2 = 1$, $\hat{\theta}_{b1} = 0$, $\hat{\theta}_{b2} = -10$

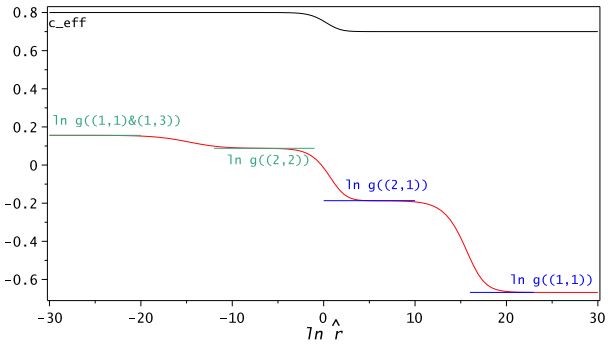

(b) $a_1 = 1$, $a_2 = 1$, $\hat{\theta}_{b1} = 0$, $\hat{\theta}_{b2} = -15$

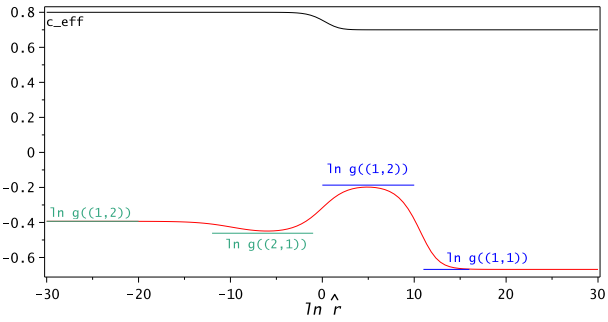

(c) $a_1 = 1$, $a_2 = 1$, $\hat{\theta}_{b1} = 40$, $\hat{\theta}_{b2} = -10$

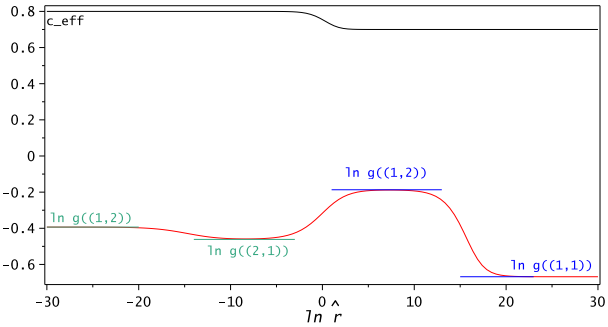

(d) $a_1 = 1$, $a_2 = 1$, $\hat{\theta}_{b1} = 40$, $\hat{\theta}_{b2} = -15$

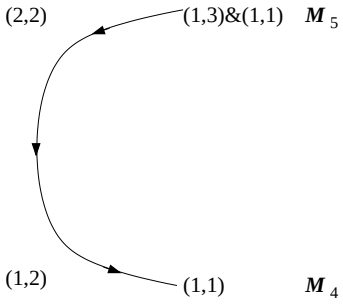

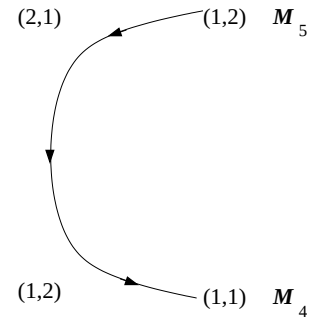

Figure 5.11: g-function flows in $\mathcal{M}A_5^{(+)}$ with $a_1 = a_2 = 1$. $c_{eff}(\hat{r})$ is also plotted to show where the bulk transition from $\mathcal{M}_5$ to $\mathcal{M}_4$ occurs. The horizontal lines show the conformal g-function values that match the plateaux of $\ln g(\hat{r})$; the green lines indicate boundary conditions in $\mathcal{M}_5$, and the blue lines those in $\mathcal{M}_4$. The diagrams on the right hand side depict the boundary condition flows, and match the $\mathcal{M}_5 \to \mathcal{M}_4$ steps of figures 5.8 and 5.7, respectively.

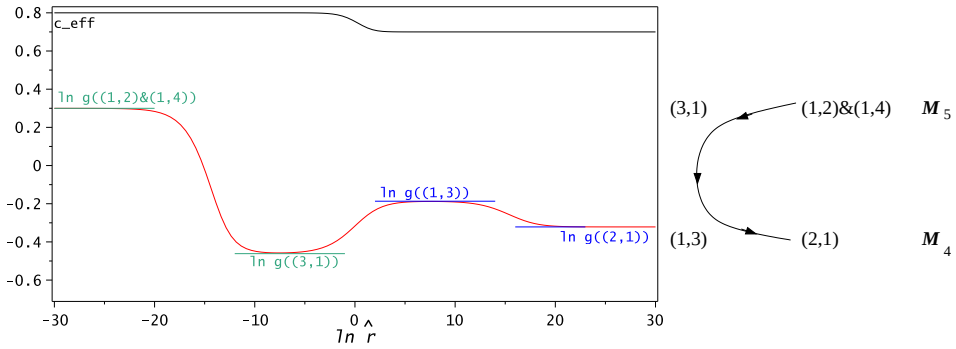

(a) $a_1 = 2$, $a_2 = 3$, $\hat{\theta}_{b1} = 15$, $\hat{\theta}_{b2} = -15$

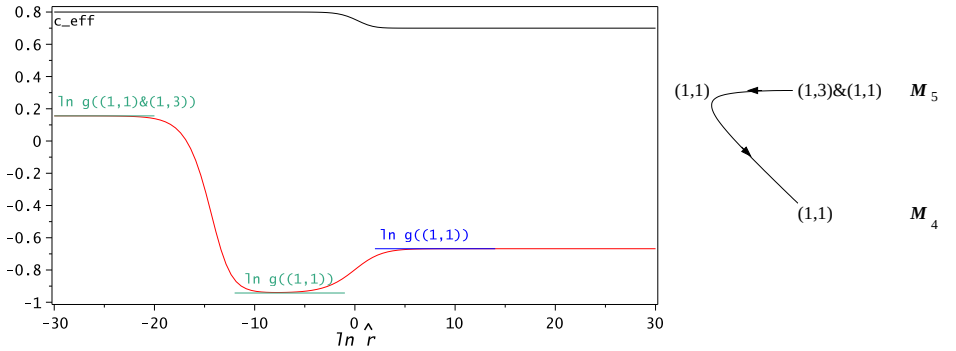

(b) $a_1 = 3$, $a_2 = 3$, $\hat{\theta}_{b1} = -15$, $\hat{\theta}_{b2} = -15$

Figure 5.12: g-function flows in $\mathcal{M}A_5^{(+)}$ with $a_1, a_2 \neq 1$. Conformal g values and $c_{eff}(\hat{r})$ are again plotted, as in figure 5.11.

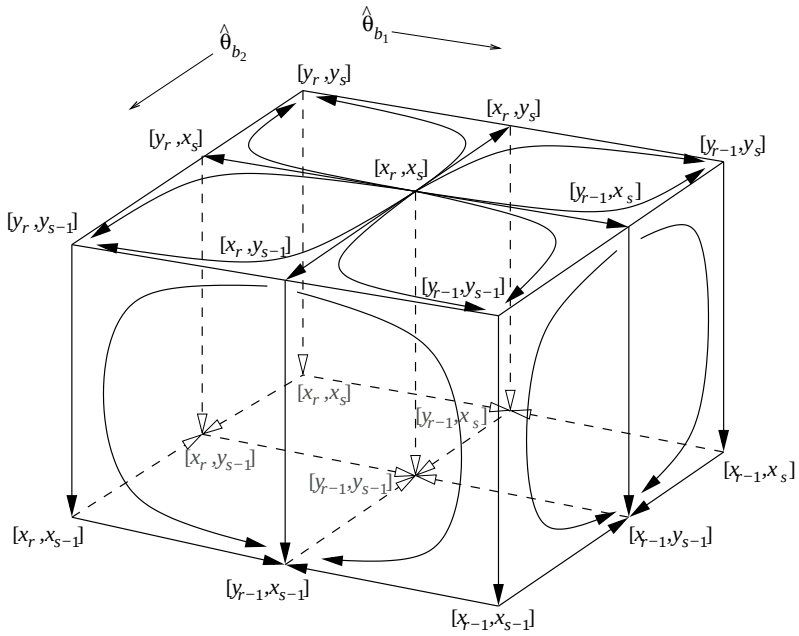

Figure 5.13: Cube of flows for $2 \leq a_1, a_2 \leq m-3$, with $r = a_1 + 1$ and $s = a_2 + 1$.

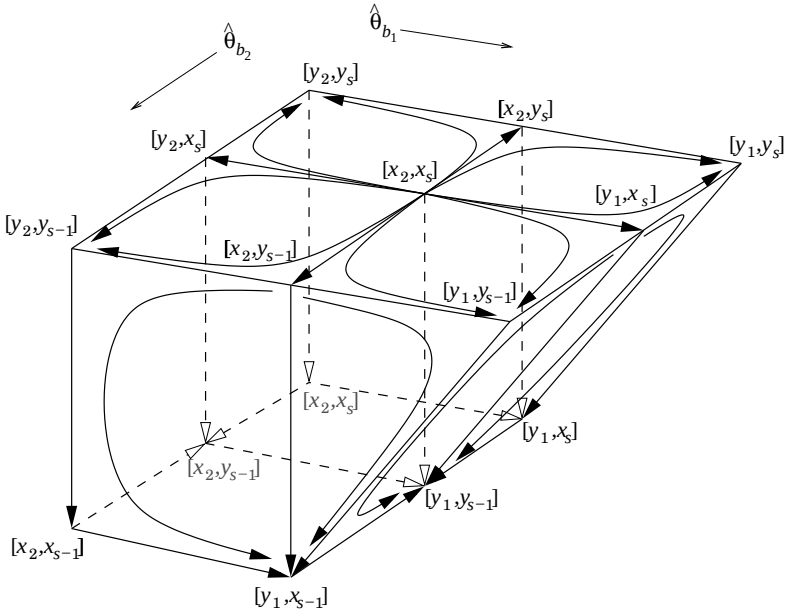

Figure 5.14: Truncation of the cube of flows for $a_1 = 1$ and $2 \leq a_2 \leq m-3$.

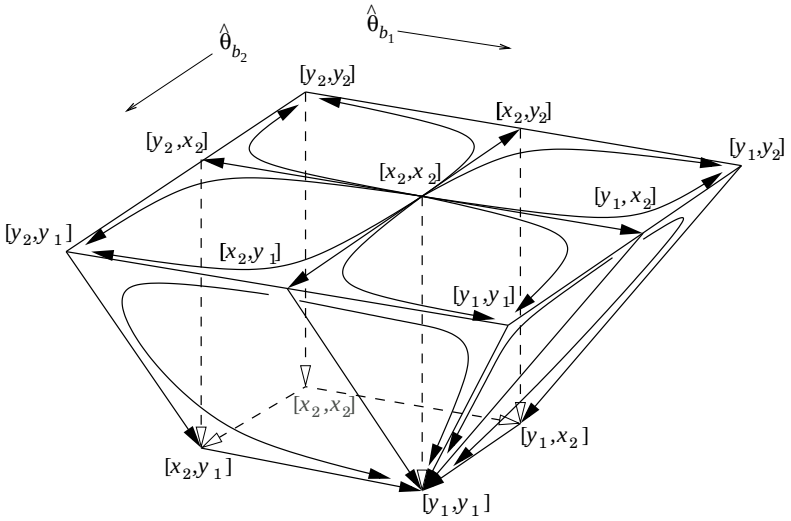

Figure 5.15: Truncation of the cube of flows for $a_1 = a_2 = 1$.

Chapter 6

Further Results on the g-function

In the previous chapter, the analysis of the g-function for the staircase model enabled exact expressions for the g-function in the $\mathcal{M}A_m^{(+)}$ models to be found, and allowed the identification of boundary flows within these models. The flows found both confirm and extend flows found perturbatively by Fredenhagen et al. [52]. In this chapter a number of further results on the g-function will be reported, which are as yet unpublished. Firstly, section 6.1 describes an analytic approach to the perturbative expansions of the exact g-function in the scaling Lee-Yang and $\mathcal{M}A_4^{(+)}$ models, which have previously only been found numerically. Secondly, in section 6.2 a proposal is made for an exact expression for an excited state g-function in the $\mathcal{M}A_m^{(+)}$ models, and the ability of this to solve the spin-flip ambiguities present in the flows identified from the ground state g-function is discussed. Finally, in section 6.3 the $\mathcal{M}A_4^{(-)}$ theory will be discussed, which interpolates between $\mathcal{M}_4$ and a massive field theory. After describing how this model emerges from analytic continuation of the $\mathcal{M}A_4^{(+)}$ model, proposals will be made for the ground state g-function in this model.

6.1 Perturbative Expansions of the Exact g-function

A means of checking a proposal for the exact g-function for a particular model is to find its expansion in small r and to compare the results to expansion coefficients found using conformal perturbation theory. This has not been attempted for the

$\mathcal{M}A_m^{(+)}$ models with $m > 4$. However, expansions were found numerically by Dorey et al. for the scaling Lee-Yang model [36] and for $\mathcal{M}A_4^{(+)}$ [41], and were found to be in agreement with conformal perturbation theory, so this at least provides confirmation of the results that underpinned the work on the staircase model. It has been possible to verify analytically how some of these expansion terms arise from the g-function expressions, and it is this work that appears in this section.

6.1.1 Expansion of the Scaling Lee-Yang Model g-function

The Lee-Yang model is the simplest non-unitary minimal model, with $c = -22/5$. It has only two bulk fields, the identity field and ϕ, which has scaling dimension $x_\phi = -2/5$. Only the boundary condition corresponding to ϕ admits a relevant perturbation by the one non-trivial boundary field, ψ, which has scaling dimension $x_\psi = -1/5$. The scaling Lee-Yang model describes the RG flow from the CFT to a massive field theory when it is perturbed by these fields:

$$S_{pert} = S_{L-Y} + \lambda \int \phi(x) d^2x + \mu \int \psi(x) dx \tag{6.1.1}$$

where λ and μ are the bulk and boundary couplings, respectively. The S-matrix for this theory is

$$S(\theta) = -(1)(2) \tag{6.1.2}$$

using a slightly different block notation from that used previously

$$(x) = \frac{\sinh\left(\frac{\theta}{2} + \frac{i\pi x}{6}\right)}{\sinh\left(\frac{\theta}{2} - \frac{i\pi x}{6}\right)}. \tag{6.1.3}$$

The reflection factor corresponding to a boundary condition labelled by b is

$$R_b(\theta) = \left(\frac{1}{2}\right)\left(\frac{3}{2}\right)\left(\frac{4}{2}\right)^{-1}\left(S\left(\theta + i\pi\frac{b+3}{6}\right)S\left(\theta - i\pi\frac{b+3}{6}\right)\right)^{-1}. \tag{6.1.4}$$

The TBA equation is

$$\varepsilon(\theta) = mR\cosh(\theta) - \int \phi(\theta - \theta')L(\theta')d\theta'. \tag{6.1.5}$$

The g-function for boundary condition α was found in [36], as the one particle-type version of equation (3.3.4):

$$\ln g_\alpha(r) = \ln g_0(r) + \ln g_1(r) \tag{6.1.6}$$

$$= \tfrac{1}{2}\sum_{n=1}^{\infty}\frac{1}{n}\int_{\mathbb{R}_n}\frac{d\theta_1}{1+e^{\varepsilon(\theta_1)}}\cdots\frac{d\theta_n}{1+e^{\varepsilon(\theta_n)}}\phi(\theta_1+\theta_2)\phi(\theta_2-\theta_3)\cdots\phi(\theta_n-\theta_1)$$

$$+\frac{1}{4}\int_{-\infty}^{\infty}\left(\phi_\alpha(\theta)-2\phi(2\theta)-\delta(\theta)\right)L(\theta)d\theta \tag{6.1.7}$$

where

$$\phi(\theta) = -\frac{i}{2\pi}\frac{d}{d\theta}\ln S(\theta) = -\frac{\sqrt{3}}{\pi}\frac{\sinh(2\theta)}{\sinh(3\theta)} \tag{6.1.8}$$

and

$$\phi_\alpha(\theta) = -\frac{i}{\pi}\frac{d}{d\theta}\ln R_\alpha(\theta) \tag{6.1.9}$$

with

$$\int\phi(\theta)d\theta = -1, \quad \int\phi_\alpha(\theta)d\theta = -2. \tag{6.1.10}$$

The focus here will be on the $\mathbb{1}$ boundary condition (corresponding to $R_0(\theta)$), for which expansions arising from perturbed conformal field theory are given in [29]. Since there is no boundary perturbation for this boundary condition, dimensional considerations mean that the small r perturbative expansion of $\ln g(r)$ is expected to take the form

$$\ln g(r) = fr + \sum_{n=0}^{\infty} d_n^{(\alpha)}\left(\lambda R^{12/5}\right)^n \tag{6.1.11}$$

where $\lambda \propto m^{12/5}$, $r = mR$ as before, and f is the free energy per unit length. To find the expansion of $\ln g(r)$ analytically from (6.1.7) the expansion of $\varepsilon(\theta)$ for small r is needed. The 'kink' TBA equation is that which arises when $r\cosh\theta$ is replaced by $\frac{1}{2}re^\theta$ in (6.1.5). In [29] the expansion of the kink pseudoenergy for small re^θ is given as

$$\varepsilon_{kink}(\theta) = \ln\frac{1+\sqrt{5}}{2} + C_1\left(re^\theta\right)^{6/5} + C_2\left(re^\theta\right)^{12/5} + \cdots \tag{6.1.12}$$

where

$$C_1 = \frac{2^{-7/5}\pi^{7/5}\Gamma\left(\frac{1}{5}\right)}{\cos\frac{\pi}{5}\Gamma\left(\frac{2}{5}\right)\Gamma^2\left(\frac{3}{5}\right)\Gamma\left(\frac{4}{5}\right)}\left(\frac{\Gamma\left(\frac{2}{3}\right)}{\Gamma\left(\frac{1}{6}\right)}\right)^{6/5}, \quad C_2 = \left(\frac{1}{\sqrt{5}} - \frac{1}{2}\right)C_1^2. \tag{6.1.13}$$

This can be used to find expansions for $L(\theta)$ and $1/(1+e^{\theta})$, since $\varepsilon(\theta)$ behaves like $\varepsilon_{kink}(\theta)$ for small re^{θ} and positive θ. Firstly, $L_{kink}(\theta) = \ln(1+e^{-\varepsilon_{kink}(\theta)})$ so writing $\varepsilon_{kink}(\theta) = C_0 + \alpha$ where $C_0 = \ln((1+\sqrt{5})/2)$ and α is small gives

$$\begin{aligned}
&\ln(1+e^{-(C_0+\alpha)}) \\
\approx &\ln(1+e^{-C_0}(1-\alpha+\frac{\alpha^2}{2})) \\
= &\ln\left((1+e^{-C_0})\left(1+\frac{\left(-\alpha+\frac{\alpha^2}{2}\right)e^{-C_0}}{1+e^{-C_0}}\right)\right) \\
\approx &\ln(1+e^{-C_0}) - C_1\frac{e^{-C_0}}{1+e^{-C_0}}(re^{\theta})^{6/5} \\
&\quad + \left(\frac{C_1^2}{2}\left(\frac{e^{-C_0}}{1+e^{-C_0}} - \left(\frac{e^{-C_0}}{1+e^{-C_0}}\right)^2\right) - C_2\frac{e^{-C_0}}{1+e^{-C_0}}\right)(re^{\theta})^{12/5}
\end{aligned} \tag{6.1.14}$$

so

$$\begin{aligned}
L_{kink}(\theta) = &\ln\left(\frac{1+\sqrt{5}}{2}\right) - \frac{3-\sqrt{5}}{2}C_1(re^{\theta})^{6/5} \\
&\quad + \left(\frac{(-2+\sqrt{5})C_1^2}{2} - \frac{(3-\sqrt{5})C_2}{2}\right)(re^{\theta})^{12/5} + \cdots .
\end{aligned} \tag{6.1.15}$$

Similarly

$$\begin{aligned}
&\frac{1}{1+e^{\varepsilon_{kink}(\theta)}} \\
\approx &\frac{1}{1+e^{C_0+\alpha}} \\
\approx &\frac{1}{1+e^{C_0}(1+\alpha+\frac{\alpha^2}{2})} \\
\approx &\frac{1}{1+e^{C_0}} - \frac{C_1e^{C_0}}{(1+e^{C_0})^2}(re^{\theta})^{6/5} \\
&\quad + \left(C_1^2\left(\frac{e^{2C_0}}{(1+e^{C_0})^3} - \tfrac{1}{2}\frac{e^{C_0}}{(1+e^{C_0})^2}\right) - \frac{C_2e^{C_0}}{(1+e^{C_0})^2}\right)(re^{\theta})^{12/5}
\end{aligned} \tag{6.1.16}$$

so

$$\frac{1}{1+e^{\varepsilon_{kink}(\theta)}} = \tfrac{1}{2}(3-\sqrt{5}) + (2-\sqrt{5})C_1(re^{\theta})^{6/5} + \left(\frac{9-4\sqrt{5}}{2}C_1^2 + (2-\sqrt{5})C_2\right)(re^{\theta})^{12/5} + \cdots . \quad (6.1.17)$$

Since the g-function is dependent on both positive and negative values of θ an 'anti-kink' expansion $\varepsilon_{anti-kink}(\theta) = \varepsilon_{kink}(-\theta)$ and its related functions must also be included. Noting that the constant term in the expansion of the full $\varepsilon(\theta)$ must be the same as that for $\varepsilon_{kink}(\theta)$, the kink and anti-kink expansions are combined to find the following expansions for small $re^{|\theta|}$:

$$\varepsilon(\theta) = \ln\frac{1+\sqrt{5}}{2} + 2C_1\cosh\left(\frac{6\theta}{5}\right)r^{6/5} + 2C_2\cosh\left(\frac{12\theta}{5}\right)r^{12/5} + \cdots \quad (6.1.18)$$

$$\begin{aligned} L(\theta) &= \sum_{k=0}^{\infty} B_k \cosh\left(\frac{6k\theta}{5}\right) r^{6k/5} \\ &= \ln\left(\frac{1+\sqrt{5}}{2}\right) - (3-\sqrt{5})C_1\cosh\left(\frac{6\theta}{5}\right)r^{6/5} \\ &\quad + \left((-2+\sqrt{5})C_1^2 - (3-\sqrt{5})C_2\right)\cosh\left(\frac{12\theta}{5}\right)r^{12/5} + \cdots \end{aligned} \quad (6.1.19)$$

$$\begin{aligned} \frac{1}{1+e^{\varepsilon(\theta)}} &= \sum_{k=0}^{\infty} A_k \cosh\left(\frac{6k\theta}{5}\right) r^{6k/5} \\ &= \tfrac{1}{2}(3-\sqrt{5}) + 2(2-\sqrt{5})C_1\cosh\left(\frac{6\theta}{5}\right)r^{6/5} \\ &\quad + \left((9-4\sqrt{5})C_1^2 + 2(2-\sqrt{5})C_2\right)\cosh\left(\frac{12\theta}{5}\right)r^{12/5} + \cdots . \end{aligned} \quad (6.1.20)$$

Inserting these expansions into (6.1.7) then gives

$$\ln g_\alpha(r) = \frac{1}{4}\int_{-\infty}^{\infty} (\phi_\alpha(\theta) - 2\phi(2\theta) - \delta(\theta)) \left(\sum_{k=0}^{\infty} B_k \cosh\left(\frac{6k\theta}{5}\right) r^{6k/5} \right) d\theta$$
$$+\tfrac{1}{2}\sum_{n=1}^{\infty} \frac{1}{n} \int_{\mathbb{R}_n} \prod_{i=1}^{n} d\theta_i \left(\sum_{k=0}^{\infty} A_k \cosh\left(\frac{6k\theta_i}{5}\right) r^{6k/5} \right) \phi(\theta_1+\theta_2)\phi(\theta_2-\theta_3)\cdots\phi(\theta_n-\theta_1). \tag{6.1.21}$$

To find the expansion of $\ln g$ in powers of r it needs to be determined for which terms it is possible to swap the sums in the expansions of $L(\theta)$ and $1/(1+e^\theta)$ with the integrals. For large $|\theta|$, both $\phi(\theta)$ and $\phi_{\mathbb{1}}(\theta) \sim 1/e^{|\theta|}$. This means that upon swapping the integral and the sum in $\ln g_1(r)$, the $k=0$ and $k=1$ terms of the $\phi(2\theta)$ part are convergent, but only the $k=0$ term of the $\phi_{\mathbb{1}}(\theta)$ part is convergent. $\ln g$ is finite, and so what remains after subtracting off convergent terms should itself be convergent. Therefore, considering the convergent terms described above separately should not affect other terms in the expansion, and should reproduce terms expected from the expansions given in [29] and [36].

The first thing to check is that when d_0 is found from the $k=0$ constant terms, it is equal to the conformal g-function value for the $\mathbb{1}$ boundary condition [29]

$$\ln g_{\mathbb{1}} = \frac{1}{4}\ln\frac{5-\sqrt{5}}{10}. \tag{6.1.22}$$

The constant terms can be pulled outside the integrals in (6.1.21) so that for $\ln g_0(r)$ the constant term is

$$\begin{aligned} &\tfrac{1}{2}\left(A_0 \int \phi(2\theta)d\theta + \frac{A_0^2}{2}\int \phi(\theta_1+\theta_2)\phi(\theta_2-\theta_1)d\theta_1 d\theta_2 + \cdots \right) \\ &= \tfrac{1}{2}\sum_{n=1}^{\infty} \frac{(-A_0)^n}{2n} = -\frac{1}{4}\ln(1+A_0) \\ &= -\frac{1}{4}\ln\left(\frac{5-\sqrt{5}}{2}\right) \end{aligned} \tag{6.1.23}$$

and for $\ln g_1(r)$ it is

$$\frac{1}{4}\ln\left(\frac{1+\sqrt{5}}{2}\right)\int_{-\infty}^{\infty}\left(\phi_{\mathbb{1}}(\theta)-2\phi(2\theta)-\delta(\theta)\right)d\theta=\left(-\frac{1}{2}+\frac{1}{4}-\frac{1}{4}\right)\ln\left(\frac{1+\sqrt{5}}{2}\right). \tag{6.1.24}$$

Adding these together gives

$$d_0=-\frac{1}{4}\ln\left(\frac{5-\sqrt{5}}{2}\right)-\tfrac{1}{2}\ln\left(\frac{1+\sqrt{5}}{2}\right)=\frac{1}{4}\ln\left(\frac{5-\sqrt{5}}{10}\right) \tag{6.1.25}$$

as expected.

Moving on to the $r^{6/5}$ term, swapping the integral and sum in the $\phi_{\mathbb{1}}$ term produces a divergent term as discussed above. In [29] the coefficient of $r^{6/5}$ in the expansion of $\int_{-\infty}^{\infty}\phi_{\mathbb{1}}(\theta)L(\theta)d\theta$ was found numerically to be zero, so this will be assumed to be true. However, it is possible to find the $r^{6/5}$ term in the expansion for $\ln g_0(r)$ and the other parts of $\ln g_1(r)$ analytically.

From (6.1.21) the coefficient of $r^{6/5}$ in the expansion of $\ln g_0$ is

$$\begin{aligned}&\tfrac{1}{2}\left(\int A_1\cosh\left(\frac{6\theta}{5}\right)\phi(2\theta)d\theta+\frac{2}{2}\int A_0A_1\cosh\left(\frac{6\theta_1}{5}\right)\phi(\theta_1+\theta_2)\phi(\theta_2-\theta_1)d\theta_1d\theta_2\right.\\&\qquad\left.+\frac{3}{3}\int A_0^2A_1\cosh\left(\frac{6\theta_1}{5}\right)\phi(\theta_1+\theta_2)\phi(\theta_2-\theta_3)\phi(\theta_3-\theta_1)d\theta_1d\theta_2d\theta_3+\cdots\right)\\&=\frac{A_1}{2}\sum_{n=1}^{\infty}\int(A_0)^{n-1}\cosh\left(\frac{6\theta_1}{5}\right)\phi(\theta_1+\theta_2)\phi(\theta_2-\theta_3)\cdots\phi(\theta_n-\theta_1)d\theta_1\cdots d\theta_n.\end{aligned} \tag{6.1.26}$$

To evaluate the integrals in the above sum, first consider the term

$$\int\cosh\left(\frac{6\theta_1}{5}\right)\phi(\theta_1+\theta_2)\phi(\theta_2-\theta_1)d\theta_1d\theta_2. \tag{6.1.27}$$

Performing a change of variables $u=\theta_1+\theta_2$, $v=\theta_2-\theta_1$, which has Jacobian $1/2$,

gives

$$\begin{aligned}\cosh\left(\frac{6\theta_1}{5}\right) &= \cosh\left(\frac{3}{5}(u-v)\right)\\ &= \cosh\left(\frac{3u}{5}\right)\cosh\left(\frac{3v}{5}\right) - \sinh\left(\frac{3u}{5}\right)\sinh\left(\frac{3v}{5}\right).\end{aligned} \tag{6.1.28}$$

The variables can now be separated, and since $\phi(\theta)$ is an even function only the cosh terms in the above give a non-zero contribution once the integral is performed. So

$$\int \cosh\left(\frac{6\theta_1}{5}\right)\phi(\theta_1+\theta_2)\phi(\theta_2-\theta_1)d\theta_1 d\theta_2 = \tfrac{1}{2}\left(\int \cosh\left(\frac{3u}{5}\right)\phi(u)du\right)^2. \tag{6.1.29}$$

For the higher terms in the sum similar changes of variables can be performed so that $\theta_1 = (u_1 - u_2 - u_3 - \cdots - u_n)/2$. Then, after repeatedly applying the double angle formula to $\cosh\left(\frac{6\theta_1}{5}\right)$, only one term involves no sinh factors, and hence only this term, $\cosh\left(\frac{3u_1}{5}\right)\cosh\left(\frac{3u_2}{5}\right)\cdots\cosh\left(\frac{3u_n}{5}\right)$, gives a non-zero contribution once integrated. Hence the coefficient of $r^{6/5}$ in the expansion of $\ln g_0$ is given by

$$\begin{aligned}&\frac{A_1}{4A_0}\sum_{n=1}^{\infty}(A_0)^n\left(\int\cosh\left(\frac{3u}{5}\right)\phi(u)du\right)^n\\ =&\frac{A_1}{4A_0}\left(\frac{1}{1+\frac{1}{2}A_0(1+\sqrt{5})}-1\right)\\ =&-\frac{C_1}{2}\left(2-\sqrt{5}\right),\end{aligned} \tag{6.1.30}$$

where the integral identity

$$\int_0^\infty \frac{\sinh(ax)\cosh(bx)}{\sinh(cx)}dx = \frac{\pi}{2c}\frac{\sin\frac{a\pi}{c}}{\cos\frac{a\pi}{c}+\cos\frac{b\pi}{c}} \qquad \text{for } c>|a|+|b| \tag{6.1.31}$$

has been used to give

$$\int\cosh\left(\frac{3u}{5}\right)\phi(u)du = -\tfrac{1}{2}(1+\sqrt{5}) \tag{6.1.32}$$

and the summation identity

$$\sum_{n=1}^{\infty} x^n = \frac{1}{1-x} - 1 \tag{6.1.33}$$

has also been used.

Turning to the convergent terms of $\ln g_1(r)$, using (6.1.19) the coefficient of $r^{6/5}$ from expansion of the $-\frac{1}{2}\phi(2\theta)$ term is

$$\begin{aligned}
&-\tfrac{1}{2}\left(-(3-\sqrt{5})C_1\right)\int_{-\infty}^{\infty}\phi(2\theta)\cosh\left(\frac{6\theta}{5}\right)d\theta \\
=&-\frac{\sqrt{3}}{2\pi}(3-\sqrt{5})C_1\int_{-\infty}^{\infty}\frac{\sinh(4\theta)}{\sinh(6\theta)}\cosh\left(\frac{6\theta}{5}\right)d\theta \\
=&-\frac{\sqrt{3}}{2\pi}(3-\sqrt{5})C_1\left(\frac{\pi}{6}\frac{\sin\frac{2\pi}{3}}{\cos\frac{2\pi}{3}+\cos\frac{\pi}{5}}\right) \\
=&\frac{1}{4}\left(1-\sqrt{5}\right)C_1,
\end{aligned} \tag{6.1.34}$$

where the integral identity (6.1.31) has again been used. The coefficient of $r^{6/5}$ coming from the $\delta(\theta)$ term can be read off from the expansion of $L(\theta)$ giving $\frac{(3-\sqrt{5})C_1}{4}$. So, adding these to the $\ln g_0$ term gives

$$C_1\left(-\frac{1}{2}\left(2-\sqrt{5}\right)+\frac{1}{4}\left(1-\sqrt{5}\right)+\frac{1}{4}\left(3-\sqrt{5}\right)\right)r^{6/5}=0 \tag{6.1.35}$$

which, combined with the zero-valued numerical result for the $\phi_{\mathbb{1}}$ term gives the $r^{6/5}$ term in the expansion of $\ln g(r)$ to be zero. This is as expected, since there is no boundary perturbation here so the regular part of the expansion is expected to be in powers of $r^{12/5}$.

6.1.2 Expansion of the $\mathcal{M}A_4^{(+)}$ g-function

The aim of this section to confirm analytically some of the expansion coefficients for the $\mathcal{M}A_4^{(+)}$ g-function with one boundary parameter which were found numerically in [41]. In this theory the bulk perturbing field $\phi_{1,3}(x,\bar{x})$ has scaling dimension $x_{bulk}=6/5$ and the boundary perturbing field $\phi_{1,3}(x)$ has scaling dimension $x_{bound}=3/5$. This means that with bulk coupling λ and boundary coupling μ, the

perturbative expansion of the g-function is expected to take the form [41]

$$\begin{aligned}\ln g(r) =& fr + \sum_{m,n=0}^{\infty} c_{m,n}^{(\alpha)} \left(\mu R^{2/5}\right)^m \left(\lambda R^{4/5}\right)^n \\ =& fr + \sum_{m,n=0}^{\infty} c_{m,n}^{(\alpha)} \left(\nu r^{2/5}\right)^m \left(\kappa r^{4/5}\right)^n \end{aligned} \tag{6.1.36}$$

where κ is related to λ by the equation $\lambda = \kappa M^{4/5}$ and ν is a function of the boundary parameter θ_b and is related to the boundary coupling μ by $\mu = \nu(\theta_b)M^{2/5}$. Note that the theory is only being considered after it has emerged from the double-scaling limit of the staircase model, so the 'hat' has been dropped from the $\hat{r}$ variable used in the previous chapter.

As was described in section 3.3 and derived in detail in section 5.1, the g-function for this model was found in [41] to be

$$\ln g(r) = \ln g_0(r) + \ln g_b(r) \tag{6.1.37}$$

$$= \ln g_0(r) + \ln g_{b1}(r) + \ln g_{b2}(r) + \ln g_{b3}(r) \tag{6.1.38}$$

where

$$\ln g_0 = \sum_{j=1}^{\infty} \frac{1}{2j-1} \int \frac{d\theta_1}{1+e^{\varepsilon(\theta_1)}} \cdots \frac{d\theta_{2j-1}}{1+e^{\varepsilon(\theta_{2j-1})}} \phi(\theta_1+\theta_2)\phi(\theta_2+\theta_3)\cdots\phi(\theta_{2j-1}+\theta_1) \tag{6.1.39}$$

$$\ln g_{b1} = -\tfrac{1}{2}\ln 2 \tag{6.1.40}$$

$$\ln g_{b2} = \int \left(\phi_{\left(\frac{3}{4}\right)}(\theta) - \phi(2\theta)\right) L(\theta) d\theta \tag{6.1.41}$$

$$\ln g_{b3} = \int \phi(\theta-\theta_b) L(\theta) d\theta \tag{6.1.42}$$

with $\phi(\theta) = 1/(2\pi\cosh(\theta))$ and

$$\phi_{\left(\frac{3}{4}\right)}(\theta) = \frac{-\sin\left(\frac{3\pi}{4}\right)}{2\pi\left(\cosh(\theta) - \cos\left(\frac{3\pi}{4}\right)\right)}. \tag{6.1.43}$$

so that

$$\int \phi_{\left(\frac{3}{4}\right)}(\theta) d\theta = -\frac{1}{4}. \tag{6.1.44}$$

$\varepsilon(\theta)$=$\varepsilon_1(\theta)$ satisfies the TBA system

$$\varepsilon_1(\theta) = \tfrac{1}{2} r e^{\theta} - \int_{\mathbb{R}} \phi(\theta - \theta') L_2(\theta') d\theta' \tag{6.1.45}$$

$$\varepsilon_2(\theta) = \tfrac{1}{2} r e^{-\theta} - \int_{\mathbb{R}} \phi(\theta - \theta') L_1(\theta') d\theta'. \tag{6.1.46}$$

As in the Lee-Yang case, the approach here will be to use the expansions of the pseudoenergies to determine terms in the expansion of $\ln g(r)$. If the $\frac{1}{2} r e^{-\theta}$ term is removed from the $\varepsilon_2(\theta)$ equation then the reduced equations are known as the kink TBA equations, and the pseudoenergies that solve them are denoted $\varepsilon_a^{kink}(\theta)$. For small r and positive θ, the original pseudoenergies behave like the kink pseudoenergies, and so as in the Lee Yang case the small $r \exp|\theta|$ expansions of $\varepsilon_1(\theta)$ and $\varepsilon_2(\theta)$ can be found from the expansions of the kink pseudoenergies. These are given in [18] as

$$\varepsilon_a^{kink}(\theta) = A_0' + A_1' \psi_a^{(2)} (r e^{\theta})^{4/5} + A_2' \psi_a^{(3)} (r e^{\theta})^{6/5} + \cdots \tag{6.1.47}$$

where

$$\psi^{(2)} = (1, 1), \quad \psi^{(3)} = (1, -1) \tag{6.1.48}$$

and

$$A_0' = -\ln\left(\frac{1+\sqrt{5}}{2}\right). \tag{6.1.49}$$

The expansion of the full $\varepsilon(\theta) = \varepsilon_1(\theta)$ is then given by combining the expansions of $\varepsilon_1^{kink}(\theta)$ and $\varepsilon_2^{kink}(-\theta)$ which results in

$$\varepsilon(\theta) = -\ln\left(\frac{1+\sqrt{5}}{2}\right) + 2A_1' \cosh\left(\frac{4\theta}{5}\right) r^{\frac{4}{5}} + \cdots \tag{6.1.50}$$

$$L(\theta) = \ln\left(\frac{3+\sqrt{5}}{2}\right) - 2A_1' \frac{e^{-A_0'}}{1+e^{-A_0'}} \cosh\left(\frac{4\theta}{5}\right) r^{\frac{4}{5}} + \cdots \tag{6.1.51}$$

$$\frac{1}{1+e^{\varepsilon(\theta)}} = \tfrac{1}{2}(\sqrt{5}-1) - 2A_1' \frac{e^{A_0'}}{\left(1+e^{A_0'}\right)^2} \cosh\left(\frac{4\theta}{5}\right) r^{\frac{4}{5}} + \cdots \tag{6.1.52}$$

where

$$\frac{e^{-A_0'}}{1+e^{-A_0'}} = \tfrac{1}{2}(\sqrt{5}-1) \quad \text{and} \quad \frac{e^{A_0'}}{\left(1+e^{A_0'}\right)^2} = -2+\sqrt{5}. \tag{6.1.53}$$

The above can be used to find the constant and $r^{4/5}$ terms in the expansions of the various components of $\ln g$. First, consider the $\theta_b = 0$ case. The constant term here should equal that of the (0+) boundary condition, which has conformal g-function value $\frac{1}{4}\ln\frac{5+2\sqrt{5}}{20}$. For $\ln g_0(r)$, since

$$\int d\theta_1 \cdots d\theta_{2j-1}\phi(\theta_1+\theta_2)\phi(\theta_2+\theta_3)\cdots\phi(\theta_{2j-1}+\theta_1) = \frac{1}{2^{2j}}, \tag{6.1.54}$$

the constant term in the expansion of $\ln g_0$ is equal to

$$\begin{aligned}
&\sum_{j=1}^{\infty}\frac{1}{2j-1}\left(\tfrac{1}{2}(\sqrt{5}-1)\right)^{2j-1}\int d\theta_1\cdots d\theta_{2j-1}\phi(\theta_1+\theta_2)\phi(\theta_2+\theta_3)\cdots\phi(\theta_{2j-1}+\theta_1)\\
=&\tfrac{1}{2}\sum_{j=1}^{\infty}\frac{1}{2j-1}\left(\frac{\sqrt{5}-1}{4}\right)^{2j-1}\\
=&\frac{1}{4}\ln\left(\frac{5+2\sqrt{5}}{5}\right).
\end{aligned} \tag{6.1.55}$$

The constant term coming from the $\phi_{(\frac{3}{4})}$ term in $\ln g_{b2}(r)$ is $-\frac{1}{4}\ln\frac{3+\sqrt{5}}{2}$, and that coming from the $-\phi(2\theta)$ term is also $-\frac{1}{4}\ln\frac{3+\sqrt{5}}{2}$. These are cancelled by the constant term in the $\ln g_{b3}(r)$ expansion, which is $\frac{1}{2}\ln\frac{3+\sqrt{5}}{2}$. So adding these results to $\ln g_{b1}(r)$ which is itself a constant, in the $\theta_b = 0$ case the constant term for the full g-function is

$$\frac{1}{4}\ln\left(\frac{5+2\sqrt{5}}{5}\right) - \tfrac{1}{2}\ln 2 = \frac{1}{4}\ln\left(\frac{5+2\sqrt{5}}{20}\right) \tag{6.1.56}$$

as expected.

Moving on to the coefficient of $r^{4/5}$, for $\ln g_0(r)$ consider the first few terms in the infinite series. For $j=1$ the relevant coefficient is

$$\int \frac{2(2-\sqrt{5})A_1'\cosh\left(\frac{4\theta}{5}\right)}{2\pi\cosh(2\theta)}d\theta = \frac{(2-\sqrt{5})A_1'}{2\pi}\int\frac{\cosh\left(\frac{2u}{5}\right)}{\cosh u}du \tag{6.1.57}$$

where the change of variable $u = 2\theta$ has been used. For $j=2$ the coefficient of $r^{4/5}$

is

$$\frac{3}{3(2\pi)^3}\int \frac{\frac{1}{4}(\sqrt{5}-1)^2 2(2-\sqrt{5})A_1' \cosh\left(\frac{4\theta_1}{5}\right)}{\cosh(\theta_1+\theta_2)\cosh(\theta_2+\theta_3)\cosh(\theta_3+\theta_1)}d\theta_1 d\theta_2 d\theta_3$$
$$= \tfrac{1}{2}\left(\frac{\sqrt{5}-1}{2}\right)^2 2(2-\sqrt{5})A_1'\left(\int \frac{\cosh\left(\frac{2u}{5}\right)}{2\pi\cosh u}du\right)^3, \tag{6.1.58}$$

which is evaluated by performing the change of variables $u_1 = \theta_1 + \theta_2$, $u_2 = \theta_2 + \theta_3$ and $u_3 = \theta_3 + \theta_1$ which has Jacobian $1/2$ and allows the variables in the integrand to be separated once the addition formula has been applied to the cosh term in the numerator. The integral is evaluated as $(\sqrt{5}-1)/2$ using the identity

$$\int_{-\infty}^{\infty}\frac{\cosh ax}{\cosh bx}dx = \frac{\pi}{b}\sec\frac{a\pi}{2b} \quad \text{for } b > |a|. \tag{6.1.59}$$

Generalising these terms, the full coefficient of $r^{4/5}$ coming from $\ln g_0$ is

$$(2-\sqrt{5})A_1'\sum_{j=1}^{\infty}\left(\frac{\sqrt{5}-1}{2}\right)^{2j-2}\left(\int\frac{\cosh\left(\frac{2u}{5}\right)}{2\pi\cosh u}du\right)^{2j-1} = (2-\sqrt{5})A_1'\sum_{j=1}^{\infty}\left(\frac{\sqrt{5}-1}{2}\right)^{4j-3}$$
$$= -A_1'\sum_{j=1}^{\infty}\left(\tfrac{1}{2}\left(7-3\sqrt{5}\right)\right)^j$$
$$= \frac{5-3\sqrt{5}}{10}A_1'. \tag{6.1.60}$$

Moving to $\ln g_b$, $\ln g_{b1}$ is just a constant so makes no contribution to the $r^{4/5}$ term. For the $\phi_{(\frac{3}{4})}$ term in $\ln g_{b2}$, the coefficient of $r^{4/5}$ is

$$\frac{\left(\sqrt{5}-1\right)A_1'}{2\sqrt{2}\pi}\int\frac{\cosh\left(\frac{4\theta}{5}\right)}{\cosh(\theta)-\cos\frac{3\pi}{4}}d\theta = (\sqrt{5}-1)A_1' \tag{6.1.61}$$

using the identity

$$\int_{-\infty}^{\infty}\frac{\cosh ax-\cos t_1}{\cosh bx-\cos t_2}dx = \left(\frac{\pi}{b}\frac{\sin\frac{a(\pi-t_2)}{b}}{\sin t_2\sin\frac{a\pi}{b}} - \frac{\pi-t_2}{b\sin t_2}\cos t_1\right) \tag{6.1.62}$$

with $t_1 = \pi/2$, $t_2 = 3\pi/4$, $a = 4/5$ and $b = 1$. For the $-\phi(2\theta)$ term the coefficient

of $r^{4/5}$ is

$$(\sqrt{5}-1)A_1' \int \phi(2\theta)\cosh\left(\frac{4\theta}{5}\right)d\theta = \frac{(\sqrt{5}-1)A_1'}{2\pi}\int \frac{\cosh\left(\frac{4\theta}{5}\right)}{\cosh(2\theta)}d\theta \tag{6.1.63}$$

$$= \frac{(3-\sqrt{5})}{2}A_1'. \tag{6.1.64}$$

Finally, for $\ln g_{b3}$ at $\theta_b = 0$ the coefficient of $r^{4/5}$ is

$$(1-\sqrt{5})A_1' \int \phi(\theta)\cosh\left(\frac{4\theta}{5}\right)d\theta = \frac{(1-\sqrt{5})A_1'}{2\pi}\int \frac{\cosh\left(\frac{4\theta}{5}\right)}{\cosh(\theta)}d\theta \tag{6.1.65}$$

$$= -2A_1'. \tag{6.1.66}$$

Adding all these together gives the full $r^{4/5}$ term in the expansion $\ln g(r)$ with $\theta_b = 0$ as

$$\frac{A_1'}{10}(-10+2\sqrt{5})r^{4/5}. \tag{6.1.67}$$

Turning now to $\theta_b = -\infty$, the constant term in this case should agree with the conformal g-function value of the (0) boundary condition, which equals $\frac{1}{4}\ln\frac{5-\sqrt{5}}{10}$. In this case, $\ln g_{b3}$ is constant and equal to $\frac{1}{2}\ln 2$, so the constant term in the expansion of $\ln g(r)$ is

$$\frac{1}{4}\ln\left(\frac{5+2\sqrt{5}}{5}\right) - \tfrac{1}{2}\ln\left(\frac{3+\sqrt{5}}{2}\right) = \frac{1}{4}\ln\frac{5-\sqrt{5}}{10} \tag{6.1.68}$$

as expected. The $r^{4/5}$ coefficient of the expansion of $\ln g(r)$ is that of the $\theta_b = 0$ case with the $\ln g_{b3}$ coefficient subtracted off and so becomes

$$\frac{A_1'}{10}(10+2\sqrt{5})r^{4/5}. \tag{6.1.69}$$

To summarise, the expansions in the two boundary parameter cases are

$\ln g(r)$	$\theta_b = 0$	$\frac{1}{4}\ln\left(\frac{5+2\sqrt{5}}{20}\right) + \frac{A_1'}{10}(-10+2\sqrt{5})r^{4/5} + \cdots$
	$\theta_b = -\infty$	$\frac{1}{4}\ln\left(\frac{5-\sqrt{5}}{10}\right) + \frac{A_1'}{10}(10+2\sqrt{5})r^{4/5} + \cdots$

In [41] the coefficients of $r^{4/5}$ for the above values of the boundary parameter were given exactly by evaluating correlation functions in perturbed conformal field theory. Assuming equality between the $\theta_b = 0$ result found above and that of [41]

allows A_1' to be evaluated, and this can then be substituted into the above $\theta_b = -\infty$ result to check its consistency with the $\theta_b = -\infty$ result of [41].

When $\theta_b = 0$, the coefficient of $r^{4/5}$ is given in [41] as

$$\frac{B(-1/5, 3/5)\kappa}{2(2\pi)^{-1/5}\eta^3} \tag{6.1.70}$$

where $B(x, y)$ is the Euler beta function $B(x, y) = \Gamma(x)\Gamma(y)/\Gamma(x + y)$,

$$\kappa = \frac{1}{2\sqrt{2}(3\pi)^{1/5}}\sqrt{\frac{\Gamma(7/10)}{\Gamma(3/10)}} \tag{6.1.71}$$

and $\eta = \sqrt{(1 + \sqrt{5})/2}$. So, for the result found above to be in agreement with this requires

$$A_1' = \frac{10}{-10 + 2\sqrt{5}} \frac{B(-1/5, 3/5)\sqrt{\frac{\Gamma(7/10)}{\Gamma(3/10)}}}{4\sqrt{2}(3/2)^{1/5}\left(\frac{(1+\sqrt{5})}{2}\right)^{3/2}}. \tag{6.1.72}$$

To simplify this note that

$$\frac{2^{3/2}}{(-10 + 2\sqrt{5})(1 + \sqrt{5})^{3/2}} = -\frac{2^{3/2}}{\sqrt{320}\sqrt{1 + \sqrt{5}}} = -\frac{\sqrt{\sqrt{5} - 1}}{\sqrt{160}} \tag{6.1.73}$$

so

$$A_1' = -\frac{5}{\sqrt{160}} \frac{B(-1/5, 3/5)\sqrt{\frac{\Gamma(7/10)}{\Gamma(3/10)}}\sqrt{\sqrt{5} - 1}}{2\sqrt{2}(3/2)^{1/5}}. \tag{6.1.74}$$

Substituting this into the above result for $\theta_b = -\infty$ gives the coefficient of $r^{4/5}$ to be

$$\frac{A_1'}{10}\left(10 + 2\sqrt{5}\right) = -\frac{\left(10 + 2\sqrt{5}\right)}{2\sqrt{160}} \frac{B(-1/5, 3/5)\sqrt{\frac{\Gamma(7/10)}{\Gamma(3/10)}}\sqrt{\sqrt{5} - 1}}{2\sqrt{2}(3/2)^{1/5}} \tag{6.1.75}$$

$$= -\frac{B(-1/5, 3/5)\sqrt{\frac{\Gamma(7/10)}{\Gamma(3/10)}}\sqrt{\frac{1+\sqrt{5}}{2}}}{4\sqrt{2}(3/2)^{1/5}} \tag{6.1.76}$$

$$= -\frac{B(-1/5, 3/5)\kappa\eta}{2(2\pi)^{-1/5}}. \tag{6.1.77}$$

This matches exactly the result given in [41] for $\theta_b = -\infty$.

6.2 The Excited State g-function in $\mathcal{M}A_m^{(+)}$

The g-function that has been explored so far is defined as the inner product between a boundary state and the bulk ground state. If the inner product under consideration is instead between a boundary state and a bulk excited state then this is described as the excited state g-function. For a conformal theory, the value of this g-function for boundary condition (a, b) and an excited state corresponding to a conformal field of conformal dimension $h_{c,d}$ is [52]

$$g^{(c,d)}(m,a,b) = \frac{\sqrt{\frac{8}{m(m+1)}}(-1)^{1+ad+bc}\sin\frac{(m+1)\pi ac}{m}\sin\frac{m\pi bd}{m+1}}{\sqrt{\sqrt{\frac{8}{m(m+1)}}\sin\frac{\pi c}{m}\sin\frac{\pi d}{m+1}}}. \tag{6.2.1}$$

The focus here will be on the state corresponding to the field of conformal dimension $h_{2,2}$ so that

$$g^{(2,2)}(m,a,b) = \frac{\left(\frac{8}{m(m+1)}\right)^{1/4}\sin\frac{2\pi a}{m}\sin\frac{2\pi b}{m+1}}{\sqrt{\sin\frac{2\pi}{m}\sin\frac{2\pi}{m+1}}}. \tag{6.2.2}$$

$g^{(2,2)}$ does not have the spin-flip symmetry possessed by the ground state g-function ($g(m,a,b) = g(m,m-a,b)$), which means that in most cases it is possible to use this excited state g-function to distinguish between a boundary condition and its spin-flip conjugate. Since

$$g^{(2,2)}(m,m-a,b) = -\frac{\left(\frac{8}{m(m+1)}\right)^{1/4}\sin\frac{2\pi a}{m}\sin\frac{2\pi b}{m+1}}{\sqrt{\sin\frac{2\pi}{m}\sin\frac{2\pi}{m+1}}} = -g^{2,2}(m,a,b) \tag{6.2.3}$$

with $a \in \{1,\cdots,m-1\}$ and $b \in \{1,\cdots,m\}$, $g^{(2,2)}(m,a,b)$ is only equal to $-g^{(2,2)}(m,a,b)$ when $a = m/2$ (for m even) or $b = (m+1)/2$ (for m odd), and in these cases $a = m-a$ or $b = m+1-b$ respectively, so the boundary conditions in question are self-conjugate under the spin-flip. So, if the value of the $\mathcal{M}A_m^{(+)}$ ground state g-function is equal to the conformal g-function value of (a,b) and $(m-a,b)$ for some values of boundary parameters $(\theta_{b1},\theta_{b2})$ near a minimal model $\mathcal{M}_m$, then knowledge of $g^{(2,2)}$ for those values of the boundary parameters would determine which of the

two boundary conditions was the correct identification. In most cases this is also true if the boundary parameters are such that they correspond to a superposition of Cardy boundary conditions when the theory is close to a minimal model. There are a few ambiguities which remain, and these will be discussed at the end of this chapter. For now attention will be turned to finding an off-critical expression for $g^{(2,2)}$ in $\mathcal{M}A_m^{(+)}$.

To check that the flows between boundary conditions identified in section 5.2 are correct, an expression for $g^{(2,2)}(r)$ must be found that is defined at all points along the RG flow in $\mathcal{M}A_m^{(+)}$ and agrees with the conformal values of $g^{(2,2)}$ (6.2.2) in the UV and IR limits, just as was done in defining an exact expression for the ground state g-function $g(r)$ in section 5.3. Klassen and Melzer [55] proposed that for m even the TBA equations for pseudoenergies $\varepsilon_a^{(2,2)}(\theta)$ for the state corresponding to the field $\phi_{(2,2)}$ are

$$\begin{aligned}
\varepsilon_1^{(2,2)}(\theta) &= \frac{1}{2} r\, e^{\theta} - \int_{\mathbb{R}} \phi(\theta-\theta') L_2^{(2,2)}(\theta')\, d\theta' \\
\varepsilon_a^{(2,2)}(\theta) &= -\int_{\mathbb{R}} \phi(\theta-\theta') (L_{a-1}^{(2,2)}(\theta') + L_{a+1}^{(2,2)}(\theta'))\, d\theta' \qquad a = 2 \ldots m-3 \\
\varepsilon_{m-2}^{(2,2)}(\theta) &= \frac{1}{2} r\, e^{-\theta} - \int_{\mathbb{R}} \phi(\theta-\theta') L_{m-3}^{(2,2)}(\theta')\, d\theta'
\end{aligned} \tag{6.2.4}$$

where

$$L_a^{(2,2)}(\theta) = \ln\left(1 + t_a e^{-\varepsilon_a^{(2,2)}(\theta)}\right) \tag{6.2.5}$$

with

$$t_a = \begin{cases} -1 & \text{for} \quad a = \frac{m-2}{2} \ \text{ or } \ a = \frac{m}{2} \\ 1 & \text{otherwise} \end{cases} . \tag{6.2.6}$$

The difference between this and the ground state TBA is simply due to the change of the sign accompanying $\exp(-\varepsilon_a(\theta))$.

These pseudoenergies have a plateaux behaviour similar to that of the ground state. In the UV limit $r \ll 1$ the central plateau of each $\varepsilon_a^{(2,2)}$ is labelled by $x_{a+1}^{(2,2)}$ and the right and left hand plateaux are labelled by $y_a^{(2,2)}$ and $y_{a+1}^{(2,2)}$ respectively,

with

$$x_a^{(2,2)} = \begin{cases} 0 & \text{for } a = 1 \text{ or } a = m \\ \left| \frac{\sin \frac{(m-1-2a)\pi}{m+1} \sin \frac{(m+3-2a)\pi}{m+1}}{\sin^2 \frac{2\pi}{m+1}} \right| & \text{for } a = 2, \cdots, m-1 \end{cases} \tag{6.2.7}$$

and

$$\left\{ y_a^{(2,2)} \right\}_{a=1}^{m-1} = \left\{ 0, \hat{y}_1, \cdots, \hat{y}_{(m-6)/2}, 0, 1, 0, \hat{y}_1, \cdots, \hat{y}_{(m-6)/2}, 0 \right\}, \quad \hat{y}_r = \frac{\sin \frac{2r\pi}{m} \sin \frac{2(r+2)\pi}{m}}{\sin^2 \frac{2\pi}{m}}. \tag{6.2.8}$$

In the IR limit, the central plateau of $\exp(-\varepsilon_a^{(2,2)}(\theta))$ is equal to $x_a^{(2,2)}$ at $\mathcal{M}_{m-2}$ for $a = 2 \cdots m-3$, and zero for $a = 1$ and $a = m-2$. The left and right hand plateau are the same as in the UV limit.

A proposal has been made by Watts [56] as to how the ground state g-function can be converted into $g^{(2,2)}$ in the case of a single boundary parameter. He looked at flows occurring within a minimal model $\mathcal{M}_m$ and so used the kink TBA system

$$\begin{aligned} \varepsilon_1^{kink}(\theta) &= -\int_{\mathbb{R}} \phi(\theta - \theta') L_2^{kink}(\theta')\, d\theta' \\ \varepsilon_a^{kink}(\theta) &= -\int_{\mathbb{R}} \phi(\theta - \theta') (L_{a-1}^{kink}(\theta') + L_{a+1}^{kink}(\theta'))\, d\theta' \qquad a = 2 \ldots m-3 \\ \varepsilon_{m-2}^{kink}(\theta) &= \frac{1}{2} r\, e^{\theta} - \int_{\mathbb{R}} \phi(\theta - \theta') L_{m-3}^{kink}(\theta')\, d\theta'. \end{aligned} \tag{6.2.9}$$

The pseudoenergies $\varepsilon_a^{(2,2),kink}$ for the $(2,2)$ excited state follow by using the same sign-changing prescription as described above. The flow investigated was in the ratio of the g-function with that of the $(1,1)$ boundary condition, both for the ground state and the $(2,2)$ excited state. For the ground state this is given by

$$\ln \left(\frac{\ln g_{\mathcal{M}_m}(r)}{\ln g(m,1,1)} \right) = \int_{\mathbb{R}} \phi(\theta - \theta_{b1}) L_a^{kink}(\theta) d\theta \tag{6.2.10}$$

and Watts found that the expected flow in the excited state g-function is found by replacing $L_a^{kink}(\theta)$ by $L_a^{(2,2),kink}(\theta)$ so that

$$\ln \left(\frac{\ln g_{\mathcal{M}_m}^{(2,2)}(r)}{\ln g^{(2,2)}(m,1,1)} \right) = \int_{\mathbb{R}} \phi(\theta - \theta_{b1}) L_a^{(2,2),kink}(\theta) d\theta. \tag{6.2.11}$$

Since only a single boundary parameter was used, the flows seen were between those of the forms $(1,a)$ and $(b,1)$.

In terms of the two boundary parameter $\mathcal{M}A_m^{(+)}$ ground state g-function (5.3.33), the situation studied by Watts is reproduced when r is such that the theory is close to a minimal model, and one of the terms in $\ln g_{b3}$ vanishes, such as is the case if a_2 is taken to equal 0 or $m-1$ (or similarly for a_1). It therefore seems natural to generalise to the two parameter situation and to propose that for $\mathcal{M}A_m^{(+)}$ with m even (the situation where Klassen and Melzer's excited state TBA equations apply), the full exact equation for $\ln g^{(2,2)}(r)$ is found from the ground state g-function $\ln g(r)$ (5.3.33) by replacing each occurrence of $\exp(-\varepsilon_a(\theta))$ with $t_a \exp(-\varepsilon_a^{(2,2)})(\theta)$. Following the prescribed pattern and adding suitable constant terms, the proposal for $\ln g^{(2,2)}(r)$ is

$$\begin{aligned}\ln g^{(2,2)}_{a_1a_2}(r,\theta_{b1},\theta_{b2}) = \\ \ln\left(\left(\frac{2}{m}\right)^{1/4}\sqrt{\sin\frac{2\pi}{m}}\right) + \int d\theta \left(\phi_{\left(\frac{3}{4}\right)}(\theta)-\phi(2\theta)\right)\ln\left(1-e^{-\varepsilon^{(2,2)}_{(m-2)/2}(\theta)}\right) \\ + \ln g_A^{(2,2)}(r) + \ln g^{(2,2)}_{b3\ a_1a_2}(r) + \left(\left\lfloor\frac{2a_1}{m}\right\rfloor + \left\lfloor\frac{2a_2}{m}\right\rfloor\right)\pi i \end{aligned} \tag{6.2.12}$$

with $(a_1,a_2)\in\{0,\cdots,m-1\}$ as before and $\left\lfloor\frac{2a_i}{m}\right\rfloor$ being the greatest integer less than or equal to $2a_i/m$.

$$\begin{aligned}\ln g_A^{(2,2)}(r) = \\ \sum_{n\,odd}\frac{1}{2n}\int \mathrm{antiTr}\left(\prod_{i=1}^{n} A^{(2,2)}(\theta_i)\,d\theta_i\right)\phi(\theta_1-\theta_2)\phi(\theta_2-\theta_3)\cdots\phi(\theta_{n-1}-\theta_n)\phi(\theta_n+\theta_1)\end{aligned} \tag{6.2.13}$$

and $A^{(2,2)}(\theta)$ is the matrix defined by

$$A^{(2,2)}(\theta) = \frac{1}{1+t_a e^{\varepsilon_a^{(2,2)}(\theta))}} l_{a,b}. \tag{6.2.14}$$

with $l_{a,b}$ the incidence matrix of the A_{m-2} Dynkin diagram. Also,

$$\ln g^{(2,2)}_{b3\ a_1a_2}(r,\theta_{b1},\theta_{b2}) = \sum_{i=1}^{2}\int_{\mathbb{R}} d\theta\,\phi(\theta-\theta_{b_i})\ln(1+t_{a_i}e^{-\epsilon^{(2,2)}_{a_i}(\theta)}). \tag{6.2.15}$$

Finally, the πi terms are included to allow the expression to distinguish between boundary conditions that are conjugate under the spin-flip symmetry, since when exponentiated it determines if the value of the excited g-function is positive or negative. There will still be an overall ambiguity in relating the boundary parameters to specific boundary conditions, since the same flows would be identified with $(\theta_{b1},-\theta_{b2})$, $(a_1,m-1-a_2)$ if the coefficient of πi was replaced with $1+\left\lfloor\frac{2a_1}{m}\right\rfloor-\left\lfloor\frac{2a_2}{m}\right\rfloor$. However, it is the ratios of $g^{(2,2)}_{a_1a_2}(r,\theta_{b1},\theta_{b2})$ at different values of r that are important in determining which boundary conditions flow to one another, and this is unaffected by any constant terms in (6.2.12). Unlike the situation for the ground state g-function, the ratio of the excited state g-function of two boundary conditions changes when either is replaced by its spin-flip conjugate. So, the combined information of the ground state and excited state g-functions is able to determine which boundary flows occur, up to certain ambiguities that arise when superpositions appear in the flows, and these will be discussed at the end of this section.

A check on this proposal is to evaluate $\ln g^{(2,2)}(r)$ in its UV and IR limits in the situation where $\ln g^{(2,2)}_{b3}(r)$ equals zero, which occurs if $a_1,a_2\in\{0,m-1\}$. In this situation the ground state g-function was equal to that of the $(1,1)$ boundary condition in the UV and IR limits (and that of its spin-flip conjugate). The excited state g-function is therefore expected to be equal to that of one or other of these boundary conditions, which for $\mathcal{M}_m$ have the values

$$g^{(2,2)}(m,1,1) = \left(\frac{8}{m(m+1)}\right)^{\frac{1}{4}}\sqrt{\sin\frac{2\pi}{m}\sin\frac{2\pi}{m+1}} \tag{6.2.16}$$

$$g^{(2,2)}(m,m-1,1) = -\left(\frac{8}{m(m+1)}\right)^{\frac{1}{4}}\sqrt{\sin\frac{2\pi}{m}\sin\frac{2\pi}{m+1}}. \tag{6.2.17}$$

Since both $\ln g_A$ and the other non-constant term in the boundary-independent part of $\ln g^{(2,2)}$ have their support close to $\theta=0$, in the UV limit each factor of $\exp(-\varepsilon^{(2,2)}_a(\theta))$ can be replaced by $x^{(2,2)}_a$. In this limit, the matrix $A^{(2,2)}$ is denoted

by $A_{UV}^{(2,2)}$, where

$$A_{UV}^{(2,2)} = \frac{x_{a+1}^{(2,2)}}{x_{a+1}^{(2,2)} + t_a} l_{a,b}. \tag{6.2.18}$$

Using the same methods as in section 5.2.1, in the UV limit $\ln g_A^{(2,2)}$ becomes

$$\ln g_A^{(2,2)}(r \ll 1) = \frac{1}{8} \ln \frac{\mathrm{Det}\left(1 + \frac{1}{2}A^{(2,2)}J_{m-2}\right)}{\mathrm{Det}\left(1 - \frac{1}{2}A^{(2,2)}J_{m-2}\right)}, \tag{6.2.19}$$

where J_{m-2} is as defined in section 5.2.1. The eigenvalues of $A^{(2,2)}J_{m-2}$ have been found for all even values of m up to $m = 12$ using Maple, and in each case are the elements of the following set, which will be assumed to be correct for all m even

$$\left\{2\cos\frac{4\pi}{m+1}, 2\cos\frac{6\pi}{m+1}, 2\cos\frac{8\pi}{m+1}, \cdots, 2\cos\frac{m\pi}{m+1}\right\}, \quad \text{all with multiplicity two.} \tag{6.2.20}$$

So,

$$\begin{aligned}
\ln g_A^{(2,2)}(r \ll 1) &= \frac{1}{8} \ln \prod_{a=2}^{m/2} \frac{\left(1 + \cos\frac{2a\pi}{m+1}\right)^2}{\left(1 - \cos\frac{2a\pi}{m+1}\right)^2} \\
&= \frac{1}{8} \ln \prod_{a=2}^{m/2} \frac{\cos^4\frac{a\pi}{(m+1)}}{\sin^4\frac{a\pi}{(m+1)}} \\
&= \frac{1}{8} \ln \left(\frac{\sin^4\frac{\pi}{(m+1)}}{(m+1)^2\cos^4\frac{\pi}{(m+1)}} \right) \\
&= \ln \left(\sqrt{\frac{\sin\frac{\pi}{(m+1)}}{\sqrt{m+1}\cos\frac{\pi}{(m+1)}}} \right).
\end{aligned} \tag{6.2.21}$$

Also, in the UV limit

$$\int d\theta \left(\phi_{\left(\frac{3}{4}\right)}(\theta) - \phi(2\theta)\right) \ln\left(1 - e^{-\varepsilon_{(m-2)/2}(\theta)}\right)\Big|_{r\ll 1} = -\tfrac{1}{2} \ln \left(1 - \frac{\sin\frac{\pi}{m+1}\sin\frac{3\pi}{m+1}}{\sin^2\frac{2\pi}{m+1}}\right). \tag{6.2.22}$$

For $(a_1, a_2) = (0, 0)$, adding all the terms together gives $\ln g^{(2,2)}(r \ll 1)$ to be

$$\begin{aligned}
&\ln\left(\left(\frac{2}{m}\right)^{1/4}\sqrt{\sin\frac{2\pi}{m}}\right) + \int d\theta\left(\phi_{\left(\frac{3}{4}\right)}(\theta) - \phi(2\theta)\right)\ln\left(1 - e^{-\varepsilon^{(2,2)}_{(m-2)/2}(\theta)}\right) + \ln g_A^{(2,2)}\Big|_{r\ll 1} \\
&= \ln\left(\left(\frac{2}{m(m+1)}\right)^{\frac{1}{4}}\frac{\sqrt{\sin\frac{\pi}{m+1}\sin\frac{2\pi}{m}\sin\frac{2\pi}{m+1}}}{\sqrt{\cos\frac{\pi}{m+1}\left(\sin^2\frac{2\pi}{m+1} - \sin\frac{\pi}{m+1}\sin\frac{3\pi}{m+1}\right)}}\right) \\
&= \ln\left(\left(\frac{8}{m(m+1)}\right)^{\frac{1}{4}}\sqrt{\sin\frac{2\pi}{m}\sin\frac{2\pi}{m+1}}\right), \qquad (6.2.23)
\end{aligned}$$

which is the logarithm of the excited state g-function of the $(1, 1)$ boundary at $\mathcal{M}_m$. $(a_1, a_2) = (m-1, m-1)$ gives the same result but with a factor of $2\pi i$ added to it. Once exponentiated, this therefore gives the same $g^{(2,2)}$ value as the case above, so again the boundary condition is $(1, 1)$. For $(a_1, a_2) = (0, m-1)$ or $(a_1, a_2) = (m-1, 0)$ the additional term is πi, so the corresponding boundary condition has $g^{(2,2)}$ value that is the negative of that of $(1, 1)$. The boundary condition that is identified with these cases is therefore $(m-1, 1)$. In section 5.2 it was predicted that in the RG flow from $\mathcal{M}_m$ to $\mathcal{M}_{m-1}$ the $(1, 1)|_{\mathcal{M}_m}$ boundary condition flows to $(1, 1)|_{\mathcal{M}_{m-1}}$, and $(m-1, 1)|_{\mathcal{M}_m}$ flows to $(m-1, 1)|_{\mathcal{M}_{m-1}}$. To check whether this is indeed the case, the IR limit of $\ln g^{(2,2)}(r)$ must also be calculated.

In the IR limit, each factor of $\exp(-\varepsilon_1^{(2,2)}(\theta))$ and $\exp(-\varepsilon_{m-2}^{(2,2)}(\theta))$ can be replaced by zero, and for all other values of a $\exp(-\varepsilon_a^{(2,2)}(\theta))$ becomes $x_a^{(2,2)}|_{\mathcal{M}_{m-2}}$. So, labelling the matrix $A^{(2,2)}$ in this limit by $A_{IR}^{(2,2)}$ and recalling that $x_1|_{\mathcal{M}_{m-2}} = x_{m-2}|_{\mathcal{M}_{m-2}} = 0$, $\ln g_A^{(2,2)}$ becomes

$$\begin{aligned}
\ln g_A^{(2,2)}(r \gg 1) &= \frac{1}{8}\ln\frac{\mathrm{Det}\left(1 + \frac{1}{2}A_{IR,m}^{(2,2)}J_{m-2}\right)}{\mathrm{Det}\left(1 - \frac{1}{2}A_{IR,m}^{(2,2)}J_{m-2}\right)} \qquad (6.2.24) \\
&= \frac{1}{8}\ln\frac{\mathrm{Det}\left(1 + \frac{1}{2}A_{UV,m-2}^{(2,2)}J_{m-4}\right)}{\mathrm{Det}\left(1 - \frac{1}{2}A_{UV,m-2}^{(2,2)}J_{m-4}\right)} \\
&= \ln\left(\sqrt{\frac{\sin\frac{\pi}{(m-1)}}{\sqrt{m-1}\cos\frac{\pi}{(m-1)}}}\right). \qquad (6.2.25)
\end{aligned}$$

In addition,

$$\begin{aligned}
&\int d\theta \left(\phi_{\left(\frac{3}{4}\right)}(\theta) - \phi(2\theta)\right) \ln\left(1 - e^{-\varepsilon_{(m-2)/2}(\theta)}\right)\Big|_{r\gg 1} \\
&= \int d\theta \left(\phi_{\left(\frac{3}{4}\right)}(\theta) - \phi(2\theta)\right) \ln\left(1 - x^{(2,2)}_{(m-2)/2}|_{\mathcal{M}_{m-2}}\right) \\
&= -\tfrac{1}{2} \ln\left(1 - \frac{\sin\frac{\pi}{m-1}\sin\frac{3\pi}{m-1}}{\sin^2\frac{2\pi}{m-1}}\right). \qquad (6.2.26)
\end{aligned}$$

Adding these to the constant term in the $(a_1, a_2) = (0, 0)$ case gives $\ln g^{(2,2)}(r \gg 1)$ as

$$\begin{aligned}
&\ln\left(\left(\frac{2}{m}\right)^{1/4}\sqrt{\sin\frac{2\pi}{m}}\right) + \int d\theta \left(\phi_{\left(\frac{3}{4}\right)}(\theta) - \phi(2\theta)\right) \ln\left(1 - e^{-\varepsilon^{(2,2)}_{(m-2)/2}(\theta)}\right) + \ln g_A^{(2,2)}\Big|_{r\gg 1} \\
&= \ln\left(\left(\frac{8}{m(m-1)}\right)^{\frac{1}{4}}\sqrt{\sin\frac{2\pi}{m-1}\sin\frac{2\pi}{m}}\right) \qquad (6.2.27)
\end{aligned}$$

which is equal to the logarithm of the excited state g-function of the $(1, 1)$ boundary at $\mathcal{M}_{m-1}$. As in the UV limit, (a_1, a_2) gives the same result, and $(a_1, a_2) = (0, m-1)$ and $(a_1, a_2) = (m-1, 0)$ correspond to the $(m-1, 1)$ boundary condition. So the boundary flows from the UV to the IR are $(1, 1)|_{\mathcal{M}_m} \to (1, 1)|_{\mathcal{M}_{m-1}}$ and $(m-1, 1)|_{\mathcal{M}_m} \to (m-1, 1)|_{\mathcal{M}_{m-1}}$, in agreement with the predictions made earlier.

The examples below will demonstrate how the excited state g-function can be used to verify the predictions made by the ground state g-function when $\ln g_{b3}(r)$ and $\ln g^{(2,2)}_{b3}(r)$ are non-zero. The excited state g-function values are tabulated at various points in the RG flow, as are the boundary condition predictions made from the ground state g-function in section 5.2. Where there are superpositions of boundary conditions it will be checked that the excited state g-function is able to uniquely distinguish which superposition appears. Where there is no ambiguity then if the value of the logarithm of the conformal excited state g-function (6.2.2) of this prediction agrees with $\ln g^{(2,2)}(r)$ at the corresponding point in the RG flow then the predicted boundary condition does indeed appear in the boundary flow in question. If there is not agreement then its spin-flip conjugate must appear.

• $\mathcal{M}A_4^{(+)}$: $\theta_{b1} \gg 0$, $\theta_{b2} \ll 0$, $|\theta_{b1}| \ll |\theta_{b2}|$ both finite, $a_1 = 1$ and $a_2 = 2$.

Point in RG flow	$\ln g_{b3}^{(2,2)}(r)$	$\ln g^{(2,2)}(r)$
$r \to 0$	$\ln\left(1 - \frac{\sin\frac{\pi}{5}\sin\frac{3\pi}{5}}{\sin^2\frac{2\pi}{5}}\right)$	$\ln\left(\left(\frac{2}{5}\right)^{\frac{1}{4}} \frac{\sin^2\frac{\pi}{5}}{\sin^{3/2}\frac{2\pi}{5}}\right) + \pi i$
$\lvert\theta_{b1}\rvert \ll \ln\frac{1}{r} \ll \lvert\theta_{b2}\rvert$	$\frac{1}{2}\ln\left(1 - \frac{\sin\frac{\pi}{5}\sin\frac{3\pi}{5}}{\sin^2\frac{2\pi}{5}}\right)$	$\ln\left(\left(\frac{2}{5}\right)^{\frac{1}{4}} \frac{\sin\frac{\pi}{5}}{\sqrt{\sin\frac{2\pi}{5}}}\right) + \pi i$
$0 \ll \ln\frac{1}{r} \ll \lvert\theta_{b1}\rvert$	0	$\ln\left(\left(\frac{2}{5}\right)^{\frac{1}{4}} \sqrt{\sin\frac{2\pi}{5}}\right) + \pi i$
$\ln\frac{1}{r} \ll 0$	0	$\ln\left(\frac{1}{2^{1/4}}\right) + \pi i$

Point in RG flow	Ground state plateau configuration	B.C. prediction from $\ln g(r)$	$g^{(2,2)}$(B.C.)
$r \to 0$	$[x_2, x_3]\rvert_{\mathcal{M}_4}$	$(1,4)\&(1,2)$	$-\left(\frac{2}{5}\right)^{\frac{1}{4}} \frac{\sin^2\frac{\pi}{5}}{\sin^{3/2}\frac{2\pi}{5}}$
$\lvert\theta_{b1}\rvert \ll \ln\frac{1}{r} \ll \lvert\theta_{b2}\rvert$	$[x_2.y_3]\rvert_{\mathcal{M}_4}$	$(3,2)$	$-\left(\frac{2}{5}\right)^{\frac{1}{4}} \frac{\sin\frac{\pi}{5}}{\sqrt{\sin\frac{2\pi}{5}}}$
$0 \ll \ln\frac{1}{r} \ll \lvert\theta_{b1}\rvert$	$[y_1, y_3]\rvert_{\mathcal{M}_4}$	$(3,1)$	$-\left(\frac{2}{5}\right)^{\frac{1}{4}} \sqrt{\sin\frac{2\pi}{5}}$
$\ln\frac{1}{r} \ll 0$	$[x_1, x_3]\rvert_{\mathcal{M}_3}$	$(1,3)$	$-\frac{1}{2^{1/4}}$

The only superposition that appears is $(1,4)\&(1,2)$. From (6.2.2), $g^{(2,2)}((1,4))$ and $g^{(2,2)}((1,2))$ are not negatives of one another, and so the superposition created by replacing either or both boundary conditions with their spin-flip conjugates (which would give the same ground state g-function value) cannot give the same $g^{(2,2)}$ value, so the combined ground state and excited state g-function values uniquely identify the boundary condition as $(1,4)\&(1,2)$. Therefore, at each point in the flow, the value of the excited state g-function given by $\ln g^{(2,2)}(r)$ agrees with that of the boundary condition predicted by the proposed rules (5.2.72) for the ground state boundary condition. The excited state g-function has therefore verified the flow which begins at the $(1,4)\&(1,2)$ boundary condition of $\mathcal{M}_4$, and then undergoes pure boundary transitions first to $(3,2)$ and then to $(3,1)$, before undergoing the bulk transition to $\mathcal{M}_3$ after which the boundary condition is $(1,3)$. The flow is illustrated in figure 6.1.

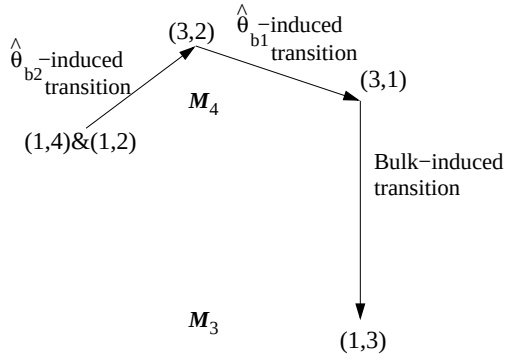

Figure 6.1: Boundary condition flow in $\mathcal{M}A_4^{(+)}$ found by combining the values of $\ln g(r)$ and $\ln g^{(2,2)}(r)$ for finite θ_{b1} and θ_{b2} with $\theta_{b1} \gg 0$, $\theta_{b2} \ll 0$ and $|\theta_{b1}| \ll |\theta_{b2}|$, and with $a_1 = 1$ and $a_2 = 2$.

• $\mathcal{M}A_6^{(+)}$: $\theta_{b1} \ll 0$, $\theta_{b2} \gg 0$, $|\theta_{b1}| \ll |\theta_{b2}|$ both finite, $a_1 = 3$ and $a_2 = 4$.

Point in RG flow	$\ln g_{b3}^{(2,2)}(r)$	$\ln g^{(2,2)}(r)$
$r \to 0$	$\frac{1}{2}\ln\left(1 - \frac{\sin\frac{3\pi}{7}\sin\frac{\pi}{7}}{\sin^2\frac{2\pi}{7}}\right) + \frac{1}{2}\ln\left(1 + \frac{\sin\frac{5\pi}{7}\sin\frac{\pi}{7}}{\sin^2\frac{2\pi}{7}}\right)$	$\ln\left(\left(\frac{1}{7}\right)^{\frac{1}{4}} \frac{\sin\frac{\pi}{7}\sin\frac{3\pi}{7}}{\sin^{3/2}\frac{2\pi}{7}}\right) + 2\pi i$
$\lvert\theta_{b1}\rvert \ll \ln\frac{1}{r} \ll \lvert\theta_{b2}\rvert$	$\frac{1}{2}\ln\left(1 - \frac{\sin\frac{3\pi}{7}\sin\frac{\pi}{7}}{\sin^2\frac{2\pi}{7}}\right)$	$\ln\left(\left(\frac{1}{7}\right)^{\frac{1}{4}} \frac{\sin\frac{\pi}{7}}{\sqrt{\sin\frac{2\pi}{7}}}\right) + 2\pi i$
$0 \ll \ln\frac{1}{r} \ll \lvert\theta_{b1}\rvert$	0	$\ln\left(\left(\frac{1}{7}\right)^{\frac{1}{4}} \sqrt{\sin\frac{2\pi}{7}}\right) + 2\pi i$
$-\lvert\theta_{b1}\rvert \ll \ln\frac{1}{r} \ll 0$	0	$\ln\left(\left(\frac{1}{5}\right)^{\frac{1}{4}} \sqrt{\sin\frac{2\pi}{5}}\right) + 2\pi i$
$-\lvert\theta_{b2}\rvert \ll \ln\frac{1}{r} \ll -\lvert\theta_{b1}\rvert$	$\frac{1}{2}\ln\left(1 - \frac{\sin\frac{3\pi}{5}\sin\frac{\pi}{5}}{\sin^2\frac{2\pi}{5}}\right)$	$\ln\left(\left(\frac{1}{5}\right)^{\frac{1}{4}} \frac{\sin\frac{\pi}{5}}{\sqrt{\sin\frac{2\pi}{5}}}\right) + 2\pi i$
$\ln\frac{1}{r} \ll -\lvert\theta_{b2}\rvert$	$\frac{1}{2}\ln\left(1 - \frac{\sin\frac{3\pi}{5}\sin\frac{\pi}{5}}{\sin^2\frac{2\pi}{5}}\right)$	$\ln\left(\left(\frac{1}{5}\right)^{\frac{1}{4}} \frac{\sin\frac{\pi}{5}}{\sqrt{\sin\frac{2\pi}{5}}}\right) + 2\pi i$

Point in RG flow	Ground state plateau configuration	B.C. prediction from $\ln g(r)$	$g^{(2,2)}$(B.C.)
$r \to 0$	$[x_4, x_5]\|_{\mathcal{M}_6}$	$(1,4)\&(1,2)$	$\left(\frac{1}{7}\right)^{\frac{1}{4}} \frac{\sin\frac{\pi}{7}\sin\frac{3\pi}{7}}{\sin^{3/2}\frac{2\pi}{7}}$
$\lvert\theta_{b1}\rvert \ll \ln\frac{1}{r} \ll \lvert\theta_{b2}\rvert$	$[x_4, y_4]\|_{\mathcal{M}_6}$	$(4,4)$	$\left(\frac{1}{7}\right)^{\frac{1}{4}} \frac{\sin\frac{\pi}{7}}{\sqrt{\sin\frac{2\pi}{7}}}$
$0 \ll \ln\frac{1}{r} \ll \lvert\theta_{b1}\rvert$	$[y_4, y_4]\|_{\mathcal{M}_6}$	$(3,1)\&(1,1)$	$\left(\frac{1}{7}\right)^{\frac{1}{4}} \sqrt{\sin\frac{2\pi}{7}}$
$-\lvert\theta_{b1}\rvert \ll \ln\frac{1}{r} \ll 0$	$[x_4, x_4]\|_{\mathcal{M}_5}$	$(1,3)\&(1,1)$	$\left(\frac{1}{5}\right)^{\frac{1}{4}} \sqrt{\sin\frac{2\pi}{5}}$
$-\lvert\theta_{b2}\rvert \ll \ln\frac{1}{r} \ll -\lvert\theta_{b1}\rvert$	$[y_3, x_4]\|_{\mathcal{M}_5}$	$(3,4)$	$\left(\frac{1}{5}\right)^{\frac{1}{4}} \frac{\sin\frac{\pi}{5}}{\sqrt{\sin\frac{2\pi}{5}}}$
$\ln\frac{1}{r} \ll -\lvert\theta_{b2}\rvert$	$[y_3, y_4]_{\mathcal{M}_5}$	$(2,1)$	$\left(\frac{1}{5}\right)^{\frac{1}{4}} \frac{\sin\frac{\pi}{5}}{\sqrt{\sin\frac{2\pi}{5}}}$

Again, it needs to be checked that the superpositions are uniquely determined. In each of the predicted superpositions, both boundary conditions have $g^{(2,2)}$ values which are not the negatives of one another, so the same $g^{(2,2)}$ value could not be reproduced by replacing either or both boundary conditions with their spin-flip conjugate. The combined ground state and excited state information uniquely determines the superposition. So, the agreement between the final columns of the two tables verifies the flow in $\mathcal{M}A_6^{(+)}$ that begins at $(1,4)\&(1,2)$, undergoes pure boundary flows first to $(4,4)$ and then to $(3,1)\&(1,1)$, and then undergoes the bulk transition to $\mathcal{M}_5$ after which the boundary condition is $(1,1)\&(1,3)$. There are then two further pure boundary flows, first to $(3,4)$, and finally to $(2,1)$. The flow is depicted in figure 6.2.

Flows between boundary conditions can be seen more explicitly by creating three-dimensional plots consisting of the values of the ground state and excited g-functions as found from the formulae (5.3.33) and (6.2.12), respectively, plotted against the effective central charge for $r \in \mathbb{R}^+$, so that the flow can be tracked as it moves between consecutive minimal models $\mathcal{M}_m$ and $\mathcal{M}_{m-1}$. Figure 6.3 shows the flows that arise at $\mathcal{M}A_6^{(+)}$ when θ_{b1} is held fixed and equal to zero, with $a_1 = 3$, and θ_{b2} is taken at various values along the full real line, with a_2 taking each of the values $\{1,2,3,4\}$ in turn. The local minima and maxima in the $(g^{(2,2)}, g)$ plane at $c = 6/7$ and $c = 4/5$ indicate the fixed points in the flows when the bulk theory is close to the respective minimal models $\mathcal{M}_6$ and $\mathcal{M}_5$, and the corresponding boundary conditions are labelled. The thicker close-to-vertical flow lines mark the meeting

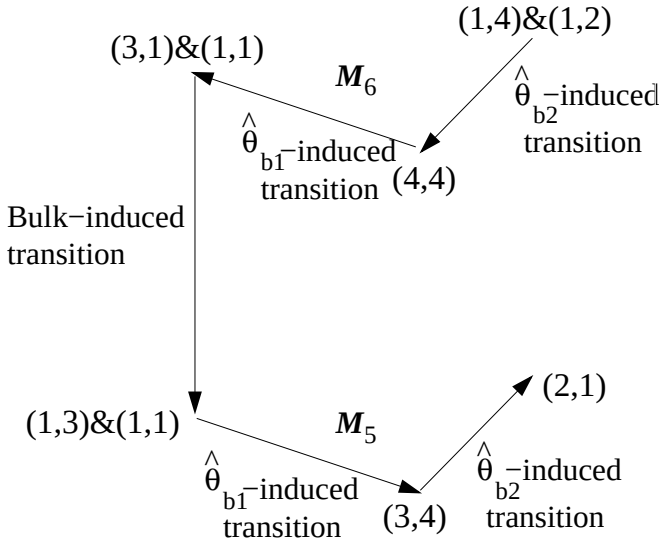

Figure 6.2: Boundary condition flow in $\mathcal{M}A_6^{(+)}$ found by combining the values of $\ln g(r)$ and $\ln g^{(2,2)}(r)$ for finite θ_{b1} and θ_{b2} with $\theta_{b1} \ll 0$, $\theta_{b2} \gg 0$ and $|\theta_{b1}| \ll |\theta_{b2}|$, and with $a_1 = 3$ and $a_2 = 4$.

of the flows arising from each value of a_2, with $a_2 = 1$ appearing on the far right and the others following in order. These lines are naturally thicker due to certain flows arising from consecutive values of a_2 both taking these values. Part of the flow depicted in figure 6.2 appears in the far left a_4 section, but since θ_{b1} is held fixed at zero there are no θ_{b1} induced flows and the bulk transition occurs once the $(4,4)$ boundary condition is reached at $\mathcal{M}_6$, so the flow seen is $(1,4)\&(1,2)|_{\mathcal{M}_6} \to (4,4)|_{\mathcal{M}_6} \to (3,4)|_{\mathcal{M}_5} \to (3,5)|_{\mathcal{M}_5} (\cong (2,1)|_{\mathcal{M}_5})$ rather than the more complex flow depicted in figure 6.2. The truncation of flows of the type depicted in figure 5.14 can be seen in the $a_2 = 1$ and $a_2 = 4$ sections of the plot, where the number of fixed points decreases from three to two in moving from the $\mathcal{M}_6$ to the $\mathcal{M}_5$ level.

Another example of flows is shown in the plot in figure 6.4. Here the flows are those that arise from $a_1 = 1$ with $\theta_{b1} \to \infty$ (though to create the plots the maximum value of $\ln\left(\frac{1}{r}\right)$ was taken to be 20 so θ_{b1} was set at 30). These choices mean that the only boundary conditions to appear are those of the form $(a,1)$ and $(1,b)$, and so when r is such that the theory is close to a minimal model the conditions of Watts'

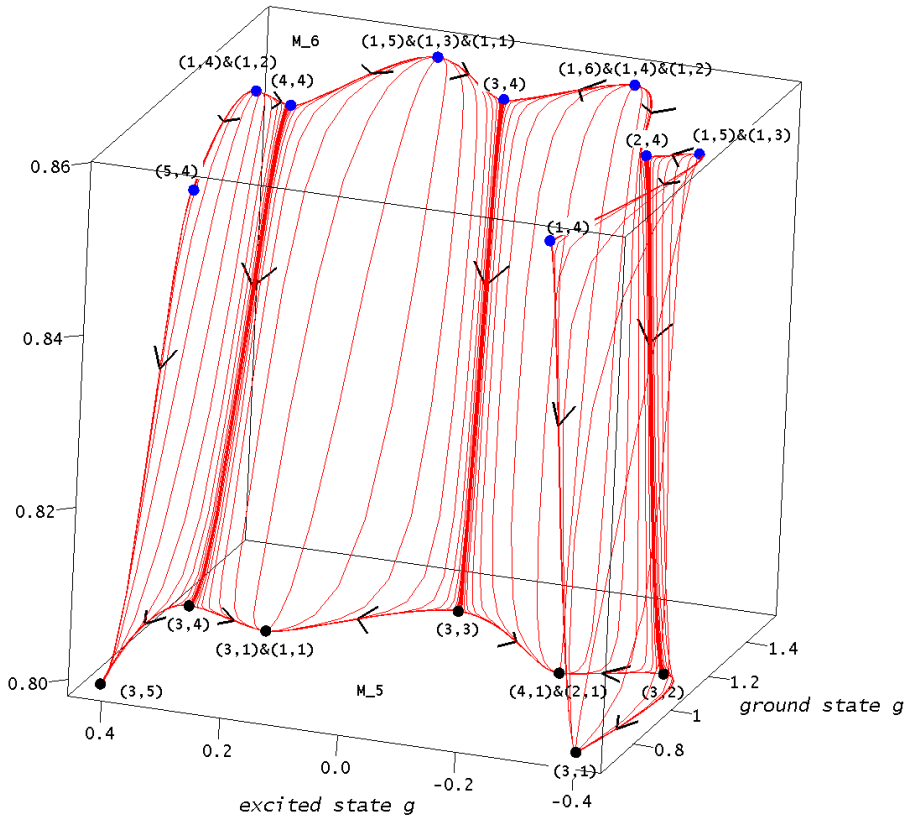

Figure 6.3: $g(r)$ and $g^{(2,2)}(r)$ plotted with a_1=3, $\theta_{b1} = 0$, and $\theta_{b2} = -30 \cdots 30$ in steps of 2 at $\ln r = -20 \cdots 20$ for each value of $a_2 \in \{1, 2, 3, 4\}$ in turn. The vertical axis is the effective central charge $c_{eff}(r)$.

paper are reproduced. Watts plots

$$\frac{g(r)}{g(m,1,1)} \qquad \text{against} \qquad \frac{g^{(2,2)}(r)}{g^{(2,2)}(m,1,1)} \Big/ \frac{g(r)}{g(m,1,1)} \,.$$

So, recalling that close to a minimal model $\mathcal{M}_m$,

$$\ln g(r) - \ln g_{b3}(r) = \ln g(m,1,1) \quad \text{and}$$
$$\ln g^{(2,2)}_{a_1 a_2}(r) - \ln g^{(2,2)}_{b3\, a_1 a_2}(r) - \left(\left\lfloor \frac{2a_1}{m} \right\rfloor + \left\lfloor \frac{2a_2}{m} \right\rfloor \right) \pi i = \ln g^{(2,2)}_{a_1 a_2}(m,1,1),$$

to make the comparison with Watts' results clear the values plotted here are

$$\text{Ground state:} \qquad g'(r) = g_{b3}(r) \qquad \text{and} \tag{6.2.28}$$

$$\text{Excited state:} \qquad (g^{(2,2)}_{a_1 a_2})'(r) = \frac{g^{(2,2)}_{b3\,a_1 a_2}(r) \exp\left[\left(\left\lfloor \frac{2a_1}{m} \right\rfloor + \left\lfloor \frac{2a_2}{m} \right\rfloor\right) \pi i\right]}{g_{b3}(r)}. \tag{6.2.29}$$

The aerial view of the plots shown in figure 6.5 shows how at $c = 6/7$ and $c = 4/5$ these plots match the $\mathcal{M}_6$ and $\mathcal{M}_5$ curves in figure 3 of Watts' paper.

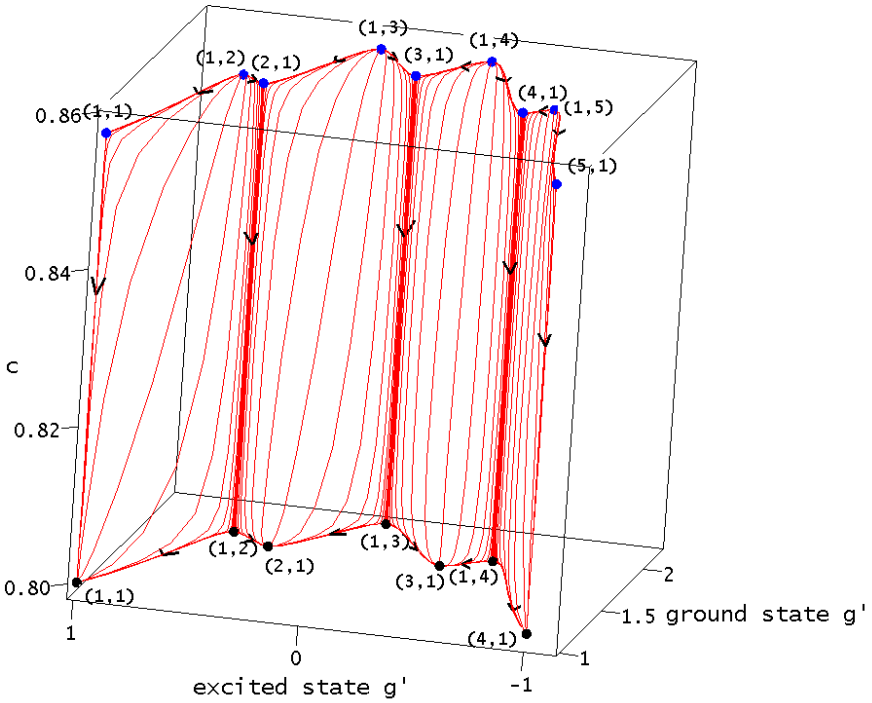

Figure 6.4: $g'(r)$ and $(g^{(2,2)})'(r)$ (defined above) for $\mathcal{M}A_6^{(+)}$ plotted with $a_1 = 1$ and $\theta_{b1} = 30$, and $\theta_{b2} = -30 \cdots 30$ in steps of 2 at $\ln r = -20 \cdots 20$ for each value of $a_2 \in \{1, 2, 3, 4\}$ in turn. The vertical axis is $c_{eff}(r)$. The ground state and excited state g-functions have been normalised so that they match the plots in Watts' paper, as described in the main text.

In all the examples above the combined information from the ground state and excited state g-functions made it possible to identify uniquely the superpositions of boundary conditions that appeared. However, this is not always the case, as will

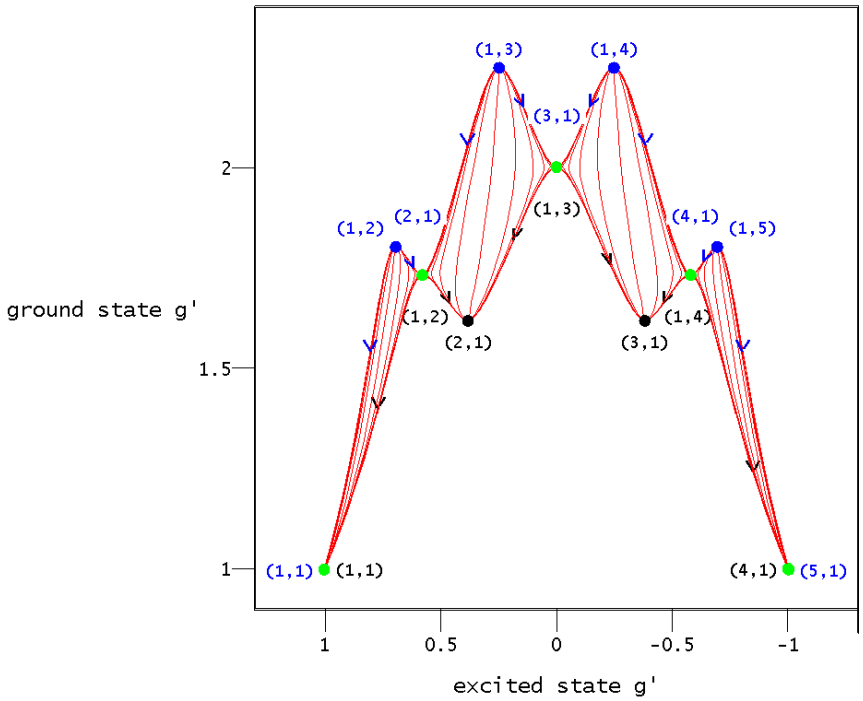

Figure 6.5: 'Aerial view' of figure 6.4. The flows in $\mathcal{M}_6$ and $\mathcal{M}_5$ are denoted by blue and black boundary conditions and arrows respectively. The five green dots indicate points where the g-values of certain $\mathcal{M}_6$ and $\mathcal{M}_5$ boundary conditions coincide in the $(g'(r), (g^{(2,2)})'(r))$ plane.

be explored below. In section 5.2 the superpositions that were identified with the $[x_r, x_s]$ and $[y_r, y_s]$ plateau configurations were of the forms

$$(1) \qquad (1,p)\&(1,p+2)\&(1,p+4)\&\cdots\&(1,q) \qquad \text{and} \qquad (6.2.30)$$

$$(2) \qquad (p,1)\&(p+2,1)\&(p+4,1)\&\cdots\&(q,1) \qquad (6.2.31)$$

respectively. However, the ground state g-function value of the superpositions above would be the same if any number of the boundary conditions making up the super-

position was replaced by their spin-flip conjugates. It is usually possible for the excited state g-function $g^{(2,2)}$ to identify which of these possible superpositions is the correct one, but there are certain exceptions. These occur when the sum of the $g^{(2,2)}$ values of a subset of the boundary conditions making up the superposition is equal to the sum of these values when each member of the subset has been replaced by its spin-flip conjugate. For a superposition of type (1) such an ambiguity arises if some subset consisting of k non-self-conjugate boundary conditions $(1, p_i)$ with $i = 1 \cdots k$ satisfies

$$\sum_{i=1}^{k} g^{(2,2)}(1, p_i) = \sum_{i=1}^{k} g^{(2,2)}\overline{(1, p_i)} = \sum_{i=1}^{k} g^{(2,2)}(m-1, p_i) \tag{6.2.32}$$

which from (6.2.2) means that

$$\sum_{i=1}^{k} \sin \frac{2\pi p_i}{m+1} = -\sum_{i=1}^{k} \sin \frac{2\pi p_i}{m+1}. \tag{6.2.33}$$

This equation can be satisfied if the subset of boundary conditions consists of one or more pairs of boundary conditions $(1, p_r)$ and $(1, p_s)$ such that

$$|p_r - p_s| = \frac{m+1}{2} \quad \text{or} \quad p_r + p_s = m + 1. \tag{6.2.34}$$

The latter case is of no consequence, since then $(1, p_r)$ and $(1, p_s)$ are conjugates of one another so conjugating both of these makes no difference to the superposition itself. However, the former case does change the superposition, so if that is satisfied then $g^{(2,2)}$ is unable to distinguish between the superposition containing $(1, p_r)$ and $(1, p_s)$ and that containing $\overline{(1, p_r)}$ and $\overline{(1, p_s)}$. Since p_r and p_s are integers this situation can only occur if m is odd. Furthermore, the form of the original superposition (6.2.30) means that $|p_r - p_s|$ is even, so m must equal 3 (mod 4), and for the ambiguity to arise there must be at least $(m+5)/4$ boundary conditions in the superposition. The boundary condition $(1, 1)\&(1, 3)$ at $\mathcal{M}_3$ obeys these conditions but in reality there is no ambiguity, since $\overline{(1, 1)} = (1, 3)$ and so taking the conjugate of both boundary conditions reproduces the same superposition. The first real ambiguity occurs at $\mathcal{M}_7$, and can only occur in superpositions containing three or more bound-

ary conditions. In particular $g^{(2,2)}((1,1)\&(1,3)\&(1,5)) = g^{(2,2)}((1,7)\&(1,3)\&(1,3))$ and $g^{(2,2)}((1,3)\&(1,5)\&(1,7)) = g^{(2,2)}((1,5)\&(1,5)\&(1,1))$. Other more occasional ambiguities, similar to the accidental ambiguities described in section 5.2, can arise if the subset of the superposition consists of three boundary conditions where

$$\sin\frac{2\pi p_1}{m+1} = \pm 1 \quad \text{and} \quad \sin\frac{2\pi p_2}{m+1} = \sin\frac{2\pi p_3}{m+1} = \mp\tfrac{1}{2}.$$

However, these only occur when $m+1$ is a multiple of twelve, and in longer superpositions that those already known to possess ambiguities. So, $g^{(2,2)}$ allows the exact identification of type (1) superpositions containing less than $(m+5)/4$ boundary conditions at $m \equiv 3 \pmod 4$, and of type (1) superpositions of all lengths for $m \not\equiv 3 \pmod 4$.

The ambiguities around the type (2) superpositions arise in a similar manner, occurring if one or more pairs of boundary conditions $(p_r, 1)$ and $(p_s, 1)$ satisfy

$$|p_r - p_s| = \frac{m}{2}. \tag{6.2.35}$$

Here $m/2$ must be even so $m \equiv 0 \pmod 4$, and such an ambiguity can only arise in a superposition of length $(m+4)/4$. Although the $(3,1)\&(1,1)$ boundary condition at $\mathcal{M}_4$ satisfies these conditions, $\overline{(3,1)} = (1,1)$ so conjugating both elements leads to the same superposition. So, the first ambiguity arises at $\mathcal{M}_8$, where $g^{(2,2)}((1,1)\&(3,1)\&(5,1)) = g^{(2,2)}((7,1)\&(3,1)\&(3,1))$ and $g^{(2,2)}((3,1)\&(5,1)\&(7,1)) = g^{(2,2)}((5,1)\&(5,1)\&(1,1))$. As for the type (1) superpositions, there are occasional ambiguities, occurring when m is a multiple of twelve, but again these occur in longer superpositions than those already identified as containing ambiguities. So, in general, $g^{(2,2)}$ can be used to identify exactly the type (2) superpositions containing less than $(m+4)/4$ boundary conditions at $\mathcal{M}_m$ for $m \equiv 0 \pmod 4$, and type (2) superpositions of all lengths for all other values of m.

6.3 The $\mathcal{M}A_4^{(-)}$ g-function

6.3.1 $\mathcal{M}A_4^{(+)}$ to $\mathcal{M}A_4^{(-)}$ by Analytic Continuation

As was discussed in section 2.1, the interpolating theory $\mathcal{M}A_4^{(+)}$ describes the RG flow induced by the perturbation of the minimal model $\mathcal{M}_4$ by the field $\phi_{1,3}$, and this corresponds to the term $\lambda \int \phi_{1,3}\, d^2x$ being added to the action of the conformal field theory, with the bulk coupling $\lambda > 0$. The IR limit of this flow is the $\mathcal{M}_3$ minimal model, but as was described in section 1.2, the IR fixed point of an RG flow from a conformal field theory need not itself be a conformal field theory, and can instead be described by a massive field theory. Such a flow arises when $\mathcal{M}_4$ is again perturbed by $\phi_{1,3}$ but this time with $\lambda < 0$, and the interpolating theory that emerges is known as $\mathcal{M}A_4^{(-)}$. Zamolodchikov found that, up to the sign change, both theories have the same relationship between λ and the crossover scale M: $\lambda_{\mathcal{M}A_4^{(+)}} = \kappa M^{4/5} = -\lambda_{\mathcal{M}A_4^{(-)}}$, where $\kappa = 0.418695516\cdots$ [18, 44].

The TBA system for $\mathcal{M}A_4^{(-)}$ was found by Zamolodchikov [44]

$$\begin{aligned}\varepsilon_1(\theta) &= r\cosh(\theta) - \int_{-\infty}^{\infty} \phi(\theta-\theta')L_2(\theta')d\theta' \\ \varepsilon_2(\theta) &= -\int_{-\infty}^{\infty} \phi(\theta-\theta')L_1(\theta')d\theta',\end{aligned} \tag{6.3.1}$$

where as for $\mathcal{M}A_4^{(+)}$, $\phi(\theta) = \frac{1}{2\pi\cosh(\theta)}$ and $L_a(\theta) = \ln(1+\exp(-\varepsilon_a(\theta)))$. The effective central charge is

$$c_{eff}(r) = \frac{3r}{\pi^2}\int_{\mathbb{R}} d\theta \cosh(\theta) L_1(\theta). \tag{6.3.2}$$

The TBA system is clearly similar to that of $\mathcal{M}A_4^{(+)}$ (2.3.22), with the values of the plateaux which make up $L_1(\theta)$ and $L_2(\theta)$ coming from the same set of values as are taken by the plateaux in the $\mathcal{M}A_4^{(+)}$ pseudoenergies (5.1.9): when $r < 1$ $L_1(\theta) = 0$ and $L_2(\theta) = \ln 2$ for $|\theta| \gg \ln(1/r)$ and $L_1(\theta) = L_2(\theta) = \ln((3+\sqrt{5})/2)$ for $|\theta| \ll \ln(1/r)$; when $r > 1$ $L_1(\theta) = 0$ for all θ and $L_2(\theta) = \ln 2$. Zamolodchikov observed [44] that the effective central charge $c_{eff}(r)$ in the two theories must be related to one another, at least in their perturbative expansions, by analytic continuation to complex r. This is because $c_{eff}(r)$ has a regular perturbative expansion in powers

of $\lambda r^{4/5}$; changing the sign of λ moves the theory from $\mathcal{M}A_4^{(+)}$ to $\mathcal{M}A_4^{(-)}$, and in the expansion this change can be effected by instead continuing r to $\rho\exp(-5\pi i/4)$ with $\rho \in \mathbb{R}^+$. Dorey and Tateo [57] showed that analytic continuation was not only of use perturbatively, but could be applied directly to the TBA system in the scaling Lee Yang model to find new TBA systems describing excited states. Dorey, Dunning and Tateo [58] found that analytic continuation could also be used to move between massless and massive TBA systems of particular models, and Dorey and Miramontes [59] explored this further in the context of the homogeneous sine-Gordon models [60, 61].

The emergence of the $\mathcal{M}A_4^{(-)}$ TBA system from the analytic continuation of the $\mathcal{M}A_4^{(+)}$ system can be seen by considering the asymptotic behaviour of the Y-systems of the theories in the spirit of [59]. These are systems of equations which are satisfied by any solution to the TBA equations [62], and have the same form in both $\mathcal{M}A_4^{(+)}$ and $\mathcal{M}A_4^{(-)}$ [18, 44]:

$$\begin{aligned} Y_1\left(\theta+\frac{i\pi}{2}\right)Y_1\left(\theta-\frac{i\pi}{2}\right) &= 1+Y_2(\theta) \\ Y_2\left(\theta+\frac{i\pi}{2}\right)Y_2\left(\theta-\frac{i\pi}{2}\right) &= 1+Y_1(\theta) \end{aligned} \tag{6.3.3}$$

where $Y_a(\theta) = \exp(-\varepsilon_a(\theta))$. The Y-functions have the periodicity property

$$Y_1\left(\theta+\frac{5\pi i}{2}\right) = Y_2(\theta) \qquad Y_2\left(\theta+\frac{5\pi i}{2}\right) = Y_1(\theta). \tag{6.3.4}$$

Although the Y-system is the same for both theories, the theory to which a particular solution to the Y-system corresponds can be seen by considering the asymptotic behaviour of $Y_a(\theta)$. For $\mathcal{M}A_4^{(+)}$ this is

$$\begin{aligned} Y_1(r,\theta) &\xrightarrow{\theta\to+\infty} \exp\left(\frac{-re^{\theta}}{2}\right) \\ Y_1(r,\theta) &\xrightarrow{\theta\to-\infty} 1 \\ Y_2(r,\theta) &\xrightarrow{\theta\to+\infty} 1 \\ Y_2(r,\theta) &\xrightarrow{\theta\to-\infty} \exp\left(\frac{-re^{-\theta}}{2}\right) \end{aligned} \tag{6.3.5}$$

but for $\mathcal{M}A_4^{(-)}$

$$\begin{aligned} Y_1(r,\theta) &\xrightarrow{\theta\to+\infty} \exp\left(\frac{-re^{\theta}}{2}\right) \\ Y_1(r,\theta) &\xrightarrow{\theta\to-\infty} \exp\left(\frac{-re^{-\theta}}{2}\right) \\ Y_2(r,\theta) &\xrightarrow{\theta\to+\infty} 1 \\ Y_2(r,\theta) &\xrightarrow{\theta\to-\infty} 1 \end{aligned} \tag{6.3.6}$$

Analytically continuing r to $\rho\exp(-5\pi i/4)$ in the $\mathcal{M}A_4^{(+)}$ TBA system (2.3.22) and shifting θ in order to make the relationship with the asymptotic behaviour of $\mathcal{M}A_4^{(-)}$ clear leads to the following asymptotic behaviour in the analytically continued $\mathcal{M}A_4^{(+)}$ Y-functions

$$\begin{aligned} Y_1\left(e^{-\frac{5\pi i}{4}}\rho,\theta+\frac{5\pi i}{4}\right) &\xrightarrow{\theta\to+\infty} \exp\left(-\frac{\rho e^{\theta}}{2}\right) \\ Y_1\left(e^{-\frac{5\pi i}{4}}\rho,\theta-\frac{5\pi i}{4}\right) &\xrightarrow{\theta\to-\infty} 1 \\ Y_2\left(e^{-\frac{5\pi i}{4}}\rho,\theta+\frac{5\pi i}{4}\right) &\xrightarrow{\theta\to+\infty} 1 \\ Y_2\left(e^{-\frac{5\pi i}{4}}\rho,\theta-\frac{5\pi i}{4}\right) &\xrightarrow{\theta\to-\infty} \exp\left(-\frac{\rho e^{-\theta}}{2}\right). \end{aligned} \tag{6.3.7}$$

Using the periodicity properties (6.3.4) then gives

$$\begin{aligned} Y_1(e^{-\frac{5\pi i}{4}}\rho,\theta+\frac{5\pi i}{4}) = Y_2(e^{-\frac{5\pi i}{4}}\rho,\theta-\frac{5\pi i}{4}) &\xrightarrow{\theta\to-\infty} \exp\left(-\frac{\rho e^{-\theta}}{2}\right) \\ Y_2(e^{-\frac{5\pi i}{4}}\rho,\theta+\frac{5\pi i}{4}) = Y_1(e^{-\frac{5\pi i}{4}}\rho,\theta-\frac{5\pi i}{4}) &\xrightarrow{\theta\to-\infty} 1. \end{aligned} \tag{6.3.8}$$

So defining $Y_a'(\rho,\theta) = Y_a(e^{-\frac{5\pi i}{4}}\rho,\theta+\frac{5\pi i}{4})$, the new Y-system $Y_a'(\rho,\theta)$ has asymptotic

behaviour

$$\begin{aligned} Y_1(\rho,\theta) &\xrightarrow{\theta\to+\infty} \exp\left(-\frac{\rho e^{\theta}}{2}\right) \\ Y_1(\rho,\theta) &\xrightarrow{\theta\to-\infty} \exp\left(-\frac{\rho e^{-\theta}}{2}\right) \\ Y_2(\rho,\theta) &\xrightarrow{\theta\to+\infty} 1 \\ Y_2(\rho,\theta) &\xrightarrow{\theta\to-\infty} 1 \end{aligned} \tag{6.3.9}$$

which is the same as for $\mathcal{M}A_4^{(-)}$ (6.3.6). So, the analytic continuation acts on the pseudoenergies in the following way:

$$\varepsilon_{1,\mathcal{M}A_4^{(+)}}(\theta) \xrightarrow{r\to\rho\exp\left(-\frac{5\pi i}{4}\right)} \varepsilon_{1,\mathcal{M}A_4^{(-)}}\left(\theta-\frac{5\pi i}{4}\right) = \varepsilon_{2,\mathcal{M}A_4^{(-)}}\left(\theta+\frac{5\pi i}{4}\right) \tag{6.3.10}$$

$$\varepsilon_{2,\mathcal{M}A_4^{(+)}}(\theta) \xrightarrow{r\to\rho\exp\left(-\frac{5\pi i}{4}\right)} \varepsilon_{2,\mathcal{M}A_4^{(-)}}\left(\theta-\frac{5\pi i}{4}\right) = \varepsilon_{1,\mathcal{M}A_4^{(-)}}\left(\theta+\frac{5\pi i}{4}\right). \tag{6.3.11}$$

This effect can be seen in figures 6.6 and 6.7, which show contour plots of the $\mathcal{M}A_4^{(+)}$ pseudoenergies at $r=\rho\exp(\psi)$ as ψ is continued from 0 to $-5\pi i/4$, and also of the $\mathcal{M}A_4^{(-)}$ pseudoenergies for real r. As the analytic continuation is performed, singularities of $L_a(\theta)$, which appear as concentric patterns in the plots, move position. If these cross the real axis then the integration contour used in the TBA system has to be deformed away from the real axis (as was done in [57]), in order to avoid passing through the singularities. The deformation of the integration contour is also depicted in the figures.

It is also possible to see numerically how analytic continuation takes the $\mathcal{M}A_4^{(+)}$ $c_{eff}(r)$ (defined via (2.3.25)) to the $\mathcal{M}A_4^{(-)}$ $c_{eff}(r)$ (6.3.2). Zamolodchikov found that for $\mathcal{M}A_4^{(+)}$, $c_{eff}(r)$ has the perturbative expansion [18]

$$c_{eff,\mathcal{M}A_4^{(+)}}(r) = \frac{7}{10} + \frac{3}{2\pi}r^2 + \sum_{n=2}^{\infty} a_n \left(\lambda r^{4/5}\right)^n \tag{6.3.12}$$

whereas in $\mathcal{M}A_4^{(-)}$ it has the expansion [44]

$$c_{eff,\mathcal{M}A_4^{(-)}}(r) = \frac{7}{10} + \sum_{n=2}^{\infty} b_n \left(\lambda r^{4/5}\right)^n. \tag{6.3.13}$$

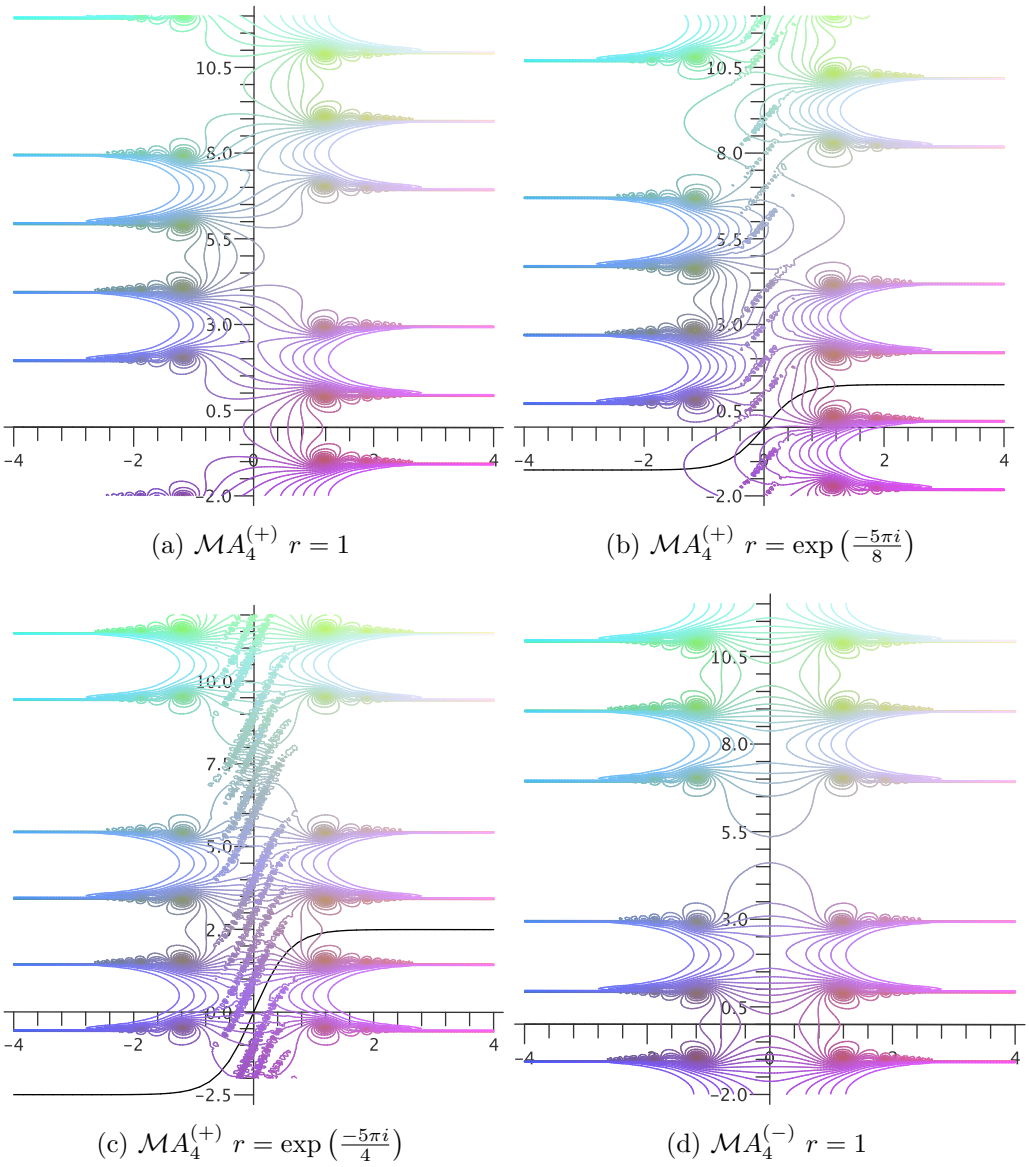

(a) $\mathcal{M}A_4^{(+)}$ $r = 1$

(b) $\mathcal{M}A_4^{(+)}$ $r = \exp\left(\frac{-5\pi i}{8}\right)$

(c) $\mathcal{M}A_4^{(+)}$ $r = \exp\left(\frac{-5\pi i}{4}\right)$

(d) $\mathcal{M}A_4^{(-)}$ $r = 1$

Figure 6.6: Contour plots of $\frac{|1+Y_1(\theta)|}{1+|1+Y_1(\theta)|}$ with the horizontal and vertical axes being the real and complex parts of θ, respectively, in units of $\frac{\pi}{2}$. The plots in 6.6a, 6.6b and 6.6c correspond to the $\mathcal{M}A_4^{(+)}$ TBA system as the argument of r moves from 0 to $-\frac{5\pi i}{4}$. The concentric patterns occur around zeros of $1+Y_1$. As the argument of r increases in magnitude, these zeros move in the positive $\mathrm{Im}(\theta)$ direction for positive $\mathrm{Re}(\theta)$, and in the negative $\mathrm{Im}(\theta)$ direction for negative $\mathrm{Re}(\theta)$. The tanh-shaped curves show how the integration contour used to solve the TBA system must be deformed to avoid the singularities as they cross the real axis. The diagonal lines of small circular contours close to the imaginary axis are artefacts of the numerics used to generate the data. In 6.6d the plot corresponds to the $\mathcal{M}A_4^{(-)}$ TBA system. Comparing this with 6.6c, other than the diagonal lines just mentioned, the matching is clear between 6.6c and 6.6d shifted by $\theta \to \theta - \frac{5\pi i}{4}$.

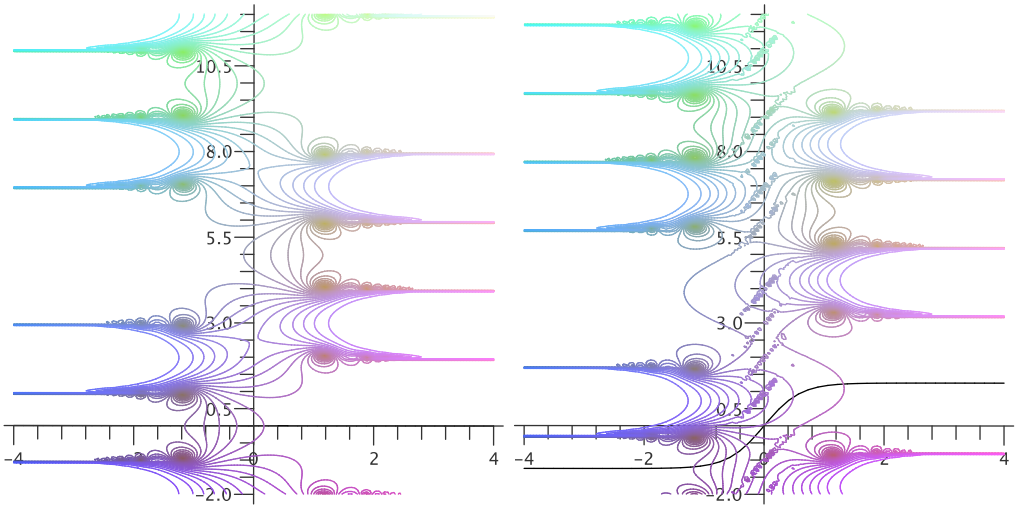

(a) $\mathcal{M}A_4^{(+)}$ $r = 1$

(b) $\mathcal{M}A_4^{(+)}$ $r = \exp\left(\frac{-5\pi i}{8}\right)$

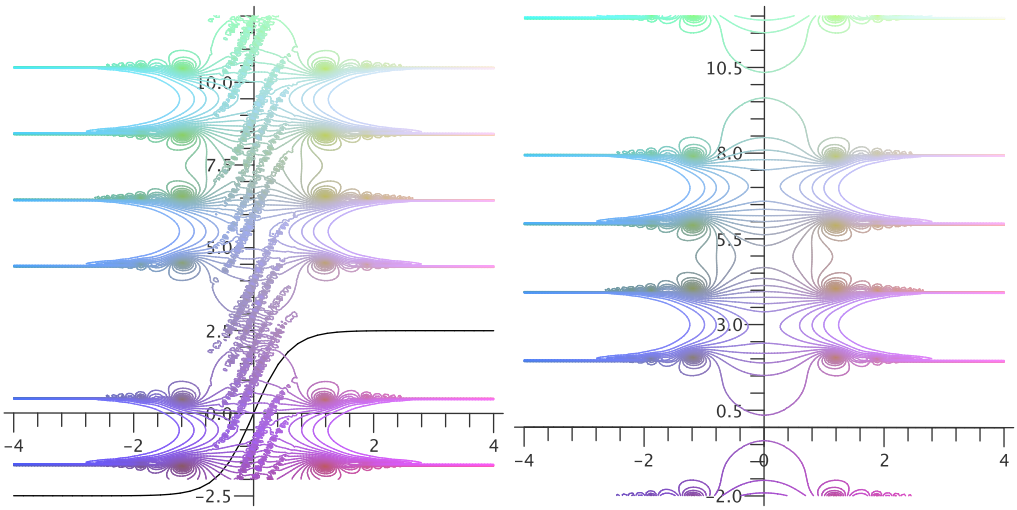

(c) $\mathcal{M}A_4^{(+)}$ $r = \exp\left(\frac{-5\pi i}{4}\right)$

(d) $\mathcal{M}A_4^{(-)}$ $r = 1$

Figure 6.7: Contour plots of $\frac{|1+Y_2(\theta)|}{1+|1+Y_2(\theta)|}$. 6.7a, 6.7b and 6.7c show the analytic continuation of the $\mathcal{M}A_4^{(+)}$ TBA system, and 6.7d corresponds to the $\mathcal{M}A_4^{(-)}$ TBA system at $r = 1$. It matches 6.7c when shifted by $\theta \to \theta - \frac{5\pi i}{4}$.

Analytic continuation $r \to \rho \exp(-\frac{5\pi i}{4})$ should map the terms making up the sum in $c_{eff,\mathcal{M}A_4^{(+)}}(r)$ to $c_{eff,\mathcal{M}A_4^{(-)}}(r)$. This was seen numerically by evaluating

$$c'_{eff,\mathcal{M}A_4^{(+)}}(r) = c_{eff,\mathcal{M}A_4^{(+)}}(r) - \frac{3}{2\pi}r^2 \tag{6.3.14}$$

at $r = \rho \exp(-\frac{5\pi i}{4})$ using Fortran, which produced the fit

$$\begin{aligned} &0.69999999999985 + 6.2584802217353 \times 10^{-11} r^{4/5} - 0.39535852554392 r^{8/5} \\ &+0.164671495497996 r^{12/5} - 0.00442294682565 r^{16/5} - 0.006084462740218 r^4 \\ &-0.00113457797974 r^{24/5}. \end{aligned} \tag{6.3.15}$$

Using the $\mathcal{M}A_4^{(-)}$ TBA system for real r produces the following fit for $c_{eff,\mathcal{M}A_4^{(-)}}(r)$

$$\begin{aligned} &0.70000000000000 - 9.7105172596272 \times 10^{-13} r^{4/5} - 0.39535851867431 r^{8/5} \\ &+0.16467119535971 r^{12/5} - 0.00441678527165 r^{16/5} - 0.00614380663949 r^4 \\ &-0.00091844415724 r^{24/5} \end{aligned} \tag{6.3.16}$$

which matches well with the analytically continued fit above. It has also been possible to plot the analytically continued $c'_{eff,\mathcal{M}A_4^{(+)}}(r)$ for values of r less than about $\ln r = 1$ (for larger values of r the singularities in $L(\theta)$ seen in the pseudoenergy plots get too close to the imaginary axis for the numerical integration to succeed). This plot and that of $c_{eff,\mathcal{M}A_4^{(-)}}$ are shown in figure 6.8, with clear matching between them.

6.3.2 The g-function

As was discussed in section 6.1, in $\mathcal{M}A_4^{(+)}$ the perturbative expansion of the g-function with one boundary parameter θ_b takes the form

$$\ln g(r) = fr + \sum_{m,n=0}^{\infty} c_{m,n}^{(\alpha)} \left(\nu r^{2/5}\right)^m \left(\kappa r^{4/5}\right)^n \tag{6.3.17}$$

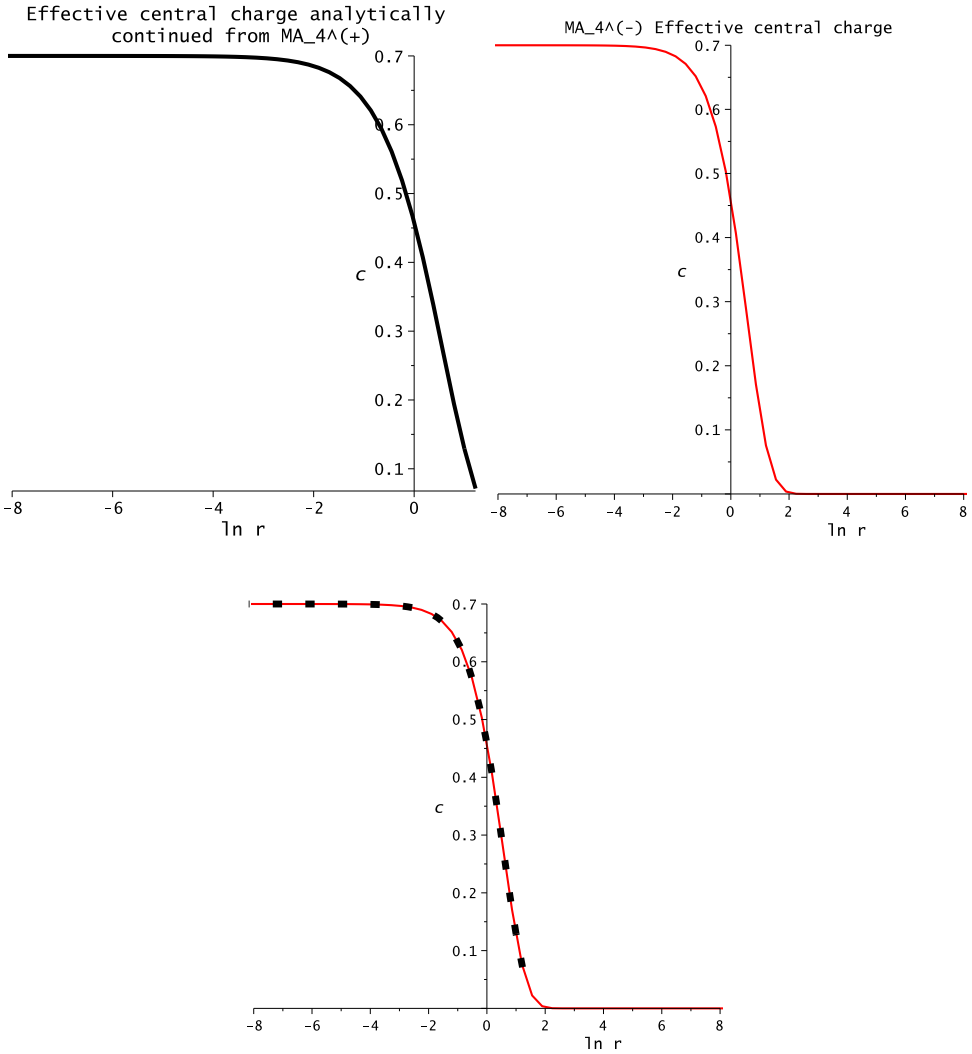

Figure 6.8: Separate and combined plots of the analytically continued $c_{eff,\mathcal{M}A_4^{(+)}}(r)$ and of $c_{eff,\mathcal{M}A_4^{(-)}}$. The final plot combines the first two, with the dotted line plotting $c_{eff,\mathcal{M}A_4^{(-)}}$.

where $\lambda = \kappa M^{4/5}$ and ν is a function of θ_b. When there is no boundary perturbation, the regular part of the expansion is purely in powers of $r^{4/5}$. This occurs when $\theta_b = 0$, and when θ_b is taken to $\pm\infty$ before r is varied. Then

$$\ln g(r) = fr + \sum_{n=0}^{\infty} d_n^{(\alpha)} \left(\kappa r^{4/5}\right)^n \tag{6.3.18}$$

In [41] the expansions were found numerically for these values of θ_b. At $\theta_b = -\infty$ (which corresponds to the (0) boundary condition) the expansion was found to be

$$\begin{aligned}\ln g(r) =& -0.3214826953191671 - 0.3535533905994r + 0.5337825122412r^{4/5} \\ & - 0.017417394r^{8/5} + 0.0133024r^{12/5} - 0.00130r^{16/5} \\ & - 0.0008r^4 + \cdots .\end{aligned} \tag{6.3.19}$$

The $\theta_b = \infty$ case (which describes flows from the (+) boundary condition) is found by subtracting $\ln(2)/2$, giving constant term -0.668056285599137. The constant and $r^{4/5}$ terms were confirmed analytically in section 6.1 as

$$\ln g(r) = \frac{1}{4}\ln\left(\frac{5-\sqrt{5}}{10}\right) - \tfrac{1}{2}\ln 2 + \frac{A_1'}{10}(10+2\sqrt{5})r^{4/5} + \cdots \tag{6.3.20}$$

$$= -0.6680562855991361 + 0.5337825122395083r^{4/5} + \cdots \tag{6.3.21}$$

where

$$A_1' = -\frac{5}{\sqrt{160}}\frac{B(-1/5,3/5)\sqrt{\frac{\Gamma(7/10)}{\Gamma(3/10)}}\sqrt{\sqrt{5}-1}}{2\sqrt{2}(3/2)^{1/5}}, \tag{6.3.22}$$

in agreement with the above. For $\theta_b = 0$, which describes flows from the (0+) boundary condition, the perturbative expansion was found numerically to be

$$\begin{aligned}\ln g(r) =& -0.1868444605395363 + 0.1464466094005r - 0.2038867770734r^{4/5} \\ & - 0.008541178r^{8/5} - 0.0020624r^{12/5} + 0.00151r^{16/5} - 0.0004r^4 + \cdots\end{aligned} \tag{6.3.23}$$

and the constant and $r^{4/5}$ terms were again confirmed analytically in section 6.1 as

$$\ln g(r) = \frac{1}{4}\ln\left(\frac{5+2\sqrt{5}}{20}\right) + \frac{A_1'}{10}(-10+2\sqrt{5})r^{4/5} + \cdots \tag{6.3.24}$$

$$\approx -0.1868444605395326 - 0.2038867770751854r^{4/5} + \cdots . \tag{6.3.25}$$

Since $\mathcal{M}A_4^{(+)}$ and $\mathcal{M}A_4^{(-)}$ only differ in the sign of λ, the perturbative expansion of the g-function for $\mathcal{M}A_4^{(-)}$ in these boundary cases should follow from (6.3.18)

upon shifting $\lambda \to -\lambda$, or equivalently $\kappa \to -\kappa$. So, the coefficients of $r^{4n/5}$ in the $\mathcal{M}A_4^{(+)}$ and $\mathcal{M}A_4^{(-)}$ expansions have the same absolute value but differ by a sign for n odd and are equal for n even. An expression for the exact g-function for $\mathcal{M}A_4^{(-)}$ must therefore obey these rules in its perturbative expansion.

Using the methods outlined at the end of section 3.3, a proposal was made by Pozsgay for an exact expression for the $\mathcal{M}A_4^{(-)}$ g-function [63]. Part of his proposal involved an infinite sum:

$$\ln g_1(r) = \sum_{j=1}^{\infty} \frac{1}{2j} \int_{\mathbb{R}^{2j}} \frac{d\theta_1}{1+e^{\varepsilon_1(\theta_1)}} \frac{d\theta_2}{1+e^{\varepsilon_2(\theta_2)}} \cdots \frac{d\theta_{2j}}{1+e^{\varepsilon_2(\theta_{2j})}} \phi(\theta_1+\theta_2)\phi(\theta_2-\theta_3)\cdots\phi(\theta_{2j}-\theta_1) \tag{6.3.26}$$

where $\varepsilon_1(\theta)$ and $\varepsilon_2(\theta)$ solve the $\mathcal{M}A_4^{(-)}$ TBA system (6.3.1). Notice that the sum here is over even powers, whereas in the $\mathcal{M}A_4^{(+)}$ g-function, $\ln g_0$ was a sum over odd powers (3.3.7). This confirmed indications coming from the A_2 homogeneous sine-Gordon model, which is a theory involving two massive particles from which $\mathcal{M}A_4^{(-)}$ emerges under certain choices of parameters in the limit where one of the particle masses is taken to zero. Pozsgay's full proposal for the g-function did not have the expected perturbative expansion. However, a study of the differences between the expected expansion and that arising from Pozsgay's proposal suggested what the other terms in the g-function should be and led to the following proposal [64] for flows from the (+) boundary condition (which in the $\mathcal{M}A_4^{(+)}$ theory corresponds to $\theta_b = \infty$):

$$\ln g(r) = \ln g_1(r) + \ln g_2(r) \tag{6.3.27}$$

where $\ln g_1$ is given above and

$$\ln g_2(r) = \frac{1}{4} \int_{-\infty}^{\infty} d\theta \, (2\phi(\theta) - \delta(\theta)) \, (L_1(\theta) + L_2(\theta)) - \ln 2. \tag{6.3.28}$$

To test this proposal, its perturbative expansion must be compared to the above $\mathcal{M}A_4^{(+)}$ results, to check that the corresponding coefficients in each theory have the same absolute value, and that the expected sign-changing behaviour is observed. Using similar analytic methods to those implemented in section 6.1, $\ln g_1$ has the

expansion

$$\frac{1}{4}\ln\left(\tfrac{1}{2}\left(\frac{5-\sqrt{5}}{5}\right)\right)+\tfrac{1}{2}\ln 2+\frac{15-7\sqrt{5}}{10}A_1' r^{4/5}+\cdots \tag{6.3.29}$$

$$\approx 0.0250908949608091-0.0240655695515436 r^{4/5}+\cdots \tag{6.3.30}$$

This has been verified by solving the massive TBA numerically and calculating g_1 using Fortran before fitting it to a series of the above form using Maple:

$$\begin{aligned}\ln g_1(r) =&0.025090894960809-2.62\times 10^{-9} r-2.44\times 10^{-13} r^{2/5}\\ &-0.024065569380745 r^{4/5}+1.30\times 10^{-8} r^{6/5}+0.008563591929185 r^{8/5}\\ &+0.000001591227208 r^2-0.001605162176630 r^{12/5}\\ &+0.000042286794764 r^{14/5}+0.000370663456047 r^{16/5}.\end{aligned} \tag{6.3.31}$$

As expected, it appears that the coefficients of odd powers of $r^{2/5}$ can be assumed to be zero. Furthermore, the coefficient of r appears to be zero, and this is also to be expected in this boundary independent part of the g-function [41]. Implementing these observations leads to a more constrained fit

$$\begin{aligned}\ln g_1(r) =&0.025090894960809-0.024065569551547 r^{4/5}+0.008563741458027 r^{8/5}\\ &-0.001594289252229 r^{12/5}+0.000445356012558 r^{16/5}\\ &-0.000114795125707 r^4-0.000013470755383 r^{24/5}\end{aligned} \tag{6.3.32}$$

which can be seen to be in agreement with the terms found analytically.

Moving to $\ln g_2$, the constant and $r^{4/5}$ terms in its expansion can again be found analytically. The integral contributes no constant term, so the constant is just $-\ln 2$ and the $r^{4/5}$ term is

$$\left(\frac{\sqrt{5}-5}{2}\right)A_1' r^{4/5}\approx -0.5097169427532075 \tag{6.3.33}$$

Finding the expansion of the integral part numerically gives

$$\begin{aligned}\ln g_2(r) + \ln 2 = &- 7.15 \times 10^{-16} + 0.500000022397917r + 2.08 \times 10^{-12}r^{2/5} \\ &- 0.509716944150008r^{4/5} - 1.11 \times 10^{-7}r^{6/5} - 0.025979871791119r^{8/5} \\ &- 0.000013386108369r^2 - 0.0116171698725921r^{12/5} - \\ &0.000351892088096r^{14/5} - 0.001133705655781r^{16/5}. \end{aligned} \tag{6.3.34}$$

Again it seems correct to constrain the regular part to powers of $r^{4/5}$, and to drop the constant term, giving

$$\begin{aligned}\ln g_2(r) + \ln 2 = &\\ &0.500000000014746r - 0.509716942690669r^{4/5} - 0.025981136515188r^{8/5} \\ &- 0.011708160725455r^{12/5} - 0.001750837361228r^{16/5} \\ &+ 0.000917387731753r^4 + 0.000259141783205r^{24/5}. \end{aligned} \tag{6.3.35}$$

Adding the analytically obtained expansions of $\ln g_1$ and $\ln g_2$ gives

$$\begin{aligned}\ln g(r) =& \frac{1}{4}\ln\left(\tfrac{1}{2}\left(\frac{5-\sqrt{5}}{5}\right)\right) - \tfrac{1}{2}\ln 2 + \frac{15-7\sqrt{5}-25+5\sqrt{5}}{10}A_1' r^{4/5} + \cdots \\ =& \frac{1}{4}\ln\left(\tfrac{1}{2}\left(\frac{5-\sqrt{5}}{5}\right)\right) - \tfrac{1}{2}\ln 2 - \frac{10+2\sqrt{5}}{10}A_1' r^{4/5} + \cdots. \end{aligned} \tag{6.3.36}$$

Comparison with the $\mathcal{M}A_4^{(+)}$ $\theta_b = \infty$ result shows that both the constant term and the $r^{4/5}$ coefficient are as expected, with the expected sign change in the $r^{4/5}$ term. Adding the numerical fits gives

$$\begin{aligned}\ln g(r) = &\\ &- 0.668056285599136 + 0.500000000006609r - 0.533782512240741r^{4/5} \\ &- 0.017417394874754r^{8/5} - 0.013302459608256r^{12/5} - 0.001305180754752r^{16/5} \\ &+ 0.0007982488821876r^4 + 0.000267720630612r^{24/5}, \end{aligned} \tag{6.3.37}$$

which is in good agreement with the regular part of (6.3.19), with the expected sign

changes. This therefore seems a good proposal for the g-function for this particular boundary case.

The next step is to see how this expression for the g-function can be adapted for flows starting from the (0+) boundary condition (the case corresponding to $\theta_b = 0$ in the $\mathcal{M}A_4^{(+)}$ situation). The formula for the $\mathcal{M}A_4^{(+)}$ g-function for this boundary situation hints at how an expression can be found for $\mathcal{M}A_4^{(-)}$. Going from the $\theta_b = \infty$ to the $\theta_b = 0$ expressions for the $\mathcal{M}A_4^{(+)}$ g-function just involves adding the term $\int_{-\infty}^{\infty} \phi(\theta) L_{(1,\mathcal{M}A_4^{(+)})}(\theta) d\theta$ (where $L_{(1,\mathcal{M}A_4^{(+)})}(\theta)$ solves the massless TBA equations (2.3.22)). An equivalent term must be found in the $\mathcal{M}A_4^{(-)}$ case to add to (6.3.27). Considering the perturbative expansion of the $\mathcal{M}A_4^{(+)}$ term, the regular part of its $\mathcal{M}A_4^{(-)}$ counterpart must have coefficients of the same absolute value, and exhibit the sign-changing behaviour described previously. These sign-changes can be effected by taking the expansion in the $\mathcal{M}A_4^{(+)}$ case and analytically continuing r to $re^{-5i\pi/4}$. So, it should be possible to find the required additional term by analytically continuing $\int_{-\infty}^{\infty} \phi(\theta) L_{(1,\mathcal{M}A_4^{(+)})}(\theta) d\theta$.

Using the $\mathcal{M}A_4^{(+)}$ TBA equations (2.3.22) the integral can be rewritten as

$$\int_{-\infty}^{\infty} \phi(\theta) L_{(1,\mathcal{M}A_4^{(+)})}(\theta) d\theta = -\varepsilon_{(1,\mathcal{M}A_4^{(+)})}(0) + \tfrac{1}{2} r. \tag{6.3.38}$$

$\varepsilon_{(1,\mathcal{M}A_4^{(+)})}(\theta)$ has a regular perturbative expansion in powers of $r^{4/5}$, so it is this part of the above for which it makes sense to consider the continuation. Using (6.3.10), the continuation has the following effect on this term:

$$-\varepsilon_{(1,\mathcal{M}A_4^{(+)})}(0) \to -\varepsilon_{(1,\mathcal{M}A_4^{(-)})}(-5\pi i/4) = -\varepsilon_{(1,\mathcal{M}A_4^{(-)})}(5\pi i/4), \tag{6.3.39}$$

where the fact that the massive pseudoenergies are symmetric has been used.

This produces a numerical fit where the coefficients of the r term and the odd

powers of $r^{2/5}$ can be assumed to be zero. Constraining the fit as before leads to

$$\begin{aligned}&0.481211825059603 + 0.737669289314415r^{4/5} + 0.008876215908657r^{8/5}\\&+ 0.015364903506098r^{12/5} + 0.002820720013630r^{16/5} - 0.000387956360825r^4\\&- 0.000297171684214r^{24/5}.\end{aligned} \tag{6.3.40}$$

As before, the constant and $r^{4/5}$ terms can be analytically verified. $\varepsilon_{(1,\mathcal{M}A_4^{(-)})}(\theta)$ has expansion

$$\varepsilon_{(1,\mathcal{M}A_4^{(-)})}(\theta) = -\ln\left(\frac{1+\sqrt{5}}{2}\right) + 2A_1'\cosh\left(\frac{4\theta}{5}\right)r^{\frac{4}{5}} + \cdots . \tag{6.3.41}$$

and so

$$-\varepsilon_{(1,\mathcal{M}A_4^{(-)})}(5\pi i/4) = \ln\left(\frac{1+\sqrt{5}}{2}\right) + 2A_1'r^{4/5} + \cdots \tag{6.3.42}$$

$$\approx 0.4812118250596035 + 0.7376692893146938r^{4/5} + \cdots . \tag{6.3.43}$$

Adding this to (6.3.36) gives the same constant term as appears in (6.3.24), and the same absolute value but opposite sign for the $r^{4/5}$ coefficient, as expected. Adding the numerical fit to the expansion for the $\mathcal{M}A_4^{(-)}$ g-function for the (+) boundary condition (6.3.37) gives

$$\begin{aligned}&- 0.186844460539532 + 0.500000000006609r + 0.203886777073673r^{4/5}\\&- 0.008541178966097r^{8/5} + 0.002062443897842r^{12/5} + 0.001515539258878r^{16/5}\\&+ 0.000410292521362r^4 - 0.000029451053602r^{24/5}.\end{aligned} \tag{6.3.44}$$

Again, the expected relationship with (6.3.23) is observed. Therefore, the proposal for flows in $\mathcal{M}A_4^{(-)}$ from the (0+) boundary condition is

$$\ln g(r) = \ln g_1(r) + \ln g_2(r) - \varepsilon_1\left(\frac{5\pi i}{4}\right). \tag{6.3.45}$$

with $\varepsilon_1(\theta)$ solving the $\mathcal{M}A_4^{(-)}$ TBA system.

Ideally, the aim would be to find an expression for the $\mathcal{M}A_4^{(-)}$ g-function for all boundary situations, i.e. those corresponding to $\theta_b \neq 0, \pm\infty$ in $\mathcal{M}A_4^{(+)}$. This involves determining how θ_b should be analytically continued to move from the massless to the massive case. It is expected that the massive boundary parameter should be related in a simple way to the boundary parameter used by Chim when he analysed the massive tricritical Ising model in [49]. However, it has not yet been possible to find what this relationship should be, so the question of finding the full exact g-function for $\mathcal{M}A_4^{(-)}$ remains open.

Chapter 7

Conclusions

In this final chapter, the main results of the thesis will be summarised, and the open questions arising from these results will be discussed.

It has been seen how the analysis of the g-function in the staircase model enabled the identification (up to certain ambiguities) of the flows between boundary conditions that occur both within unitary minimal models and as a result of bulk flows between consecutive models. In the limits corresponding to a single boundary parameter, these flows confirmed the perturbative results of Fredenhagen et al. [52], and new flows emerged when the second boundary parameter also induced changes in the value of the g-function. Furthermore, considering the staircase model equations in certain double-scaling limits allowed the extraction of expressions for the exact g-function for the $\mathcal{M}A_m^{(+)}$ interpolating theories. Pozsgay's alternative approach to the exact g-function suggests a means of verification of these equations; this was done for the $\mathcal{M}A_4^{(+)}$ case in [40], and although a full proof has not been found, he has made checks on the first few terms of the $\ln g_0$ expression in $\mathcal{M}A_5^{(+)}$ and $\mathcal{M}A_6^{(+)}$ [63], which seem to give good indications of the matching of his results with those reported in section 5.3. Scope for further work lies in the possibility that further boundary parameters could be included in the staircase model reflection factor in addition to the two already considered. Such a boundary configuration does not follow directly from boundary sinh-Gordon theory, but arises when defects are placed next to the original two-parameter boundary [65,66], and investigation of the g-function of such a model might allow further boundary flows to be identified.

It has been possible to confirm analytically some perturbative results on the scaling Lee-Yang model and on $\mathcal{M}A_4^{(+)}$, which had previously only been found numerically. This provides additional confirmation of the exact g-function results which were the foundations on which the expressions for the staircase g-function were built. However, since the methods used only allowed the first couple of terms in the expansions to be found, it remains an open question as to how the higher terms can be found analytically.

It has also been possible to make proposals for the $\mathcal{M}A_4^{(-)}$ g-function for certain values of the boundary parameter, but as was discussed in section 6.3 an expression valid for all values of the boundary parameter has so far proved elusive. Further work is therefore needed on the relationship between the boundary parameter and the boundary coupling to determine exactly how the boundary parameter behaves under the analytic continuation that takes $\mathcal{M}A_4^{(+)}$ to $\mathcal{M}A_4^{(-)}$.

Exact g-function equations have been found for an excited state in the $\mathcal{M}A_m^{(+)}$ theories in the cases where m is even, and it has been seen that the combined information from the ground state and excited state g-function allows the unique identification of boundary flows in the majority of cases. This is also an area that could be explored further. Only the g-function arising from the inner product of a boundary state with the bulk state corresponding to the $\phi_{2,2}$ field was considered here. However, other excited states could be considered, and indeed Klassen and Melzer [55] proposed TBA equations for the $(m/2, m/2)$ state in $\mathcal{M}A_m^{(+)}$ with m even. This might be a means to uniquely identify those flows involving the boundary condition superpositions which were not uniquely determined by the ground state and $(2,2)$-excited state g-functions. Expressions for the $(2,2)$-excited state g-function are also still to be found for $\mathcal{M}A_m^{(+)}$ when m is odd. Klassen and Melzer [55] found that, unlike for m even, it was not possible to find a simple way to adapt the ground state TBA system to find the excited state TBA system in this case. Indeed, for the $(m/2, m/2)$ excited state they found that the TBA system which worked for m even actually led to a system describing flows between minimal models with non-diagonal modular invariants (the so-called D_n minimal models) for m odd [67]. It therefore seems that to find the $(2,2)$-excited state for m odd may prove rather more

complex than for m even.

There are, however, other ways of considering excited states. Dorey and Tateo [57] found in the Lee-Yang model that TBA equations for excited states could be found from the ground state TBA system by analytic continuation of the bulk coupling, or equivalently of r, around singularities of the ground state energy, and these equations match those found by Bazhanov et al. [68] using alternative methods. These results indicate that the g-function for excited states might arise from analytic continuation of the ground state expression. However, the process is more difficult than for the TBA itself, as the infinite sum part of the g-function involves multiple integrals which make the process of dealing with the residues that arise from the deformation of the contour more complex. Another possibility lies in the Truncated Conformal Space Approach, which has been used by Takacs and Watts [69] to find excited state g-functions for boundary flows in the Lee-Yang model. If this could be extended to bulk flows, and in particular to the $\mathcal{M}A_m^{(+)}$ interpolating theories, then it would provide both a useful means of checking the TBA results already found, and an alternative approach to finding expressions for other excited states. There is therefore great scope for exploring this issue further.

Bibliography

[1] P. Dorey, R. Tateo, and R. Wilbourne, "Exact g-function flows from the staircase model," *Nucl.Phys.* **B843** (2011) 724–752, `arXiv:1008.1190 [hep-th]`.

[2] R. Pathria, *Statistical Mechanics* . Elsevier, second ed., 1996.

[3] N. Goldenfeld, *Lectures on phase transitions and the renormalization group*, vol. 85 of *Frontiers in physics*. Addison-Wesley, 1992.

[4] K. Peeters and M. Zamaklar, "Euclidean Field Theory." `http://www.maths.dur.ac.uk/users/kasper.peeters/pdf/eft.pdf`, 2011. Lecture notes for the M.Sc. in Elementary Particle Theory at Durham University.

[5] J. L. Cardy, *Scaling and renormalization in statistical physics*. Cambridge University Press, 1996.

[6] M. Blume, V. J. Emery, and R. B. Griffiths, "Ising Model for the lamda Transition and Phase Separation in He-3- He-4 Mixtures," *Phys. Rev.* **A4** (1971) 1071–1077.

[7] K. G. Wilson, "The Renormalization Group: Critical Phenomena and the Kondo Problem," *Rev.Mod.Phys.* **47** (1975) 773. Cargese lecture notes (1973).

[8] P. Christe and M. Henkel, *Introduction to conformal invariance and its applications to critical phenomena*, vol. M16 of *Lect. Notes Phys.* Springer-Verlag, 1993.

[9] P. Di Francesco, P. Mathieu, and D. Senechal, *Conformal field theory*. Springer, 1997.

[10] M. Henkel, *Conformal invariance and critical phenomena*. Springer, 1999.

[11] P. Pfeuty and G. Toulouse, *Introduction to the Renormalization Group and to Critical Phenomena*. Wiley, 1977. Translated by G. Barton.

[12] J. L. Cardy, "Conformal Invariance and Statistical Mechanics," in *Fields, strings and critical phenomena. Proceedings, 49th Session of the Les Houches Summer School in Theoretical Physics, NATO Advanced Study Institute, Les Houches, France, June 28 - August 5, 1988*, E. Brezin and J. Zinn-Justin, eds. Elsevier, 1989.

[13] J. L. Cardy, "Boundary conformal field theory," `arXiv:hep-th/0411189 [hep-th]`. To apper as entry in Encyclopedia of Mathematical Physics.

[14] A. Belavin, A. M. Polyakov, and A. Zamolodchikov, "Infinite Conformal Symmetry in Two-Dimensional Quantum Field Theory," *Nucl.Phys.* **B241** (1984) 333–380.

[15] A. Zamolodchikov, "Integrable field theory from conformal field theory," *Adv.Stud.Pure Math.* **19** (1989) 641–674.

[16] A. Zamolodchikov, "Renormalization Group and Perturbation Theory Near Fixed Points in Two-Dimensional Field Theory," *Sov.J.Nucl.Phys.* **46** (1987) 1090.

[17] D. Friedan, Z. Qiu, and S. H. Shenker, "Conformal Invariance, Unitarity and Two-Dimensional Critical Exponents," *Phys. Rev. Lett.* **52** (1984) 1575–1578.

[18] A. Zamolodchikov, "From tricritical Ising to critical Ising by thermodynamic Bethe ansatz," *Nucl.Phys.* **B358** (1991) 524–546.

[19] R. Eden, P. Landshoff, D. Olive, and J. Polkinghorne, *The Analytic S-matrix*. Cambridge University Press, 1966.

[20] A. B. Zamolodchikov and A. B. Zamolodchikov, "Factorized S-matrices in two dimensions as the exact solutions of certain relativistic quantum field theory models," *Ann. Phys.* **120** (1978) 253.

[21] S. J. Parke, "Absence of particle production and factorization of the S matrix in (1+1) -dimensional models," *Nucl. Phys.* **B174** (1980) 166.

[22] P. Dorey, "Exact S matrices," `arXiv:hep-th/9810026 [hep-th]`.

[23] A. Zamolodchikov, "Integrals of Motion and S Matrix of the (Scaled) T=T(c) Ising Model with Magnetic Field," *Int.J.Mod.Phys.* **A4** (1989) 4235.

[24] A. Zamolodchikov, "Thermodynamic Bethe ansatz in relativistic models: scaling three state Potts and Lee-Yang models," *Nucl.Phys.* **B342** (1990) 695–720.

[25] P. Dorey, "Exact finite-size effects in relativistic field theories." Conference on Integrability in Gauge and String Theory, Utrecht, 2008.

[26] T. R. Klassen and E. Melzer, "The Thermodynamics of purely elastic scattering theories and conformal perturbation theory," *Nucl.Phys.* **B350** (1991) 635–689.

[27] P. Fendley and H. Saleur, "Massless integrable quantum field theories and massless scattering in (1+1)-dimensions," `arXiv:hep-th/9310058 [hep-th]`.

[28] J. L. Cardy, "Boundary Conditions, Fusion Rules and the Verlinde Formula," *Nucl.Phys.* **B324** (1989) 581.

[29] P. Dorey, I. Runkel, R. Tateo, and G. Watts, "g function flow in perturbed boundary conformal field theories," *Nucl.Phys.* **B578** (2000) 85–122, `arXiv:hep-th/9909216 [hep-th]`.

[30] R. E. Behrend, P. A. Pearce, V. B. Petkova, and J.-B. Zuber, "Boundary conditions in rational conformal field theories," *Nucl.Phys.* **B570** (2000) 525–589, `arXiv:hep-th/9908036 [hep-th]`.

[31] N. Ishibashi, "The Boundary and Crosscap States in Conformal Field Theories," *Mod. Phys. Lett.* **A4** (1989) 251.

[32] I. Affleck and A. W. W. Ludwig, "Universal noninteger 'ground state degeneracy' in critical quantum systems," *Phys. Rev. Lett.* **67** (1991) 161–164.

[33] S. Ghoshal and A. B. Zamolodchikov, "Boundary S matrix and boundary state in two-dimensional integrable quantum field theory," *Int.J.Mod.Phys.* **A9** (1994) 3841–3886, arXiv:hep-th/9306002 [hep-th].

[34] E. Corrigan, "Integrable field theory with boundary conditions," arXiv:hep-th/9612138 [hep-th].

[35] E. Merzbacher, *Quantum Mechanics*. Wiley, third ed., 1998.

[36] P. Dorey, D. Fioravanti, C. Rim, and R. Tateo, "Integrable quantum field theory with boundaries: The Exact g function," *Nucl.Phys.* **B696** (2004) 445–467, arXiv:hep-th/0404014 [hep-th].

[37] P. Dorey, A. Lishman, C. Rim, and R. Tateo, "Reflection factors and exact g-functions for purely elastic scattering theories," *Nucl.Phys.* **B744** (2006) 239–276, arXiv:hep-th/0512337 [hep-th].

[38] A. LeClair, G. Mussardo, H. Saleur, and S. Skorik, "Boundary energy and boundary states in integrable quantum field theories," *Nucl.Phys.* **B453** (1995) 581–618, arXiv:hep-th/9503227 [hep-th].

[39] F. Woynarovich, "O(1) contribution of saddle point fluctuations to the free energy of Bethe Ansatz systems," *Nucl.Phys.* **B700** (2004) 331–360, arXiv:cond-mat/0402129 [cond-mat].

[40] B. Pozsgay, "On O(1) contributions to the free energy in Bethe Ansatz systems: The Exact g-function," *JHEP* **1008** (2010) 090, arXiv:1003.5542 [hep-th].

[41] P. Dorey, C. Rim, and R. Tateo, "Exact g-function flow between conformal field theories," *Nucl.Phys.* **B834** (2010) 485–501, arXiv:0911.4969 [hep-th].

[42] A. B. Zamolodchikov, "Resonance factorized scattering and roaming trajectories," *J.Phys.A* **A39** (2006) 12847–12862.

[43] P. E. Dorey and F. Ravanini, "Staircase models from affine Toda field theory," *Int.J.Mod.Phys.* **A8** (1993) 873–894, arXiv:hep-th/9206052 [hep-th].

[44] A. Zamolodchikov, "Thermodynamic Bethe ansatz for RSOS scattering theories," *Nucl.Phys.* **B358** (1991) 497–523.

[45] A. Kirillov and N. Reshetikhin, "Exact solution of the integrable XXZ Heisenberg model with arbitrary spin. I. The ground state and the excitation spectrum," *J.Phys.A* **A20** (1987) 1565–1585.

[46] M. Lassig, "Multiple crossover phenomena and scale hopping in two-dimensions," *Nucl. Phys.* **B380** (1992) 601–620, arXiv:hep-th/9112032.

[47] E. Corrigan and G. Delius, "Boundary breathers in the sinh-Gordon model," *J.Phys.A* **A32** (1999) 8601–8614, arXiv:hep-th/9909145 [hep-th].

[48] S. Ghoshal, "Bound state boundary S matrix of the Sine-Gordon model," *Int.J.Mod.Phys.* **A9** (1994) 4801–4810, arXiv:hep-th/9310188 [hep-th].

[49] L. Chim, "Boundary S matrix for the tricritical Ising model," *Int.J.Mod.Phys.* **A11** (1996) 4491–4512, arXiv:hep-th/9510008 [hep-th].

[50] I. Affleck, "Edge Critical Behaviour of the 2-Dimensional Tri-critical Ising Model," *J. Phys.* **A33** (2000) 6473–6480, arXiv:cond-mat/0005286.

[51] G. Watts, "On the boundary Ising model with disorder operators," *Nucl.Phys.* **B596** (2001) 513–524, arXiv:hep-th/0002218 [hep-th].

[52] S. Fredenhagen, M. R. Gaberdiel, and C. Schmidt-Colinet, "Bulk flows in Virasoro minimal models with boundaries," *J.Phys.A* **A42** (2009) 495403, arXiv:0907.2560 [hep-th].

[53] Gradshteyn, I. S. and Ryzhik, I. M., *Table of integrals, series, and products*. Elsevier/Academic Press, Amsterdam, Seventh ed., 2007. Translated from the Russian, Translation edited and with a preface by Alan Jeffrey and Daniel Zwillinger.

[54] K. Graham, "On perturbations of unitary minimal models by boundary condition changing operators," *JHEP* **0203** (2002) 028, arXiv:hep-th/0111205 [hep-th].

[55] T. R. Klassen and E. Melzer, "Spectral flow between conformal field theories in (1+1)-dimensions," *Nucl.Phys.* **B370** (1992) 511–550.

[56] G. Watts, "Moduli space coordinates and excited state g-functions," *JHEP* **1202** (2012) 059, arXiv:1107.0236 [hep-th].

[57] P. Dorey and R. Tateo, "Excited states by analytic continuation of TBA equations," *Nucl.Phys.* **B482** (1996) 639–659, arXiv:hep-th/9607167 [hep-th].

[58] P. Dorey, C. Dunning, and R. Tateo, "New families of flows between two-dimensional conformal field theories," *Nucl.Phys.* **B578** (2000) 699–727, arXiv:hep-th/0001185 [hep-th].

[59] P. Dorey and J. Luis Miramontes, "A T-duality interpretation of the relationship between massive and massless magnonic TBA systems," *J.Stat.Mech.* **0612** (2006) P12016, arXiv:hep-th/0609224 [hep-th].

[60] P. Dorey and J. L. Miramontes, "Aspects of the homogeneous sine-Gordon models," arXiv:hep-th/0211174 [hep-th].

[61] O. Castro-Alvaredo, A. Fring, C. Korff, and J. Miramontes, "Thermodynamic Bethe ansatz of the homogeneous Sine-Gordon models," *Nucl.Phys.* **B575** (2000) 535–560, arXiv:hep-th/9912196 [hep-th].

[62] A. B. Zamolodchikov, "On the thermodynamic Bethe ansatz equations for reflectionless ADE scattering theories," *Phys.Lett.* **B253** (1991) 391–394.

[63] B. Pozsgay, "g-functions for non-diagonal scattering theories." Private communication, 2011.

[64] P. Dorey, B. Pozsgay, and R. Wilbourne, "The exact $\mathcal{M}A_4^{(-)}$ g-function." In preparation.

[65] P. Bowcock, E. Corrigan, and C. Zambon, "Some aspects of jump-defects in the quantum sine-Gordon model," *JHEP* **0508** (2005) 023, `arXiv:hep-th/0506169 [hep-th]`.

[66] Z. Bajnok and Z. Simon, "Solving topological defects via fusion," *Nucl.Phys.* **B802** (2008) 307–329, `arXiv:0712.4292 [hep-th]`.

[67] T. R. Klassen and E. Melzer, "RG flows in the D series of minimal CFTs," *Nucl.Phys.* **B400** (1993) 547–573, `arXiv:hep-th/9110047 [hep-th]`.

[68] V. V. Bazhanov, S. L. Lukyanov, and A. B. Zamolodchikov, "Integrable quantum field theories in finite volume: Excited state energies," *Nucl.Phys.* **B489** (1997) 487–531, `arXiv:hep-th/9607099 [hep-th]`.

[69] G. Takacs and G. Watts, "Excited State G-Functions from the Truncated Conformal Space," *JHEP* **1202** (2012) 082, `arXiv:1112.2906 [hep-th]`.